2.5 GEOLOGY AND SEISMOLOGY

Waterford 3 is situated along the west (right descending) bank of the Mississippi River, about 25 miles west of New Orleans, Louisiana. It is located in the southern portion of the Gulf Coastal Plain geologic province. The southern portion of the Gulf Coastal Plain is the Mississippi River deltaic plain physiographic province. The Mississippi River has dominated the development of geologic and physiographic features in the deltaic plain since the beginning of Neogene. The deltaic plain is characterized by low marshy terrain, much of which is covered by water. The higher natural ground within the deltaic plain generally occurs along the natural levees of existing and abandoned stream courses.

The deltaic plain is an area where extensive exploration and exploitation of petroleum has occurred. As a result of exploration near the site, deep boring data are available that provide identification of strata characteristic of the site to depths of 12,000 ft. In addition, 74 borings were drilled within the site to depths up to 500 ft., to define the site stratigraphic and hydrostratigraphic sequences and to determine the engineering properties of subsurface materials.

The regional geologic structures in the deltaic plain consist of salt structures, their overlying attendant faults, and growth faults. The growth faults represent previously unstable areas which were at the leading slope of sediment accumulation. The subsurface data demonstrate that such regional structures cannot affect the Waterford site.

→(DRN 01-464)

The site is within a region of infrequent and minor seismic activity. The maximum earthquake associated with the site region is the Donaldsonville earthquake of October 19, 1930, which has an epicentral intensity of nearly VI Modified Mercalli (MM). The nuclear plant has been designed for a maximum horizontal ground surface acceleration of 0.1g, about two times greater than the maximum acceleration appropriate for the Donaldsonville earthquake. In November 1982, the U.S. Geological Survey (USGS) in its capacity as advisor to the U.S. Nuclear Regulatory Commission (NRC) on geologic and seismic siting issues, provided clarification of its position with respect to consideration of the Charleston earthquake of 1886 in seismic design decisions. The clarification was contained in a letter from James Devine to Robert Jackson dated November 18, 1982 (90).

←(DRN 01-464)

This clarification perceived uncertainty about earthquake causes in the East, the uncertain geologic characteristics of seismic source zones, and the difficulty that has been experienced in making licensing decisions that properly take account of these uncertainties within the constraints of the deterministic regulation, 10CFR100, Appendix A. This has been referred to as the "Charleston earthquake issue."

→(DRN 01-464; 02-217)

The Seismicity Owner's Group (SOG) was formed to develop and perform analyses to resolve the Charleston earthquake issue. The entire SOG methodology and implementing interpretations for application to probabilistic seismic hazard computations were documented, referenced (91) and submitted to the NRC for review in July 1986. The NRC issued an SER in September 1988 accepting the SOG's methodology and implementing interpretations. Following receipt of the NRC SER, the SOG performed site-specific seismic hazard computations at 57 sites. The EPRI site specific methodology and results for Waterford 3 were documented in Reference (92) LP&L reviewed the methodology and results of the seismic hazard computation, and the review was documented in Reference (93). The review concluded the seismic hazard at Waterford 3 is very low. The mean percentile annual probability of exceeding 0.10 g is 8.0E-6 and of

←(DRN 01-464; 02-217)

→(DRN 02-217)

exceeding 0.05g, the annual probability is 3.0E-5. The SOG concluded, on the basis of the overall methodology and the site specific probabilistic seismic hazard computations, the Charleston earthquake issue has no material impact on the safety of nuclear power plants in the central and eastern U.S. The site specific seismic hazard computations for the 57 sites were provided by the SOG to the NRC in April 1989.

←(DRN 02-217)

All seismic Category I systems, equipment and components are supported within a common rigid, reinforced concrete structure. The foundation is designed as a part of the structure so that the combined foundation and structure act as an integral unit. The structure and its mat foundation are referred to as the nuclear plant island structure (NPIS).

The NPIS bears at elevation -47 ft. MSL. At this level the plant island is completely compensated and imparts an average stress to the underlying strata approximately equal to the pre-existing in situ effective stresses.

The sandy aquifers which exist beneath the site are of sufficient density to preclude liquefaction during the postulated most severe earthquake conditions.

The only natural slope in the area of the site is the right descending (west) bank of the Mississippi River, located about 960 ft. east of the NPIS. This bank slopes to the north at an angle of about seven degrees (8H:IV) and its failure could not adversely affect the plant.

The geologic studies of the site and surrounding area were made by Law Engineering Testing Company. These studies include interpretations of geologic literature, geologic maps, topographic maps, remote sensing data, surface mapping, subsurface borings, geophysical refraction surveys, electric logs and laboratory tests. Subsections 2.5.1 through 2.5.5 present the conclusions drawn from these data.

2.5.1 BASIC GEOLOGIC AND SEISMIC INFORMATION

2.5.1.1 Regional Geology

The following section provides basic information describing the physiography, geologic history, stratigraphy and structural geology of the region around the site. The geologic features influencing potential subsidence, collapse and man's activities are provided in Subsection 2.5.1.3; the groundwater conditions of the region are discussed in Subsection 2.4.13.

2.5.1.1.1 Physiography and Geomorphology

The Waterford 3 site is located near river mile 129 Above Head of the Passes (AHP) (Figure 2.5-1). The site is located within the Gulf Coastal Plain physiographic province (Figure 2.5-2). The Gulf Coastal Plain extends about 600 miles inland from the coast along the site longitude, 90 degrees west, approximately 200 miles inland along longitude 88 degrees west and approximately 300 miles inland along longitude 94 degrees west.

The northern margin of the Gulf Coastal Plain is bounded by five major physiographic provinces: Ouachita province, Ozark Plateau province, Central Lowlands province, Interior Low Plateaus province, and the Southern Appalachians province. The locations of these physiographic provinces are shown on Figure 2.5-2. The topography of the adjacent physiographic provinces has been mainly developed along structural features in Paleozoic and older rocks.

The Gulf Coastal Plain is bounded to the south by the Gulf of Mexico. The Mississippi enbayment section of the Gulf Coastal Plain is subdivided into three major physiographic areas (Figure 2.5-2), as is the submerged area of the Gulf (Figure 2.5-3). The description of these six physiographic areas are as follows:

a) Mississippi River Valley and Adjacent Lowlands (Figure 2.5-2)

The Mississippi River and its tributaries follow a broad, north-south trending lowland that begins at the head of the Mississippi embayment, near the junction with the Ohio River, and extends southwest about 600 miles to the Gulf. This lowland is composed of an alluvial plain that extends from the Ohio confluence to near the Atchafalaya River in Louisiana and a deltaic plain that continues to the Gulf of Mexico.

The alluvial plain of the Mississippi River valley includes the alluvial valleys of the Mississippi River and its tributaries. Most tributary streams enter the Mississippi River from the west. These include the Arkansas, Red, and Missouri Rivers which supply the main sediment load of the Mississippi River. The major tributary that enters from the east is the Ohio River. The alluvial plain ranges from about 25 to 125 miles wide and slopes from a surface elevation of about +300 ft. MSL near the mouth of the Ohio River to about +30 ft. MSL at the northern margin of the deltaic plain. The slope is uniform, gradually decreasing downstream.

The meandering Mississippi River and its tributaries are aggrading streams, with the present course defined by ridges or natural levees which are higher than most other areas of the floodplain. The combination of natural levees and two major ridges, Crowleys Ridge and Macon Ridge, have divided the alluvial valley into several shallow basins. These basins include: The St. Francis basin, White River lowland, Arkansas lowland, Yazoo basin, Boeuf basin, Ouachita lowland, Tensas basin, and Lower Tensas basin. The basins, or lowlands, are typically areas of very low relief and poor drainage, marked frequently with scars associated with abandoned stream channels. Within the alluvial valley, the only areas of significant topographic relief are the natural levees of the Mississippi River and larger tributaries, and the two ridges previously mentioned.

Crowley's Ridge extends 200 miles from southeastern Missouri to central Arkansas. It rises as much as 200 ft. above the surrounding lowlands. Macon Ridge extends about 100 miles from southeastern Arkansas into northern Louisiana. The ridges are the highest divides within the valley. (1)

A narrow band of fluviatile terraces and deeply dissected loess hills occurs along the eastern bank of the Mississippi River valley from the Ohio River, to southwestern Mississippi.

The deltaic plain is generally composed of broad basins separated by narrow, sinuous natural levee ridges which are associated with existing and abandoned distributary courses. Prominent basins include the Atchafalaya basin and Pontchartrain basin, which are characterized by swampland, shallow lakes and coastal marshlands. The marshlands include numerous large and small interconnected lakes. Bays are formed between the mainland and several offshore islands. The area occupied by lakes and bays increases toward the Gulf.

Natural levee ridges and a few isolated beach ridges are the higher ground within the deltaic plain. These ridges project as much as 25 ft. above the marshlands and are generally a few hundred yards to a few miles wide. The natural levees, except for those associated with major distributaries, slope into and are covered by the marsh. Natural levees which have been associated with major distributaries are usually continuous to the Gulf, although local topographic relief of the levee is no more than a few feet. Several isolated natural topographic highs within the deltaic plain are due to uplifts over salt domes.

The major topographic features of the deltaic plain are Teche ridge, LaFourche ridge, Metairie ridge, St. Bernard ridge and the existing course of the Mississippi River. The Teche and LaFourche ridges mark abandoned distributaries which once carried a major portion of the total river flow. Metairie ridge is a combination of an abandoned distributary and beach ridge.

Several offshore islands are also included within the deltaic plain. Most of these low, narrow, generally arcuate features have been isolated from the coastland by subsidence and erosion.

Numerous artificial topographic features occur within the deltaic plain. These include shell mounds built on some natural levees by prehistoric inhabitants; levees built along the Mississippi River and other drainage courses; lakes which have been enlarged by dredging for construction materials and fill; and the numerous canals and spoil piles built for navigation and drainage.

b) Eastern and Western Hills (Figure 2.5-2)

Bordering both sides of the northern portions of the Mississippi River valley are a series of low hills with local relief of 50 to 150 ft. The surface elevations in these areas are generally between +400 and +600 ft. MSL, with a maximum elevation of about +800 ft. MSL. The Eastern Hills consist of arcuate trending bands separated by broad lowlands, and have a maximum width of about 150 miles. The Western Hills are east-west trending cuestas separated by lowlands and extend about 200 miles across.

c) Southern Hills (Figure 2.5-2)

Gulfward from the Eastern Hills and Western Hills, a prominent wold on the Catahoula formation forms the northern margin of the Southern Hills. From surface elevations generally exceeding +400 ft. MSL along the wold, coastwise terrace surfaces slope gently gulfward in a belt attaining a 160 mile width. Valleys of major trunk streams which flow gulfward, such as the Mississippi, Pearl and Sabine, narrow where they incise the wold. The drainage basins of smaller trunk streams, such as the Amite, Tickfaw and Tangipahoa, are completely contained within the gulfward dip slopes that form the Southern Hills.

d) Northern Gulf of Mexico Continental Shelf (Figure 2.5-3)

The Southern Hills terminate against the deltaic plain or the shore of the Gulf of Mexico. The northern Gulf of Mexico continental shelf extends from the shore line southward for a distance ranging from 10 to 130 miles (Figure 2.5-3). The northern portion of the continental shelf slopes gently southward and extends to a maximum depth corresponding to about -400 ft. MSL. The shelf is generally smooth, except at local channels and ridges extending from the coast. Relief of these features is about 6 to 30 ft. Numerous knolls and mounds of up to 60 ft. relief are present on the deeper shelf.

e) Northern Gulf of Mexico Continental Slope (Figure 2.5-3)

The northern Gulf of Mexico continental slope includes all of the relatively steeply sloping area between the edge of the continental shelf and the deep abyssal Gulf. The slope ranges from about 50 to 200 miles wide and is typically one of irregular, hummocky topography, except at the edge of the Florida shelf, where regular topography and a steep, uniform gradient occurs. The depth of the slope varies from -400 ft. MSL to over -6000 ft. MSL within the northern continental slope area. Local relief within the area of irregular topography may approach 2500 ft.. About 90 miles south of the site, the Mississippi trough incises the Mississippi River alluvial fan portion of the slope. Most of the fan lies on the abyssal floor of the Gulf of Mexico.

f) Gulf of Mexico Floor (Figure 2.5-3)

The physiographic change from the continental slope to the Gulf of Mexico floor is marked by a decrease in slope on the Mississippi alluvial fan, and elsewhere in the northern Gulf by the steep West Florida and Sigsbee escarpments. The Gulf of Mexico floor is an area about 600 miles long and from 100 to more than 300 miles wide; it ranges in depth from -9000 to more than -12,000 ft. MSL. The area is characterized by a gentle, low relief, sloping surface which flattens to the Sigsbee plain. The plain is essentially featureless with the exception of several clustered mounds, the Sigsbee knolls, located near its center. The Sigsbee knolls rise as much as 900 ft. above the plain.

2.5.1.1.2 Geologic History

The discussion of the geologic history of the northern Gulf region is developed chronologically, beginning with events that occurred during late Paleozoic, and briefly tracing the history of the Gulf of Mexico basin and significant geologic features located north of the basin. The sequence of events included within this time interval are mainly responsible for geologic conditions presently existing in the northern Gulf region.

a) Late Paleozoic Era (310 to 230 Million Years Before Present - MYBP)

Numerous origins have been suggested for the Gulf of Mexico oceanic basin and are outlined in Subsection 2.5.1.1.4. Based on geophysical data, it has been determined that oceanic crustal rocks have underlain the present Gulf at least since late Paleozoic or early Mesozoic time. (See References 2, 3, 4 and 5).

The late Paleozoic Ouachita orogenic belt (Figure 2.5-8), which essentially surrounds the northern portion of the present Gulf, was a controlling influence on development of the Gulf basin. This orogenic belt is known from intermittent outcrops in Mexico. Also, surface and subsurface data(6) demonstrate its continuity from the west Texas Marathon area through central Texas to the Ouachita Mountains of Oklahoma and Arkansas and thence southeastward to the Mississippi-Alabama border. Sedimentation was occurring along the Ouachita belt, which was a geosyncline, prior to Middle Pennsylvanian (300 MYBP).

During late Pennsylvanian (280 MYBP), the Ouachita orogeny occurred, a major event of the Appalachian revolution. This event terminated sedimentation within the geosyncline.

During the Permian period (230 MYBP), the uplifted Ouachita orogenic belt was undergoing erosion and supplying sediments to the south. Postorogenic sediments have been drilled on the Texarkana platform in northeastern Texas.(7) Additional sediments may have been supplied to the area from the western edge of the Appalachian Mountains which were affected by the Permian Allegheny orogeny.

b) Triassic-Jurassic Periods (230 to 135 MYBP)

The Triassic period was marked by epeirogenic uplift of the continental area of the northern Gulf region, which was followed in late Triassic by block faulting. This faulting resulted in graben development along the southern flank of the Ouachita orogenic belt in southern Arkansas. Graben development during this period has been substantiated by the penetration of redbed deposits (Eagle-Mills formation) which are characteristic of Triassic graben-fill in other areas.(8) Igneous activity occurred in the southern portion of the Ouachita orogenic belt contemporaneous with graben development and filling. A basement high occurs in southern Mississippi and central Louisiana which has been postulated (9) to have had its origin in late Triassic (181 MYBP). This basement high, which separated areas of evaporite deposition, has been called the Hancock ridge (Figure 2.5-8).

Widespread evaporite deposition occurred during early and middle Jurassic to form thick sequences of salt and anhydrite, the Louann salt. Evaporite deposition may have occurred throughout the shallow water Gulf region, as a nearly continuous sheet, possibly including what is now the central Gulf; this is evidenced by salt on the abyssal Sigsbee plain. The evaporite thins (or was not deposited) over the Hancock ridge and other similar highs. One such high is the Sabine uplift (Figure 2.5-8), which may have been a minor positive feature as early as late Paleozoic. Drilling has demonstrated the absence of salt over this uplift, either through non-deposition or flowage.(7)

During the late Jurassic, the sea transgressed northward, producing carbonate deposition which overlapped redbed deposits and salt along the margin of the Gulf basin. Subsequently, these carbonates were buried by deposition of clastics from the north and east, predominantly from Appalachian source areas. In response to this sedimentary loading, salt mobilization began in the late Jurassic and initiated faulting at the northern margin of the salt basin. The Gilbertown-Pollard fault zones in Alabama and northwestern Florida[10] (Figures 2.5-8 and 2.5-10) were the initial hingeline faults which occurred peripheral to the Gulf basin. Along this trend, in central Mississippi, the Phillips fault (Figure 2.5-10) developed, downthrown to the Gulf Basin.(11) These and other hingeline faults underwent recurrent movements until late Tertiary (2 MYBP).

c) Cretaceous Period (135 to 65 MYBP)

The early Cretaceous was characterized by development of an extensive barrier reef at the shelf edge, which nearly surrounded the deepening Gulf basin. Behind this barrier reef, an extensive carbonate lagoon developed, overlapping the southwestern extension of the Ouachita trends in Texas and Mexico. Epeirogenic depression of the oceanic crust of the Gulf basin and continuing development of the reef created topographic escarpments, which survive today as the West Florida (Figure 2.5-3) and Campeche escarpments. Continuous reef building and carbonate deposition over the shelf maintained the shallow-water environment and, coupled with the depression of oceanic crust, accounts for the presence of thick carbonate deposits surrounding the early Cretaceous Gulf basin.

The foregoing pattern of gulfward subsidence was accompanied by continued hingeline flexing along the periphery of the basin on the gulfward side of the Ouachita trend. Locally, in the northeastern Texas - southern Arkansas region, the flexure was accompanied by the initiation of the Talco and South Arkansas fault systems(12) (Figure 2.5-8).

Diapirism, which began in the Jurassic, continued in the Cretaceous and was occurring within the interior salt basins. The domeless region south of the Mississippi salt basin lies over the Hancock ridge where evaporite deposition was thin or absent. The lack of a thick salt source accounts for the general absence of salt diapirs in this area.

During middle Cretaceous, widespread sea level regression occurred, associated with structural warping and igneous activity. Warping accentuated or developed positive structures such as the Sabine uplift, Monroe-Sharkey uplift, and Jackson dome (Figure 2.5-8). This uplift was in contrast to developing negative features such as the East Texas basin, North Louisiana basin, and Mississippi embayment (Figure 2.5-8 and 2.5-10). During this interval, a northeast trending fault zone developed in the continental region north of the Mississippi embayment (New Madrid area). These faults had a southern terminus in the upper portion of the Mississippi embayment, north of the Ouachita belt. Igneous activity extended primarily from Mississippi to the Rio Grande. Igneous intrusions formed the core of the Jackson dome, and were widespread beneath the Monroe-Sharkey uplift and along the inner edge of the present coastal plain.

During late Cretaceous, the sea transgressed above its level of early Cretaceous, flooding the continent as far north as southern Missouri, in the newly formed Mississippi embayment and extending to the west into the region of the developing Rocky Mountain geosyncline. In the northern Gulf, it is likely that only the central portion of the Ouachita orogen, mountains located in Oklahoma and Arkansas, remained above sea level.

During late Cretaceous and early Tertiary, the Laramide orogeny occurred, terminating the Rocky Mountain geosyncline and uplifting the present Rocky Mountains. This uplift caused regression of the Gulf of Mexico from its connection with the Rocky Mountain eosyncline. The newly uplifted mountains were to become the major source of sediment to the Gulf basin in the Cenozoic.

d) Tertiary Period (65 to 2 MYBP)

The Tertiary was characterized by rapid clastic sedimentation along the western and northern margins of the Gulf of Mexico basin, contrasted with carbonate shelf deposition in Florida and Yucatan. In the latter areas, the shelves established during early Cretaceous were perpetuated, but where clastic deposition was predominant, as in Louisiana and Texas, the clastics deeply buried the older shelves and barrier reefs and extended as ramps gulfward, into the Gulf oceanic basin.

During early Tertiary, rapid localized sedimentation created the Gulf geosyncline. During Tertiary, the geosynclinal depocenters were located along the present Texas coast and were under the influence of the Rio Grande. The axis of the geosyncline extended into central Louisiana. During late Tertiary, Miocene and Pliocene (22 to 2 MYBP), the influence of the Mississippi River began to dominate and depocenters shifted eastward to offshore Louisiana. Continued hingeline flexing along the periphery of the basin was accompanied by the first expression of the Balcones and Mexia fault systems in central Texas, and the Pickens fault system in central Mississippi, as well as continuing movement elsewhere along previously established peripheral faults (Figure 2.5-8). The Fisher fault zone also developed along the south flank of the Sabine uplift (Figure 2.5-10).

The localization of sedimentary loading also initiated growth faulting (contemporaneous faulting) and intrusion and deformation by underlying salt or clay. Tertiary growth (contemporaneous) faulting consists of a series of generally gulfward concave faults in Louisiana and Texas. Initiation of faulting was related to slumping along the unstable outer shelf, often in association with the mobilization of salt or clay. Faulting was perpetuated by differential loading over the area caused by increased sediment accumulation on the downthrown or gulfward block. Salt intrusions caused some of the faulting. From either cause, the faulting was associated with the gulfward progression of the geosynclinal axis from central Louisiana to offshore near the present shelf edge. The age of initiation and cessation of faulting becomes progressively younger moving gulfward. The northernmost faults which were active during the Eocene (53 to 36 MYBP), occur in central Louisiana. Progressing gulfward, Miocene (22 to 5 MYBP) faults and diapirs affected most of present southern Louisiana and nearshore areas. Pliocene (5 MYBP) faults occurred south of the present coastline.

During the time that the geosyncline was developing, two significant uplifts occurred to the north in central Alabama and Mississippi (Figure 2.5-10). These were the formation of the Hatchetigbee anticline, which occurred during late Oligocene, and the Wiggins uplift, which occurred during Eocene, both of which may have been associated with the deformation of salt.

e) Quaternary Period (2 MYBP to Present)

The thickest Pleistocene (2 HYBP to 11,000 YBP) sediments in the geosyncline occur north of the present shelf edge, offshore from the Texas-Louisiana boundary. The location of the depocenter has been the same during the recent epoch.

The oldest Quaternary salt structures occur closest to the present shore and appear as large, isolated salt diapirs. Pleistocene and recent salt structures have developed and are developing further south on the present continental shelf and slope, where active sedimentation is occurring. The Sigsbee escarpment (Figure 2.5-3) marks the physiographic change from continental slope to abyssal Gulf. This escarpment is a wall, or ridge of salt, which is being pushed southward by the geosynclinal accumulations of sediments behind it (Ref. 5,13).

The Baton Rouge fault (Figure 2.5-10) is a lower Tertiary growth fault along the south flank of the Hancock ridge. Faulting along this system was active during the Pleistocene and continued until the present (see Subsection 2.5.3.2).

Geophysical studies have shown that slumping is currently occurring in unstable sediments at the edge of the outer shelf in the northern Gulf. The areas of active movement are the Texas continental shelf, along the edge of the outer shelf, and on the slope. The active faults are mainly related to movement of salt.(13)

The Gulf region has been affected by five periods of Pleistocene glaciation and intervening periods of glacial retreat. Glaciation, as such, had no direct effect on the northern Gulf coast, but the associated fluctuations in sea level caused the development of numerous depositional and erosional features.

During periods of glacial maxima, sea levels may have been as much as 450 ft. below present sea level. (14) Increased drainage gradients allowed deep dissection, erosion, and oxidation of the preexisting surface. The eroded channels, such as the Mississippi trough (Figure 2.5-3), extended far out on the shelf, beyond the lowered shoreline. Lower sea levels allowed groundwater levels to fall, which caused some subsidence through consolidation of sediments. Coastal conditions existed near the edge of the present continental shelf, causing the formation of deltaic and shoreline features.

Sea level transgressions during the periods of glacial retreat allowed deposition of mainly glacially derived sediments over large, previously terrestrial areas. Coastal features developed far inland, about 100 miles north of the current shoreline.

The sediments deposited during the transgressions now appear as topographic terraces in their outcrop zones.

The current sea level transgression began about 18,000 years ago and rose to near its present level by about 5000 years ago.(14)

Estuaries existing along the Gulf and other coasts are the result of dissection during sea level regression and submergence of the eroded troughs during the last transgression.

Since the end of Wisconsin glaciation, the Mississippi River has been building the delta systems of southernmost Louisiana.

The Mississippi has developed seven recent delta systems, as shown on Figure 2.5-4. The features associated with each successive system have become less distinct with age due to subsidence (generally from geosynclinal influence or sediment consolidation). The only actively aggrading delta is the 550 year old Balize system that the Mississippi now occupies. Due to artificial restrictions and the position of the present Balize delta in deep water near the edge of the continental shelf, the sediment carried by the Mississippi River is only very slowly increasing the emerged land area.

2.5.1.1.3 Stratigraphy

Recent seismic velocity data(9) has inferred that a cross section through the northern Gulf coast consists of a sequence of sediments reaching up to about 57,000 ft- thick. Below the sediments, continental crust is 40,000 to 60,000 ft. thick at the northern margin of the coastal plain. It thins and eventually pinches out to the south, beneath southern Louisiana. Underlying the continental crust is oceanic crust, 40,000 to 70,000 ft. thick beneath the coastal plain and 20,000 to 25,000 ft. thick beneath the Gulf. Figure 2.5-5 demonstrates these relationships through the Louisiana region of the Gulf Coastal Plain. The following section contains a discussion of the Gulf coast sedimentary sequence, consisting of Mesozoic and Cenozoic sediments. Figure 2.5-6 is a regional stratigraphic column of the northern Gulf coast sedimentary sequence, showing the names and subdivisions used in this text. Figure 2.5-7 is the surface geology map of the central Gulf Coastal Plain.

a) Pre-Upper Jurassic

The Eagle Mills formation unconformably overlies Paleozoic rocks in peripheral portions of the coastal plain, primarily in Arkansas. The Eagle Mills consists of continental, redbed sandstones, silt stones, and shales which were deposited in the block faulted graben of southern Arkansas during early Mesozoic. These sediments were injected by basic igneous intrusions during deposition. The Eagle Mills formation does not crop out, but has been encountered at a depth of 1800 ft. in central Arkansas, where 7,000 ft. was penetrated by drilling before encountering Paleozoic limestone(8).

Unconformably overlying the Eagle Mills formation, is the Louann group, made up of the Werner and Louann formations(8). The Werner formation consists of conglomerates, anhydrites, red sandstones and silt stones. Sparse data are available relative to its thickness or areal extent. The Louann formation is an evaporite and consists of up to 5,000 ft. of salt (6). The greatest thicknesses of the Louann occur in four major interior salt basins: the Rio Grande basin; the East Texas basin; the North Louisiana basin and the Mississippi salt basin; and the Texas-Louisiana coastal and offshore basin (Figure 2.5-8). Other salt basins are known around the western and southern periphery of the Gulf. The Louann was probably deposited over the entire northern Gulf basin. Therefore, Jurassic salt of some thickness is a general occurrence, except in areas which maintained an elevation above the salt accumulation during deposition, or areas where uplift forced the salt to flow laterally off the uplifted area into the surrounding basins. The basins are separated by preexisting structural highs or Mesozoic/Cenozoic uplifts. Due mainly to isostatic imbalance, from subsequent sedimentation, movement of salt has occurred within the basins causing domal or anticlinal structures to penetrate younger sediments and, in some cases, to the ground surface. A generalized regional cross section indicating salt diapirism is shown on Figure 2.5-9.

b) Upper Jurassic (135 MYBP)

Beginning in Upper Jurassic, a normal marine environment of deposition developed in the Gulf. As the result of widespread sea level transgression, the Louann salt is overlapped in the northern Gulf region by the Upper Jurassic Louark group, which is composed of the Norphlet, Smackover, and Haynesville formations. In the type area of southern Arkansas and northern Louisiana, thicknesses exceeding 1000 ft. have been estimated.(8) In the updip facies in southern Arkansas and northern Louisiana, the Louark group consists of basal continental or nearshore clastics, overlain by nearshore marine carbonates, shales, and evaporites. Basinward, the group grades to dark marine carbonates.

The Louark group is unconformably overlain by the Cotton Valley group, which is made up of the Bossier and Schuler formations. The updip Cotton Valley, in southern Arkansas and northern Louisiana, consists of non-marine red shales, sandstones and conglomerates, which grade gulfward to marine, partly indurated and cemented sands, shales and marls very similar to the underlying Louark. The Cotton Valley group, which does not crop out, exceeds 4000 ft. in thickness in southern Mississippi(6).

c) Cretaceous (135 to 65 MYBP)

The Lower Cretaceous is marked by the presence of a carbonate barrier reef, the Stuart City reef, which developed at the shelf edge, and nearly encircles the Gulf basin. Northward of the reef, deposition occurred in a lagoonal environment where thick, generally carbonate sequences, are present. Because of the great depth at which Cretaceous strata occur gulfward of the reef, beyond present well depths, stratigraphic information is mainly limited to the Cretaceous shelf facies.

The Coahuilan series is lowermost Cretaceous in age and consists of the Hosston and Sligo formations. The Hosston unconformably overlies and oversteps the underlying Upper Jurassic Schuler, to rest directly upon Paleozoic rocks in Mississippi and Alabama.

In northern Louisiana, the Coahuilan consists mainly of shale and sandstone. Gulfward, it becomes more shaley and limey. The thickness of the Coahuilan series in southern Mississippi is 2400 ft. The Coahuilan series crops out in small areas in southwestern Arkansas and southeastern Oklahoma, within the Western Hills.

The upper part of the Lower Cretaceous, the Comanchean series, consists of the Trinity, Fredericksburg, and Washita stages. The Trinity stage is lowermost

Comanchean and contains all strata between the Hosston-Sligo and the lowermost Fredericksburg (middle Comanchean). In the subsurface section of southern Arkansas and northern Louisiana, the Trinity consists of several formations, including; Pine Island, James, Rodessa, Ferry Lake, Mooringsport and Paluxy.

The Trinity strata are generally sandstones and shales in the updip areas toward the north, becoming predominantly limestones, marls, and shales toward the Gulf basin. The updip sediment types imply fluctuations within a nearshore marine environment of deposition. They are shown by deep wells to attain a maximum thickness of more than 4000 ft. downdip from the outcrop area. The outcrop area in the northern Gulf region is located in southwestern Arkansas and southeastern Oklahoma, in the northernmost part of the Western Hills, adjacent to the Ouachita Mountains.

The upper Comanchean, Washita-Fredericksburg (undifferentiated) stage, crops out in the Western Hills of Texas, Oklahoma, and Arkansas. The updip facies of the Washita-Fredericksburg in northern Mississippi consist of sandstones, mudstones, and shales which grade basinward to dark, marine limestones and shales in northern Louisiana. The thickness of the Washita-Fredericksburg is 2300 ft. in southern Mississippi.

The Lower Cretaceous and Upper Cretaceous are separated by a major unconformity which was formed by erosion during widespread sea level regression, ending in Upper Cretaceous. A subsequent widespread transgression during late Cretaceous deposited the Gulfian series. The Upper Cretaceous, Gulfian series, has been subdivided into five stages: the Woodbine, Eagle Ford, Austin, Taylor, and Navarro. In the Gulf region, rocks of these ages lie unconformably on rocks of Lower Cretaceous, Jurassic, and older ages as a result of the marine transgression.

Lowermost Gulfian or Woodbine sediments occur as far north as central Tennessee and directly overlap rocks of the Ouachita orogen in eastern Arkansas and Mississippi. The updip rocks are redbeds consisting of coarse grained clastics and volcanics. The downdip rocks are of marine origin and darker, and finer grained than their updip equivalents.

Upper Gulfian or Eagle Ford, Austin, Taylor and Navarro, occur as sandstones and shales from central Tennessee to northern Louisiana. In their northernmost extent, these deposits accumulated in a continental or nearshore environment. In their southern extent, they accumulated in a shallow marine environment and also include significant deposits of water-laid volcanic materials. During Austin, Taylor, and Navarro stages, thick deposits of shelf and reefal chalks and marls accumulated in southern Louisiana, Mississippi, Alabama and Texas. Reefal carbonates, primarily Navarro in age, are present over the Jackson dome and Monroe uplift.

Gulfward dipping rocks of Upper Cretaceous age crop out along the northern margin of the Gulf Coastal Plain in the location of the Eastern and Western Hills, forming the cuesta and lowland topography typical of these areas.

d) Cenozoic (65 to 0 MYBP)

The Cenozoic sediments of the Gulf coast are part of a geosynclinal complex of continental, deltaic, and marine deposits. The axes of thickest strata within particular time units roughly parallel the Gulf coast and are characterized by fluvial and marginal or transitional sediments landward of the depocenters, grading seaward to marine sediments. The Gulf coast Cenozoic is commonly divided into two systems, the lower Tertiary Paleogene (65 to 22 MYBP) and the upper Tertiary Neogene (22 to 2 MYBP). These systems generally correspond to the time periods when thickest sediments collected in depocenters off the Texas and Louisiana coast, respectively. Figure 2.5-6 shows the chronologic relationship of these systems to the subdivision of the Tertiary into epochs.

In the northern Gulf coast, the Paleogene is subdivided into several stages: the Midway, Sabine-Wilcox, Claiborne, Jackson, and Vicksburg. Gulfwide correlation within these Paleogene stages is difficult and has led to the assignment of numerous formational breakdowns.

The Paleogene system is essentially characterized by updip deltaic clastics and downdip marine shales. The position of the transition between marine and deltaic corresponds to the position of sea level during deposition. The thickest Paleogene sediments are located along the Texas coast, accumulating to over 35,000 ft- In Louisiana, Paleogene sediments are thinner, just over 10,000 ft., and are generally more arenaceous. Paleogene downdip facies are similar throughout the Gulf coast (15).

Paleogene outcrops extend from the northern edge of the Southern Hills in Louisiana northward through the Mississippi embayment of Tennessee, into Kentucky and westward into Arkansas and Texas, except where covered by Mississippi River alluvium. They comprise the major portion of the cuestas and lowlands of the Eastern and Western Hills.

The Neogene in the northern Gulf coast is typified by a major regressive sequence: the Miocene Catahoula and overlying Plio-Pleistocene deposits of similar facies. As in the Paleogene, stratigraphic correlations of any one formation are difficult to make over broad areas within the Gulf region due to facies changes.

Sea level changes were generally less extreme during the Neogene than the Paleogene. The basal Neogene strata, the Catahoula formation, laps onto the Paleogene only as far north as Vicksburg, Mississippi and its emerged outcrop zone is confined to the land surface within the Southern Hills. The Neogene updip lithology is principally non-marine soft sandstones and shales, which are more than 5000 ft. thick in southern Louisiana. These interfinger into a downdip, offshore sequence of marine shales. The entire sequence exceeds a thickness of 25,000 ft. in the depocenter, located on the shelf, southeast of the mouth of the Mississippi River.

The Quaternary depocenters are located at the edge of the continental shelf just south of the present mouth of the Mississippi River (15). The thickness of Quaternary strata is estimated to be approximately 12,000 ft. (16). The sediments at the depocenter are alternating neritic (shelf) hard clays and silts and littoral (shoreline) dense sands and hard silts and clays, the latter corresponding to glacial maximum (17)(18). Gulfward of the depocenter, turbidity currents transported clays into the area of the Mississippi trench and cone, and off the slope to the abyssal continental rise.

The marine sands and clays grade shoreward from the depocenter into shallower marine facies and then to continental facies. These diverse sediments represent the same transgressive and regressive glacial stages and crop out in what has been called coastwise terraces. The terraces are alluvial surfaces which were active during interglacial deltaic advances. Each terrace represents a variety of sediments, generally deltaic toward the coast, grading to fluvial further inland.

Four Pleistocene coastal surfaces have traditionally been identified and their names have also been applied stratigraphically to the subsurface formations which were thought to be of equivalent age. These are, starting with the oldest: Williana, Bently, Montgomery and Prairie (1), (19), (20). Their equivalents were correlated into the subsurface of the Mississippi delta area where the "upper marine beds" were identified as Aftonian or Williana (1)(18). Subsequent revisions have recognized the oldest terrace as Citronelle (preglacial Plio-Pleistocene in age) (21)(22), and similarly placed the base of the upper marine beds in the upper Pliocene (16). The most extensive post Citronelle coastwise terrace is the coastwise Prairie or Port Hickey which is late Pleistocene in age, 75,000 to 100,000 years old. Its oxidized surface dips gulfward beneath recent sediments.

The northern Gulf has been in an interglacial period, with sea level at approximately its present level during the last 5000 years. Sedimentation has dominated subsidence in the Mississippi delta and the shoreline has been extended southward to the very edge of the continental shelf by means of a sequential series of seven delta systems (see Figure 2.5-4). The deltaic sediments consist of irregularly distributed organic clays, silts and fine sands, which vary in thickness from a few feet in the northern delta, to over 700 ft. at the present Mississippi River mouth (23).

2.5.1.1.4 Structural Geology

Opinions concerning the origin of the Gulf oceanic basin are divided between belief that: (1) it has existed as an oceanic basin since Precambrian (4), (2) it may be a product of oceanization, (3) it may be due to polymorphic phase changes in the crust, or (4) the Gulf is the product of late Paleozoic, post Ouachita, or early Mesozic seafloor spreading (3), (5), (7). By whichever cause, geophysical studies have shown that continental crust underlies the Gulf Coastal Plain generally north of the location of the Cretaceous (Stuart City) reef and oceanic crust is present south of the reef (5)(9). Structural features within the Gulf Coastal Plain have developed from adjustments within the crust and in the stratigraphic sequence above this crustal framework. This discussion will cover the major structural features of the Gulf Coastal Plain, the areas surrounding the Gulf Coastal Plain and the northern Gulf of Mexico. Figure 2.5-10 is a regional structure map showing the locations of the major structural features of these areas.

a) Structural Features Surrounding the Gulf Coastal Plain

The Ouachita orogenic belt is a complexly deformed zone which was formed by intense northward compressional forces more than 230 MYBP. The gulfward portion of the orogene consists of several overthrust sheets composed of tightly folded, metamorphosed, Paleozoic sediments. During the orogeny, these sheets were thrust from south to north and broken by high angle reverse faults and cross faults. The southern boundary of the area affected by the Ouachita orogeny probably corresponds to the position of the peripheral faults along the hingeline flexures, which were developed in sediments during Jurassic through Tertiary. The northern portion of the orogenic belt consists of the Arkoma and Black Warrior basins, which are east-west trending folds gradually decreasing in amplitude northward (6). The Ozark uplift, the Pascola arch and the Nashville dome form a preorogenic trend north of the Ouachita orogenic belt (24).

Data from deep wells allows the extension of the Ouachita orogene south-eastward beneath coastal plain sediments to a point within 50 miles of the proven southwestward extension of the Appalachian trend. Geophysical data are inadequate to determine the relationship of the two orogenic trends at their projected junction (7). To the southwest, the orogene is overlapped by Cretaceous sediments, but is probably continuous to the Marathon Mountain region of southwest Texas.

The southern Appalachians generally consist of Paleozoic and Precambrian rocks which were metamorphosed, folded and faulted during late Paleozoic. On the northwestern side, the rocks consist of folded and faulted sediments. On the southeastern side, they consist of intensely deformed metamorphic and intrusive rocks. With the exception of unfaulted plateaus on the northern edge, southwest-northeast trending faults, overthrust to the northwest, occur throughout the Appalachian system. These trends extend into the subsurface in southwest Alabama, where subsurface data for their further continuation are unavailable.

The New Madrid zone is located north of and beneath the northern end of the Mississippi embayment within Illinois, Missouri, Kentucky, Tennessee and Arkansas. This area consists of a series of generally northeast-southwest trading faults which displace sediments as young as Pleistocene. Subsurface data show that some faults of this system extend across the northwest-southeast trending Pascola arch in northeastern Arkansas and northwestern Tennessee. Recent seismic studies, however, show that the faults do not enter the Arkoma basin of north-central Arkansas, where the basin is in part buried beneath sediments of the Mississippi embayment but rather die out north of Memphis, Tennessee (25). There is no indication of the New Madrid tectonic activity south of the northern boundary of the Ouachita orogene.

b) Non-Geosynclinal Structural Deformation within the Gulf Coastal Plain

Postorogenic (since 230 MYBP) structural deformation within the Gulf Coastal Plain has taken the form of hingeline faulting around the periphery of the Gulf basin and epeirogenic or more localized uplift and downwarp. Broad regional uplift occurred during the Triassic period and regional depression or downwarp began in late Jurassic.

Cretaceous (135 MYBP) crustal depression is attributed to gravitational adjustment of the crust due to the weight of extensive carbonate sequences around the margin of the Gulf. Crustal adjustments of a lesser regional magnitude have continued under the influence of Cenozoic sediment accumulations. The result of this depression is that oceanic crust beneath the Gulf is about 18,000 ft. deeper than oceanic crust beneath the Atlantic Ocean (5).

Faulting along the gulfward margin of the Ouachita belt, possibly due to relaxation of orogenic compressional forces, began in late Triassic (181 MYBP) with the formation of a block faulted graben in southern Arkansas, resulting in displacements of several thousand feet. The southern fault boundary of the block faulted graben is located in northeastern Louisiana. It is less well defined than the northern fault because of sparse subsurface data (8).

Along the gulfward margin of the southward concave Ouachita orogene, an extensive system of enechelon grabens developed along the hingeline, displacing strata from upper Jurassic (135 MYBP) to Quaternary (2 MYBP). Fault systems along this trend include the Balcones, Mexia-Talco, South Arkansas, Phillips, Pickens and Gilbertown-Pollard faults (Figure 2.5-10). Maximum displacements along this fault zone range between 1500 to 2000 ft. (See References 6, 11 and 12). Activation of faulting along this trend, which began during the Jurassic period and terminated at the end of Tertiary (2 MYBP), has been related to basinward flexing, hinging at this fault zone. The movement may be due to several causes, with the dominant cause possibly varying in different portions of the fault zone. Initial movements may have been related to relaxation of orogenic compressional forces, later accompanied or replaced by collapse or down-warping of the Gulf sedimentary basin (6). Salt mobilization and movement gulfward from the inner margin of the Mississippi salt basin has been related to graben collapse along the Gilbertown-Pollard fault system (10) and beneath the Talco graben, in the East Texas basin (12). Well data showing stratigraphic thickening on the downthrown block and increased displacement with depth in several locations along the graben trend, suggest that recurrent or continuous faulting occurred over a long period of time and was at least partially contemporaneous with deposition (6) (12) . Other Tertiary age faults occur on the periphery of the Sabine uplift (Rodessa and Fisher faults) and the southern end of the East Texas basin (Mt. Enterprise fault).

The Sabine, Monroe-Sharkey uplifts, the Jackson dome, the Mississippi and East Texas embayments and the North Louisiana syncline (North Louisiana salt basin) were enhanced by mid-Cretaceous structural warping. The Sabine uplift, East Texas basin and possibly others, were in existence prior to this warping, but their present form was more or less determined by it.

The Sabine uplift is a broad, domal uplift underlain by a basement high. The basement high is pre-Jurassic, but the local structures on the dome are probably related to Cretaceous or younger warping. The development of the Monroe-Sharkey uplift and the Jackson dome was initiated by Cretaceous warping and was modified by igneous intrusion (6). These features are evident as positive anomalies on the regional Bouguer gravity anomaly map (Figure 2.5-11).

The negative areas developed or rejuvenated by Cretaceous structural warping are the Mississippi and East Texas embayments and the North Louisiana syncline. These are similar depressed areas and are directly related to surrounding structural highs. Except for the Mississippi embayment, the development of structural features in these areas is related to mobilization of Jurassic salt. This mechanism will be discussed later in this section.

c) Structural Features Associated with the Development of the Gulf Geosyncline

Salt structures exist above the salt basins in the southern portion of the Gulf Coastal Plain, which are shown on Figure 2.5-8. These structures were mainly developed during the Tertiary (65 to 2 MYBP). Salt structures similar to those which exist in the interior salt basins are presently developing offshore beneath the continental slope about 140 miles south of the site.

Salt movement under the influence of sediment accumulation in the geosyncline is depicted by Figure 2.5-9. Downdip lateral movement of salt into the Mississippi and East Texas salt basins was related to faulting above the margin along the Gilbertown-Pollard and the Mexia-Talco fault zones respectively (10) (12) . Lateral salt movement into the Gulf basin has created the Sigsbee escarpment, the leading edge of a huge salt wedge (Figure 2.5-3).

Vertical movement is responsible for the development of salt domes, ridges, and other such features. The presence of irregularities in the salt, or in the sediments above or below, combined with the density imbalance between salt and denser overlying sediments, initiates vertical movement of the salt, deforming the sedimentary strata. Motion is sustained through geologic time by continued sedimentary loading. Two types of salt domes develop under these conditions, piercement domes and deep-seated, non-piercement domes. During the development of piercement domes, periods of slow sedimentation or erosion and resulting weight imbalance allow the salt to rise to a position of isostatic equilibrium. At this point, the dome may be near enough to the surface to create a topographic high over which surface erosion prevails. Unconformable contacts between the sediments and the salt will develop if the process of vertical motion, quiescence, and erosion is repeated many times. When the rate and volume of sedimentation becomes great enough that the salt motion will no longer keep pace, the dome becomes buried beneath sediments, sometimes thousands of feet thick. The movement of the dome ceases as the basal or source layer salt is depleted and the dome and sediments react to isostatic balance (26). Development of piercement salt domes are most common in the salt dome basins. Deep seated domes are located along the periphery of the basin where basal salt supply is thinner. Active development of domes is occurring gulfward of the geosynclinal axis, on the continental slope (Figure 2.5-9). Salt movements been estimated to be a maximum of about one foot per 100 years (27).

Development of salt domes may cause the formation of localized complex systems of normal faults which often cause graben development in the sedimentary strata above the dome. The arching of overlying sediments, causes shearing and fracturing of the deformed strata. Development of secondary or complementary faults occurs as stress continues to increase during salt uplift. Salt piercement drags adjacent beds upward, imposing dips approaching vertical along the flanks of the dome.

→(DRN 01-464; 02-217)

In contrast to localized salt dome faulting, regional faulting in the Gulf CoastalPlain is in the form of a series of an echelon, concave gulfward fault trends known as contemporaneous faults or growth faults. Faults of this type are located within the Texas Louisiana coastal salt basin in southern Louisiana and coastal Texas, south of the Cretaceous reef trend, and offshore from these areas. The position and period of activity of particular growth faults is directly related to the sedimentation history of the Gulf geosyncline since the beginning of its activity. The names and locations of the growth fault systems in southern Louisiana are shown on Figure 2.5-10. The period of activity for

←(DRN 01-464; 02-217)

→(DRN 02-217)

each growth fault system is shown on Table 2.5-1. As shown on this table, the activity of the northern-most growth fault system, Bancroft, terminated prior to the Miocene (22 MYBP). The growth fault systems in the site area (Scott, Grand Chenier, and Lake Sand) all terminated during the Miocene, at least 5.5 MYBP.

←(DRN 02-217)

The axis of maximum deposition within the geosyncline generally corresponds with the position of the topographic break between the continental shelf and slope (16). The initiation of growth faulting occurs along the outer shelf, gulfward of the depocenter, where the instability of the slope causes sediments gulfward of the fault position to begin to slump. Other factors pertinent to the development of growth faults have been described (See References 16, 28, 29 and 30). In addition to slope instability, the presence of structurally weaker salt or clay is closely related to development of growth faults and may possibly be the dominant mechanism for fault initiation. Growth faults, once initiated, are perpetuated by differential sediment loading across the stable and downthrown blocks. This results in the development of thicker sedimentary sequences on the downthrown fault block. The period of growth activity on a particular fault may be determined by comparing the relative increase in stratigraphic thickness across the fault for a series of correlative units. The period of maximum activity corresponds to the stratigraphic unit which increases most in thickness, and the cessation of growth faulting is indicated by the stratigraphic unit in which no thickening occurs across the fault plane (31).

A characteristic of growth faults is the development of "rollover", or reversal of dip toward the fault plane, in the downthrown block. Apparent reversals of dip are due to rotational slumping of the downthrown sediment mass contemporaneous with deposition. The slumping may be associated with the development of minor complementary or antithetic faults (6) (28). The degree of rollover varies laterally and vertically along the fault, and the localized rollover anticlinal structures are sought as structural traps favorable to petroleum.

Fault movement under the influence of differential sedimentary loading is contemporaneous with deposition. For this reason, strain accumulations leading to sudden movements, generating seismic energy, do not occur. The only current slumping (growth faulting) is occurring near the continental slope, about 140 miles south of the site. Most growth faults in southern Louisiana have an average southward dip of 40 to 60 degrees, which generally increases upward and decreases downward. It is generally accepted that growth fault dips decrease with depth, to the point where they become essentially bedding plane faults or the fault may terminate within mobile salt or clay. The result of this decrease in dip is that growth fault planes are entirely within the sedimentary sequence and are not extensions of deeply buried tectonic structures within the basement.

During the Quaternary, normal faulting has occurred at the northern periphery of the Louisiana coastal salt basin, about 30 miles north of the site. These faults form escarpments due to displacement of late Pleistocene terrace surfaces and extend from the vicinity of Baton Rouge, east-southeast nearly 100 miles along the north side of the Pontchartrain basin, to the Pearl River. These faults are downthrown to the basin. They are attributed to differential compaction and gulfward tilting of the South Louisiana salt basin sedimentary mass toward the area of the thick subsiding wedge of geosynclinal sediments. Three faults have been identified north of Baton Rouge. Starting with the northernmost, they are: the Zachary, Scotlandville-Denham Springs and Baton Rouge faults (Figure 2.5-10). These faults are discussed in Subsection 2.5.3.2.

The Vacherie, Louisiana ground fissure which developed in 1943 is described in detail in Subsection 2.5.3.2.2. The causal mechanism for fissuring is local sediment consolidation and subsidence and is dissimilar to faulting. The fissure is shown on Figure 2.5-12.

d) Significance of Linears

In addition to structural features determined by surface mapping, borings, and geophysical data, structural trends have been suggested from linears observed on aerial photographs. Linear trends determined by physiographic alignments and tonal anomalies on aerial photographs were mapped by Fisk in the central Gulf Coastal Plain and assumed by him to represent fracture and fault patterns (1). These consisted of two general orientations: northeast-southwest and northwest-southeast (Figure 2.5-13). The actual known faults in the same region generally strike east-west, peripheral to the Gulf basin, and consequently contrast with the orientations that Fisk postulated.

Only one of Fisk's identified linear trends corresponds to any known structural feature or trend. Fisk's northernmost NW-SE linear appears to correspond to the position of the NW-SE extension of the Baton Rouge fault system north of Lake Pontchartrain. The significance of the Baton Rouge fault to the plant has been discussed in Subsection 2.5.3.2 of the FSAR.

The contention that such linears represent faults or even lines of accumulating strain has not been substantiated by the mass of accumulated subsurface evidence in the Gulf Coastal Plain area.

The contrasting orientations between regional linear trends and known structural trends in Louisiana forms the primary reason for discounting Fisk's linears as evidence of geologic structures. However, a detailed study of linear trends in the site area was undertaken in an attempt to correlate those trends with geologic structure. These studies are presented in Subsection 2.5.1.2.

2.5.1.2 Geology of Site and Surrounding Area

This section describes the geologic conditions at the site and within an area of about 50 square miles surrounding the site. The site consists of over 3,000 acres along the west (right descending) bank of the Mississippi River (Figure 2.5-14). The plant island is situated within the property in section 26 of Township 12 South and Range 20 East. The location of the plant island superimposed on the site topography is presented on Figure 2.5-15.

The geologic studies of the site and surrounding area were based on interpretations of geologic literature, geologic maps, topographic maps, remote sensing data, surface mapping, subsurface borings, geophysical reflection and refraction surveys, geophysical logs and laboratory tests.

2.5.1.2.1 Physiography of Site and Surrounding Area

The site and surrounding area lie within the Mississippi River deltaic plain physiographic province. The deltaic plain is described in Subsection 2.5.1.1.1 and is characterized by flat topography near sea level, with extensive areas covered by water, swamp, or marsh. In the site and surrounding area, the physiography is dominated by the present Mississippi River. The site is located on the outside or eroding bend of the river, between miles 129 and 130 AHP. At the site, the Mississippi river has a maximum depth of about 110 ft. and is 2200 ft. wide.

The site is located almost entirely upon the natural levee of the Mississippi River (Figure 2.5-16). The southernmost portion of the property, about two miles southwest of the plant site, is fresh-water swamp adjacent to the natural levee. The surface elevations of the natural levee on the property range between near sea level in the southwestern portion to about 14 ft. MSL near the river, at the base of the man-made, flood-control levee. The crest of the Mississippi River flood-control levee, which is the highest point on the site, is about +30 ft. MSL. The lowest elevations on the site occur in the swamp, at the southwestern end of the property. In this area elevations are one to two ft. above sea level. Figure 2.5-15 shows the topography of the northern portion of the property, in the vicinity of the plant island.

2.5.1.2.2 History of Site and Surrounding Area

The geologic history of the Gulf basin, including the Mississippi River deltaic plain, is discussed in Subsection 2.5.1.1.2. The deltaic plain has developed over the northern flank of the Gulf geosyncline since Tertiary (2 MYBP).

During early Jurassic (181 MYBP), several thousand feet of evaporities (Louann salt) developed above oceanic crust in the area that is now the Texas-Louisiana coastal basin, including the Mississippi River deltaic plain. From Jurassic through Paleogene (22 MYBP), deep seas existed in this area and deposited an estimated 15,000 ft. of continuous marine clays. During Cretaceous, an extensive barrier reef developed to the north along the coastal shelf edge and the surface vertical projection of this reef presently defines the northern limits of the Mississippi River deltaic plain.

Throughout Paleogene, the geosynclifial sedimentation was occurring throughout the northern Gulf with its depoaxis in coastal Texas west of the present Mississippi River deltaic plain. The geosyncline received rapid sedimentation with accumulations up to 10,000 ft. in the site. At the close of Paleogene or early Neogene, the depoaxis shifted to southern Louisiana and this position has persisted until the present.

During Neogene, the area of the deltaic plain received rapid sedimentation with accumulations up to 15,000 ft. in the site area. During this rapid accumulation, the leading edge of the sediment mass was unstable. This instability resulted in basinward slumping and growth fault development. This was accompanied by mobilization of the underlying salt and marine clay. Series of growth fault systems are mapped which mark the migration of the sediment edge gulfward. The growth faults near the site are an extension of the Grand Chenier fault system, as shown on Figure 2.5-10. By early Pliocene (5 MYBP), the active areas had moved south of the present coastline. As deposition progressed southward, the landward portions of sediments became stable and deposition occurred over the previously faulted areas. As sediment load increased gulfward, hingeline flexing occurred along the northern margin of the deltaic plain, over the southern flank of Hancock ridge.

Figure 2.5-17 illustrates the Miocene and younger statigraphic sequence beneath the site.

During the Pleistocene, deltaic deposition by the Mississippi River was interrupted by several periods of sea level rise and fall associated with cyclic world-wide glaciation. The youngest Pleistocene deposit in the site area forms a firm, erratically oxidized surface (23) at approximately -40 feet MSL underlying Recent Mississippi River deposits. This surface is relatively undissected with few major entrenchments (23). The Mississippi River has scoured a channel deeply into the Pleistocene in the area and the width of this entrenchment is controlled by the amount of river migration (23). At the site the trench is about two miles wide. Elevations on the top of the Pleistocene on both sides of the trench are similar, so that correlation across the trench is certain.

The regional slope on this buried surface is approximately two feet per mile to the southeast, becoming more easterly east of the site. To the northwest this surface rises above sea level (present swamp level) and forms the emergent Pleistocene surface in Ascension Parish. The profile (Figures 2.5-30f and 2.5-30g) depicts the regular southeastward slope through this area from an elevation of +30 feet MSL in northern Ascension Parish to -60 feet MSL along the southwestern shoreline of Lake Pontchartrain.

Where the surface is exposed as a terrace in Ascension Parish, it is part of the youngest widespread coastline terrace in Louisiana, generally termed Coastwise Prairie, or alternatively, Port Hickey, Hammond or Beaumont. This surface is a deltaic plain (83) deposited during the Sangamon interglacial stage 80,000 years or more ago (84). Dissection and oxidation occurred during lowered sea level associated with the Wisconsin glacial stages. On the basis of Figure 2.5-30g and previously published contour maps (87, 23), it is our conclusion that this oxidized surface is indeed Pleistocene and correlative to the Coastwise Prairie (Port Hickey of River Bend PSAR) in the Baton Rouge area.

A 1975 study (86) of Lake Pontchartrain mapped this level throughout the Lake Pontchartrain area and northeastward to the Baton Rouge fault zone on the northeast margin of the Lake. This study also recognized an older, deeper oxidized layer. Both layers are present in the subsurface on the south side of the Baton Rouge fault zone, northeast of Lake Pontchartrain. The study (86) consequently discussed the alternate possibilities that the emergent Prairie on the upthrown, north side of the fault correlates with the upper or lower oxidized layer on the buried downthrown side. A correlation to the upper layer indicates a fault displacement of less than 10 feet and confirms our identification of this surface as Coastwise Prairie in the Waterford site area. In this case, the lower, oxidized layer possibly represents an older interglacial surface.

A correlation to the lower level would indicate a fault displacement of approximately 55 feet and require the upper oxidized layer south of this fault to represent a younger surface, possibly Deweyville, as suggested by Kolb et al.(86). Such a correlation would also signify that the oxidized layer at Waterford is also Deweyville. If so, however, the evidence presented on Figure 2.5-30g is contradicted.

Other reasons for doubting the validity of this alternate interpretation include:

a) The general geology of the area depicted on Plate 2 of the 1975 study (86), displays Prairie terrace on both the upthrown and downthrown sides of most of the individual faults of the Baton Rouge fault system. Throws of less than 20 feet are thus indicated. The 55 foot displacement required if the upper oxidized level is to be designated Deweyville, is much greater than recognized elsewhere on the surface along the entire trend of the Baton Rouge fault system in Southeastern Louisiana.

b) The specific fault south of Slidell, Louisiana along which this large displacement is postulated, has outcropping Prairie above sea level on its downthrown side both to the east and to the west along the fault as depicted on Plate 2 (86). The occurrence to the east is especially noteworthy because the Prairie surface extends approximately three miles southwest of the fault as a peninsula surrounded by recent deposits. To account for the throw on the fault in this area being less than 10 feet, whereas it would be 55 feet further west, a north northwest - south southeast problematic branch fault has been depicted. This is an anomalous orientation to the usual west northwest - east southeast trend of the faults in the area. Furthermore, a similar branch fault would also be required, but is not depicted on the west side of the area of postulated 55 foot throw for the same reason.

c) The Deweyville terrace depicted on Plate 2(86) is a fluviatile terrace associated with the Pearl River. While its coastwise equivalent undoubtedly occurs somewhere Gulfward from that point, it is difficult to account for it being present under such a widespread area long the north shore of Lake Pontchartrain and yet being separated from the Pearl River occurrence by the southward extending Prairie peninsula as mapped northeast of the lake.

Post-glacial deltaic deposition by the Mississippi River began with the Sale-Cypremort delta system about 5500 years ago. Between that time and the present, the surface geology of the site area has developed under the deposition, subsidence, and erosion associated with the formation and eventual abandonment of the several delta systems of the Mississippi River. Figure 2.5-4 shows the area affected by each delta system. Deltaic deposition is represented at the site by about 50 ft. of unconsolidated alluvial deposits described as soft clays and silty clays with occasional sand lenses or pockets, which unconformably overlie the Pleistocene Prairie formation.

2.5.1.2.3 Geologic Structure of Site and Surrounding Area

The site and surrounding area lie above the north flank of the Gulf geosyncline. The Gulf geosyncline has been at its present position since early Miocene (22 MYBP) and its axis is located south of the site. The north flank of the geosyncline is a broad east-west trending regional structure which dips to the south at about three degrees (32). Continued downwarping of the Gulf geosyncline since Miocene has resulted in the gulfward thickening of sediments producing this attitude within the sedimentary sequences. The geosyncline is not related to structural features within the deltaic plain.

The geologic structures which exist near the site were developed in thick sedimentary sequences during Neogene. They consist of non-tectonic structures associated with salt and clay mobilization and growth faults associated with sediment instability at the shelf edge.

The mechanisms for these structures are discussed in Subsection 2.5.1.1.4.

Faulting in the site and surrounding area was thoroughly investigated by analyzing existing subsurface data, including the spontaneous potential and resistivity logs of 151 oil wells; the records of ten deep seismic reflection lines; and the analysis of various published and unpublished geologic maps. The locations of oil wells used in this analysis are shown on Figure 2.5-18 (see Table 2.5-2 for the oil wells used in this study). Aerial photography interpretation techniques were utilized to identify any surface features which could be manifestations of subsurface structures.

Analysis of the electric logs of the oil wells allowed the identification of several continuous (across the site area) and correlatable marker horizons. Figure 2.5-17 presents an example log showing these marker horizons. Based on these correlations, several graphic interpretations were derived. The plan locations of the sedimentary structures near the site are shown on Figures 2.5-19 through 2.5-24. Figures 2.5-25, 26, 27, 27a, and 27b are geologic sections drawn through selected oil wells to show buried structures and the attitude of bedding. The structures within five miles of the site include the west flank of the Good Hope salt dome and its associated faulting and seven growth faults which are a portion of the fault trend designated as the Grand Chenier fault system in western Louisiana.

The nearest salt dome to the site is the Good Hope dome which is centered about six miles east of the site. It is a piercement type salt dome buried by 9580 ft. of Miocene and younger sediments. The sediments overlying the dome were uplifted and faulted by the rising salt mass during the period of its development. Salt dome uplift ceased during the Miocene epoch (5.5 to 22.5 MYBP). These faults are shown on Figures 2.5-19, 2.5-23, and 2.5-24. Active petroleum production is occurring from numerous wells drilled in the uplifted and faulted dome.

The development of growth faults has been discussed in Subsection 2.5.1.1.4. The relationship of the site to the Cenozoic growth fault systems is shown on Figure 2.5-10. The site is located along the eastward extension of the Grand Chenier fault system. This system is related to thickening of upper Miocene strata in the downthrown block (6). Three faults related to this system are shown on Figure 2.5-27. Faults of the Scott and Lake Sand fault systems lie about 10 miles north and 15 miles south of the site, respectively.

Fault zone 3 (Figure 2.5-19), the northernmost growth fault is 4.5 miles north of the Waterford site and trends in an easterly direction for approximately 1.7 miles at a depth of about 9,000 feet, causing sediments to be downthrown to the south. Missing stratigraphic sections, which occur in wells 98, 99, 107 and 103 are the evidence for this fault. The maximum fault displacement is 70 feet in well 99. Cross sections D and E (Figures 2.5-27a and 2.5-27b) indicate that there is no evidence for the fault above a depth of 8,000 feet, indicating that faulting apparently ceased in the middle Miocene, about 14 MYBP.

Fault Zone 4 (Figure 2.5-19) is located approximately 3.5 miles north of the Waterford site and trends in an easterly direction for approximately 1.6 miles at a depth of about 9,000 feet. Missing stratigraphic sections, which occur in wells 96 and 108 indicate that the sediments have been downthrown to the south. The maximum displacement is 130 feet in well 96. Cross Sections D and E, (Figure 2.5-27a and 2.5-27b) indicate that there is no evidence for the fault above a depth of about 8,000 feet, indicating that faulting ceased in the middle Miocene, about 14 MYBP.

The Norco fault, (Figure 2.5-19) is generally described as a Miocene growth fault which strikes east-west in the site vicinity and overall is slightly concave gulfward. This fault is named for the Norco field, where gas and oil have been produced from a rollover structure on the downthrown block of the fault. The average dip of the fault plane is 47 degrees to the south. Correlation of oil well electric log signature indicates that the stratigraphic displacement decreases from about 150 ft. at a depth of 9500 ft. to about 10 ft. at 6000 ft. deep. The fault terminates upward at a depth slightly shallower than -6000 ft. MSL. According to Thorsen (33), the period of maximum activity of this fault occurred during early to middle Miocene. In addition, Thorsen shows that faulting essentially ceased, during middle Miocene, about 14 MYBP. Studies performed to date the cessation of faulting in the site area determined that the paleontological marker fossils Rangia cuneata and Rangia johnsoni occur at about -4900 ft. MSL in the site area. These fossils are indicative of the top of Miocene sediments.

This correlation indicates that growth faulting which is contemporaneous with sediment deposition ceased prior to the deposition of the upper 1000 ft. of Miocene sediments. Faulting ceased at least 5.5 MYBP and possibly more than 14 MYBP.

To the east, the Norco fault is joined by a smaller growth fault and at least one fault associated with the Good Hope salt dome. The small growth fault strikes north-northwestward and dips to the west-southwest at about 52 degrees. This fault plane appears to bend around the western flank of the salt dome and may have formed, at least in part, due to uplift of the Good Hope dome. Displacement across the fault is about 150 ft. at 9500 ft. deep. Figure 2.5-23 shows that the fault is not present at a depth of 6000 ft. Activity on this Norco splay fault probably ceased at the same time as did activity on the Norco fault.

Fault 2B (Figure 2.5-19) joins the Norco fault and is directly related to movement of the Good Hope dome. This fault is a normal fault striking northwestward and dipping at about 37 degrees to the northeast. The cause of faulting in this case is not the gulfward slumping associated with growth fault development. This fault occurred as an adjustment to the rising domal salt mass during the Miocene when the salt dome formed. The fault terminates upward between 4500 and 6000 ft. deep. This termination depth is beneath the previously described early Miocene paleontological markers and indicates cessation of activity during the Miocene.

Another normal fault related to movement of Good Hope dome, Fault 2C (Figure 2.5-19), strikes in a north-northeasterly direction and dips to the east-southeast and has a maximum displacement of 680 feet near the center of the dome. Fault 2B intersects fault 2C and they correspond to faulting related to salt movement mapped by Smith.(89)

A second growth fault, Fault "B" occurs 1.5 to three miles south of the Norco fault. Fault "B" is present in the subsurface beneath the site. It is a slightly undulating, but generally gulfward concave growth fault which strikes from east-west to west-northwest in the immediate site vicinity. It dips southward at between 47 and 50 degrees. The interpreted maximum displacements on the fault are 150 ft. at 10,000 ft. deep and 120 at 6300 ft. Structural contours on electric log marker horizon three (Figure 2.5-22) show no indication of faulting at about 4800 ft. deep. The fault, therefore, terminates upward between 6300 and 4800 ft. deep, probably near 5000 ft. deep. The paleontological marker fossils Rangia cuneata and Rangia johnsoni occur above the top of faulting. This relationship indicates that activity on Fault "B" ceased prior to 5.5 MYBP and the fault has subsequently been buried by 5000 or more feet of post-Miocene sediments.

Fault "C" is the southernmost growth fault in the site area. It has an undulating fault plane which is generally concave, gulfward. To the east, Fault "C" parallels Fault "B" at a distance of one to two miles south. A small, deeply buried growth fault connects Faults "B" and "C" at a location just east of the site. To the west, Fault "C" branches, one limb bending northwestward to join Fault "B", the other trending southwestward out of the site area.

Fault "C" dips southward at about 47 degrees. The displacement on Fault "C" is 350 ft. at 10,500 ft. deep. It decreases to 160 ft. at 6600 ft. deep and the fault is absent at 5100 ft. The fault terminates upward between 6600 and 5100 ft. deep. This depth of burial indicates that fault activity ceased about 5.5 MYBP, based on the paleontological marker fossils Rangia cuneata and Rangia johnsoni which occur at about 5300 ft.

The small fault which connects Faults "B" and "C" strikes north-northwest and dips to the southwest at about 47 degrees. Its length, at 10,000 ft. deep is about one mile. At 10,000 ft. there is about a 50 ft. displacement. The fault is not present at 6500 ft. deep. The upward termination of the fault is probably buried by 9000 ft. of middle Miocene and younger sediments. Cessation of fault activity occurred much more than 5.5 MYBP.

Correlation of electric log marker horizons indicates that late Miocene and younger sediments (above the top of faulting) in the site area are flat to gently undulating with a gentle southward dip of about one degree. The sediments above the Good Hope dome and the Norco and Lucy oil field rollover structures (Figures 2.5-20 through 2.5-22) are the only significant variances from this general structural trend. These are localized structures and their influence on overlying stratigraphy diminishes toward the surface.

The geologic structure of the upper 500 ft. of sediments within the site boundaries is characterized by nearly flat lying sediments which can be traced laterally by stratigraphic horizons. The continuity of these horizons has been confirmed by electric log signatures and lithologic identity. The simplicity of the structure at the site is shown by geologic cross sections shown in Figures 2.5-28 and 2.5-29. Structural contours on three Pleistocene aquifers, the Gramercy, Norco, and Gonzales-New Orleans , also illustrate that the sediments dip gently with minor undulations and no faulting.

The excavation for the Waterford 3 seismic Category I structural mat was cut 60 ft. deep to approximately elevation -48 ft. MSL. The excavation, which exposed the upper several feet of the Pleistocene Prairie formation over an area 380 ft. by 267 ft. was mapped in detail (Figure 2.5-30). In the excavation, the Prairie formation at foundation level consists of horizontally bedded layers of silts and clays. The conditions encountered compare very favorable with the data taken from site borings. Mapping of the excavation disclosed no anomalies or discontinuities which might indicate conditions which could adversely affect the integrity of the foundation materials.

In performing the geologic studies of the site and surrounding areas, various forms of remote sensing data were utilized to supplement surface and subsurface data. The purpose of this analysis was to aid in the interpretation of depositional history of this portion of the Mississippi River Deltaic plain and to determine if surficial expression exists for any of the deep underlying geologic structure.

The types of remote sensing data which were used include: low-altitude black and white photographs, low-altitude color and color infrared photographs, high-altitude color infrared photographs, U. S. Air Force side-looking radar imagery, black and white and near infrared images from the ERTS satellite and color infrared photography from Skylab. Areas of specific interest were also visually examined from aircraft and on the ground.

Areas of anamolous photographic tone were common features for which an explanation was not immediately apparent. Black and white and color infrared photography was examined in the study of these areas. They were determined to be minor topographic anomalies which are accentuated by surface water conditions. Such topographic anomalies are explained as old features of deltaic deposition for which only subtle expression remains due to the combination of deltaic subsidence and man's activities. Areas of tonal anomaly are indicated on Figure 2.5-31.

Linear trends mapped by Fisk (34) in the central Gulf Coastal Plain have been discussed in Subsection 2.5.1.1.4. One of these linear trends extends through the area surrounding the site. The evidence for this linear trend is apparently the general southeastward course of the Mississippi River through the site area in combination with the course of the river near its mouth. The study of remote sensing data identified several linear trends based on alignments of stream courses or deflections in stream courses.

These trends and the one mapped by Fisk are shown on Figure 2.5-31. Descriptions of the features identified by the remote sensing study are presented in Table 2.5-3.

As a basis for determining whether there is a correlation between the anomalous tones and linear trends and any subsurface structure, a structural contour map of the top of the Pleistocene in the site area has been prepared and is presented in Figure 2.5-31a. The top of the Pleistocene is a depositional surface of deltaic origin. Originally it was a relatively flat surface except for minor irregular backswamps, natural levees, etc. During Wisconsin time (10,000-15,000 BP), the surface was tilted and a lowering of sea level caused local entrenchment and local erosion. This resulted in the present day surface, which has, for the most part, been preserved.

Data for the structural contour map was obtained from nearby plants, Louisiana Highway Department, U.S. Army Corps of Engineers, and LP&L files. As Figure 2.5-31a indicates, within a five mile radius of the site, the top of Pleistocene deposits is fairly uniform except for the areas occupied by point bar deposits. Here the Pleistocene has been scoured away and replaced with recent alluvium.

As Figure 2.5-31a indicates, no geologic structure or deformation is apparent from the top of the Pleistocene. The contours of the surface of the Pleistocene show very little variation in a north-south direction where displacements would be expected if faulting were present. In a northwest-southeast direction on both sides of the site, the variation across a total distance of about eight miles is on the order of seven ft. This is representative of the regional trend in the area. Moreover, in the immediate site area, where boring control is quite good, the surface is essentially flat, ranging from about -40 to -43 ft. MSL. The contours of the Pleistocene surface correlate with Kolb's (1962) interpretation of the regional geology and his contours of the top of the Pleistocene. He has mapped large drainage swales trending southwest and east northeast away from the site. The -79 and -73 data points (Figure 2.5-31a) located southeast of the site are interpreted as being the head of the swale previously mapped by Kolb (1962).

In addition to the relatively subdued contours of the top of the Pleistocene, contours of individual strata down to about -5000 ft. show no indication of faulting (see Figures 2.5-26 and 2.5-27).

In the process of determining if there is a correlation of the anomalous tones and linear trends to any subsurface structure, the tonal anomalies and linear trends shown in Figure 2.5-31 were compared to fault surfaces in the site area shown in Figure 2.5-19. This comparison indicated that the anomalous tones and linear trends are not related to subsurface structure.

The tonal anomalies noted in the site area are substantially different from those visible along the Baton Rouge fault system, located some 30 miles north of the site. Here the topographic relief is on the order of 10 to 15 ft., whereas at the site area, topographic lows are on the order of two ft. Based on the above, we conclude there is no relationship between the tonal anomalies noted in the aerial photos and geologic structure located 5000 ft. or deeper.

2.5.1.2.4 Stratigraphy of the Site and Surrounding Area

It is estimated that the normal position of the Louann salt formation occurs at a depth of at least 40,000 ft. beneath the site (9) (35). Continuous marine shales overlie the Louann extending upward to a depth of about 10,500 ft. The marine shales range in age from upper Jurassic to middle Miocene.

In the area near the site, petroleum test wells have penetrated the upper 11,000 ft. of sediments, as shown on Figure 2.5-17. These test wells have encountered shale alternating with thin sandstone layers between depths of 10,500 and 7,500 ft., overlain by massive sandstone interbedded with scales which extend upward to a depth of 4,900 ft. The top of the Miocene at the site is indefinite, but probably occurs at a depth of about 4,900 ft. The overlying Pliocene sediments are about 3,000 ft. thick.

Lithologically, they are similar to the Miocene sediments, consisting mainly of clays and relatively thin sand layers.

Above the top of Pliocene beds, sediments from about 1,900 to 1,100 ft. deep are classified as Plio-Pleistocene (36) (37) . The Plio-Pleistocene deposits consist of interbedded sands and clays, probably representing nearshore marine and marine depositional environments. The Plio-Pleistocene deposits make up the Citronelle formation. Above the Citronelle, Pleistocene sands and clays continue to a depth of about 50 ft. At the site, the Pleistocene sands include the Gramercy, Norco, and Gonzales - New Orleans aquifers which are discussed in detail in Subsection 2.4.13.1.2. These aquifers occur at 210, 335, and 610 ft. deep, respectively, beneath the site and are 100, 125, and 250 ft. thick. Recent deltaic organic clay and silty clays overlie the Pleistocene.

To investigate the stratigraphy and engineering properties of the upper 500 ft. of

→ (DRN 01-360)

materials, a total of 74 soil borings have been drilled within the immediate plant site. The drilling was carried out by the Eustis Engineering Company, New Orleans, Louisiana and the testing by Eustis and Law Engineering. The locations of borings are shown on Figure 2.5-33. At selected boring locations, electric and gamma logging were performed by Schlumberger Well Services for geologic correlative purposes. These electric logs are presented as Figures 2.5-32(a) through 2.5-32(f). Figures 2.5-32(a) through 2.5-32(f) are classified as historical pursuant to Waterford 3 Site Procedure W4.504 and Nuclear Energy Institute (NEI) 98-03. The figures have been physically removed from the UFSAR. However, the figures are incorporated by reference, and thus they continue to be a part of the UFSAR. These figures are available for reference and use in Document Control, and they may be found as record ER-W3-01-0268-00-00 / DRN 01-360. Five refraction lines were run at the site by Law Engineering to aid in investigating shallow subsurface conditions. Figure 2.5-33 shows the locations of these lines and Figure 2.5-34 presents typical selected portions of the data. Figures 2.5-35 through 2.5-38 are cross sections showing the interpreted velocity interfaces.

← (DRN 01-360)

The geologic conditions of the upper 500 ft., which is the deepest penetration of the site borings, are presented by geologic cross sections, Figures 2.5-28 and 2.5-29. The units defined by the borings are described in the following subsections. The elevations of the various strata vary across the site. Therefore, the elevations and thicknesses described below are representative of the plant island, unless otherwise noted.

→(DRN 01-464)

The upper 50 ft. of materials are recent alluvial deposits described as soft clays and silty clays with occasional sand lenses or pockets. At approximately 50 ft. of depth, or elevation -40 ft. MSL, and extending to great depths, there is a marked change in soil strata indicating the top of the Pleistocene soils. The upper part of these soils are stiff, gray and tan clays with occasional silt lenses. These clays extend to about elevation -320 ft. MSL and contain only two significant and continuous silty sand strata. One is from about elevation -77 ft. MSL to elevation -92 ft. MSL. These silty sands are dense to very dense as indicated by high standard penetration test results. The stratum below the stiff clays from elevation -320 ft. MSL to at least elevation -500 ft. MSL (the deepest elevation penetrated), is a very dense gray silty sand.

←(DRN 01-464)

2.5.1.2.5 Engineering Significance of Site Geologic Features

Detailed descriptions of the soil types encountered by the site boring program and the engineering properties of these soils as determined by detailed laboratory testing are discussed in Subsection 2.5.4.2.

The dynamic behavior of material beneath the site during prior earthquakes is discussed in Subsection 2.5.2.1.3.

Subsection 2.5.1.2.3 discusses all structural features beneath the site which might be considered as possible structural weaknesses. No zones of alteration or irregular weathering exist in the site area.

Over 40,000 ft. of mostly unconsolidated sediments lie above the crystalline basement rock beneath the site. No unrelieved residual stresses exist in the unconsolidated foundation materials.

No materials exist at the site which could be unstable due to their mineralogy. Subsection 2.5.4.2 discusses the physical properties of the foundation materials and addresses their stability.

Subsection 2.5.1.3 discusses the effects of man's activities in the site area.

2.5.1.3 Mineral Exploitation and Geologic Subsidence

The southern Gulf Coast Plain is an area of extensive petroleum reserves and withdrawals. Major petroleum exploitation is being accomplished in the Texas Louisiana Coastal basin in association with salt structures and growth faults. Petroleum production and potential in areas surrounding the site are discussed in Subsection 2.5.1.3.1.

In the deltaic plain, subsidence is recognized by correlating the age of marker beds with depth, by submerged geologic features recognizable on remote sensing data, and by precise surface level nets. Regional subsidence, which is occurring, is attributed to: (1) crustal depression as a result of increased sediment load and (2) compaction of thick sequences of sediments. Superimposed on regional subsidence are isolated subsidence effects resulting from man's activities, specifically fluid withdrawals from shallow depths. Subsidence mechanisms are discussed in Subsection 2.5.1.3.3.

2.5.1.3.1 Petroleum Production

Numerous oil and gas test wells have been drilled in the site area. The majority of these wells were dry and never in production. Figure 2.5-18 shows wells which have been drilled near the site and indicates wells which were never produced or produced and later abandoned and those which remain in production. Figure 2.5-39 shows wells or fields in the site area which have been productive.

The nearest petroleum production to the site was from the Union of California #1 Milliken and Farwell well. This oil well is about one-half mile west of the site and is located on a low relief anticline. It was drilled in 1946 and abandoned in 1947. Several other wells were drilled in this, area but were not producers.

The Taft field is also on a low relief anticline, located about two miles southeast of the site. This field had one gas well which was drilled in 1957 and plugged in 1960. No production was recorded.

The Lucy field is three miles west of the site and presently has five gas wells producing from Upper Miocene sands. These wells appear also to be located on a low relief anticline, probably a rollover structure on the downthrown block of the Norco fault.

The Norco field is located northeast of the site along the subsurface Norco fault which was investigated by Thorsen (31) and is discussed in Subsection 2.5.1.2.4. One oil well and five gas wells were drilled at this field. The oil well and two gas wells have been abandoned. Three gas wells are still producing. The closest producer is located about two miles northeast of the site.

The Lac Des Allemandes field is located about five miles south-southwest of the site. The field consists of one oil and seven gas wells which were drilled in 1955. These wells produce from a rollover structure on east-west subsurface faults.

The largest producing fields near the site are the Good Hope field, centered six miles east of the site, and the Paradis field, 10 miles south of the site. Good Hope, discovered in 1944, now has 43 oil wells and one gas well producing from Miocene deposits. Paradis, discovered in 1939, has 64 producing oil wells and 47 gas wells. Both these fields are located on known salt domes.

2.5.1.3.2 Future Petroleum Production Near the Site

The possibility of petroleum production from the Middle Tertiary sands, which comprise the producing horizons at other fields in the area, has been tested by six wells drilled within one mile of the plant island. One of these, the Union of California #1 Milliken and Farwell, completed in 1946, produced 4,021 barrels of oil and 1313 million cubic ft. of casing head gas from a depth of 8770-8785 ft. before being abandoned the following year.

The closest well to the site is the Union of California #2 Milliken and Farwell drilled to 9934 ft. in 1946, about 400 ft. east of the plant island. The deepest of the six nearby tests, the Shell #1 Milliken and Farwell, was drilled to 11,003 ft. in 1953, about 1000 ft. northwest of the plant island. At that depth, this well terminated in the base of the Middle Tertiary sand sequence without encountering abnormal pressures.

The two deepest wells in the adjacent area provide definitive information on the base of the Middle Tertiary sands and the underlying occurrence of thick Middle Tertiary shales:

Well	Location From Site	Depth (ft.)	Deepest Sand (ft.)	Penetration of Underlying Shale (ft.)
Hawthorne & Union of Texas #1 Camille Roussel	7 mi. WNW	13,431	11,190	2241
Sunray DX #1 St. Charles School Board	4 mi. SW	14,508	12,250	2258

From these data, it is concluded that all sands at the site shallower than 14,000 ft. have been tested.

Deeper horizons that conceivably could prove productive of petroleum in the site area are the Lower Tertiary Wilcox formation and the Middle Cretaceous Lower Tuscaloosa-Duntzler formations. These are regressive sand sequences that contain productive sands along the margins of the Gulf Basin, but their sand facies may possibly extend basinward beneath the site. The nearest Wilcox production is 50 miles to the northwest in Alsen Field, East Baton Rouge Parish below 10,000 ft. The nearest lower Tuscaloosa-Dantzler production is 60 miles ENE in Ansley field, Hancock County, Mississippi also below 10,000 ft.

Only two wells, approximately on depositional strike with the site, were drilled sufficiently deep to test the Wilcox formation. These are fifty miles to the east in Lake Borgne. One of these, the Placid #1 State Lease 5407 well, holds the Louisiana depth record of 25,600 ft. It penetrated the Tuscaloosa-Dantzler sequence and bottomed in a 3500 foot shale sequence. Using equivalent isopachs beneath the "Het" paleontological horizon, the Wilcox would be present at 13,580 ft. and the lower Tuscaloosa at 16,900 ft. in the site area. Potential production from these horizons would be too deep to experience compaction associated with fluid withdrawal.

2.5.1.3.3 Regional Subsidence

Various authors have attributed the subsidence of the geosyncline to several mechanisms acting independently or in combination: (1) preexisting isostatic inequilibrium, (2) sediment loading and attendant isostatic adjustments, (3) variations in underlying crust, (4) lateral sub-crustal thinning, (5) phase changes at the crustmantle interface and (6) lateral salt migration (see References 6, 9, 15, 38, and 39). Subsidence of geosynclinal proportions began in the Cenozoic, probably related to the movement of depocenters southward, off the more bouyant continental crust, onto oceanic crust. The location of maximum crustal depression of the geosyncline has varied with the geosyncline depocenter location as it moved from coastal Texas to the Louisiana shelf edge. Crustal subsidence beneath the sedimentary sequence in southern Louisiana is estimated at about 12,000 ft- (Figure 2.5-5). Regional subsidence due to crustal downwarping is a very broad, long-term phenomenon which could not be detected over a distance of several miles or within a few hundred years. Consequently, subsidence from this mechanism would not directly affect any individual structure or site.

In addition to general basin subsidence, sediment compaction is a significant source of subsidence in the Gulf coastal area. Several mechanisms affect sediment compaction., however, the dominant mechanism relates to porosity changes in the clay mass. Powers(40) and Burst(41) reviewed the work of numerous authors and summarize water loss and associated subsidence in two major stages:

a) Pore water and excess clay-water interlayers are removed by overburden pressure. This mechanism, though effective to a depth of about 6000 ft. is most effective in the upper few hundred feet. In this process, the water content of sediments is reduced from about 70 or 80 percent, for a typical deltaic clay, to about 30 percent.

b) Diagenesis of montmorillonite to illite and related water loss associated with potassium absorption and increased temperature of the deep burial environment. This process is generally effective within a depth range of about 6000 to 12,000 ft. Below about 12,000 ft. little dehydration effects are recognized.

Jones (42) cites that alteration of montmorillonite is initiated at a temperature of about 80°C and is effective to a temperature of about 120°C. He hypothesizes a volume change of roughly one half associated with this dehydration. Montmorillonitic clays represent about 60 to 80 percent of clay deposited in the northern Gulf during the Neogene; therefore, significant potential subsidence may be associated with dehydration and diagenesis of montmorillonite.

It is important to note that for subsidence to occur, due to either mechanism, a path for the escape of excess water must exist. Interconnected sand layers normally provide the escape route, but where one is not present, the water remains in place.

Subsidence measurements have been made over the past 30 to 40 years in the Gulf Coastal Plain. Several studies are cited below which emphasize recent subsidence in southern Louisiana. These studies, which are short term or rely on point readings, are subject to variations due to local, natural or man-induced subsidence mechanisms.

Shephard (see 144 in bibliography) indicates a rate of subsidence of 0.03 ft. per year based on data from U.S. Corps of Engineers tidal gauges in the Head of Passes, Louisiana region. Using data collected over a 12 year period (1959-1970), Swanson and Thurlow (see 147 in bibliography) report subsidence rates carrying from 0.037 to 0.143 ft. per year at five south Louisiana locations.

Figure 2.5-40 shows changes in bench mark elevations over a 26 year period (1938 to 1964) along a U.S. Coast and Geodetic Survey first-order level line, located near the Mississippi River between Baton Rouge and Head of Passes. Figure 2.5-41 shows the location of bench marks along this line.

The average subsidence rates developed from these data indicate that, in the vicinity of the site, the subsidence rate in the past 26 years has been on the order of 0.01 to 0.02 ft. per year. The higher subsidence rates recorded at stations south of the site, near Head of Passes, are in an area of present deltaic sedimentation. This rate of subsidence is of the same order of magnitude as the rates reported in previous studies cited above. More importantly, the average slope of the subsidence measurements between Baton Rouge and Head of Passes, excluding the effects of major groundwater withdrawals, is only 0.0015 ft. per mile per year. This gradient could not be detected over a single site or structure. It is concluded that regional subsidence cannot directly affect any structure or series of structures at the site.

2.5.1.3.4 Groundwater Related Subsidence

→(DRN 01-464)

Subsidence of the land surface may result when groundwater pressure is reduced by pumping as demonstrated by several case histories (16) (45) (46). The reduction in pressure can induce compaction of aquifers composed of unconsolidated and semiconsolidated alluvial sediments. Adjacent fine-grained beds of silt and clay may also be compacted by the removal of groundwater. Land subsidence depends on the subsurface lithology and on the magnitude and duration of the artesian pressure decline. Subsidence is mostly inelastic, and thus permanent.

←(DRN 01-464)

Groundwater conditions for the region and site area are discussed in detail in Subsection 2.4.13. The Gramercy, Norco, and Gonzales-New Orleans aquifers of Pleistocene age are the principal aquifers in the region. The Gramercy aquifer is not a principal aquifer in the site area, but because of the convergence area of the Gramercy and the underlying Norco aquifer, groundwater levels in the Gramercy aquifer are influenced by pumpage at Norco. The potentiometric surface of the Gramercy aquifer is shown for the site area in Figure 2.4-34. The Gramercy aquifer is not continuous in the vicinity of the site.

The Norco aquifer is the principal aquifer in the site area. The major use of the aquifer is at the Norco refinery which is about 3 miles northeast of the site. The water levels in the Norco aquifer quickly adjust to changes in pumpage because of the nearby source of recharge afforded by the large area of convergence with the overlying Gramercy aquifer. The potentiometric surface of the Norco aquifer in the site area is shown in Figure 2.4-35. As shown in Figure 2.4-36, groundwater levels in the Norco aquifer have gradually risen since 1965 as a result of the decreased usage of groundwater at the Norco refinery.

The largest groundwater consumption in the region occurs in the New Orleans area from the

Gonzales-New Orleans aquifer. The groundwater levels beneath the site are shown in Figure 2.4-37. Water levels in the Gonzales-New Orleans aquifer are not continuing to decline in the New Orleans area as observed from 1906 to 1963, but have leveled off during the period from 1968 to early 1974, and have begun to rise from late 1974 to the present.

There has been local subsidence at Norco in addition to the regional subsidence. Surveyed levels at Norco show the maximum local subsidence to be about 0.6 foot during the 26 year period from 1938 to 1964. The zone of local subsidence at Norco is "bowl shaped" with the greatest amount (0.6 foot) near the center of the area. The level data along the River show that subsidence due to pumping at Norco is limited to a one mile radius of Norco. No subsidence beyond the total (regional) subsidence was measured at the bench marks across the River from the Waterford site during the 26 year period.

A second area of concentrated groundwater withdrawal is the La Place Community which is about four miles north of the Waterford site. There has been local subsidence in the La Place area; a maximum of about 0.4 ft. during the 26 year period from 1938 to 1964. This area is also "bowl shaped" and is less than one mile in radius.

Concentrated pumping at Norco and La Place has caused localized subsidence, a maximum of which is 0.6 foot during a 26 year period. The areas which have subsided are "bowl shaped" and one mile or less in radius. There has not been any local subsidence at the site due to pumping at Norco or La Place. In addition, we understand that Norco is using more river water and less groundwater each year for operations; thus reducing the rate of localized subsidence at Norco. This is confirmed by the rising piezometric levels at Norco as shown in Figure 2.4-36. Since the Norco is the principal aquifer in the site area, subsidence due to groundwater withdrawals from other aquifers in the region is not anticipated at the site. In addition, groundwater levels in the area of largest consumption in the region (New Orleans) are no longer continuing to decline.

2.5.1.3.5 Subsidence Due to Hydrocarbon Production

Oil and gas production have long been recognized as a source of ground subsidence. However, notable subsidence above producing oil gas fields is the exception rather than the rule (47). Yerkes and Castle (43) report the results of an extensive survey of surface deformations associated with hydrocarbon-production in the United States. Twenty-six documented occurrences of subsidence associated with oil and gas production are presented by the authors, 22 occurrences in California and four in Texas. There is no reported occurrence of land subsidence due to hydrocarbon extraction in Louisiana.

a) Subsidence Mechanisms

Numerous publications address the subject of the mechanism of ground subsidence over producing oil and gas fields.

Most studies attribute subsidence to reservoir compaction. Compaction results from an increase in effective stress in the production zone, associated with the decrease in reservoir fluid concurrent with fluid extraction.(48) Allen (49) discusses two basic mechanisms most commonly considered as components of compaction: (1) compaction of unconsolidated reservoir sands and (2) compaction due to dewatering of shales (clays), interbedded with reservoir sands.

Estimates of shale compaction have been made based on the assumption that shale compaction would produce free mobile water which would show up in oil production. Gilluly and Grant (50) found that water production in the Wilmington field was minor and concluded that subsidence related to shale compaction was insignificant. Using a similar technique, D'Appolonia and Lambe (51), in their study of the Bolivar Coastal Field, concluded that shale compression accounted for between 10 and 30 percent of the total reservoir subsidence.

The ratio of reservoir compaction to overburden subsidence has also been studied and is generally considered to be greater than unity; i.e., surface subsidence generally less than compaction within the reservoir. Geertsma(47) indicates the ratio of reservoir depth to lateral extent of pressure reduction is the key parameter effecting the percent of reservoir compaction which will be expressed as surface subsidence. In contrast, Knapp and Vlis (48) suggest that the volume of reservoir compaction will be expressed by an essentially equal volume of subsidence at the surface. However, surface subsidence will be spread out over a larger area and subsidence at a given point at the surface will not necessarily be equal to the magnitude of the reservoir compaction below that point.

Studies of the general mechanism of subsidence and the relationship between reservoir compaction and surface subsidence are important considerations in an attempt to predict the magnitude and rate of subsidence due to hydrocarbon extraction. To date, attempts to accurately predict subsidence have not been very successful. This lack of success, as related to the Wilmington field at Long Beach, is summarized by D'Appolonia and Lambe . Numerous investigators made unsuccessful attempts to predict the future subsidence in this area utilizing techniques ranging from mathematical model studies, to utilization of laboratory test data, to extrapolation from past subsidence history. Based on the review of these studies, the authors conclude that: (1) curve fitting is not a reliable method of estimating future subsidence and (2) surface subsidence and fluid pressure decline data used together with one-dimensional compression theory are not adequate to define the factors controlling the magnitude and rate of future subsidence.

b) Geologic Characteristics of Oil and Gas Fields Experiencing Subsidence

Most literature on subsidence in petroleum producing areas is related to four fields where major subsidence has occurred: (1) Goose Creek, Texas (greater than three ft.), (2) Wilmington field, Long Beach (29 ft.), (3) Inglewood field, Baldwin Hills (8 to 10 ft.) and (4) Bolivar Coastal Field, Venezuela (about 11 ft.). Except for the Inglewood field, these production areas are located in coastal zones where subsidence was easily observed (due to flooding). Subsidence in inland fields may not be as readily noticed. Baldwin Hills is an obvious exception, due to the resultant failure of the Baldwin Hills reservoir.

The Goose Creek field subsidence was first discussed by Pratt and Johnson.(52) Production was from a gentle dome structure, apparently not related to salt intrusion. Oil was extracted from Pliocene-Miocene beds at depths between 1000 and 4000 ft. The production zone consisted of interbedded clays and unconsolidated sands. Field development was initiated in 1917 and subsidence was recognized almost immediately as low-lying areas began to flood. Water drive was weak and apparently solution-gas drive was a primary production mechanism.

Production in the Wilmington field started in 1936 with subsidence first recognized in 1937 and measured in 1940. Total settlements have exceeded 29 ft; however, a repressurizing program initiated in 1958 has essentially arrested significant subsidence in most of the field. The structure of the field is that of a faulted gently arched anticline. Approximately 6000 ft. of Recent to Miocene strata unconformably overlie a pre-Tertiary schist. Primary production is from the 2000 to 4000 foot depth, from Pliocene and Miocene interbedded shales and unconsolidated or poorly consolidated sands. The zone between about 3000 and 4000 ft. (comprising the upper and lower terminal zones) have contributed most of the surface subsidence. Natural-water drive in the Wilmington field is weak.

The Inglewood field (Baldwin Hills), an elongate faulted anticline, is one of several along the Newport-Inglewood uplift which has experienced subsidence. Production, initiated in 1924, is from nine zones ranging from a depth of 1000 to 10,000 ft. Interbedded soft shales and uncemented sands comprise the stratigraphic sequence. Most production is from a Pliocene sequence, the Vickers zone, between depths of 1000 and 3000 ft. The primary recovery mechanism is solution-gas drive.

Production from the Bolivar Coastal Fields, on the northeast shore of Lake Maracaibo, is from faulted, slightly tilted strata. Producing zones range in depth from 1000 to 10,000 ft. and are Cretaceous-Eocene and Miocene age. However, the Cretaceous is a poor producer and studies have shown little or no subsidence associated with production from the Eocene (indurated shales and cemented sands). Most production and associated compaction is from Miocene strata at depths of 1000 to 4500 ft. Areas of maximum subsidence coincide with areas of greatest pressure decline and thickest Miocene producing zones. Solution-gas and natural-water drive are both recovery mechanisms.

Studies of these fields, and others which have undergone subsidence to a lesser magnitude, indicate several common geologic characteristics. These include:

1) Production is from Miocene or younger deposits.

2) Production is from uncemented sand members interbedded with clay shales.

3) Reservoir depths are less than 5000 to 6000 ft. Production from deeper zones has not been associated with subsidence.

4) Significant subsidence occurs only after excess reservoir fluid pressures have been dissipated.

5) Solution gas drive, and related weak water drive, is the principal recovery mechanism - associated with rapid dissipation of excess reservoir fluid pressure.

c) Subsidence Bowl Characteristics

Limited data is available on the geometry of surface subsidence zones above the few producing oil and gas fields where vertical movements have been documented. However, where studies have been made, the area of subsidence is bowl-shaped, with contours of vertical movements following a roughly elliptical shape (51). Studies on this characteristic indicate that the outer limit of significant subsidence is closely associated with the zone of production. Yerkes and Castle (43) present data from fields where surface subsidence has been documented. In six instances, data is presented which includes both the area of maximum production and the area of subsidence. The ratio of subsidence area to production area, as determined from these cases, ranges from 1.8 to 4.4 (1.8, 2.2, 2.3, 2.6, 2.7, and 4.4). Assuming approximately circular areas of production and subsidence, the radius to the edge of the subsidence bowl would be about 1.3 to 2.1 times that of the radius to the edge of the production area.

D'Appolonia and Lambe (51) show vertical profiles through the minor axis of subsidence bowls for six fields (Goose Creek, Wilmington field, Baldwin Hills, and three fields at the Bolivar coastal complex). The slope of the subsidence is steepest at the bowl center and flattens toward the edges. They have analyzed these profiles to determine average slope of the subsidence bowls at the point where vertical displacement is equal to 25 percent of the maximum subsidence at the center of the bowl. Values of average slope at this point for the six cases discussed above ranges from 0.0005 to 0.0029. Additional studies of the profiles of Goose Creek and Wilmington field indicate that the slope of the subsidence bowls at the edge of the area of production is equal to or less than 0.0011.

d) Subsidence Potential of Near-Site Petroleum Production

The location of petroleum fields and individual wells from which oil or gas is being or has been produced is shown on Figure 2.5-41. The nearest major production is the Good Hope field which is centered about six miles east of the site. The productive zone, which occurs between 7000 and 9000 ft deep, has an area of approximately 1700 acres. About 100 wells, most producing oil, have been drilled over the dome.

For complete conservatism, it was assumed that future production at Good Hope may ultimately result in subsidence. The relationship of this subsidence to the site is pertinent. The previously described characteristics of subsidence bowls indicate that the slope of subsidence bowls at the edge of the area of production is equal to or less than 0.001 and that this slope diminishes to essentially zero at a distance of 1.3 to 2.1 times the radius of the production area.

These figures are based on roughly circular producing areas. Converting the 1700 acre area of Good Hope to an equivalent circular area (Good Hope is actually shaped like a half-circle), the outer limit of subsidence 2.1 times the productive radius is more than four miles east of the plant island. Consequently, it is concluded on the most conservative basis, that existing producing areas could not result in subsidence at the site.

The other nearby fields, the Norco field with six wells which have been produced and the Lucy gas fields with only five productive. wells typify rollover anticlinal structures associated with growth faults. Production at Norco occurs between 8300 and 10,100 ft. deep. At Lucy, gas production occurs at about 10,200 ft. deep. Consequently, this field is too deep to generate surface subsidence. According to the studies discussed earlier in the subsection, production shallower than 5000 to 6000 ft. is required. However, if it is assumed that subsidence is possible at either field and the productive areas drawn to include all of the widely spaced wells at each field, the maximum outer limit of subsidence (2.1 times field radius) would not occur within about 1.5 miles of the plant island.

e) Subsidence Due to Salt Dome Utilization

Shallow, piercement salt domes are utilized in Louisiana for the production of salt and sulfur, quarrying and underground storage. Table 2.5.1.4, lists 23 south Louisiana salt domes that have been utilized for one or more of these purposes.(26) (53).

Caprock, consisting of anhydrite, gypsum and limestone, overlies the salt on most domes. The limestone outcrop of the caprock was formerly quarried on Pine Prairie dome. Some caprock contains free sulfur, which is produced by the Frasch process in which hot water is circulated to melt the sulfur and return it to the surface in molten form. The underlying salt is produced by underground openshaft mining or by brine in which fresh water is pumped into the salt resulting in solution, and the return of brine to the surface. This process is also used to dissolve underground chambers that are used for storage of hydrocarbons, usually liquefied petroleum gas, in the impermeable salt.

Surface subsidence has been noted in conjunction with underground sulfur removal. According to the Freeport Sulfur Company, which operates the Lake Washington (Grand Ecaille) mine, 53 miles southeast of the site and the Grand Isle-Block 18 offshore mine, surface subsidence is monitored periodically.

Sulfur is produced from caprock deposits less than 2000 ft. deep in each case. A surface subsidence bowl is produced that is essentially limited to the production area and amounts to less volume than the sulfur removed.

Surface subsidence above salt domes, attributable to salt mining, has also occurred. Documented mine failures and resultant surface subsidence have occurred over shallow salt domes 100 to 200 miles from the site, but there have been no known cases nearer the site. Where salt mining is occurring, particular care is taken to leave sufficient support pillars to avoid mine collapse and to place the mine far enough away from the sides and top of the salt to maintain the integrity of the workings.

In addition to artificially induced subsidence (mine collapse), natural solution of shallow salt domes by groundwater has produced sinks and depressions at the ground surface. Such naturally induced features are only associated with very shallow salt domes.

In all of these instances, the area of collapse or subsidence is restricted to the surface overlying the salt dome; this must be regarded as an unstable area. However, these conditions do not extend laterally away from the domes.

The nearest shallow piercement dome to the site is Sorrento, located 22 miles northwest. Active brine production and Liquid Propane gas storage is occurring at the Sorrento dome. The next closest shallow piercement dome is Chacahoula, 29 miles southwest. Table 2.5-5 lists all salt domes within 50 miles of the site and indicates whether utilization other than for oil and gas production is occurring or has occurred.

Six salt domes are located within 20 miles of the site; all are productive of oil and gas, but none have been utilized for any other purpose. All six have caprock and/or salt too deeply buried for mining or brine or sulfur production. These domes are Good Hope, five miles east with salt at 9580 ft.; Paradis, seven miles south with salt at 13,538 ft.; Bayou Des Allemands, 15 miles south with caprock at 7552 ft. and salt at 7560; Bayou Couba, 15 miles southeast with salt at 6160 ft.; Hester, 16 miles west with salt at 6780 ft.; and Raceland, 17 miles south with salt at 8170 ft.

Geologic and geophysical data indicate that no salt dome exists in the site area with the exception of the Good Hope and Paradis domes which are five and seven miles, respectively, from the site. Each of these domes is deep-seated with salt deeper than 9500 ft. and hence too deep for economic utilization for underground storage, salt, sulfur, or other caprock mineralization. The nearest dome for which such use is feasible is the Sorrento dome, 22 miles away. Consequently, subsidence associated with removal of salt, sulfur, or other caprock mineralization from salt domes is not a site related problem.

2.5.2 VIBRATORY GROUND MOTION

2.5.2.1 Seismicity

Figure 2.5-42d shows the seismic coverage within five miles of the Waterford 3 site.

Epicentral locations for all recorded earthquakes in the central Gulf Coastal Plain, including the Mississippi embayment, which have a reported intensity of about IV-V Modified Mercalli (MM) or greater, are plotted on Figure 2.5-42. Historic earthquake data were assembled between latitude 27.5° to 37.3° North and longitude 86° to 96° West. Tables 2.5-6, 2.5-7, and 2.5-8 are a listing of these earthquakes with additional pertinent data. The earthquake data has been compiled from U.S. Department of Commerce reports on U.S. Earthquakes, 1928 through 1972 (55) the Earthquake History of the United States revised through 1970 (56)' and Preliminary Determination of Epicenters Listing issued by the U.S. Geological Survey (57) and reports by Moneymaker (see Refs. 58,59,60, and 61).

As shown on Figure 2.5-42 and Table 2.5-6, ten small earthquakes have occurred within about 200 miles of the site. These earthquakes include:

a) The Donaldsonville earthquake with an epicentral intensity of less than VI MM which occurred on October 19, 1930 was located about 32 miles west of the site.

b) The Gulfport earthquake with an epicentral intensity of V MM which occurred February 1, 1955 was located about 87 miles east of the site.

c) The Baton Rouge earthquake with an epicentral intensity of V MM which occurred on November 19, 1958 was located about 43 miles northwest of the site.

d) The Gulf of Mexico earthquake with a recorded magnitude of 4.8 which occurred on November 5, 1963 was located 191 miles southwest of the site.

e) The Mississippi earthquake with a recorded magnitude of 2.9 which occurred on September 9, 1975 was located about 86 miles northeast of the site.

f) The southern Alabama earthquake with an epicentral intensity of V MM which occurred on December 10, 1974 was located 202 miles northeast of the site.

g) The Mississippi earthquake with a recorded magnitude of 3.0 which occurred on October 22, 1976 was located about 184 miles northeast of the site.

h) The Mississippi-Alabama earthquake with a recorded magnitude of 3.6 which occurred on May 5, 1977 was located about 183 miles northeast of the site.

i) The Mississippi-Alabama earthquake with a recorded magnitude of of 3.3 which occurred on June 9, 1978 was located about 183 miles northeast of the site.

j) The Mississippi-Alabama earthquake with a recorded magnitude of 3.5 which occurred on December 10, 1978 was located about 180 miles northeast of the site.

The Donaldsonville and Baton Rouge earthquakes are discussed in greater detail in the following two subsections. In addition, a summary of intensity data is presented in Table 2.5-9 for these two earthquakes, the Gulfport earthquake, and the New Madrid series.

2.5.2.1.1 Donaldsonville Earthquake

The Donaldsonville earthquake has a recorded maximum intensity of less than VI MM and was felt over 15,000 square miles(56). Donaldsonville, Louisiana is about 32 miles west-northwest of the site. Instrumental data for this event is not available.

On Sunday morning, October 19, 1930, at about 6:15 a.m., an earthquake occurred near Donaldsonville, Louisiana. The epicenter was recorded as being latitude 30° North and longitude 91° West. This point is near Donaldsonville, Louisiana. In 1930, the U. S. Coast and Geodetic Survey reported, "The outstanding feature of the Louisiana shock was the irregular distribution of intensity of the central zone and the relatively large area of the zone. These features indicate a rather deep-seated origin (62). The U.S. Coast and Geodetic Survey isoseismal map (Figure 2.5-43) shows the maximum intensity V-VI Rossi-Forel scale (RF) which generally corresponds to V MM.

Neumann and Bodle, of the U. S. Coast and Geodetic Survey, in 1932, determined the epicentral location by drawing isoseismals using Postmaster and citizen reports and newspaper account (63). Neumann and Bodle state, "This earthquake was not recorded in any satisfactory manner on any seismograph."

They list a maximum intensity of VII RF and an area over which the tremor was felt of 15,000 square miles (intensity VII RF generally corresponds to intenslty VI MM). Intensities V-VII RF are listed for Morgan City (Berwick), Des Allemandes, Donaldsonville, Franklin, Napoleonville, and White Castle.

The initial evaluation by the U. S. Coast and Geodetic Survey assigned intensity V-VI RF which compares with V MM. The subsequent 1932 evaluation by the U. S. Coast and Geodetic Survey apparently took into account the structural damage reported to chimneys and windows. The remaining evidence for intensity VI MM is the report of broken windows at the Donaldsonville hotel. It is concluded that the maximum epicentral intensity for the Donaldsonville earthquake was greater than V MM and less than VI NM and is therefore classified as less than VI MM.

2.5.2.1.2 Baton Rouge Earthquake

On November 19, 1958, an earthquake was reported to have been felt in the Baton Rouge, Louisiana area with an intensity of V Modified Mercalli. Newspaper reports (see Table 2.5-9) indicate that several persons felt a tremor in the Baton Rouge area.

The seismograph at Loyola University in New Orleans did not record any event at the time of the tremor. Other authorities were reportedly checked and such things as explosions and jets cracking the sound barrier were ruled out.

Several water well records for the date of this reported earthquake were checked. No fluctuation in groundwater level was reported at the designated time. Several of the water wells checked reported a large fluctuation during the 1964 Alaskan earthquakes.

The exact origin of this reported earthquake is still in question. It may have been a surface disturbance and only felt locally. There was no observed change or surface disturbance along the Baton Rouge Fault Zone following this reported earthquake.

2.5.2.1.3 Behavior During Prior Earthquakes

New Orleans, Louisiana was settled in 1718 by the French. During the greater than 250 year period since New Orleans was settled, only three shocks of the 1811-1812 New Madrid series, and the 1930 Donaldsonville earthquake have probably been felt at the site and surrounding area.

Records at New Orleans indicate that only the largest intensity earthquakes of the New Madrid series were felt in the New Orleans area. The New Madrid series of earthquakes had three events rated XII Modified Mercalli (MM) epicentral intensity (55). Table 2.5-9 summarizes intensity data from this series of events. Nuttli (64) compiled all available references on this series of events. He rated the intensity at New Orleans resulting from the December 16, 1811 event as intensity III MM based on a report by Fuller of the U.S.G.S. Fuller relates that, "The earthquake was felt at New Orleans, but was not severe". He reported that Natchez (Mississippi) felt four shocks with some resulting damage. The January 23, 1812 event was assigned an intensity IV-V MM at New Orleans by Nuttli. This was based on the account in the Louisiana Gazette and Daily Advertiser on January 24, 1812, "A slight shock of an earthquake was felt in this city yesterday morning, about nine o'clock. The wind was from the southward, light and gentle, and the morning fine ... it lasted but a few seconds and but few felt it. At that time all is bustle in the city - but many proofs, such as clocks stopping, glass shades, and different kinds of glassware and crockery shaking, the feelings of many who were either writing or reading, prove the fact. We may expect to bear more on the subject from the northward and eastward". At New Orleans, the February 7, 1812 event was assigned an intensity V MM by Nuttli. This intensity was based on the article in the New York Post on March 5, 1812, "New Orleans, February 8" - "There was another shock of an earthquake felt in this city yesterday morning about half past three o'clock - It's said to have been much more strong than the one felt some time ago".

An isoseismal map of the Donaldsonville earthquake which occurred on October 19, 1930 is shown in Figure 2.5-43. This figure shows that the site experienced between intensities IV and V Rossi Forel scale (IV MM) during this earthquake.

In summary, the New Madrid series of earthquakes of epicentral intensity XII MM and the Donaldsonville earthquake are probably the only seismic events that have been felt in the site and surrounding area during the past 250 years. The greatest intensity experienced at the site during the historic record was V MM or less. There is no physical evidence to indicate any earthquake effects at the site.

2.5.2.2 Geologic Structures and Tectonic Activity

The lithologic, stratigraphic, structural and historical conditions of the site and surrounding region are discussed in Subsections 2.5.1.2 and 2.5.1.1, respectively. Following is a summary of these sections, emphasizing the Mississippi River deltaic plain.

The site is within the Gulf Coastal Plain geologic province which encompasses the coastal region from the Rio Grande River to the western border of Florida. The region surrounding the site has an almost continuous history of sedimentary deposition in the Gulf geosyncline. The geosyncline's axis of deposition is parallel to the coast. Sedimentary deposits, ranging in age from Triassic to present, have accumulated to thicknesses exceeding 50,000 ft. within the geosyncline.

Near the base of the geosyncline is the Louann salt formation, which was deposited during the Jurassic period (135 to 181 MYBP). The depth to the Louann salt is estimated to be in excess of 40,000 ft. in the site area. The Louann salt formation, under the increasing pressures of sedimentation, intrudes upward at isolated points and produced most of the localized geologic structures of the geosyncline. The structures vary from small low-relief anticlines to large, steeply dipping salt dome intrusions.

The Gulf geosyncline is a broad regional downwarping of oceanic crust overlain by thick sedimentary deposits in the southern half of the Gulf Coastal Plain. The geosyncline has an arcuate trend which varies from east-west, in Louisiana, to north-south, in south Texas and which dips gulfward about three degrees. The oceanic crust of the Gulf geosyncline is overlain by thick Jurassic salt and over 40,000 ft. of sediments. Marine conditions, characterized by clay deposition, persisted from Jurassic into the Cenozoic. These deposits are overlain by a regressive deltaic sequence. There are no seismogenic structures identified within the sedimentary sequences above the geosyncline floor. The existence of a thick salt layer at the base of the sediments should, in effect, establish a zone on which long term stress (tangential shear) cannot be sustained. This would effectively separate stress accumulation in the sediments from stress accumulation in the crust.

The northern portion of the Gulf Coastal Plain province is characterized by continental crust with varying thickness which was partly controlled by late Triassic block faulting. Thick Jurassic salt accumulations occur in previously low areas. The salt occurs over the majority of the area and provides a zone which cannot sustain long term stress. Therefore, stress accumulations within the crust would be independent of the overlying sediments. Differential sedimentation was replaced by a stabilized shelf in Lower Cretaceous (135 MYBP), bounded gulfward by the Stuart City barrier reef which was in turn partly controlled by a southern basement high.

A "hinge line" partly marked by faulting which terminated in Tertiary (2 MYBP), separates the Gulf Coastal Plain from the Paleozoic, Ouachita orogenic belt. From the hinge line inland, the Ouachita province includes sediments, which were folded and faulted during late Paleozoic (280 to 230 MYBP), as well as relatively undeformed areas such as the Arkoma-Black Warrior basin. Cretaceous igneous activity, such as the Monroe-Sharkey uplift and the Jackson dome, occur within the Ouachita orogenic belt.

The Ouachita orogenic belt borders the Precambrian craton which is broken by the New Madrid faulted zone in the area of the Mississippi enbayment north of Memphis. Faults in this system may be related to present earthquake activity.

In addition to geologic individuality - crustal types, basement structure and sedimentary thickness - each of the three broad regions have displayed distinct earthquake distributions over the past 250 years. Figure 2.5-42 shows the number of earthquakes and their relative size which have occurred in the central Gulf Coastal Plain. The distribution of earthquakes for each of the regions described above is as follows:

Region	Number of Occurrences With Epicentral Intensity V MM or Greater	Maximum Epicentral Intensity MM
Gulf Coastal Plain	15	VI*
Ouachita Deformed Crust Province	25	VI-VII
New Madrid Faulted Zone	94	XII

*See Subsection 2.5.2.3

With the exception of the New Madrid events, these earthquakes generally have a random distribution within their respective regions and are not identified with a specific tectonic structure. The New Madrid seismic zone lies within a 70 km-wide by 100 km-long, northeast striking graben which has been defined by magnetic data (Hamilton, 1981). A 100 km-long seismicity trend coincides with the axis of the graben, with another northeast striking trend along the graben's northwest margin. A third, lower activity seismicity trend has been correlated with the southeastern edge of the graben.

2.5.2.3 Corelation of Earthquake Activity with Geologic Structures or Tectonic Provinces

The geologic structures of this region have been discussed in Subsection 2.5.2.2. The scattered earthquakes which have occurred in this region cannot be identified with any geologic structures. Consequently, the region has been divided into three provinces, each having unique crustal pattern, geologic history and earthquake history. Figure 2.5-42 is a plot of earthquake epicenter locations superimposed on these provinces.

The site is located in the Gulf Coastal Plain province. There have been 17 historic seismic events with epicenters located within this province. However, only ten events have occurred in the province within about 200 miles of the site. These ten events include: (1) an epicentral intensity of nearly VI MM event which occurred on October 19, 1930 at Donaldsonville, Louisiana, (2) an intensity V MM event which occurred on February 1, 1955 at Gulfport, Mississippi, (3) an intensity V MM event which occurred on November 19, 1958 at Baton Rouge, Louisiana, (4) an event with a recorded magnitude of 4.8 which occurred on November 5, 1963 on the Texas-Louisiana continental slope, (5) an event with a recorded magnitude of 2.9 which occurred on September 9, 1975 in southern Mississippi, (6) an event with a recorded magnitude of 3.0 which occurred on December 10, 1974 in southern Alabama, (7) the Mississippi earthquake with a recorded magnitude of 3.0 which occurred on October 22, 1976 was located about 184 miles northeast of the site, (8) the Mississippi-Alabama earthquake with a recorded magnitude of 3.6 which occurred on May 5, 1977 was located about 183 miles northeast of the site, (9) the Mississippi-Alabama earthquake with a recorded magnitude of 3.3 which occurred on June 9, 1978 was located about 183 miles northeast of the site, and (10) the Mississippi Alabama earthquake with a recorded magnitude of 3.5 which occurred on December 10, 1978 was located about 180 miles northeast of the site. The largest earthquake, the Donaldsonville event, is discussed in detail in Subsection 2.5.2.1.1.

In addition to the ten seismic events which occurred within about 200 miles of the site, seven other events with epicentral intensities IV-V MM or greater have been recorded in the Gulf Coastal Plain province. Of these seven events, six had epicentral intensities of V MM. One earthquake within this province had an epicentral intensity VII MM. This earthquake was the "Rusk" (Texas) event that occurred on January 8, 1891. This earthquake is not considered typical of the province since its felt area was extremely small as compared with lesser intensity earthquakes characteristic or the region. The Rusk earthquake is discussed in Section 2.5.2.4.

The largest earthquake in the Gulf Coastal Plain province (other than the "Rusk" event) is the Donaldsonville earthquake which occurred on October 19, 1930 with an epicentral intensity of less than VI MM.

The Ouachita deformed crust province consists of Paleozoic metasediments, which were folded and faulted during late Paleozoic (230 MYBP) and the relatively undeformed Arkoma-Black Warrior basin sediments. This province contains cretaceous igneous rocks. Twenty-five seismic events of epicentral intensity IV-V MM or greater have been recorded in this province. Of these events, the intensity of one is unknown. Of the other 24 one had an estimated intensity of IV-V (magnitude 2.9). 18 events had intensities of V MM (five of these are estimated from magnitudes between 3.2 and 4.2), four events had intensities of VI MM (one estimated from a magnitude of 4.5), and the largest event had an epicentral intensity of VI-VII MM. The largest event in this province was 403 miles distant from the site.

Figure 2.5-42 shows a zone of intense seismic activity, the New Madrid faulted zone, centered about 400 miles north of the site. The New Madrid faulted zone is composed of a series of faults that trend across the Pascola arch in a northeasterly-southwesterly direction. The southerly extension of these faults and associated seismic activity, dies out near Memphis, Tennessee, where the faulted zone terminates at the Arkoma-Black Warrior basin, the northern edge of the Ouachita deformed crust province. The largest seismic events recorded in the New Madrid faulted zone were three intensity XII MM events which occurred during the earthquake series from December 16, 1811 to February 7, 1812 (Subsection 2.5.2.1.3). The closest approach of the New Madrid faulted zone to the site is about 340 miles.

2.5.2.4 Maximum Earthquake Potential

Tables 2.5-6, 2.5-7, and 2.5-8 list the historic earthquakes between latitude 27.5° to 37.3° North and longitude 86° to 96° West, having an epicentral intensity IV-V or greater on the Modified Mercalli scale (MM). These events are shown on Figure 2.5-42 with provinces of unique crustal patterns, geologic history, and earthquake history. Subsection 2.5.2.3 discusses the relationships of recorded earthquakes with tectonic structures and provinces.

The largest earthquakes of historic record in the United States are the three events of intensity XII MM that occurred near New Madrid, Missouri during the 1811-1812 series of earthquakes. This area lies within the New Madrid faulted zone. Nuttli (64) has drawn isoseismals for the December 16, 1811 event. If Nuttli's isoseismals are adjusted to fit the February 7, 1812 event (an epicentral intensity of XII MM to which he assigned an intensity V MM at New Orleans, Louisiana) and then superimposed on Memphis, Tennessee (the closest point of the New Madrid faulted zone to the site), an intensity slightly greater than V MM is indicated at the site for a postulated recurrence of an earthquake with an epicentral intensity XII MM.

The 1882 Arkansas earthquake is reported to have been felt over an area of 135,000 square miles (isoseismals not available). Assuming an approximately circular felt area, the distance from the epicenter to the felt area edge would be about 210 miles. The point on the Ouachita deformed crust province closest to the site is approximately 180 miles. Therefore, if the 1882 Arkansas earthquake were to be translated to the closest approach of the Ouachita deformed crust province it would be felt at the site with about intensity IV MM.

Although the Rusk (Texas) earthquake apparently caused intensity VII damage over a small area, the earthquake was only felt at Rusk. Typically, an intensity VII earthquake would have a much larger felt area. For example, the October 22, 1882 Arkansas earthquake (VII MM) was felt over 135,000 square miles and the October 19, 1930 Donaldsonville earthquake (less than VI MM) was felt over 18,000 square miles. In respect to felt area, the Rusk earthquake is similar to the April 9, 1932 Mexia-Wortham (Texas) earthquake (V-VI) which was felt over an area of 1,000 square miles.

Assessment of damage reports from the Rusk earthquake is difficult because violent weather conditions with damaging winds were occurring at the time of the earthquake. Also, two earthquake shocks were reported which may imply that two separate small earthquakes occurred rather than one of larger intensity. The earthquake intensity of VII MM was based on chimney damage. It is possible that the earthquake or earthquakes damaged but did not topple the chimneys and that high winds associated with the storm, did much of the damage. Unless many chimneys are completely downed, they are poor indicators of earthquake intensity due to the variable nature of their construction. Since only a few chimneys were toppled without other corroborative damage reports, there is only weak evidence for an intensity assignment of VII MM for the Rusk earthquake. It is most likely that the Rusk earthquake is not of intensity VII MM and should instead be considered as a very small, shallow earthquake which occurred with a severe storm.

Excluding the "Rusk" event, the largest recorded earthquake in the province is the Donaldsonville (Louisiana) event, which occurred on October 19, 1930, and had an epicentral intensity of less than VI MM.

In accordance with 10CFR100, Appendix A, dated November 13, 1973, the Donaldsonville earthquake is defined as the maximum earthquake for the Waterford site.

2.5.2.5 Seismic Wave Transmission Characteristics of the Site

2.5.2.5.1 Properties of Foundation Soils

Samples taken from exploratory borings were utilized in a comprehensive laboratory testing program to determine the physical properties such as densities and classifications of soils at the site. A complete description of this testing program including results is presented in Subsection 2.5.4.2. A program of field geophysical surveys and laboratory testing was performed to determine the seismic and elastic soil properties. These properties included shear wave (V_s) and compression wave (V_p) velocities, shear moduli, Young's moduli and Poisson's ratios, which are characteristics of the site soils. This program included up-hole, cross-hole, and refraction seismic surveys and cyclic triaxial tests in conjunction with literature searches. The investigative procedures and results are described in Subsections 2.5.4.2 and 2.5.4.4.

2.5.2.5.2 Shear Modulus of Elasticity

The shear modulus of elasticity was calculated for the Pleistocene soils based on the shear wave velocity profile given in Figure 2.5-76. The average shear wave velocity for the upper Pleistocene soils is about 1,000 ft. per second and the corresponding shear modulus of elasticity is 27×10^3 psi.

The average shear wave velocity for the lower Pleistocene soils (below elevation -317 ft. MSL) is approximately 1,600 ft. per second which corresponds to a shear modulus of elasticity of 69×10^3, psi.

For a complete discussion of strain dependent shear modulus and a correlation of laboratory measured and field measured shear moduli refer to Subsection 2.5.4.2.

2.5.2.5.3 Percent Damping

Percent damping for the upper Pleistocene soils was determined by comparison of laboratory test data of Pleistocene materials with published values of percent damping. The damping as a function of shear strain is presented on Figure 2.5-78. The percent damping is approximately five percent at low shear strain levels (up to 3×10^{-4} in./in.), it increases to 8 percent at shear strains of 10^{-3} in./in. and further increases to 20 percent at a shear strain of 10^{-2} in./in. The strain-dependent percent damping for the lower Pleistocene and Class A backfill are presented on Figures 2.5-79 and 89 respectively.

Refer to Subsection 2.5.4.2 for a discussion of the selection of the damping properties.

2.5.2.5.4 Seismic Wave Transmission Characteristics

Seismic wave transmission characteristics of the site were determined by using the computer program SHAKE (66). The model and the associated shear moduli used for the analysis are presented in Figure 2.5-91. The soil properties such as unit weight, shear modulus and damping of the Class A backfill and the underlying Pleistocene soils were obtained from laboratory testing, field geophysical surveys, boring information, and published literature.(67) For the analysis a parametric study was conducted utilizing three different sets of shear moduli from the upper and lower Pleistocene materials. This analysis represented the occurrence of the maximum potential earthquake. Since Waterford site is a deep soil site, the model used for study was set 400 ft. deep to incorporate the Class A backfill, the upper Pleistocene and part of the lower Pleistocene soils. The groundwater table was taken at elevation +8 ft. MSL.

The significant and fundamental frequencies at the site were in the range of 0.2 to 0.4 cycles per second, which correspond to the periods of 5 to 2.5 seconds. The analysis indicated little amplification through the stiff Pleistocene soils and the Class A backfill as is the case of a long period soil column. This long period soil column was insensitive to the effect of the stiffening and/or softening of the underlying Pleistocene clay and sand. A detailed discussion of the methodology used for performing the analysis is presented in Subsection 2.5.4.7. Results from the study such as accelerations at different depths, and the associated shear moduli, and the significant frequencies are presented in Table 2.5-10. Based on the results of the analyses, it was concluded that very little high frequency wave transmission is possible within the Waterford site materials.

2.5.2.6 Safe Shutdown Earthquake

The U.S. Nuclear Regulatory Commission's (NRC) Standard Review Plan (June, 1975) for Section 2.5-2, Vibratory Ground Motion, states that the Safe Shutdown Earthquake" is as conservative as that which would result at the site from the Maximum Earthquake Potential (determined in Subsection 2.5.2.4)." Recently published in the Federal Register, Vol 42, No. 6, Monday, January 10, 1977, was an Amendment to 10CFR100, Appendix A which mainly consisted of three conditions relating to selection of the Safe Shutdown Earthquake (SSE). These conditions are " (1) Where the highest intensity of historically reported earthquakes is determined to have been experienced at the site taking into consideration site foundation conditions, (2) where seismicity in the immediate site vicinity is significantly higher than that generally existing in the tectonic province as a whole, (3) where there exists in proximity to the site tectonic structure demonstrably like that found where larger earthquakes in the tectonic province have occurred historically."

We have considered these conditions in the selection of the SSE and have concluded that they are not applicable to the Waterford site. Therefore, the SSE for the site is based on a hypothetical earthquake with epicentral intensity VI MM occurring adjacent to the site.

During the preparation of the Waterford PSAR in 1970, we utilized the Hershberger intensity - acceleration relationship (69). As previously described, the NRC published a Standard Review Plan for Section 2.5.2 in 1975 which generally states that the SSE seismic design acceleration should be at least as conservative as the 1975 Trifunac-Brady mean re-lationship. As shown on Figure 2.5-44, intensity VI MM corresponds to a horizontal surface acceleration of 0.05g according to the conservative Hershberger relationship. According to the Trifunac-Brady relationship, intensity VI MM corresponds to a horizontal surface acceleration of 0.06g.

In order to comply with the minimum accepted acceleration as stipulated by 10CFR100, Appendix A, Waterford 3 was designed for a maximum horizontal ground surface acceleration of 0.10g. This very conservative surface acceleration is double the maximum acceleration appropriate for the maximum earthquake which has occurred in the site's tectonic province during the past 250 years. The peak vertical acceleration for the postulated SSE is 2/3 peak horizontal acceleration.

2.5.2.6.1 Synthetic Earthquake and its Response

A synthetic earthquake record with a maximum acceleration of 0.10g was developed (Figure 2.5-45) to generate response spectra as shown in Figures 3.7-1 and 3.7-2. In simulating the earthquakes a maximum duration of 20 seconds was used in the model, of which 0 to two seconds was used for the rising period, two to seven seconds for the constant maximum acceleration period, and seven to 20 seconds for the receding period. These durations were selected based on the available data of the duration of the earthquakes in this region. The shape of the response spectra of the simulated earthquake for a single degree of freedom approximates N. M. Newmark's Spectrum Curve as discussed in his paper "Design Criteria for Nuclear Reactors Subject to Earthquake Hazards", Urbana, Illinois, May 25, 1967. The maximum amplification, at two percent critical damping is approximately 3.5, greater than the value shown in the Housner Spectra of TID 7024, but less than the Newmark value.

2.5.2.6.2 Amplification and Spectral Shift

Mathematical analyses have been made to determine the effect of the sediments at the site on earthquake intensity. If it is assumed that the earthquake forces are imposed at the dense sands at a depth of 330 ft. (or deeper), there is little amplification through the stiff Pleistocene clay and Recent sediments above because the fundamental period for the clay-recent sediment column is long. There is some attenuation of the higher frequency short period components of vibration through the long Pleistocene-Recent column. However, from the design point of view the conservative approach is to ignore the high frequency losses and consider the same frequency-acceleration spectra at all levels within the Pleistocene.

Based on these studies a conservative approach which considered the recommended acceleration response to occur at the surface of the Pleistocene clays at a depth of about 50 ft. below the ground surface was utilized.

2.5.2.7 Operating Basis Earthquake

The Operating Basis Earthquake (OBE) for the Waterford site is postulated to have peak horizontal and vertical accelerations of 0.05g and 0.033g, respectively. These are one-half of the corresponding accelerations postulated for the SSE in Subsection 2.5.2.6.

The horizontal and vertical response spectra for the postulated OBE conditions at the Waterford site will be one-half of those for the SSE and are presented on Figures 3.7-3 and 3.7-4 for two percent, and on Figures 3.7-7 and 3.7-8 for five percent damping.

The probability of a seismic event equaling or exceeding the OBE was computed using standard statistical methods. The region surrounding the site was subdivided into areas of similar seismicity, and the statistical properties of seismic events were developed for each area. The effects of events in neighboring provinces were attenuated to the site. The annual probability of events of each intensity greater than or equal to V MM at the site was computed. Horizontal accelerations for each intensity were taken from the 1975 Trifunac-Brady relationship. The annual probability for an event greater than or equal to 0.05g was interpolated from the results of this computation, and the probability of occurrence of one or more such events was computed. The results of these computations indicated a probability of 2.6 percent over the 40 year life of the plant.

2.5.3 SURFACE FAULTING

2.5.3.1 Geologic Conditions of the Site

The geologic conditions of the site and the surrounding area have been described in the Subsections 2.5.1.1 and 2.5.1.2. Fault mechanisms and the history of faulting in the Gulf Coastal Plain have been discussed in Subsection 2.5.1.1. It is concluded that no seismic generative faults are known to exist within 200 miles of the site. Figure 2.5-10 shows the locations of known faulting within this region.

Many growth faults which occurred during Miocene (22 to 5 MYBP) are buried beneath the surface in the Gulf geosyncline south of the Cretaceous reef trend. Growth faults of the Grand Chenier system in the site and surrounding area were studied in detail as described in Subsections 2.5.1.2 and 2.5.3.2. The latest movements along the youngest fault of the Grand Chenier system, the site and surrounding area, was more than 5,500,000 years ago.

As discussed in Subsection 2.5.1.1.4, these faults were initiated and perpetuated by differential sediment loading on the continental slope, and by salt movement on the outer continental shelf. Faults of this type are active today along the present outer continental shelf, about 140 miles south of the site. Movement along these active faults, leading to sediment thickening on the downthrown block, is contemporaneous with sedimentation; thus, residual stresses, which could lead to a sudden release of seismic energy, cannot accumulate. These faults are non-seismic.

2.5.3.2 Evidence of Fault Offset

2.5.3.2.1 Baton Rouge Fault Zone

The Baton Rouge fault system extends east-southeastward from the Mississippi River to the Pearl River along the north side of Lake Pontchartrain. It is a fairly continuous, partially en-echelon zone attributed to differential compaction and gulfward flexing of the sedimentary mass along the north flank of the Gulf geosyncline province. The Zachary, Scotlandville-Denham Springs, and the Baton Rouge faults are a part of this system. The widths of the individual faults within this system are less than 500 ft. The closest point of any of these faults to the site is 22 miles to the north.

Recorded vertical displacements along the Baton Rouge faults, determined from subsurface well data, varies from 200 to 450 ft.(68). The shallowest subsurface information indicates an offset of 350 ft. at depths above 2,000 ft. Durham and Peeples believe that the recurrent nature of fault movement, as demonstrated by the existence of surface escarpments, indicates that the Pleistocene has been the main period of fault activity (34). Some of these faults have been active from at least late Pliocene (2 MYBP) to the present. However, as is characteristic of growth faults, these faults do not accumulate strain and are non-seismic.

2.5.3.2.2 Vacherie Fissure

On April 12, 1943, at 2:00 A.M., a fissure suddenly developed in the ground surface at Vacherie, 16 miles due west of the site, in Section 20, T12S R17E on the west (right descending) side of the river. The fissure was approximately perpendicular to the river and initially 1600 ft. long, with its center about 2500 ft. from the levee. The fissure elongated at both ends during the ensuing three days until it extended from 1200 ft. from the levee to 6500 ft. from the levee, a length of 5300 ft.

Although there has been no noticeable movement since April 15, 1943, it is prudent to determine: (1) whether additional movement could occur at this location during the life of the project, (2) whether this could affect the proposed project, and (3) whether similar fissuring could develop at the project site. The answer to the first question is possibly yes; the answer to the remaining two is no. The rationale behind these answers is developed below.

a) Description of Fissure

→(DRN 01-464)

The location of the fissure is shown approximately on Figure 2.5-12. It eventually extended from 1200 ft. south of the levee to 6500 ft. south. Its path was generally south-southeastward, but in the form of a greatly elongated reverse curve slightly concave eastward north of the railroad (a length of 2900 ft.) and slightly concave westward, south of the railroad, a length of 2200 ft. At the railroad it offset to the west more than 100 ft.

←(DRN 01-464)

The northern end of the fissure was a hair line crack which gradually increased in width to 1.5 in. in a distance of 1200 ft. The width increased to as much as 6 in., 1600 ft. from its beginning and about 2800 ft. south of the levee, with a number of arc-like branches or parallel curving cracks. The width decreased to less than one-half in., 2900 ft. from the beginning or 4100 ft. south of the levee. Beyond the railroad the fissure continued as a 100 ft. wide zone of parallel cracks, with widths varying between one-eighth and one-half in.

In the northernmost 900 ft. and the southernmost 2500 ft., there was little or no vertical displacement across the fissure. In the central part, the west side was lower, with the maximum difference nearly eight in. The zones of maximum crack width and maximum offset were centered about 1600 ft. from the beginning of the crack or 2800 ft. south of the levee.

The fissure was first discovered by the occupant of a small cabin 2100 ft. south of the levee, who was awakened by a tremor sound. Daylight disclosed a three inch fissure beneath the house and several of its stone pillars displaced. The crack continued to grow in length, both north and south, and increased its displacement. At 12:50 A.M April 13, a day later, a slight tremor was felt by observers on the railroad. The tracks subsided two inch west of the fissure and eventually required reballasting. Growth apparently ceased April 15. As far as can be determined there has been no movement since.

The general appearance of the crack can be seen in Figures 2.5-46 and 2.5-47 which were made April 12 or 13 on the Laurn Plantation and which were furnished by Mr. Waguespack. The first shows the displacement across a furrow; the second shows the shape of the fissure across a pasture and implement yard somewhat north of the zone of greatest movement.

No trace of the crack can be seen today, even at specific locations pointed out by local residents. Infra-red aerial photographers, however, do show a narrow trace of reduced reflectivity, perpendicular to the river, 3000 ft-south of the levee. This trace occurs in the exact location pointed out by Joseph Gilbert who has lived in a cabin 250 ft. east of the fissure more than 30 years.

The resident of the cabin astride the fissure was awakened at 2:00 A.M. by a rumble such as coming from a distant explosion as well as by a small tremor. Others living in the near vicinity also felt a slight tremor; others in Vacherie, 1000 ft. away, apparently did not.

The nearest seismograph is at Loyola University in New Orleans. A letter from K. A. Maring, S. J. May 4, 1943 at H. N. Fisk, School of Geology, Louisiana State University, states that the Loyola seismographs showed no registration. The next nearest station is St. Louis University, St. Louis, Missouri. Their instruments recorded no seismic disturbance at the time of the fissuring.

b) Geological Conditions at Vacherie

The same stratigraphic sequence which occurs at the site also exists at Vacherie. However, the Vacherie structure has been distorted by the Vacherie Salt Dome which is centered on the north bank of the Mississippi River about 7000 ft. west-northwest of the north end of the fissure. The top of the dome is about 7000 ft. below sea level, and its steep conical surface passes below the fissure at depths of from 10,000 to 12,000 ft. Two faults, 8000 ft. apart and crossing the dome from north to south, have been postulated from local oil well exploration. These faults form a graben in which the strata between them have subsided 600 to 1000 ft. Their cause is probably the upward bending and stretching of the strata above the salt. The younger, less consolidated sediments that accumulated above the graben are 1000 ft. thicker than those immediately adjacent to it, a discontinuity that must be reflected in differential sediment consolidation. Possibly some vertical shear cracking accompanied this consolidation, reflecting the location of the faults but not necessarily related to any movement on the faults themselves.

Borings made by the Corps of Engineers in 1943 to investigate the Vacherie fissure found the surface of the Pleistocene sediments several feet lower between the fissure and the dome and graben than east of the fissure.

An abandoned crevassee channel and its accompanying levees extended south from Vacherie, turning eastward toward Lac des Allemandes. The current aerial photographs still show the old channel defined by darker colored sediments, as well as numerous textural changes which represent the shifting point bars. It is significant that the fissure parallels this old channel and that it nearly coincides with one of the channel boundaries as suggested by the aerial photographic tonal changes.

c) Vacherie Oil Field

Oil was discovered at the Vacherie Dome in 1936, followed by production of both gas and oil, mostly south of the river. In 1943 a well was being drilled 9000 ft. southeast of the center of the dome, just west of Highway Louisiana 20, and about 2800 ft. south of the levee. The well crossed a fault (orientation unknown) and reached salt water with a pressure exceeding 2000 psi at a depth of 8800 ft. Water flowed out of control for a short time commencing at 12:30 P.M., April 11, causing a shutdown of drilling. The fissure was first discovered about 13 hours later. The well was 1500 ft. from the fissure at its closest point; it was directly opposite the zone of maximum displacement and crack width of this fissure. The well was later plugged with cement.

d) Probable Cause of Fissuring

A number of mechanisms can be suggested from the geology of the area. The simplest is reactivation of the buried faults surrounding the salt dome. No evidence supports this theory. Fault movement is generated by increasing strain or decreasing resistance across the fault surface. While there is evidence of slow seaward tilt of the Gulf Coastal Plain, there is no suggestion of strains accumulating in this area. More important, the increased effective stress associated with oil extraction increases resistance to movement. Finally, any significant strain release from faulting producing a fissure as large as Vacherie should have registered on seismographs as near as New Orleans and St. Louis.

The sag in the Pleistocene suggest consolidation of the sediments due to their uneven thickness across the graben associated with the dome. Possibly both shear and tension cracks were produced in the past as a result. While they might reflect the position of a fault because it defines the graben, they are otherwise not related to the faulting.

Any sudden decrease in internal fluid pressure would reactivate the tension cracks at the surface, as the ground surface bends downward toward the graben. The open crack observed at Vacherie fits the mechanism perfectly. It apparently followed a surface discontinuity, the old river channel boundary, and was centered opposite the oil well that discharged water 13 hours before. The vertical displacement reflects the shear associated with the graben or possibly local slumping along a deep vertical tension crack in weak sediment. The arc-like shape of portions of the fissure, as well as local grabens support this interpretation.

There is no indication that the Vacherie Fissure produced a tremor of any sort at the site, nor is any reasonable extension of the fissure likely to come closer to the site than 15 miles. Even if fault movement were responsible for the Vacherie fissure, the trace of these faults would come no closer to the site than 15 miles.

2.5.3.2.3 Subsurface Faults Near the Site

There are three faults and four other minor faults of the Grand Chenier fault system buried beneath 5,000 to 9,000 ft. of Miocene (5.5 MYBP) and younger sediments within five miles of the site. The western flank of the Good Hope salt dome and two associated faults also lie within five miles of the site. The locations of these faults; Fault Zones 3 and 4, the Norco Fault, Faults "B" and "C", a minor splay fault off the Norco Fault, a minor fault connecting Faults "B" and "C" and the salt dome related faults are shown on Figure 2.5-19. All faulting within five miles of the site is described in detail in Subsection 2.5.1.2.3.

Fault Zone 3 is an easterly trending growth fault that displaces sediments down to the south. The evidence for this fault is found in four wells which indicate displacement on the fault ranging up to 70 feet. The location of the upward terminus of the fault is not clear, but the regional dip of the horizons above 8000 feet in depth (Cross Sections D and E, Figures 2.5-27a and 2.5-27b) is uninterrupted and structural contours on Pliocene horizons 2 & 3 (Figures 2.5-21 and 2.5-22) show no evidence of faulting in this area.

Fault Zone 4 is another small easterly trending growth fault located approximately 3.5 miles north of the Waterford site. Well data indicate that the fault displaces sediments 10 to 130 feet down to the south. The fault does not offset horizons above 8,000 feet in depth (Cross Sections D and E, Figures 2.5-27a and 2.5-27b) and contours on Pliocene horizons 2 and 3 (Figures 2.5-21 and 2.5-22) show no evidence of faulting in this area.

The Norco Fault is a east-west trending, southward dipping growth fault located north of the site. Correlation of electric log marker horizons indicates that the upward termination of faulting lies at about 6,000 ft. deep. The paleontological marker fossils Rangia cuneata and Rangia johnsoni occur above the top of faulting and indicate an age of cessation of faulting at least 5.5 MYBP, during late Miocene. At its upward termination the fault lies 1.5 miles north of the site.

To the east, a small growth fault splays off the Norco Fault with a north-northwest strike and westward dip. The fault bends around the western flank of the Good Hope salt dome and may have formed at least in part in reaction to the salt uplift. The fault terminates upward between 6,000 and 9,500 ft. deep. Activity on the fault probably ceased at about the same time as did activity on the Norco Fault. The small Norco splay fault is three miles east of the site at a depth of 8,000 ft. Fault "B" is a growth fault which strikes from east-west to west-northwest and dips southward. The buried fault plane lies beneath the site property limits, but south of the plant island. At its upward termination depth, about 5,000 ft. deep, the fault is about 1,000 ft. south of the plant island. The fault terminates beneath the late Miocene paleontological markers Rangia cuneata and Rangia johnsoni, indicative of an age of cessation of activity greater than 5.5 MYBP.

Fault "C" is the southernmost growth fault in the site area. The fault has a general east-west undulating fault plane trend and dips to the south. Westward, the fault bifurcates, one limb bending north to join fault "B", the other bending south. The fault terminates upward at about 6,000 ft. deep beneath the late Miocene paleontological markers mentioned

previously. The age of cessation of faulting is therefore about 5.5 MYBP. At its upward termination of 6,000 ft. deep, the fault is two miles south of the plant island.
Faults "B" and "C" are connected by a small fault which strikes north-northwest and dips to the west. Faulting terminates upward at about 9,000 ft. deep, beneath the upper Middle Miocene paleontological marker Bigenerina humbeli. This relationship indicates that fault activity ceased more than 10 MYBP. At its termination depth, the fault lies two miles southeast of the Nuclear Plant Island Structure (NPIS).

The Grand Chenier system of growth faults, in the area surrounding the site, is not an active system. The youngest faulting of these growth faults ceased at least 5.5 MYBP. In light of the age of cessation of faulting, and the fact that the faults occurred as continuing movement during sedimentation which did not allow strain build up, these faults are not capable faults.

Figure 2.5-19 shows a northwest striking, northeast dipping fault (Fault 2B) joining the Norco Fault near its eastern end. This fault is associated with the Good Hope salt dome which lies within five miles of the plant island according to detailed site area structural studies. This fault terminates upward at a depth of about 5,000 ft. This termination depth is below the late Miocene paleontological markers Rangia cuneata and Rangia johnsoni which indicates an age of cessation of activity of about 5.5. MYBP. it is probable that the cessation of salt dome uplift, the causal mechanism for this faulting, occurred at about the same time. At a depth of 5,000 ft., the fault plane lies 3.4 miles east of the NPIS. A north-north easterly striking fault (Fault 2C) intersects Fault 2B on the west flank of Good Hope dome (Figure 2.5-19). It is a normal fault and displaces sediments down to the east-southeast. This fault is part of a central graben-horst system above Good Hope dome (89). The location of the upward terminus of the fault is uncertain due to the lack of well control in the up-dip direction. However, the fault does not offset structural contours on Pliocene Horizon 3 (Figure 2.5-22).

Regardless of the period of activity of salt mobilization, the faults produced by salt domes are restricted to the area of domes. The faults known to exist above the Good Hope dome are also known to be restricted to the area of domes. These faults do not approach within 3.4 miles of the NPIS and do not constitute a hazard to any feature of the site.

2.5.3.3 - 2.5.3.8

There are no capable faults which could affect this site. Therefore, these sections do not apply.

2.5.4 STABILITY OF SUBSURFACE MATERIALS

2.5.4.1 Geologic Features

The Waterford Steam Electric Station is situated along the west (right descending) bank of the Mississippi River. It is located in the southern portion of the Gulf Coastal Plain physiographic province. This southern area is called the Mississippi River deltaic plain.

The sedimentary thickness beneath the site is estimated to be in excess of 40,000 ft. These sediments consist of the following: marine shales (between 40,000 ft. deep and 10,500 ft. deep); shale alternating with thin sandstone layers (10,500 ft. deep to 7,500 ft. deep);

massive sandstone interbedded with shale (7,500 ft. deep to 4,900 ft. deep); Pliocene alternating sands and clays (4,900 ft. deep to 1,900 ft. deep); Plio-Pleistocene interbedded sands and clays (1,900 ft. deep to 1,100 ft. deep); Pleistocene sands and clays (1,100 ft. deep to 50 ft. deep); and Recent alluvium deposits for the upper 50 to 60 ft. Subsection 2.5.1.2 presents a more detailed description, with figures, of the site geology and stratigraphy including two geological cross sections (Figure 2.5-28 and 2.5-29) of the stratigraphy in the upper 50 ft.

More complete and descriptive boring profiles for the upper 500 ft. are presented on Figure 2.5-49 through 2.5-52. The subsurface profile primarily consists of Recent alluvial deposits from grade to elevation -40 ft. MSL. This material is described as soft clays and silty clays with occasional sand lenses. Below elevation -40 ft. MSL there is a marked change in the soil strata indicating the start of Pleistocene age soils. The upper part of these soils are stiff, gray and tan clays with occasional silt lenses. These clays extend to about elevation -320 ft- MSL and contain only two significant and continuous silty sand strata. One is from elevation -77 ft. MSL to elevation -92 ft. MSL. The other is from elevation -235 ft. to elevation -245 ft. MSL. These silty sands are dense to very dense as indicated by standard penetration test results. The stratum below the stiff clays from elevation -320 ft. MSL to elevation -500 ft. MSL (the deepest elevation penetrated), is very dense gray silty sand.

The Pleistocene soil strata is further subdivided into five distinct zones, as shown on Figures 2.5-49 through 2.5-52. The zones are shown on Table 2.5-12.

All seismic Category I systems, equipment and components are supported within a common reinforced concrete structure. The foundation for the structure is a common reinforced concrete mat approximately 380 ft. long by 268 ft. wide. The foundation is designed as a part of the structure so that the combined foundation and structure act as an integral unit. The combined structure bears at elevation -47 ft. MSL (seven ft. into the stiff Pleistocene stratum). At this level, the foundation loads are completely compensated by hydrostatic uplift forces and impart an average stress to the underlying strata approximately equal to the original in situ effective stresses. Recent alluvium was removed to elevation -40 ft. MSL and the excavation back-filled with compacted sand.

There is no cavernous or karst terrain in the site area. The sediments are not subject to stress build-up with formation of deformational zones or other structural weaknesses.

Actual and potential site and regional subsidence is presented in detail in Subsection 2.5.1.3. Subsidence mechanisms discussed include petroleum production, groundwater withdrawal, gas production and crustal movement.

Subsection 2.5.4.2 discusses the engineering properties of the materials underlying the site. With the exception of the Recent alluvium, which - was removed, unstable conditions of the subsurface materials at the site due to mineralogy, lack of consolidation, or water content do not exist. The bases for concluding that the sand strata will not liquefy during the postulated SSE is discussed in Subsection 2.5.4.8.

Previous loading history of the foundation materials including deposition or sedimentation, water level fluctuations and glacial influences are discussed in Subsection 2.5.1.2. Structural irregularities such as faults are also discussed in Subsection 2.5.1.2.

2.5.4.2 Properties of Subsurface Materials

The following Subsection describes the significant engineering properties of the Recent alluvial material and the five strata investigated in the upper Pleistocene subsurface profile. Included are discussions of material classifications, strength determinations, consolidation characteristics and elastic properties. Test procedures and individual test results are presented in Appendix 2.5A. Final design values are summarized graphically on Figures 2.5-53 through 2.5-79 and numerically on Table 2.5-14.

2.5.4.2.1 Classification Characteristics

a) Moisture Content

Moisture content determinations were made on undisturbed tube and split spoon samples throughout the entire profile to a depth of 500 ft. (the deepest boring penetration depth). Results of these tests are presented on Laboratory Test Summary Table 2.5A-1 of Appendix 2.5A. Moisture content test results are also presented along side the individual boring logs on the subsurface profiles (Figures 2.5-49 through 2.5-52). The mean moisture content in the Recent alluvial material is 40 percent. Moisture content of the sandy Pleistocene material is 25 percent. Pleistocene clays and silts have a mean moisture content of 37 percent; the lower moisture contents occur above the -77 ft. MSL sands and the higher moisture contents occur below the sand layer.

b) Grain Size Distribution

Grain size distribution (GSD) ranges for each stratum are presented in Figures 2.5-53 through 2.5-59. Shown on these curves are the coarsest and finest limits of all tests performed and the mean grain size distribution for the stratum. The test results showed good agreement with preliminary visual descriptions made during the subsurface boring investigation program. Individual GSD curves are presented on Figures 2.5A-1 through 2.5A-60 of Appendix 2.5A.

c) Atterberg Limits

The plasticity characteristics of the Pleistocene silty and clayey strata are presented graphically as plots of liquid limit (LL) versus plasticity index (PI) for each stratum on Figures 2.5-60 through 2.5-65. These results are also presented numerically on the Laboratory Test Summary Table 2.5A-1 and along side the individual boring logs from the subsurface profiles (Figures 2.5-49 through 2.5-52).

Unified Soil Classification descriptions (72) for the silty and clayey strata are summarized in Table 2.5-13.

d) Unit Weight Measurements

Natural density determinations were performed on selected samples throughout the geologic profile. The mean natural density for each stratum is presented on the subsurface profiles (Figures 2.5-49 through 2.5-52) and in Table 2.5-14. Individual density test results are presented in Appendix 2.5A, Table 2.5A-1 and adjacent to the individual boring logs in the subsurface profiles (Figures 2.5-49 through 2.5-52).

e) Specific Gravity

Specific gravity (Gs) tests were performed on samples taken in the different strata. These tests were performed in conjuction with the consolidation tests. Individual (Gs) test results are presented with each consolidation test (Appendix 2.5A Figures 2.5A-16 through 2.5A-247). The mean specific gravities for each stratum are presented in Table 2.5-14.

2.5.4.2.2 Permeability

Coefficients of permeability (K) were determined using falling head permeability tests and one dimensional consolidation tests. These individual results are presented in Appendix 2.5A (Tables 2.5A-2 and 2.5A-3). For design purposes the following permeabilities were used.

Recent alluvium........................	$K = 1.5 \times 10^{-6}$ cm/sec
stiff upper Pleistocene clays..........	$K = 10^{-8}$ cm/sec
elevation -77 ft. MSL Pleistocene sands	$K = 3 \times 10^{-5}$ cm/sec

2.5.4.2.3 Strength Determinations

a) Unconfined Compression Tests

Unconfined compression (UC) tests were performed on selected undisturbed and remolded samples throughout the geologic profile to determine undrained static shear strength. UC tests were performed in the horizontal direction as well as vertically and on specimens of varying dimensions in order to investigate the Recent materials for excavation slopes. A summary plot of unconfined compressive strength (qu) and cohesion (C=qu/2) versus depth is presented graphically on Figure 2.5-66. Also shown on the plot are the final design cohesion values used for all silty and clayey materials encountered in the geologic profile. Design values for each stratum were taken as the mean of all test results within that stratum. Individual test results, including horizontal and vertical tests, undisturbed and remolded tests and specimens of varying dimensions are presented in Appendix 2.5A, Table 2.5A-1. Individual UC test results are also indicated adjacent to the boring logs on Figures 2.5-49 through 2.5-52.

b) Unconsolidated Undrained Tests

Unconsolidated undrained (UU) shear strength tests were performed on selected undisturbed samples from the Recent alluvium and Pleistocene material to determine the undrained static shear strength of these materials. These tests included triaxial compression tests and direct shear tests. Individual test results are numerically presented in Appendix 2.5A, Table 2.5A-1 as undrained cohesion (c) and undrained friction angle (ϕ). The results are also presented graphically as Mohr's envelope/plots and deviator stress versus axial strain plots in Appendix 2.5A (Figures 2.5A-61 through 2.5A-156).

Summaries of all UU tests for each stratum in which tests were performed are presented in Figures 2.5-67 through 2.5-69. These figures present maximum and minimum Mohr's strength envelopes along with the conservatively selected design envelope used. Generally the UU tests indicated higher undrained shear strengths than were obtained with the unconfined compression tests. Therefore the design strength envelopes selected based on the unconfined compression tests were conservative.

c) Consolidated Undrained Tests

Consolidated undrained triaxial shear tests with pore pressure measurements $\overline{\text{CIU}}$ were performed on selected samples of the Recent alluvium and Pleistocene clays. These tests produced drained and undrained Mohr's circle shear strength envelopes. The drained or long-term shear strength was obtained by subtracting the test load induced pore pressure buildup from the actual total stress (effective intergranular stress plus pore water stress). The undrained shear strength was obtained by plotting total stress Mohr's circles.

Individual $\overline{\text{CIU}}$ test Mohr's circle plots including deviator stress versus strain plots, are presented in Appendix 2.5A (Figures 2.5A-157 through 2.5A-160). The undrained strength envelopes are summarized in Figures 2.5-70 and 2.5-71 according to the stratum from which the test specimens were obtained. Similarly, the drained strength envelopes are summarized in Figures 2.5-72 and 2.5-74.

The undrained shear strength envelopes obtained from the CIU tests exhibited higher friction angles than the unconsolidated undrained test results from the same strata. This is due to specimen consolidation under each increasing confining pressure. For conservatism, the design envelopes used and presented on Figures 2.5-70 and 2.5-71 are the shear strengths obtained from the unconfined compression tests performed in the respective strata. This sheer strength is considerably lower than the shear strength obtained from the $\overline{\text{CIU}}$ tests, particularly in the range of in situ confining pressures.

The $\overline{\text{CIU}}$ drained shear strength envelopes for the Recent material (Figure 2.5-72) exhibited either little or no effective cohesion (c') but a high effective friction angle (ϕ). For design purposes any contributing effective cohesion (c') from these materials was ignored and the shear strength was conservatively selected as frictional resistance alone. Due to the overconsolidated state of the Pleistocene clays, the drained shear strength of these materials consisted of some effective cohesion (c') and effective frictional resistance (ϕ). The drained design envelope for the Pleistocene clays shown on Figure 2.5-74 was selected as the average of the maximum and minimum strength envelopes.

d) Consolidated Drained Tests

A series of consolidated drained (CD) triaxial tests were performed on reconstituted test specimens of the -77 ft. MSL Pleistocene sands. Due to the quick draining nature of these sandy materials, triaxial tests where the specimen is allowed to drain during shearing yielded the best estimation of the strength of the material. The effective shear strength of this material is purely frictional. The drained shear strength envelope for this material is plotted on Figure 2.5-73.

Final design shear strength values for all strata are presented as either drained (long term) or undrained (short term) strengths. These results are numerically presented on Table 2.5-14 and represent strength selections based on the above discussed criteria.

2.5.4.2.4 Consolidation Characteristics

Several one dimensional consolidation tests were performed on all strata except the -77 ft. MSL sands and the dense sands below elevation -317 ft. MSL. Individual test results are graphically presented in Appendix 2.5A, Figures 2.5A-161 through 2.5A-247. Each test is plotted as void ratio (e) versus log of effective pressure. Included is a plot of coefficient of consolidation (Cv) versus log of effective pressure, compression index, and the overconsolidation ratio (OCR) for each test. OCR is also plotted versus depth for the different strata in Figure 2.5-75 and presented numerically in Table 2.5-14. The upper Pleistocene clays at the mat level are highly overconsolidated with an OCR of 3.4. This is the result of a stage when the stratum was subjected to the combined effects of desiccation and overloading. The Pleistocene clays between tile -77 ft. MSL sands and the -317 ft. MSL sands range from low to medium overconsolidated with OCR values ranging from 1.4 to 2.4.

2.5.4.2.5 Elastic Properties

a) Elastic Properties Seismically Determined

Elastic properties of the subsurface soils were seismically determined from the cross-hole, up-hole and refraction surveys. Test results procedures and equipment used during seismic surveys are described in detail in Subsection 2.5.4.4. To summarize these results five seismic refraction traverses were made at and near the site. The locations of the traverse lines are shown in Figure 2.5-33. The results of the refraction survey is a compression wave (P-wave) profile (Figures 2.5-35 through 2.5-38) for each traverse. Compression wave velocities range from 2,000 ft. per second (fps) to 4,000 fps in the Recent material and 5,000 fps in the upper Pleistocene clays. An up-hole velocity survey was conducted in boring B-41. The results of this survey is a time-distance curve which was interpreted for P-wave velocity. The range of these results is shown versus depth on Figure 2.5-76. Shear wave (S-wave) velocities obtained using seismic cross-hole surveys are similarly presented on Figure 2.5-76. Using these results, shear modulus (G) Young's modulus (E) and Poisson's ratio (M) were determined.

Shear Modulus:

Shear modulus was calculated using the equation

$$G = \rho Vs^2$$

where ρ= mass density of the soil and Vs is the shear wave velocity of the stratum being considered. Figure 2.5-76 presents the results of the shear modulus calculations for each stratum. Presented are two sets of properties; average (G) for the Recent material, upper Pleistocene and lower Pleistocene are plotted versus depth using the solid line. These values are the result using average Vs measurements of 550 fps and 1,600 fps for the Recent, upper

Pleistocene and lower Pleistocene materials, respectively. Also presented on the same figure is a detailed plot of shear modulus versus depth for each stratum. These detailed (G) values are the result of more closely modeling the actual Vs profile with depth and were used in the ground motion analysis discussed in Subsection 2.5.4.7.

Poisson's Ratio:

Poisson's ratio (M) was computed using shear wave (Vs) and compression wave (Vp) velocities presented on Figure 2.5-76 in the equation:

$$\mu = \frac{1/2\ \frac{Vp^2}{Vs}\ - 1}{\frac{Vp^2}{Vs}\ - 1}$$

Poisson's ratios for each stratum are presented in Table 2.5-14. The results for all strata are typically between) 0.45 and 0.49. This is in good agreement with Whitman (73) who recommends a value of 0.5 for fully saturated soils. The results also agree well with the laboratory determinations of Poisson's ratio as 0.5 for all strata.

Young's Modulus:

Young's modulus of elasticity (E) was similarly calculated using the following equation:

$$E = 2G\ \ (1 + \mu)$$

where G and M are the results of previous calculations. Values of (E) for each stratum are presented in Table 2.5-14.

b) Elastic Properties From Laboratory Tests

Cyclic triaxial shear tests were performed on selected undisturbed samples of Recent alluvial material and from the upper Pleistocene clays. Results of these tests combined with field seismic data produced strain-dependent shear moduli for the different strata. Damping, as a function of strain, was similarly obtained from cyclic triaxial tests and by comparisons with accepted published damping results. Poisson's ratio was statically measured using a standard triaxial cell apparatus.

Shear Modulus:

Shear modulus (G) versus shear strain (γ) for the Recent alluvial material is presented on Figure 2.5-77. Also included on the curve is the calculation of (G) from field seismic cross-hole Vs measurements. The field data provides (G) for the low shear strain ranges (10^{-6} in./in.) and the laboratory data provides degradation of (G) with strain. Both field and laboratory determinations of (G) show good agreement.

The shear modulus curve for the upper Pleistocene materials (between elevation -40 ft. MSL and -317 ft. MSL) is presented on Figure 2.5-78. Along with the laboratory test results are superimposed the range of field measurements of (G) in the low strain ranges and calculations of (G) as per Hardin and Drnevich in the high strain ranges.(74) Field, laboratory and calculated (G) values show good correlation.

No cyclic laboratory measurements were made in the lower Pleistocene sandy material (below elevation -317 ft. MSL) so a recommended (G) versus shear Strain curve was prepared using results obtained by Seed and Idriss (75). This curve, shown on Figure 2.5-79, is typical of sandy dense material similar to the lower Pleistocene material.

Damping:

The strain dependent damping (λ) of the upper Pleistocene and Recent alluvium samples tested in the laboratory cyclic triaxial testing program was masked by hysteresis of the test apparatus. However, since the shear moduli of the samples tested are in excellent agreement with the relationship proposed by Seed (75), the use of the published (λ) -shear strain relationship is appropriate for both Recent alluvium and upper Pleistocene deposits. The damping curves for the Recent and upper Pleistocene material are presented on Figures 2.5-77 and 2.5-78 respectively.

The strain dependent damping of the lower Pleistocene sands is taken from cyclic triaxial tests performed on similar compacted sand backfill material and is presented on Figure 2.5-79.

2.5.4.3 Exploration

In order to fully investigate the materials at the site, comprehensive subsurface investigation and instrumentation programs were implemented. A total of 74 soil borings were drilled at the site by Eustis Engineering Company of New Orleans, Louisiana. Individual boring logs are presented in Appendix 2.5B. The sampling methods were done in accordance with ASTM standard procedures. To obtain disturbed samples and blow count resistance measurements ASTM D 1586 ("Penetration Test and Split - Barrel Sampling of Soils") was used. Undisturbed sampling was done in accordance with ASTM D 1587 ("Thin Walled Tube Sampling of Soils"). Penetrometer and Torevane readings were made in cut-off end sections of undisturbed tube samples in the field prior to sealing the samples with parafin. The equipment used to perform the tests consisted of the Soil Test CL-600 Torevane Shear Device and the Soil Test CL-700 Pocket Penetrometer.

Continuous undisturbed thin wall tube samples were taken in the fine grained soils (silts and clays) wherever standard penetration test results are not shown on the boring logs. Where sandy soils were encountered the split-barrel sampler was primarily used. In order to accurately define the subsurface profile the undisturbed thin wall tube samples were carefully extruded from the tubes in the field and laid out in sequential order. A shallow continuous scratch mark was made along the side of each sample and any color and material changes were recorded and are reflected in the final boring description. The undisturbed samples were then sealed in parafin.

Five seismic refraction traverses as well as cross-hole and up-hole geophysical studies were made by Law Engineering of Marietta, Georgia. Locations of seismic refraction traverses and borings are shown on Figures 2.5-33 and 2.5-48, respectively. A complete description of the geophysical program including seismic velocity plots is presented in Subsection 2.5.4.4.

Locations of instrumentation including piezometers and settlement monuments are shown on Figure 2.5-112 and are discussed in detail in Subsection 2.5.4.13.

From the results of the boring program five generalized soil profiles (Sections A-A. through E-E) were prepared and are presented in Figures 2.5-49 through 2.5-52. Through investigation of the individual boring logs, the stratigraphy proved to be very uniform, laterally, therefore the generalized soil profiles were prepared incorporating the mean thickness of the individual strata. The location of the combined strticture and backfill material relative to the generalized soil profile is presented on Figure 2.5-80.

To supplement the boring program a detailed geologic map of the final excavation was made. The Phase IV excavation stage was the final cut eight ft. vertically into the stiff Pleistocene clays, from elevation -40 ft. MSL to -48 ft. MSL, within which the combined structure mat was constructed. Refer to Subsection 2.5.4.5 for a more complete description of the excavation. The mapping program was a three-fold operation consisting of visual observations of final exposed cut vertical faces and excavation bottom. Field in-place pocket penetrometer, torvane, density and grain size tests were performed at several locations. The results of visual observations and in-place tests are presented on Figure 2.5-30. Photographs were also made of the entire Phase IV excavation and are on file at the site.

The mapping showed good agreement with the layering profile encountered through the boring program and exhibited no offsets or discontinuities across the site. Material properties were also consistent with properties measured in the laboratory. The only slight anomoly encountered was an old erosional surface in the top of the Pleistocene and was localized in the southeast corner of the Phase IV excavation where the top of the Pleistocene was eroded to elevation -46 ft. MSL. The eroded area, however, was within the Phase IV excavation and was therefore removed. The remaining eroded Pleistocene surface outside the structure was backfilled to -40 ft. MSL with a compacted clay and shell mixture shown on the south and southeast cut face profiles on Figure 2.5-30.

Additional studies of this erosional feature were performed to verify that it is not a surface expression of a deeper faulting situation. A top-of Pleistocene contour map was prepared utilizing the boring information in conjunction with the results of the mapping program. This contour map is shown on Figure 2.5-30a. The results show, with the exception of the feature, that the Pleistocene surface is, in fact, uniformly flat with no more than a two-foot variation across more than 1000-feet. The feature is shown to be confined to the area delineated by the Geologic Mapping Report.

The boring data utilized to prepare this contour map are as follows:

Boring Number	Top of Pleistocene Elevation-Ft	Boring Number	Top of Pleistocene Elevation - Ft
1	-38.5	19	-39.8
2	-40.5	21	-40.1
3	-38.7	25	-45.0
4	-39.5	26	-38.0
5	-45.1	27	-36.1
6	-39.9	28	-41.3

Boring Number	Top of Pleistocene Elevation-Ft	Boring Number	Top of Pleistocene Elevation - Ft
7	-40.4	29	-39.1
8	-39.4	30	-40.8
9	-39.4	31	-41.0
10	-40.1	34	-38.4
11	-38.8	35	-37.1
12	-38.5	36	-38.2
16	-39.5	37	-38.4
17	-38.8	38	-41.4
18	-39.1	39	-40.6
40	-38.7	59	-40.1
41	-39.3	60	-40.4
42	-40.8	61	-39.8
43	-38.1	62	-41.5
44	-39.8	63	-47.1
45	-40.3	64	-40.3
46	-40.2	65	-41.0
51	-39.5	66	-41.0
52	-39.8	67	-45.0
53	-39.9	68	-40.3
54	-39.5	69	-38.5
55	-39.9	70	-39.0
56	-38.6	71	-38.8
57	-41.4	72	-39.9
58	-40.7	73	-38.5
		74	-38.1

Four subsurface profiles were constructed in the immediate vicinity of the feature utilizing the boring and mapping information. These profiles are shown on Figures 2.5-30b, c, d and e. They show good agreement with the more generalized site profiles shown on Figures 2.5-49 through 2.5-52 and they show that the feature is confined to the top of the Pleistocene formation. The soil strata beneath the feature show no evidence of offsets or depressions and are all horizontal, thus precluding the possibility of any type of faulting activity.

2.5.4.4 Geophysical Surveys

a) Refraction Seismic Survey

Five seismic refraction traverses were made at and near the site. The location of the traverse lines are shown on Figure 2.5-33. In all of the seismic traverses, geophones were spaced at 50 ft. intervals and explosive charge of a 1/2 to 10 pounds of 90 percent gelatine dynamite, were fired at shot points located 50 to 1650 ft. from the ends of the spread.

Figure 2.5-34 is a time-distance plot of the seismic first arrival times at their respective geophone locations. The travel times have been corrected to those which would have occurred if all geophones and shot points were at zero ft. MSL. These corrections were relatively minor due to the low relief of the profile. Figures 2.5-35 through 2.5-38 are cross sections showing the interpreted velocity interfaces. A layered model was used for data analysis because the site geology is horizontally layered.

The interpreted sections indicate two velocity interfaces in the upper 50 ft. of sediments at the site. The upper interface divides materials exhibiting compressional wave velocities of 2000 fps from those with velocities of 4000 fps. This interface occurs within the Recent soft clays and silty clay, and probably corresponds to the position of the groundwater table. The compressional wave velocity below the interface, (4000 fps) is lower than is expected for saturated clays and sands. These values were measured in materials with organic and fiber content. Even though the organic materials are below the groundwater level, they contain gases which prevent their complete saturation. The values measured are typical of organic materials.

The second velocity interface occurs at about a 50 ft. depth and divides compressional wave velocities of 4000 and 5000 fps. This interface approximately marks the boundary between Recent and Pleistocene soils. The Pleistocene clays have a consistency significantly greater than the overlying soils, which results in the increased velocity.

b) Up-Hole Survey

To aid in determination of elastic moduli, an up-hole velocity survey was conducted in boring B-41. Explosive charges were fired at various depths (from -220 ft. MSL to the ground surface) and both compressional (P) and shear (S) waves were recorded by means of an array of both vertical and horizontal geophones located at the ground surface around the hole. The geophones were placed at 15 and 30 ft. horizontal offset distances from the top of the hole. The result of the survey is a time-distance curve which can be interpreted for P-wave and S-wave velocity.

Representative compressional wave velocities and their ranges, for the strata at the site, are shown on Figure 2.5-76.

c) Cross-Hole Survey

Prior to beginning the cross-hole measurements, the site had been excavated in the reactor area to approximately elevation -5 ft. MSL, a removal of some 20 ft. of overburden soils. During excavation the groundwater table had been lowered to approximately -20 ft. MSL. The area of primary interest for shear wave measurements was the Pleistocene strata between -40 ft. MSL and -220 ft. MSL. Review of the boring logs indicated that dense or hard layers occurred near approximately -90 and -160 ft. MSL. These layers were suspected of being higher velocity layers due to consistently higher penetration resistances on the boring logs. Both of these layers are of limited vertical extent and appear to be between 10 and 15 ft- thick. Therefore, these zones constituted approximately 30 ft. thickness in the entire 180 ft. of the Pleistocene formation. The remainder of the soils appeared to be relatively uniform silts and clays. Elevations for measuring cross hole velocities were selected to be -50, -65, -87, -102 and -160 ft. MSL. These elevations were selected so as-to provide representative information of the soils which constitute the majority of the Pleistocene formation and information within the two zones suspected of being higher velocity layers.

Two drill rigs were used to advance two simultaneous borings. One boring was used for generating energy, the other used for monitoring the arrival of seismic waves. The energy source used was a hammer driven soil sampler seated in the bottom of one hole. A multi-component geophone was used to record seismic arrivals in the bottom of the second hole. Both P- and S-wave arrivals were recorded.

In every case, the P-wave arrivals indicated a velocity of 4500 fps corresponding to the P-wave velocity of water.

The shear wave velocities measured by the cross hole method are shown plotted on Figure 2.5-76. The velocities ranged from a low of 730 fps at -50 ft. MSL to 1230 fps at -160 ft. MSL. Our interpretation of this shear wave velocity profile is based on: (1) the field measured values of shear wave velocity, (2) the concept that the shear wave velocity should increase as an expontential function of the effective confining pressure and, (3) the actual stratification at the site as indicated by boring logs and standard penetration tests.

The departure of the shear wave velocity profile from the measured velocity at -50 ft. MSL is a result of the unloading of the Pleistocene soils due to the excavation to -5 ft. MSL. Heave point indicators placed at the surface of the Pleistocene have indicated heave during excavation. Effective stress changes and void ratio changes could also effect the velocity at this elevation.

It was concluded that the upper Pleistocene strata (above -317 ft. MSL) should be considered to have an average seismic shear wave velocity of 1,000 fps. The resulting shear modulus of elasticity is 27 x 10^3 psi. This value is consistent with the range of shear moduli determined by laboratory tests and with the Hardin-Black and the Hardin-Drnevich equations. Based on knowledge that shear wave velocity increases as an exponential function of the effect' confining pressure and literature published by Seed and Idriss (75) the shear wave velocity profile was accordingly extended eighty ft. into the lower Pleistocene strata (below -317 ft. MSL). It was concluded that an average seismic shear wave velocity for this strata is 1600 fps with a corresponding shear modulus of elasticity of 69 x 10^3 psi.

d) Borehole Electrical Logging

→ (DRN 01-360)

Borehole electrical logging services at this site were provided by Schlumberger Services under the direction of Law Engineering Testing Company. The logging program consisted of an Induction Electrical Survey (IES) on six borings; B-3, B-5, B-7, B-26, B-41, and B-42. The IES consists of simultaneous recording of a spontaneous potential curve and a normal resistivity curve. These logs are presented as Figures 2.5-32(a) through 2.5-32(f). Figures 2.5-32(a) through 2.5-32(f) are classified as historical pursuant to Waterford 3 Site Procedure W4.504 and Nuclear Energy Institute (NEI) 98-03. The figures have been physically removed from the UFSAR. However, the figures are incorporate by reference, and thus they continue to be a part of the UFSAR. These figures are available for reference and use in Document Control, and they may be found as record ER-W3-01-0268-00-00 / DRN 01-360.

← (DRN 01-360)

2.5.4.5 Excavation and Backfill

As discussed in Subsection 2.5.4.1 Recent alluvial material in the plant area was removed to elevation -40 ft. MSL and replaced with compacted sand backfill. A one ft. thick compacted shell filter blanket was placed immediately under the common combined structure mat. This shell blanket serves to evenly distribute uplift buoyant forces on the underside of the mat as well as provide an acceptable working surface. The limit and extent of the excavation and backfill at the site is presented in plan on Figure 2.5-81 and in section on Figure 2.5-82.

Approximately 1,067,000 cubic yards of material were excavated and backfilled with 462,000 cubic yards of Class A and 369,000 cubic yards of Class B backfill. 4000 cubic yards of compacted shell were placed under the common mat.

All excavation work was performed by Boh Brothers Construction Company of New Orleans. Backfilling was done by J. A. Jones Construction Company of Charlotte, North Carolina.

2.5.4.5.1 Excavation

The excavation to -48 ft. MSL, for the combined structure, was performed in four phases. An additional excavation was extended to accommodate the design change of founding the turbine building on compacted fill rather than piles (refer to Subsection 2.5.4.14). The excavation geometry in the Recent material consisted of 4H:lV cut slopes with two 15 ft. wide berms; one at elevation -5 ft. MSL and one at elevation -22 ft. MSL. The effective slope configuration with berms was 5H:lV. With the change in turbine building design from a pile foundation to spread footings, the initial excavation was expanded approximately 200 ft. south. The Recent soils in this area had the benefit of being dewatered for a year prior to being re-excavated thus, allowing the Recent alluvial slope material to become more stiff. Therefore, the extension cut slope was made at 3H:lV.

The following stages of excavation were performed:

	Excavated			
Stage	From	To	Started	Finished
Phase I	Grade	-5 ft. MSL	April, ’72	July, ’72
Phase II	-5 ft. MSL	-22 ft. MSL	January, ’75	June, ’75
Phase III	-22 ft. MSL	-40 ft. MSL	April, ’75	August, ’75
Phase IV	-40 ft. MSL	-48 ft. MSL	October, ’75	March, ’76
Turbine Bldg. Extension	Grade	-40 ft. MSL	January, ’77	March, ’77

To facilitate the removal of the soft upper 30 ft. to 35 ft. of the Recent material, several steel tread Monaghan dragline excavators working from wood platforms were set up in a line. The material was removed by continuously working it from north to south passing the material from one dragline to the next. The lower 15 to 20 ft. of Recent material to the top of the Pleistocene (-40 ft. MSL) was excavated from north to south using backhoes. The turbine building excavation was performed by working the material down from the top of the slope with bulldozers.

The excavation for the combined structure mat (Phase IV excavation) was performed with backhoes by making an eight ft. vertical cut in the stiff Pleistocene material to elevation -48 ft. MSL. Lateral dimensions of the cut were equal to that of the common mat. The excavation was performed in strips: the initial strip was approximately 120 ft. wide running the full width of the common mat (267 ft.). The first strip was cut under the Reactor Building area. The subsequent strips (No. two through No. six) were cut north and south of strip No. one (see Figure 2.5-30). In order to minimize foundation heave caused by Phase IV excavation, concrete placements for the common mat were made simultaneously in the alternate strips, working numerically from Strip No. one to Strip No. six. This sequence of concrete placement kept the final cut in the Pleistocene material open for a minimum amount of time.

All exposed vertically cut faces were immediately gunited within eight hours of exposure to prevent desiccation prior to concrete mat placement.

To monitor the integrity of the excavation, a comprehensive instrumentation program was implemented. Refer to Subsection 2.5.4.13 for a complete discussion of the instrumentation devices, program implementation and measured results. In summary; the bottom of the excavation heaved between 0.4 ft. and 0.8 ft. prior to placement of backfill and concrete. Presently, through the imposed backfill and concrete loads, this heave is nearly recompressed back to in situ conditions, thus eliminating long term settlement of the foundation materials. Measured lateral excavation slope movements in the Recent material ranged from between 2.5 in. and five in. away from the open cut at the top of the slope, and between 1.5 in. and 3.5 in. towards the open cut at elevation -26 ft. MSL. Measured lateral slope movements in the Pleistocene materials were negligible. With excavation complete and with backfilling nearly complete, the slopes virtually stopped moving and in some instances have returned slightly towards their initial positions. Cut slopes in the Recent material did not adversely affect the integrity of the foundation material. The negligible lateral movements measured in the Pleistocene material beneath the cut slopes also were not adverse to the quality of the foundation material beneath the combined structure.

2.5.4.5.2 Dewatering

A dewatering system consisting of deep wells with submersible pumps was used to control groundwater elevations at the site. The system was installed and operated by Moretrench American Corp. of Rockaway, N.J. Presented on Figure 2.5-83 is a plan showing the locations of all dewatering wells used. The system consists of 251 dewatering wells located around the perimeter of the excavation. 217 of these perimeter wells pump from the Recent material; the ejector tips being at elevation -40 ± ft. MSL. The remaining 34 perimeter wells pump from the -77 ft. MSL Pleistocene sands. These ejector tips are at approximately elevation -95 ± ft. MSL. A second series of 12 deep pump relief wells are located around the combined structure common mat and also pump from the -77 ft. MSL sands.

The purpose of the dewatering system is to draw down the water levels in the plant area below the excavation in order to implement the design criteria presented in detail in Subsection 2.5.4.11. The design consists of regulating groundwater levels so that the reduction in effective stress resulting from removal of material is balanced by the increase in effective stress due to dewatering. In this manner much of excavation-caused heave (rebound) is prevented. The design criteria during construction consists of reloading the foundation soils with concrete and backfill loads up to 1200 psf in excess of the original in situ stress in order to further recompress excavation-caused heave. This 1200 psf overload limit is reached by maintaining a completely dewatered site while construction proceeds. Subsequent to reaching this maximum overload limit the water level will be allowed to rise and the dewatering system will be throttled down in order to induce hydrostatic uplift forces compensating further load increases and thus maintain the limit.

Prior to the installation of the pump relief well system within the central portion of the excavation, the perimeter system pumping rates ranged from between 140 gpm and 220 gpm. With the operation of the additional pump relief wells in October, 1975, overall dewatering rates increased to between 220 gpm and 360 gpm. Fluctuations in the overall pump rates were caused by changes in river elevation, mechanical malfunctions and changes in the number and efficiency of operating pumps within the system.

Flowrates for the system were monitored on a daily basis, and, a qualitative and more direct review of the performance of the system towards the design intent was made utilizing piezometric records and heave settlement measurements discussed in Subsection 2.5.4.13.

2.5.4.5.3 Backfill

2.5.4.5.3.1 Material Selection

The backfill material consists of clean sand, designated Class A material, placed immediately around seismic Category I structures from grade (+17 ft. MSL) to -40 ft. MSL and Class B material to backfill the remainder of the excavation up to natural grade. Refer to Figures 2.5-81 and 2.5-82 for a plan and cross sections of the backfill material.

Class A material is basically clean pumped Mississippi River sand with no more than 12 percent fines content. The selection of this material was based on its ability, when compacted, to safely resist static and dynamic loading conditions. Economics of availability and ease of placement also provided contributing factors in the selection of this material. Class B material is non-seismic Category I material consisting of sand or a combination of sand and clam shell filter material capable of practical compaction. The filter blanket placed immediately beneath the common mat consists of one ft. thick compacted layer of clam shells dredged from Lake Pontchartrain. This type of material was selected because of high permeability which facilitated its use in evenly distributing the hydrostatic uplift forces on the underside of the mat. It was also able to be well compacted eliminating any settlement considerations.

2.5.4.5.3.2 Material Placement

Class A and Class B backfill and the compacted shell filter blanket placement procedures were done in accordance with Ebasco Specification No. LOU 1564.482 - Filter and Backfill. This document is presented in Appendix 2.5C.

The Class A fill was spread in 15 in. thick lifts and compacted to a specified in-place relative density of 75 percent. In analyzing the compacted Class A backfill as a whole, a statistical approach was adapted based on a paper written by R.A. Pettit(76) and on a paper written by H.K. Cook(77).

→(DRN 01-464, R11-A)

This approach specified the in-place compacted Class A backfill to be a minimum relative density of 75 percent. The allowable variation for the Class A fill less than the specified density was a maximum of one standard deviation. The numerical value of the standard deviation for this material was periodically established by a series of field tests conducted during the initial compaction operation and was reported in terms of minimum allowable density required. Presented on Figure 2.5-84 is a typical cumulative statistical study of relative density calculations made for the Class A fill. These relative densities were converted from field densities by the use of the correlation curve presented in Figure 2.5-85. The correlation curve was constructed using cumulative test data or random samples taken from the fill. The following procedure was used to develop Figure 2.5-85:

←(DRN 01-464, R11-A)

1) A representative 300 lb. sample was obtained from the fill.

2) 100 lbs was sent to the field lab and 200 lbs was sent to the home lab (Peabody Testing) for parallel testing to determine a Modified Proctor compaction curve and percent finer than #200 sieve.

3) The parallel results were compared, the Proctor densities agreed to within ± 2 pcf and the percents finer than the #200 sieve agreed to within ± 3 percent. Therefore, the hole lab proceeded to perform maximum (γmax) and minimum (γmin) density determinations on the material.

4) The following equation was used to plot Figure 2.5-85:

→(DRN 06-905, R15)

$$\text{Dry Density} = \frac{\gamma\, max\, \gamma\, min}{\gamma\, max - Dd(\gamma\, max - \gamma\, min)}$$

←(DRN 06-905, R15)

Where:

Dry Density = field dry density

Dd = relative density

γmax, γmin = measured in the home lab for this material type

The curve was established by assuming various Dd values and calculating Dry Densities. The following calculations were made and plotted:

Dd (assumed)	Dry Density (calculated)
0.50	93.3
0.55	94.3
0.60	95.3
0.65	96.3
0.70	97.3
0.75	98.3
0.80	99.4
0.85	100.5
0.90	101.6

Dd (assumed)	Dry Density (calculated)
0.95	102.7
1.00	103.9
1.05	105.1
1.10	106.3
1.15	107.6
1.20	108.8
1.30	111.5
1.40	114.3
1.50	117.2

Figure 2.5-85 was developed for one family of material where maximum Proctor densities were within 2 pcf and the percents passing the #200 sieve were within 3 percent. The curve was also continuously verified by performing one relative density test for every 200 in-place density tests. All backfill placed up to and including this study belonged to one material type typified by Figure 2.5-85.

The results of this numerical analysis are typical and representative of other similar analyses performed on the Class A fill. This study indicates a mean relative density of the Class A compact fill of 94.0 percent with a standard deviation of 14.3 percent.

Only 5.2 percent of all tests fell below the minimum required 75 percent relative density, well within the allowable statistical variance of 14.3 percent for one standard deviation below 75 percent.

It is concluded from these analyses that the specified compaction criteria was met thus measuring the quality of the backfill desired.

Class B backfill was spread in layers not exceeding 10 in. thick and compacted to an in-place density of 90 percent of the Modified Proctor density.

The shell filter blanket was placed in a single lift and compacted to a one ft. thick layer. Prior to placement of the shell material a Marafi 140 filter cloth was placed over the exposed Pleistocene clays and silts in order to prevent contamination of the shell when compacted. Due to the sensitive nature of the shell to laboratory compaction by various techniques it was difficult to set a degree of compaction or relative density as a criteria for placement of the material. Settlement considerations and permeability were therefore selected as the governing criteria for the shell filter placement.

To determine these characteristics of the compacted shell material a comprehensive test fill section was established investigating several methods of placement. Permeability measurements on in situ compacted test specimens indicated sufficiently high permeabilities for all compaction efforts (approximately 10^{-1} cm/sec). This insured the high permeability required for the compacted material to operate effectively as a filter blanket.

Settlement considerations in the filter layer were resolved by utilizing the compaction effort, determined from the test fill, beyond which negligible settlement occurred by increased compaction effort.

In-place density test frequencies on the above backfill and filter materials was as follows:

Class A backfill	one test* in each lift for every 20,000 sq ft. of compacted material.
Class B backfill	one test* in each lift for every 40,000 sq ft. of compacted material.
Shell filter blanket	one test** for every 5000 sq ft. of shell filter blanket.

2.5.4.5.3.3 Backfill Quality Control

A comprehensive quality control program was implemented to insure the integrity of the compacted materials. An Ebasco Site Soils Engineer was resident at the site to insure the design intent of the earth related activities and assure compliance with the backfill procedures and tests. The areas of responsibility in performing QC activities were the following:

> Material acceptance - the performance of inspections of the backfill material to determine its acceptability were performed by Ebasco;
>
> Construction Activities - inspection of placement and compaction operations were performed by J. A. Jones Construction Company with designated inspections by Ebasco;
>
> Soils Testing - under the direction and supervision of Ebasco, field in-place and basic laboratory tests were performed by Peabody Testing of Chicago and state-of-the-art static and dynamic Class A backfill tests were performed by Woodward Clyde Consultants of Clifton, New Jersey;
>
> Documentation - all field quality control records were prepared by the proper agency stated above and then compiled into a single package for each backfill lift by Ebasco.

For a complete description of quality control responsibilities and procedures refer to procedure number QCIP-2, "Procedure For Soils Control" included in Appendix 2.5C.

2.5.4.5.3.4 Laboratory Testing

An extensive state-of-the-art laboratory testing program was performed on the Class A fill by Woodward-Clyde Consultants of Clifton, New Jersey.

The program consisted of index property tests, static, triaxial tests, cyclic, properties tests and cyclic strength (liquefaction potential) tests.

---

* ASTM - D1556, ASTM - D2167 or ASTM -D2922

** ASTM - D1556 or ASTM - D2167

A representative test sample of the Class A backfill was obtained by Peabody Testing Services under the supervision of Ebasco's qualified site soils engineer. For conservatism, static and dynamic strength tests and cyclic properties tests were performed on reconstituted samples compacted to 85 percent relative density. This density is approximately nine percent below the mean relative density of 94 percent as determined by field statistical studies, discussed in Subsection 2.5.4.5.3.2. An additional field-laboratory comparison check was made by performing several particle size analyses and a modified Proctor compaction test on the laboratory sample. The results agreed with similar tests performed on the same material in the field. This assured continuity of interpretation of the material between the field studies and laboratory tests.

The reason for the discrepancy between 100 percent relative density at 99 pcf on Table 2.5-15 and 100 percent relative density at 104 pcf on Figure 2.5-85 is that the material tested at Woodward-Clyde's laboratory is a slightly lighter material than what is represented on Figure 2.5-85. The laboratory testing is conservative because the test specimens were compacted to 85 percent relative density for that material. The mean field relative density was 94 percent. Placing and compacting this lighter material in the field with the same effort and density requirements of the heavier material results in it having a much higher in-place relative density than what was assumed.

a) Index Tests

Index tests consisted of six particle-size analyses, one performed on a composite sample and five performed on triaxial test specimens, one modified Proctor compaction test, two specific gravity tests, two maximum dry unit weight determinations (vibrating table method) and one minimum dry unit weight determination,

The results of the index properties tests are presented in Table 2.5-15. The results of the particle-size test and compaction test on the composite sample are presented graphically on Figure 2.5-86. Basically the results indicate the representative Class A backfill test sample is a very fine sand with between one percent and three percent passing the No. 200 sieve. It has a specific gravity of 2.67 and has a maximum dry unit weight of 99.9 pound per cubic ft. (pcf) at optimum moisture content of 17.8 percent from the compaction test. A maximum dry unit weight of 99.2 pcf was measured from the vibrating table test.

b) Static Strength Tests

To determine static shear strength of the material isotropically consolidated-drained (CID) tests were performed. These tests were performed under two types of loading conditions. In one series, two CID tests were performed with the loading along an active stress path (CID-A). The initial effective confining pressures were 2.5 and 5.0 ksf. In the second series, three CID tests were performed with the loading along a passive stress path (CID-P). The initial effective confining pressures in this series were 1.75, 3.38 and 5.9 ksf- An active stress path is one where the vertical stress is held constant while the horizontal stress is decreased until failure occurs. A passive stress path is one where the vertical stress is held constant while the horizontal stress is increased until failure occurs. This method of loading was utilized in order to more closely simulate the actual response of the backfill material to wall movements of the combined structures caused by earthquake loading.

Test results are presented on Figures 2.5-87 and 2.5-88. Figure 2.5-87 is a plot of the ratio of horizontal effective stress to vertical effective stress (K) versus radial strain. The plot ranges from the complete active failure stress ratio condition (Ka) through the at-rest (Ko) stress ratio condition of zero radial strain and up to the passive failure stress ratio condition (Kp). Figure 2.5-88 presents the more conventional Mohr's circle friction angles for active and passive loading. The measured Mohr's circle friction angles are 43.6 degrees and 41.6 degrees, respectively. An angle of internal friction of 40 degrees was selected for design purposes.

c) Cyclic Properties Tests

The strain dependent cyclic properties (shear modulus (G) and percent damping - λ) were determined from state-of-the-art cyclic triaxial testing. The test was performed in stages of increasing strain. Between each strain stage the excess pore water pressure was allowed to dissipate. At double amplitude shear strains smaller than 10^{-4} in./in. the loading was stress controlled and above 10^{-4} in./in. the loading was strain controlled. The testing was performed at an effective confining pressure of 3.0 ksf. The strain dependent shear modulus and damping curves are presented on Figure 2.5-89.

d) Cyclic Strength Tests

Cyclic strength (liquefaction potential) tests were performed on four reconstituted test specimens. The specimens were consolidated to an effective confining pressure of 3.0 ksf and cyclically loading using a stress controlled mode of load application. Results are graphically presented in Figure 2.5-90 as the cyclic stress ratio required to cause five percent and 10 percent double amplitude strain and initial liquefaction versus the log of the number of load cycles. For a more complete discussion of tests and results relative to possible backfill liquefaction under seismic loading, refer to Subsection 2.5.4.8.

2.5.4.6 Groundwater Conditions

Groundwater conditions for the site and surrounding area are discussed in detail in Subsection 2.4.13. The site is underlain by three relatively shallow local aquifers, two of which have been correlated with aquifers that exist on a regional scale. These aquifers and their approximate elevations in the plant area are:

AQUIFER	DESCRIPTION	ELEVATION RANGE FT. (MSL)
1	-77 Ft. Sand	-77 ft. to -92 ft.
2	Gramercy Aquifer*	-200 ft. to -312 ft.
3	Norco Aquifer	-312 ft. to -500 ft.

---

*The Gramercy aquifer is not located beneath the combined structure. It comes to within one mile SW of the immediate plant island.

Groundwater levels in the -77 ft. sands ranged from +2 ft. MSL to +10 ft. MSL during the dormant construction period from March, 73 to November, 74. Water levels in the partially open excavation stabilized at approximately +5 ft. MSL during this same period and are indicative of the water levels to be expected in the completed backfill with the termination of dewatering. Piezometers in the Recent materials (above -40 ft. MSL) indicated water levels between +3.5 ft. MSL and +8.5 ft. MSL during the same time period. Bore hole piezometers monitored prior to construction in 1970 and 1971 indicated groundwater levels varying between +4 ft. MSL and +10 ft. MSL. Evaluation of this information indicated that the design water level for the plant structure for normal operation be considered at +5 ft. MSL for an average low water condition and +8 ft. MSL for a normal water level condition.
Due to the average grade elevation of +13 ft. MSL the average high water design level was taken as +13 ft. MSL. For a maximum flood condition assuming the Mississippi River levee is breached the design water level of +30 ft. MSL was used. This value was conservatively selected from studies presented in Subsections 2.4.2 and 2.4.3.

Construction dewatering was carried out to the depth of the shallowest aquifer (-77 ft. MSL). A detailed discussion of the dewatering system is presented in Subsection 2.5.4.5. The excavation to -48 ft. MSL was accompanied by lowering the water levels in the shallow -77 ft. MSL aquifer and upper Recent material in the vicinity of the plant island. Groundwater was controlled by a system of shallow and deep wells around the periphery and interior to the excavation. Refer to Subsection 2.5.4.13 for a discussion of groundwater levels during construction. Piezometric levels in these strata were lowered and raised concurrent with excavation and backfill operations in such a manner as to minimize changes from their existing effective stress. This procedure minimized rebound or heave during excavation and recompression during the backfilling and plant construction. Post-construction water levels are expected to return to their normal water-levels.

Due to the rapid draining characteristics of the compacted backfill and the geometry of the completed plant grade, no post-construction control of groundwater levels and seepage is required. All structures are adequately designed for all anticipated hydrostatic loading conditions.

With the completion of construction no further monitoring of local wells and piezometers is required and will therefore not be done. For a discussion of the rationale behind the elimination of future monitoring of groundwater levels refer to Subsection 2.4.13.4.

Laboratory permeability tests for the in situ Recent materials and upper Pleistocene strata are presented in Subsection 2.5.4.2.

Directions of groundwater flows and gradients in the Recent material and -77 ft. MSL aquifer were evaluated relative to postulated radioactive waste leakage into the ground. The gradients used for these studies are discussed in Subsection 2.4.13.3.

2.5.4.7 Response of Soil and Rock to Dynamic Loading

The response of the subsurface material to dynamic loading was analyzed using the computer program SHAKE(66) This program computes the response associated with vertical propagation of shear waves through the linear viscoelastic soil layered system. The program incorporates nonlinear soil behavior by an equivalent linear procedure based on an average strain level. Consequently, the strain-compatible solution is obtained. The depth of model used for the

→(DRN 01-464)
response analysis was determined at 400 ft. This depth incorporated the Class A backfill material as well as the upper Pleistocene and part of the lower Pleistocene material. Strain dependent shear modulus and damping and the variation of elastic properties with depth were implemented into the response study. The post construction groundwater table was recognized at +8 ft. MSL. The model and the associated soil properties used for the analysis are presented on Figure 2.5-91.
←(DRN 01-464)
A detailed discussion of the laboratory testing and results, in conjunction with the soil properties used for the response analysis, is presented in Subsections 2.5.4.2 and 2.5.4.5. The methods and procedures used for performing geophysical surveys and the results of seismic wave velocities such as compression wave and shear wave are presented in Subsection 2.5.4.4.

The SSE was designated at the top of Pleistocene at -40 ft. MSL with the maximum acceleration of 0.1 g. The input ground surface motion used for the analysis was conservatively scaled up from the top of Pleistocene to the top of Class A backfill at +17 ft. MSL. The maximum acceleration of approximately 0.1 g was assured and maintained at the top of Pleistocene during the deconvolution process.

In order to study the effects of varying soil stiffness properties on seismic response, a parametric analysis of the soil properties was performed.. The laboratory and field measured shear moduli were increased and decreased by 25 percent of the measured shear moduli for each Pleistocene stratum and a full analysis was performed for each set of properties.

The results of these response analyses including accelerations and earthquake induced shear stresses are plotted versus depth for each set of soil properties on Figure 2.5-92. The resulting earthquake induced shear stresses were utilized to assess the potential for liquefaction. A detailed discussion of liquefaction potential, which incorporates the above results, is presented in Subsection 2.5.4.8.

The soil-structure interaction analysis was performed by using a lumpedmass spring model. A general discussion of the analysis and the rationale for using the lumped-mass spring method is presented in Subsection 3.7.2. The selection of model and the shear modulus during SSE is presented in App. 3.7A. Since all the plant seismic Category I facilities are within the nuclear plant island structure (NPIS) there are no seismic Category I buried pipelines or seismic Category I earthwork structures at the site.

2.5.4.8 Liquefaction Potential

The foundation of the seismic Category I NPIS is established in stiff clays of the upper Pleistocene formation at -47 ft. MSL. This section assesses the potential for liquefaction of the Class A backfill and Pleistocene soils as a result of shear stresses induced by ground motion generated by the Safe Shutdown Earthquake (SSE).
→(DRN 02-217)
A study of the literature describing the liquefaction phenomenon, as well as the recent detailed studies of both Niigata (Japan) and Alaskan earthquakes, indicate that the stiff clays and highly cohesive soils do not experience instability due to earthquake induced stresses. The upper Pleistocene soils are predominantly highly cohesive and their strength is due to the high degree of overconsolidation and not from the intergranular overburden stresses as would be the case in clean granular soils. Any cyclic shear stresses associated with the SSE would not tend to rearrange this predominant soil structure and induce instability
←(DRN 02-217)

→(DRN 02-217)

by building pore pressures, but instead would transmit the shears as an elastic medium.

←(DRN 02-217)

There is a thin zone of silty materials at approximately -50 ft. MSL and another very dense 15 ft. thick silty sand layer at -77 ft. MSL. In addition to these in situ cohesionless materials is the compacted Class A backfill from grade (+17 ft. MSL) to -40 ft. MSL. The following subsections will more specifically address the liquefaction capabilities of these materials.

2.5.4.8.1 Selection of Strata

All the available soil samples from the existing borings were personally observed and reviewed by Ebasco soil engineers in order to verify the classifications. All samples with silty and sandy appearances were tested for grain size distribution. Two additional borings were taken under the NPIS in order to verify the soil profile. Boring B-73 is a five in. diameter continuous sampling boring 100 ft. deep extending to approximately -105 ft. MSL. Boring B-74 is a three in. diameter continuous sampling boring extending to the same depth. Boring B-74 was taken and sliced along the center line and photographed completely in order to visually obtain the entire 100 ft. soil column beneath the structures. For a complete and detailed description of the profile refer to Subsection 2.5.4.1.

The -55 ft. MSL most granular material was selected for liquefacton studies because of the low Standard Penetration Test (SPT) blow counts encountered there. Subsequently, additional grain size analyses of these materials indicated that these materials are in fact not granular or sandy in nature but are really clayey silts and silty materials (see Figure 2.5-93). All but one sample tested had greater than 65 percent of the material by weight pass through a number 200 sieve. The silty nature of this material accounted for the low SPT blow counts.

The in-place density tests of these materials also show that they are not loose but are 85 to 90 percent relative compaction with respect to Standard Proctor (see Figure 2.5-94).

Instances of low SPT blow counts were also encountered at approximately -77 ft. MSL or the beginning of the 15 ft. thick dense granular stratum. Similarly grain size analyses were performed on samples obtained at this elevation (see Figure 2.5-95). For these tests the percentage of material by weight passing the number 200 sieve ranged from 10 to 50 percent with clay contents of between two and 12 percent. The low SPT blowcounts here are attributed to the silty nature and clay content of the material. This zone is clearly the region of transition from the stiff clays above elevation -77 ft. MSL to the dense sandy stratum below.

2.5.4.8.2 Cyclic Strength Testing Program

Cyclic triaxial strength tests were performed to determine the strength of the critical in situ strata and Class A backfill available under SSE loading. These tests were performed utilizing undisturbed samples from the strata and reconstituted samples from the backfill. Undisturbed samples of foundation soils were used so that in situ conditions would best be simulated (any soil structure in the strata to be tested would be preserved). Testing of the in situ strata was performed by Law Engineering Testing Company of Marietta, Georgia and the

Class A backfill was tested by Woodward Clyde Consultants of Clifton, New Jersey.

All undisturbed samples from the in situ strata were personally examined by Ebasco soils engineers. The most sandy and silty looking undisturbed samples were selected for cyclic triaxial testing. These samples were five in. diameter by 12 in. in height. The sample preparation procedure was as follows: each sample was lightly trimmed in order to observe the stratification in the sample; the cyclic triaxial specimens were cut from the most silty and sandy portion of the entire sample. A prism cut was taken longitudinally along the sample to represent the entire sample and the entire prism was tested for grain size distribution. A comparison of the grain size analyses of the cyclic test materials with the representative samples of the actual tested materials showed that tests were run on the most critical materials (i.e., critical with respect to liquefaction susceptibility).

Sections from each undisturbed sample were trimmed into test specimens 1.4 in. in diameter and approximately three in. long. Each specimen was encased in an impervious membrane and placed in a triaxial test chamber. The test specimen was saturated by inducing a back pressure to the interior of the specimen of 60 psi. During back pressure saturation, the chamber pressure exterior of the specimen was maintained approximately one psi above the back pressure. The pore water response was checked after back pressure saturation to ensure that the samples were saturated and "B" values of at least .99 were observed.

After the undisturbed specimens were saturated, the chamber pressure was increased above the back pressure level to be commensurate with the effective overburden stress of the samples in situ. The specimens were then allowed to consolidate under the chamber pressure by allowing drainage through the bottom of the specimen. Complete consolidation was obtained by monitoring pore water pressure dissipation and volume change of the specimen. After complete consolidation was obtained, further drainage through the base of the specimen was prevented by closing the drainage valve. The specimen was then subjected to cyclic axial loads at a frequency of one cycle per second. Cyclic deviator stresses varied from 14 to 29 psi. During loading constant monitoring of cyclic load, internal pore pressure and axial deformation was maintained. Data were collected using direct writing rectilinear oscillograph recorders. Axial loads were measured with a miniature four arm bridge load cell excited with a 2.5 kHz carrier signal. Axial strains were measured with an inductive coil linear transducer excited at 60 Hz ac current. Pore pressures were measured at the bottom of the specimen using strain diaphragm transducers. Frequency of load application activated a solenoid valve with a quick exhaust.

Tests of the Class A backfill were performed on specimens reconstituted from representative Class A material selected by the Ebasco site soils engineer. Specimens were compacted to 85 percent relative density which is less than the mean relative density of 94 percent statistically determined for all the Class A backfill placed. Refer to Subsection 2.5.4.5.3 for a more complete description of Class A backfill relative density studies.

Reconstituted two in. in diameter, four in. long backfill test specimens were prepared. Each specimen was encased in an impervious membrane and placed in the triaxial chamber. Specimen saturation was accomplished using 100 psi back pressure and a saturated effective stress of five psi above the back pressure. "B" values were typically greater than .95. With saturation complete the chamber pressure was increased to the average effective overburden stress of the in-place backfill. After complete overnight consolidation further drainage of the specimen was prevented. The test specimens were then cyclically loaded at one cycle per second with a sinewave loading starting in compression. The specimens were subjected to cyclic deviator stresses varying from 11 psi to 21 psi. During loading constant monitoring of load, pore pressure and deformation was maintained. This data was collected using a Bell & Howell Data Graph model 5-134. Axial loads were applied using an MTS test frame and an inductive coil linear transducer. Pore pressures were measured using semi-conductor strain gages on top and bottom of the test specimen and the average reading was used.

2.5.4.8.3 Failure Criteria

In the literature, failure has variously been defined as, five percent double amplitude strain, ten percent double amplitude strain, or pore pressure equal to cell confining pressure (initial liquefaction). Due to the clayey - silty nature of the critical in situ strata these materials did not liquefy as described by Seed (78). Typically, the test specimens underwent progressive strain with continuous load cycles and did not exhibit typical liquefaction. For this reason, the failure criteria established for the critical in situ (i.e. more sandy) strata was conservatively selected as five percent double amplitude strain in 10 cycles of motion. Plotted on Figure 2.5-96 is the cyclic shear strength of the in situ material available to resist five and ten percent double amplitude strain. The cyclic strength is plotted versus the log of the number of cycles to cause failure.

The Class A backfill, being completely granular, more closely resembled the initial liquefaction failure criteria whereby pore pressure equaled cell confining pressure. This coincidentally occurred at five percent double amplitude strain. The failure criteria for the Class A backfill was therefore conservatively selected as five percent double amplitude strain in 10 cycles of motion. Plotted on Figure 2.5-90 is the cyclic shear strength of the Class A backfill available to resist five and ten percent double amplitude strain and initial liquefaction. The cyclic strength is plotted versus the log of the number of cycles to cause failure.

2.5.4.8.4 Design Loading

The analysis of liquefaction potential is based on seismic loading imposed by the intensity VI MM SSE earthquake with an assigned acceleration of 0.10g at the top of Pleistocene. For a complete and detailed description of the SSE selection refer to Subsection 2.5.2.6. Using the time history of accelerations associated with the SSE, induced shear stresses were determined at different depths. A range of shear stresses was developed corresponding to a parametric input of elastic soil properties (See Figure 2.5-92). The computer program (SHAKE) was utilized in performing these analyses. A complete and detailed discussion of the methodology used is presented in Subsection 2.5.4.7. Average equivalent uniform earthquake-induced shear stresses were taken as 65 percent of the peak values and used for the liquefaction analysis (78).

2.5.4.8.5 Analysis and Conclusions

In order to assess liquefaction potential, the ratio of cyclic stress causing five percent double amplitude strain in ten cycles to the estimated shear stress produced by the SSE was determined. This ratio is essentially a factor of safety against liquefaction.

The cyclic stress causing five percent double amplitude strain in 10 cycles was determined from the laboratory data presented as curves of stress ratio versus number of cycles (Figures 2.5-90 and 2.5-96). The stress ratio was corrected by use of a factor which related the laboratory triaxial test data to stress conditions causing liquefaction in the field. In accordance with the most recent evaluations of this factor a value of 0.7 was used for all soil layers in the profile.

Figure 2.5-97 gives a comparison plot of average equivalent stresses developed during the SEE and the cyclic shear strength available to resist five percent double amplitude strain in the in situ siltry-clayey sand zones. Factors of safety against the conservative five percent double amplitude strain failure criteria are also presented.

Due to the dense state of the Class A backfill neither the five percent strain nor the initial liquefaction failure criteria could be achieved for ten cycles of motion using the maximum cyclic loading of a stress ratio of 0.5 (Refer to Figure 2.5-90). Therefore the materials are extremely safe with respect to cyclic mobility and no factors of safety are presented for the backfill material on Figure 2.5-97

For the in situ material minimum and maximum factors of safety are presented. The safety factors reflect the results of the parametric study of the ground motion analysis where the elastic shear moduli (G) of the in situ material were varied ± 25 percent of the actual measured shear moduli. The resulting factors of safety for in situ materials are all in excess of 1.5 therefore precluding the possibility of any excessive strains or liquefaction developing in the foundation materials.

The Waterford tests were compared with work done by Lee & Fitton (79) and the study verified the fact that in situ silty materials do strain rather than liquefy, and that the testing of the Waterford soils are valid. The comparison entailed a grain size comparison as well as void ratios of materials tested (see Figure 2.5-98). The comparison of the Waterford cyclic test results with those of Lee and Fitton show the tests compare quite favorably (see Figure 2.5-99) and give the assurance necessary to utilize these results as mentioned above.

2.5.4.9 Earthquake Design Basis

The establishment of the SSE and OBE are discussed in Subsections 2.5.2.6 and 2.5.2.7 respectively. In summary, the selection of the SSE is based on a hypothetical earthquake with an epicentral intensity of VI MM occurring adjacent to the site. According to the most recent and acceptable intensity-acceleration relationship by Trifunac-Brady the intensity VI MM corresponds to a horizontal surface acceleration of 0.06g. The plant was conservatively designed for 0.lg maximum horizontal ground acceleration. The peak vertical acceleration for the postulated SSE is 2/3 peak horizontal acceleration or 0.067g. The OBE for the site is postulated to have a peak horizontal acceleration of 0.05g and a peak vertical acceleration of 0.033g. These peak accelerations are one half of the corresponding peak SSE accelerations.

2.5.4.10 Static Stability

The geologic conditions underlying the site have been discussed in detail in Subsection 2.5.4.1 and the in situ and compacted backfill soil properties are discussed in Subsections 2.5.4.2 and 2.5.4.5 respectively. This Subsection discusses static analyses of the NPIS, including settlement, bearing capacity and lateral earth pressures.

2.5.4.10.1 Settlement

The settlement conditions at the site are evaluated in terms of vertical effective stress. The effective stress is defined as the combined submerged weight of the existing overburden soils, and is considered with the groundwater table at +8 ft. MSL. Presented on Figure 2.5-103 is a history of effective stress at the mat bearing level (-47 ft- MSL) from the preexcavation (in situ) condition to the final post-construction operating condition.

The in situ effective stresses were in the order of 3300 psf. The first construction stage illustrates the pressures upon completion of excavation to the bottom of mat bearing level thereby reducing the stress to zero. Next, an intermediate stage of construction is illustrated in which the effective stress at the bottom of the mat approaches 4500 psf. This is due to the weight of the concrete structures with the water table held below the mat level. The final stage illustrated is the completed stage, with the buildings completed to the final elevation, the sand backfill completed, and the groundwater table back to its initial normal water level condition of +8 ft. MSL. The final mat level bearing pressures will be 3100 psf. This is 200 psf less than the in situ soil pressures at the site. For this reason, long term post-construction settlements will not be a concern with this type of floating foundation. Refer to Subsection 2.5.4.11 for a discussion of the theory behind the floating foundation principle implemented.

Foundation heaves and settlements, however, did occur during the construction stages. These movements are presented and discussed in Subsection 2.5.4.13.

2.5.4.10.2 Bearing Capacity

Due to the net 200 psf reduction in effective pressure at the mat bearing level with the completion of construction there was no possibility of a static bearing capacity type failure occurring during normal plant operation. Bearing capacity was, however, a consideration during plant construction and during seismic loading after the plant is in operation.

To compute the bearing capacity of the Pleistocene clays at the mat bearing level during transient construction loading the following modified bearing capacity equation by Hansen (80) was used:

$$q_{ult} = cNcScdc + qNqSqdq + 1/2\gamma BN\gamma S\gamma d\gamma$$

For purely cohesive soils ($\phi = 0$) the equation reduces to

$$q_{ult} = cNcScdc + qsq$$

where q_{ult} = ultimate bearing capacity (psf)

Nc = Hansen’s bearing capacity factor (dimensionless)

c = weighted average cohesion of the Pleistocene soils to a depth equal to two thirds of the common mat width (psf)

γ = unit weight of the soil

q = backfill surcharge loading (psf)

SC = (1 + 0.2 B/L) = 1.14 (dimensionless)

Sq = (1 + 0.2 B/L) = 1.14 (dimensionless)

dc = (1 + 0.35 D/B) = * (dimensionless)

B = common mat width (ft.)

L = common mat length (ft.)

D = depth of penetration of common mat (ft.)

For $\gamma = 0$ Hansen's bearing capacity factor (Nc) is 5.14. The weighted average cohesion, c, between -47 ft. MSL and -225 ft. MSL is 1750 psf and the optimum moist backfill density was approximately 120 pcf.

The ultimate bearing capacity (q_{ult}) of the Pleistocene soils at the mat bearing level with no backfill surcharge (q = 0) is 10,300 psf. With moist backfill in place prior to complete release of the dewatering system (q = 7700 psf) the ultimate bearing capacity of the Pleistocene soil is 19,100 psf.

The largest loading imposed at the mat bearing level during construction was less than 4500 psf. This loading was imposed on the Pleistocene soil prior to release of the dewatering system and when the site was nearly completely backfilled. The resulting factor of safety against a static bearing capacity failure for this maximum construction loading was in excess of 4.0. This load will subsequently be reduced by the introduction of hydrostatic uplift forces hence further increasing the factor of safety against a bearing capacity failure beyond 4.0.

To evaluate the factor of safety against a bearing failure caused by dynamic loading Hansen's bearing capacity equation was evaluated for an operating site with the water table at +13 ft. MSL and buoyant backfill surcharge (q = 4400 psf). Refer to Subsection 2.5.4.6 for a discussion of the groundwater conditions at the site. The ultimate bearing capacity (q_{ult}) under these conditions was approximately 15,000 psf. Using methods discussed in Subsection 3.7.2.14 the factor of safety against a bearing capacity failure under dynamic loading was 2.6.

2.5.4.10.3 Earth Pressures

The NPIS was designed for static and dynamic earth pressures as discussed below:

---

* For no backfill surcharge dc = 1.0
For backfill surcharge dc = 1.08.

a) Static Earth Pressure

The combined structure was designed for at-rest pressure and hydrostatic loading. The at-rest earth pressure coefficient (K_O) of 0.5 and a buoyant unit weight of 65.5 pounds per cubic ft. (pcf) were used for the backfill material. Two hydrostatic loading conditions were used. The water level was taken at +8 ft. MSL for normal conditions and +30 ft. MSL for flood conditions. The pressure distribution used to design the below grade structure walls is shown on Figure 2.5-100. Refer to Subsection 2.5.4.6 for a discussion of the groundwater conditions at the site. For a complete description of earth pressure load combinations used in conjunction with other foundation loads refer to Section 3.8.

b) Dynamic Earth Pressure

A dynamic lateral earth pressure analysis was performed for all seismic Category I structures using the following criteria:

1) Effective displacement of structural wall relative to the soil was the arithmetic sum of the movement of the wall obtained from the dynamic analysis and the maximum relative soil displacement in the free field as determined by the SHAKE computer analysis.

2) The strain was computed from the wall movement at a particular depth divided by the horizontal component of length of the Rankine failure surface at that depth.

3) The lateral pressures were obtained by a relationship between coefficient of earth pressure vs. strain, as determined from laboratory tests (Figure 2.5-87) discussed in Subsection 2.5.4.5.3.

The dynamic earth pressure distribution used for design of the below grade structure walls is presented in Figure 2.5-101. Hydrostatic pressure under SSE loading was taken as +5 ft. MSL, i.e. low water level condition.

2.5.4.11 Design Criteria

The existence of the slightly overconsolidated Pleistocene clays at elevation -92 ft. MSL, indicated that significant long term and differential settlements could be expected for heavily loaded structures founded on individual spread footings. To eliminate differential and long term settlement considerations the heavy loads were compensated by a combined foundation structure with the Reactor Building, Reactor Auxiliary Building, and Fuel Handling Building (seismic Category I structures) located on a common mat foundation. The floating foundation principle was utilized and the combined foundation will apply an effective load to the bearing stratum clays which is approximately equal to the preconstruction overburden pressure.

All seismic Category I structures are founded in the Pleistocene formation on a common mat with a bottom elevation of -47 ft. MSL. At this level the mat bears in the upper stiff, tan and gray clays of the Pleistocene formation. The objective of the common mat foundation is illustrated in Figure 2.5-102. This figure illustrates the various soil conditions and pressures during four stages of construction shown, beginning with initial soil conditions and finishing with the completed structures and backfill in place.

The soil conditions at the site were evaluated in terms of vertical effective stresses at the mat bearing level (-47 ft. MSL). These stresses initially were 3300 psf prior to construction. The first construction stage illustrates the pressure upon completion of excavation to the bottom of mat elevations thereby reducing the stress to zero. Next, an intermediate state of construction is illustrated in which the effective stress at the bottom of the mat approaches 4500 psf. This is due to the weight of the concrete structures with the water table lowered below the mat. The final stage illustrated is with the buildings completed, the sand backfill completed, and the groundwater table back to its initial condition of +8 ft. MSL. The mat level bearing pressures for the completed stage will be 3100 psf. This is 200 psf less than the initial soil pressures at the site. For this reason, settlements will not be a concern with this type of foundation.

Since this foundation concept involves the balancing of existing soil pressures, a time history diagram of soil pressure was developed and is illustrated on Figure 2.5-103. This figure details the soil pressures at the bottom of the foundation mat. It begins with the initial soil pressure conditions and develops the pressures during the progressing phases of construction. After excavation the pressures were reduced to zero. This is analogous to the phase described earlier in Figure 2.5-102. During the concrete construction stages, the pressures increased and continued until a pressure of nearly 4500 psf was applied. This pressure was predetermined to be a maximum pressure that is desirable with this type of foundation concept. This is based on the re consolidation characteristics of the soils and was deemed to be a prudent value to maintain during the construction phase. In order to keep the soil pressure at this level or below, the water table will be allowed to rise thus compensating for further pressure increases, as shown on Figure 2.5-103. This procedure reduces the effective soil pressure and maintains the effective pressures below the 4500 psf level and establishes final effective pressures as described above. Detailed construction stages are given on Figure 2.5-104 through 2.5-111. Each diagram corresponds to the phase outlined on the aforementioned bearing pressure time history diagram. These figures illustrate the various construction features involved during each phase of the work including the sand backfilling, saturation of backfill, and other construction aspects.

In particular, the detailed foundation design considers the following principles, rationale and distinct features:

a) The base of the combined mat foundation is located at elevation -47 ft. MSL resulting in a final effective soil loading condition of 3100 psf as compared to the initial effective overburden pressure of 3300 psf.

b) Design criteria have established a 1200 psf overload above the existing effective soil pressures which may be applied only during the construction phase of the work. This is primarily to maintain a margin of pressure below the preconsolidation pressure of the materials with the lower OCR'S.

c) The excavation of the Recent deposits, consisting of soft clays, silts and sands extending to approximate elevation -40 ft. MSL and subsequent excavation of the stiff Pleistocene clays results in an elastic rebound and heave of the final exposed clay bearing strata. Refer to Subsection 2.5.4.13 for a discussion of measured foundation heave and settlement. Heave is minimized by excavating in increments and by rapid concrete placement in designated sections of the mat in a predetermined sequence to optimize recompression.

d) By conforming with the floating foundation principle, construction settlement of the seismic Category I structures is confined essentially to the recompression of the rebound and heave experienced by the Pleistocene materials with an additional preconsolidation for the higher backfill imposed loading. It is desirable to complete the major portion of this settlement during the construction period therefore the applied loading sequence is arranged with this particular aspect in consideration.

e) By applying a maximum effective loading of nearly 4500 psf the major amount of recompression takes place during the construction phase.

f) During the construction phase a dewatering system is installed around the perimeter and within the excavation to control under-seepage through silt and sand layers in and below the excavation slopes. Refer to Subsection 2.5.4.5.2 for a discussion of the dewatering system used at the site. A series of twelve recharge wells are also located around the perimeter of the mat foundation extending into the compacted shell filter blanket under the mat. The locations of these wells are shown in Figure 2.5-83. These recharge wells assist in introducing hydrostatic uplift forces to compensate for additional construction-imposed foundation loads beyond the 4500 psf allowable pressure.

In order to ensure meeting the design objectives, detailed excavation specifications and drawings were prepared. Figures 2.5-81 and 2.5-82 detail configuration of the excavation. The slopes presented on these drawings were established based on the soil properties determined from laboratory and field tests. The excavation specification detailed the construction of the concrete mat foundation such that it minimized the exposure of the stiff clays at the base of the foundation. In order to assure uniform pore pressure distribution in the clays beneath the mat upon relieving the dewatering system, a filter media consisting of compacted shell was utilized. Detailed instrumentation, consisting of electrical extensometers, mechanical heave points, pore pressure piezometers and settlement plates, were installed to monitor heave and recompression settlement of the mat foundation. Refer to Subsection 2.5.4.13 for a complete discussion of the instrumentation system. A plot plan showing the instrumentation systems which monitor foundation responses is presented on Figure 2.5-112.

The criteria for selection of design parameters and the design methods and associated factors of safety are based upon established soil mechanics procedures and have been noted in the relevant sections. References have been cited where applicable.

2.5.4.12 Techniques to Improve Subsurface Conditions

In order to improve conditions within the plant area and to prevent liquefaction around the NPIS all Recent material (initial plant grade to -40 ft. MSL) was excavated and replaced with compacted sand backfill. Further, to prevent excessive long-term consolidation settlement and differential settlement a floating foundation principle was utilized including a carefully monitored construction dewatering system to maintain foundation pressures as close as possible to their in situ state. Refer to Subsections 2.5.4.5 and 2.5.4.11 for discussions of the excavation-backfill program and the floating foundation principle respectively.

No grouting, vibroflotation rock bolting etc. beneath the NPIS was required.

2.5.4.13 Subsurface Instrumentation Program

To monitor safety related foundation soils prior to and during construction and to implement the design criteria presented in Subsection 2.5.4.11 a comprehensive subsurface instrumentation program was initiated. The scope of the program consists of monitoring of piezometric levels, foundation soil heave and settlement, excavation slope movements and site subsidence due to dewatering.

The locations of all instrumentation are shown on the Instrumentation Plot Plan (Figure 2.5-112). The instrumentation designation numbers and elevations (where applicable) are also presented on this figure. Provisions were made to continue reading various instruments located under the mat foundation by extensions through the concrete. The extent of the program consists of the following instrumentation:

Piezometers

Twenty two pneumatic type piezometers (Pl-P22) are used to measure the piezometric levels in the Recent alluvium cut slopes and Pleistocene foundation materials within the seismic Category I excavation. Piezometers Pl through P10 measure piezometric levels in the Recent alluvium which extends to elevation -40 ft. MSL. Piezometers Pll through P14 measure piezometric levels in the silty-clayey Pleistocene zone at elevation -57 ft. MSL. Piezometers P15 through P18 monitor the -77 ft. MSL Pleistocene sands and P19 through P22 monitor the materials below this sand layer. Two open hole PVC stand pipe piezometers (P23 and P24), slotted between -70 ft. MSL and -90 ft. MSL, provide additional piezometric measurements in the -77 ft. MSL Pleistocene sands. Five pneumatic piezometers (P44-P48) measure piezometric pressures in the compacted shell blanket layer underlying the NPIS.

The pneumatic piezometers are manufactured by Slope Indicator of Seattle, Washington. The device basically consists of a pneumatic readout transducer set in a borehole to a particular elevation. Nitrogen gas, fed from grade through a series of tubes to the diaphragm readout unit, equalizes the piezometric pressures acting on the diaphragm. Through this procedure, the piezometric pressure is measured.

The piezometric levels are measured in the standpipe piezometers by lowering a small bimetal probe, manufactured by Soil Test, into the standpipe. The probe is attached to a cord marked in five ft. increments. When the probe touches water a circuit in the probe is closed thus measuring the depth of the probe and piezometric level.

Piezometers are generally read on a weekly basis during normal construction operations. During any critical changes in the construction dewatering, the readings are taken as frequently as daily.

Heave Points

Nine Borros anchor heave points (Hl-H9) are located at the bottom of the seismic Category I excavation. These heave points measure the rate and amount of heave of the Pleistocene materials at the base of the excavation. Heave points Hl through H5 were placed prior to any excavation; H6 through H9 were placed after the mat had been placed.

The heave points are manufactured by Borros Co. Ltd., Stockholm, Sweden. They were assembled by lowering a 1/4 in. diameter steel rod anchor post into a one in. casing inside a borehole. Attached to the bottom of the anchor post are 1/4 in. diameter steel rods in a contracted position around the post forming the Borros anchor unit. When the anchor was at the required elevation, approximately -50 ft. MSL, the three contracted rods were expanded into a fixed anchored position.

Heave-settlement readings are made by survey crews on the main anchor posts protruding from the ground. Generally, readings are made on a weekly basis. When changes in the normal plant construction operation are made, the frequency of readings is increased to three times a week.

Extensometers

Two electrical extensometers (El and E2) are located under the central portion of the seismic Category I excavation. These devices serve to augment the heave-settlement readings obtained using the heave point system. The extensometers are only applicable, however, in measuring the movements of the upper 200 ft. of Pleistocene material.

The extensometers are manufactured by Slope Indicator Company. They were installed by drilling to elevation -250 ft. MSL (200 ft. into the Pleistocene,) and grouting a Borros anchor into position. This lower anchor is assumed to be a fixed reference point. Three additional Borros anchors were set in each extensometer borehole two ft., 10 ft. and 30 ft. below the, base of the excavation which is at -48 ft. MSL. These additional anchors are illustrated on Figure 2.5-113 by the subscripts "a", "b" and "c". Movements between the three upper anchors and the fixed lower anchor are obtained by measuring resistance changes in the electrical linear potentiometers adjacent to each of the upper anchors. The movements of the upper anchors are relative to the lowest anchor at elevation -250 ft. MSL.

Extensometer readings are taken as frequently as the heave point readings.

Inclinometers

Six inclinometers (In.1-In.6) were placed in the cut slopes around the excavation to measure horizontal north-south and east-west slope movements of the Recent alluvial material during excavation and period of open excavation. These measurements continue approximately 35 ft. into the Pleistocene material. The north and south slopes each have one inclinometer and the east and west slopes are monitored by two inclinometers each.

The inclinometers are manufactured by Slope Indicator Company of Seattle, Washington. The device consists of several five ft. long sections of plastic piping, approximately three in. in diameter connected by joints that are free to move laterally and vertically. These pipes were lowered into a borehole with backfill placed around them. The completely assembled inclinometers are 90 ft. long. To determine the lateral movement of each section a probe is lowered into the tube and the out-of-plumbness of each section is determined in both north-south and east-west directions. By knowing the out-of-plumbness and,lengths of each section, total lateral displacement in both north-south and east-west directions are determined for each section.

Each inclinometer is read on a weekly basis.

Settlement Monuments

To evaluate the effects the dewatering system has on the ionediate area surrounding the seismic Category I excavation, several settlement monuments were established and are read by survey crews on a weekly basis. These monuments are as follows:

PLANT AREA; No's 1,4,5,6,8,9,10,11 and
In.1 through In.6* (total of 14 points)

LEVEE AREA; No's W300, W200, W100,
E100, E200, E300, centerline (total of 7 points)

HIGHWAY AREA
(LA-18); No's W300, W200, W100,
E100, E200, E300, centerline (total of 7 points)

2.5.4.13.1 Instrumentation Program Implementation

To insure the implementation of the design criteria through the instrumentation program, close supervision of the program on a daily basis was maintained by a qualified site soils engineer. Each month a detailed instrumentation report was issued by the site soils engineer for a comprehensive review by the supervising soils engineer in the Ebasco N.Y. office. During crucial construction operations, frequent site visits are made by the supervising soils engineer as well as other home office engineers associated with the design of the plant. The contents of each report relative to the instrumentation program consist of the following information:

a) A cover letter written by the site soils engineer giving a brief summary discussion of the month's instrumentation readings. Any important occurrences are highlighted.

b) A location plan of all instrumentation is presented along with pertinent notes as to the condition of the instruments.

c) All piezometer readings, river levels, monthly rainfalls, heave point and extensometer readings are plotted versus time on the same drawing. Also included on the common plot is total backfill and concrete quantities placed to-date. Presenting the instrumentation in this manner facilitates the evaluation of the foundation material response relative to piezometric level changes and structural and backfill loads.

---

* Settlement readings were taken on the tops of the inclinometer tube casings.

d) Inclinometer movements are presented on two separate drawings. One drawing shows the north-south movements and the second drawing shows the east-west movement of each inclinometer. Also included on these drawings are the updated slope movements represented vectorially at elevations +14 ft. MSL and -26 ft. MSL.

e) Settlement monuments along the immediate levee area, highway (LA-18) and plant area are plotted versus time on one common drawing.

2.5.4.13.2 Measured Foundation Material Response

a) Piezometric Response

Presented on Figure 2.5-113, sheets 1 through 4 is the entire piezometric record at the site for all piezometers. The record extends from the initial start of the dewatering system (August, 1972) to March, 1983. Included in this figure are notes indicating changes in the normal construction operation. Also presented on this figure, relative to the piezometric records, are river level readings and monthly rainfall accumulations. The following presents a chronological narrative of the more significant piezometric changes from 1972 through 1977.

The site was initially dewatered in August 1972. With the entire dewatering system fully operative the piezometric levels ranged from elevation -20 ft. MSL in the recent alluvium to elevation -60 ft. MSL in the -77 ft. MSL sands and lower materials. In November 1972, with the Phase I excavation complete to elevation -5 ft. MSL, the entire construction operation was shutdown due to legal and non-construction related reasons. As shown on the records, piezometric levels in all materials rose abruptly to a stable position by March 1973. For 20 subsequent months the dewatering system remained off. The excavation filled with water and piezometric levels in all materials rose to approximately -5 ft. MSL. Fluctuation in the piezometric levels during this dormant period, particularly for the piezometers in the -77 ft. MSL sands, were caused by river level-fluctuations. In November, 1974, the dewatering system was reinstated with the resumption of construction. Piezometric levels after this second dewatering start-up were approximately 15 ft. lower than during the initial dewatering operation. It was felt that, due to the on-off-on operation, the well system was essentially purged making it more efficient. During the period of March through October, 1975, there was a general rise in the piezometric levels under the site. This rise was caused by the turning off of six deep ejector wells around the northwest corner of the excavation in order to minimize the differential settlements occurring on a nearby 500 kV transmission tower. The deep ejector wells pumping out of the -77 ft. MSL sands have immediate effect on the piezometric levels in the plant area because this sand layer is the most prominent direct recharge connection with the Mississippi River. The piezometric levels then dropped during the month of October as a result of the addition of 12 pump relief wells located around the NPIS.

Referring to notes presented on Figure 2.5-113, at that time (December, 1975) the final Phase IV excavation was started simultaneously with the concrete placements for the common mat. In order to monitor the effectiveness of the buoyant uplift forces on the underside of the mat, caused by hydrostatic recharge, five piezometers were installed in the one ft. thick compacted shell layer under the common mat. These piezometers essentially read zero until September, 1976, when they started to rise. This rise is attributed to the placement of wet backfill, constant watering of the backfill as well as rainfall. This water is directly feeding into the shell blanket effecting a rise in the piezometric levels. Considering the relatively impervious alluvial cut slopes and the highly impervious Pleistocene clays between elevations -40 and -77 ft. MSL, this water table is essentially purged and contained within the excavation area.

→(DRN 01-464)

The sharp rise in all piezometric levels at the end of December, 1976 was caused by construction activity associated with relocating the wells around the south portion of the excavation. The relocation process included jetting new wells to accommodate the increase in excavation for the Turbine Building. Following the start-up of the relocated well system, the piezometric levels stabilized themselves at their original low positions. During the end of April, 1977, however, there were substantial piezometric rises of nearly 25 ft. in the lower piezometers and nearly 10 ft. in the upper piezometers. The shell layer similarly underwent 10 ft. piezometric rises. This rise was attributed to the large increase in the river elevation and excessive rainfall. Only half of the total pump relief well capacity was utilized, six of the deep ejector wells around the northwest corner of the excavation were shut off and there was an overall reduction in well efficiency. The reduced pumping and increased river levels accounted for the rise in the lower piezometers. High rains accounted for the rise in the upper piezometers. A subsequent reduction in rainfall, and falling river elevation, increased pumping through the pump relief wells and installation of larger pumps, resulted in a return of piezometric levels toward their original low positions by the end of July 1977. In order to more effectively control the foundation movements and effective pressures, the controlled throttling down of the dewatering system was implemented in October 1977 and completed in July, 1979. This has resulted in stabilized piezometric levels which reflect the normal groundwater pressure levels at the site. These pressure levels exhibit mild fluctuations (up to five feet over a one-year period) and are dependent on the river fluctuations. Similar fluctuations were experienced during the dormant construction/dewatering period of 73/74.

←(DRN 01-464)

b) Foundation Materials Heaves - Settlements

Shown on Figure 2.5-113, sheets 1, 2 and 3 directly beneath the piezometric records are heave point and extensometer movement plots to date. The following presents a chronology of the more significant foundation displacements for the last five years.

→(DRN 02-217)

With the start of the Phase I excavation in April, 1972, the foundation materials exhibited between 0.1 and 0.3 ft. of heave. This heave was the result of excavating 20 ft. of material without the beneficial effective stress balancing by site dewatering. With the start-up of dewatering in August, 1972, resulting in an increase in effective foundation pressure, approximately 0.1 ft. of this heave was recompressed. However, the dewatering system was not in operation long enough to balance the Phase I excavation and the release of the dewatering system due to job shutdown caused elastic foundation rebound to its predewatering position. The post-shutdown heaves stabilized in February, 1973 and remained between 0.1 and 0.3 ft. until the resumption of full dewatering in November, 1974. Between November, 1974 and late January, 1975, the dewatering system was fully operative and Phase II excavation had not been started yet. Consequently, with the more

←(DRN 02-217)

→(DRN 02-217)

effective dewatering system caused by its on-off-on operation and the time lag for renewed Phase II excavation, approximately 0.15 ft. of previous foundation heave was recompressed. In January, 1975, the remaining excavation work (Phase II through IV) was started and continued for the entire year. As a result, foundation heaves increased to between 0.4 ft. and 0.8 ft. The commencement of concrete placement in December 1975, backfilling in mid 1976 and implementation of larger dewatering pumps in July 1977 resulted in recompression of the heaves incurred during the excavation phases.

←(DRN 02-217)

The average heave readings at the site were recompressed to their initial zero readings by July 1977. The continued maximum running of the dewatering system until October 1977 resulted in an average controlled movement of the heave points to an average net settlement of 0.15 ft. After October the rate of movements of these heave points was reduced and further controlled by the throttling down of the dewatering system. With the complete shutdown of the dewatering system in July 1979 the heave points stabilized to a net average settlement of 0.45 ft. and have remained stable through the final readings in June 1982 (approximately three years).

The predicted post-construction heave was initially calculated to be two in. occurring uniformly across the excavated site. There was a two to four fold difference between predicted and actual heaves incurred. As described above, the initial Phase I excavation of 20 ft. of soils without the beneficial lowering of piezometric levels decreased the effective pressures by increasing the uplift on the foundation soils. This caused more heave than calculated for the dewatered excavation procedure. The original scheme envisioned a balanced effective pressure system for the Phase I excavation, which would have resulted in no heave and potentially a settlement under the dewatered condition. This balance would have come about by the increased weight of dewatered soil and the decreased pressure due to Phase I excavation. When the dewatering was started, the foundations responded by recompressing; however, the short duration of the dewatering prior to project shutdown was not effective in recovering the heave. This long shutdown period simply allowed complete relaxation of soils due to the stress relief.

The heave experienced, in excess of the two in. predicted, is also felt to be attributed to more rapid rebounding of the foundation clays than anticipated. Early calculations, formulated during the PSAR stage, considered that approximately 20 percent of the rebound would be realized during a 10 to 12 months excavation phase. The actual measurements indicate that a more rapid rebound has been experienced, perhaps on the order of 70 to 80 percent of full rebound, under the relaxed stresses of full excavation.

The higher differential heave along the north during the Phase I excavation is attributed to the excavation procedure which essentially handled the material from north to south as well as the fact that the grade along the south, east and west sides of the excavation was raised four to five ft. for construction facilities. The north side was not surcharged with the additional fill which in essence allowed more relaxation along the north. Additionally, the piezometric pressures along the north are always somewhat higher due to the recharge from the Mississippi River. All of the above factors tend to increase the heave potential of the north side of the excavation, as is the case shown on Figure 2.5-113 for heave point HI.

The less responsive behavior of the extensometers as compared to the heave point movements is attributed to various factors. The most significant factor is that the extensometers may not be reading correctly. This is felt to be the case since the extensometers were extended to their full travel during the final excavation phases and have not responded properly since. Various correlations between heave points, mat settlements and extensometers indicated that the extensometers have been unresponsive during the reload phase of construction.

The rationale of inducing heave point settlements in a controlled manner, to 0.45 ft.below the in situ position, was to essentially preconsolidate the foundation soils and eliminate any long term settlements.

In summary close observation and interpretation of these movements as well as the piezometric responses have insured the design criteria presented in Subsection 2.5.4.11 was adhered to.

c) Slope Movements

→(DRN 01-464)

Presented on Figures 2.5-114 and 2.5-115 are up-to-date plots of the north-south and east-west slope inclinometer movements respectively. Also presented on Figure 2.5-115 are the total slope inclinometer lateral movements in any direction shown vectorially at elevation +14 ft. MSL. On Figure 2.5-114 is a similar lateral vectorial plot for elevation -26 ft. MSL. The slope movements perpendicular to the excavation are basically consistent for all inclinometers. The tops of each slope generally underwent movements back into slope. At depths of between 20 and 30 ft., no net movements in or out of the slopes occurred. Below this depth, there was a general trend for slope movement into the hole. At approximately 69 ft. depths, the limit of excavation, slope movements again return to approximately zero. Slope movements parallel to the excavation are generally of small magnitude and occur in no particular pattern. In some instances, maximum parallel slope movements occur at the top of the slope; in other cases, the maximum movements occur between depths of 20 and 40 ft. At grade the total lateral vectorial slope movements range from between 2.5 in. and five in. With the exception of Inclinometer No. four, the overall movement trend is away from the excavation. At elevation -26 ft. MSL, vectorial movements are towards the excavation, ranging from 1.5 in. and 3.5 in. With rising backfill in the excavation, the most recent slope movements have either stopped or have begun to move the opposite direction back to their original preexcavated positions.

←(DRN 01-464)

Lateral slope movements perpendicular to the hole generally occurred in the upper 55 ft. of the slope which is the Recent alluvial material with much smaller lateral movements measured at depths extending into the Pleistocene foundation material; therefore, maintaining the integrity of this material.

→(DRN 02-217)

The general slope displacement away from the excavation was the result of site area settlements and heaves caused by excavation and construction dewatering. During construction there was a combination of as much as 11 in. of foundation heave in the bottom of excavation and 18 in. of settlement at the top of slope (see description in Subsection 2.5.4.13.2b and d. This resulted in an

←(DRN 01-217)

→(DRN 02-217)

upward movement of the excavated bottom which was compensated by a general rotation of the cut slopes away from the excavation. The overall geometry of the excavation was one where the center of excavation was in heave while the top of slope was in compression with a neutral axis along the cut slope. When evaluated in this manner, the only direction the top of slope could move in order to provide relief for the center heave was away from the excavation. This movement was more of an elastic nature with slopes and foundation soils acting together rather than a slope stability failure. Had the movement been a result of a slope stability failure all points on the inclinometers would have moved in a direction toward the excavation.

←(DRN 02-217)

When evaluating horizontal movements (Figures 2.5-114 and 2.5-115) in conjunction with vertical slope movements (inclinometer settlement shown on Figure 2.5-116) it can be seen that the overall slope displacement consists of an average settlement of 1.6 ft. and an average lateral, away from the hole, movement of 0.33 ft. The combination of these two displacements results in horizontal/vertical vectorial displacement which is nearly all in the downward direction with a slight displacement away from the excavation. When evaluated this way it can be seen that the overall slope movement is normal to the flat (5 horizontal to 1 vertical) construction slope and is predominately a settlement event with lateral movements contributing a small part.

The reason for slope movements into the excavation at a depth of approximately 40 ft. is also a result of the horizontal/vertical vectorial displacement normal to the slope. These displacements caused a squeezing effect on the slope. At this depth, which is below the aforementioned neutral axis, the Recent Alluvium is softer than at the surface (see "Average Strata Properties" on Figures 2.5-4a through 52). Squeezing normal to the slope face caused the soft lower Recent Alluvium to move in the directional least resistance; i.e., into the excavation.

All the above movements occurred during excavation and have since stabilized and heaves have been recompressed with the completion of backfilling and the reduction in construction dewatering.

d) Site Area Subsidence

Settlement of the highway, levee and plant area settlement monuments as well as inclinometer settlements are plotted in Figure 2.5-116. The plots indicate that construction dewatering-imposed area settlements have leveled off and stabilized. The highest settlements were realized by the inclinometers, these being closest to the dewatering system of all settlement monuments. Inclinometer settlements ranged from 1.1 ft. to 1.8 ft.

The plant area settlement monuments exhibited nearly zero settlement for the monuments furthest from the dewatering system. Settlement began to be measurable at between 1300 and 1500 ft. from the dewatering system. Settlement in this region is approximately 0.1 ft. Within 400 ft. of the dewatering system, 0.75 ft. of settlement was measured. Settlement monument No. 8, which was in the same proximity to the dewatering system as the inclinometers, settled 1.5 ft. This is in good agreement with the inclinometer settlement measurements.

Highway and levee settlement monuments settled between 0.1 ft. and 0.6 ft. These monuments are not too representative of the area settlement because of their installation date, which was several years after initial start of construction. They are, however, indications that the settlements around the north side of the excavation in the levee area have stabilized.

The overall site area settlement response is gradual. The dewatering zone of influence for settlement is approximately one mile across. Although settlements ranged up to nearly two ft. in the immediate vicinity of the dewatering system, these settlements are total surface movements. Much of this movement occurred in the Recent alluvial material and does not in any way effect the integrity of the immediate plant foundation Pleistocene soils.

2.5.4.13.3 NPIS Settlement

The NPIS settlements have been, and are being periodically monitored throughout the entire construction period. The combined structure foundation is an integral reinforced concrete mat which was formed in 28 block placements between December 1975 and May 1976. At the outset of these block placements, their movements were monitored for total and differential settlements. Total settlements are being measured with respect to a fixed monument, well removed from the influence of construction activities. Differential settlements for the individual blocks are taken with respect to the center foundation block #6 (first block placed).

Presented on Figure 2.5-117 are time vs. settlement plots, averaged for each foundation strip. Each strip is comprised of several blocks. As indicated on the figure, each block experienced an immediate settlement of approximately 1/2 inch as a result of concrete placement. Subsequently, the entire mat experienced a fairly constant rate of settlement through 1977. Between the fourth quarter of 1977 and the second quarter of 1979, the rate of foundation settlement diminished to zero and has remained unchanged to the present (May 1981). This was the result of controlled deactivation of the dewatering system (period of foundation recharge) and the decrease in the rate of placing structural loads. It should also be noted that for the first year and a half, NPIS settlement was simply recompression of site heave experienced during the excavation phases, shown on Figure 2.5-113. Subsequently, the NPIS experienced a controlled, induced net settlement beyond the initial zero position in order to further preconsolidate the foundation soils.

→(DRN 02-899, R12-A)

Because of the stabilized settlement rates and the increased difficulty in obtaining individual block settlements in a congested NPIS, the block settlement readings were discontinued at the end of 1980. In lieu of monitoring the foundation mat blocks, plant settlement readings were transferred to four points on the exterior walls of the NPIS and four points on the containment structure in January 1981 (see key plan on Figure 2.5-117 and Figure 2.5-112a). These relocated settlement points served as monitoring points for continued post-construction settlement, as discussed in Subsection 2.5.4.13.4.

←(DRN 02-899, R12-A)

The long term settlement measurements on these relocated settlement points are plotted on Figure 2.5-117 and also confirm the stabilized plant settlement trend.

Presented on Figure 2.5-118 is a plot of differential settlement contours across the NPIS foundation. These are the maximum differential settlements (relative to block #6) experienced in the mat up to the time when the individual blocks stopped moving (August 1979). This figure shows that the maximum differential settlement across the mat does not exceed 2.5 inches. It should also be noted that the higher movements are shown at the north and south ends of the mat. This is because as each block was placed and tied into the mat system it was set relative to block #6 which had already experienced some movement. As construction proceeded away from the mat center each subsequent block experienced a larger relative movement to an already-settled block #6.

2.5.4.13.4 Post-Construction NPIS Monitoring

The NPIS basemat continues to be monitored. The basemat monitoring program provides for data collection and trending such that information allows an assessment of the structural integrity of the basemat. The monitoring program includes four major areas:

a) Basemat Settlement - This portion of the program is essentially an extension of the data measurements taken during construction and prior to plant commercial operation. Elevation data is taken by a survey on selected monitoring points. Figures 2.5-112a and 117 show the monitoring points and associated settlement previously measured through 1984.

→(DRN 02-899, R12-A)

In October 1984, prior to fuel load, some monitoring point locations were revised and additional points added in order to facilitate measurements during plant operation considering accessibility from an ALARA and security standpoint. In selecting primary monitoring points considerations were also made to minimize, as much as possible, the surveying "setups" required to achieve the monitoring point elevation, thus minimizing the errors associated with the measurement. During 1985, LP&L also added additional monitoring points which were designated as secondary monitoring points. The primary settlement monitoring points were located on the exterior walls of the NPIS and the Reactor Containment Building as shown in Figure 2.5-112b. The secondary settlement monitoring points were located on top of the basemat representing different areas of the basemat as shown in Figure 2.5-112C. The intent of establishing both primary and secondary monitoring points was to establish a correlation between them and then monitor only the points that were at grade.

←(DRN 02-899, R12-A)

The basemat movements since 1984 have not exhibited unusual behavior. Detailed evaluation and analysis of the existing monitoring data resulted in the deletion of some monitoring points and the addition of others near the edge of the basemat for a better distribution. Figure 2.5-112d shows the location on the basemat surface of the set of monitoring points which are currently utilized for settlement measurements.

→(DRN 02-899, R12-A; 06-877, R15)

Initially, post-construction NPIS elevation data was taken through surveys conducted on on a quarterly basis. Quarterly measurements were conducted for four consecutive quarters. Following the four measurements, the interval was extended as no significant changes were observed and no adverse or unexplained data has been obtained. Thereafter, three consecutive, satisfactory surveillances were required to extend the internal to the next interval stated below. The intervals were (as defined in Technical Specification Table 1.1).

←(DRN 02-899, R12-A; 06-877, R15)

Quarterly	At least once per 92 days
Semi-annually	At least once per 184 days
Annually	12 months
Refueling	At least once per 18 months

Basemat settlement measurements are conducted concurrently with surveillances or measurements associated with the crack width measurements and ground water level measurements.

→(DRN 06-877, R15)

b) Groundwater Chemistry - Actual corrosion of the basemat rebar from the groundwater surrounding the basemat is highly unlikely given the normal groundwater chemistry found in the vicinity of Waterford 3, and the minimal contact between the water and rebar. Nonetheless, water samples are taken and analyzed for chloride content from each of the two wells located one to the east and other to the west next to the NPIS. The frequency of groundwater sampling is quarterly.

←(DRN 06-877, R15)

c) Seasonal Variation of Groundwater Level - Groundwater level measurements are taken and maintained to provide data in the event that evaluation of other observed basemat phenomena becomes necessary. These measurements which are taken on a quarterly basis are performed concurrently with surveillances or measurements for other portions of the program scheduled to be performed during that quarter. The wells established for groundwater sampling provide a means to determine the groundwater level.

→(DRN 06-877, R15)

d) Crack Surveillance - The cracks in the basemat have been shown to be a result of the differential settlements experienced during the early stages of construction. Since state-of-the-art NDT inspections, calculations, and evaluations have determined that existing cracking does not imply any degradation of the designed structural integrity a crack surveillance program was established to detect significant changes in the state of the basemat. To provide further assurance that basemat integrity is not degraded from some future unanticipated mechanism or postulated event, this crack surveillance program includes obtaining quantitative data on the width of basemat cracks.

←(DRN 06-877, R15)

The program consists of taking precision measurements across representative cracks that were chosen based on location, visual appearance, crack depth from NDT measurements and accessibility. The points of crack width monitoring were selected so that several major cracks, cracks in areas of computed compression and cracks in areas of computed tension on the basemat top surface are gaged. These cracks have been instrumented to provide a measure of changes in crack width. The number of cracks instrumented has been increased from four representative cracks to fifteen. Measured changes in crack width of greater than 0.015 inches, which is the established, conservative action limit, require further evaluation and inspection of the basemat.

Baseline readings for the four representative cracks selected for crack width monitoring were taken in August, 1986. Subsequent to the baseline readings, readings were taken at 3 month intervals. Quarterly 2 measurements will be performed for four consecutive quarters before interval extension will be considered. However, subsequent measurement intervals may be extended in the same manner as described for basemat settlement. Crack width surveillance measurements are conducted concurrently with basemat settlement measurements and ground water level measurements.

→(DRN 06-877, R15)

The program also involved the performance of a photographic survey, every 18 months, of the lower portion of the Shield Building and selected exterior walls in the east and west cooling tower areas. A photographic survey in lieu of mapping of cracks was adopted because the NDT examination of Shield Building wall cracks indicated that they were shallow cracks and no correlation was found between the wall cracks and the basemat cracks. The photographic surveys were utilized to determine whether significant changes were visible, in which case the areas would have been subjected to futher investigation.

←(DRN 06-877, R15)

The first complete photographic survey of the selected walls was conducted in June, 1986. The photographic survey was continued for two additional cycles in December 1987 and May 1989. Subsequently, the phototgraphic survey was discontinued due to a lack of any significant changes.

2.5.4.14 Construction Notes

The only significant design and construction change consisted of placing the Turbine Building on spread footings in the compacted backfill. Originally this building was to be founded on piles.

The additional lateral stresses imposed by the Turbine Building footings on the adjacent seismic Category I Reactor Auxiliary Building wall were determined using a Boussinesq lateral stress distribution analysis. Due to the well distributed magnitude of the footing loads and their respective distances from the adjacent seismic Category I Structure, these additional stresses are of sufficiently low magnitude and are well within the structural capacity of the seismic Category I wall. No redesign of the Reactor Auxiliary Building was therefore required.

2.5.5 STABILITY OF SLOPES

There are no seismic Category I slopes failure of which could adversely affect the safety of the plant. Therefore this Subsection does not apply.

2.5.6 EMBANKMENTS AND DAMS

There are no seismic Category I embankments and dams at the Waterford site. Embankments are not required for impounding cooling water, nor are embankments used for flood protection. The plant is designed for a full flood condition of +30 ft. MSL where the Mississippi River levee is assumed-to be breached. Therefore, this Subsection does not apply.

SECTION 2.5: REFERENCES

1. Fisk, H. N., 1944, Geological Investigation of the Alluvial Valley of the Lower Mississippi River: Mississippi River Commission, Vicksburg, Mississippi.

2. Garrison, L. E., and Martin, R. G., Jr., 1973, Geologic Structures in the Gulf of Mexico Basin: U. S. Geological Survey Professional Paper 773, p. 85.

3. Martin, R. G.,, and Case, J. E., Geophysical Studies in the Gulf of Mexico: in Ocean Basins and Margins, Volume II, The Gulf of Mexico and Caribbean Sea, Plenum Press, New York.

4. Paine, W. R., and Meyerhoff, A. A., 1970, Gulf of Mexico Basin: Interactions Among Tectonics, Sedimentation, and Hydrocarbon Distribution: Transactions-Gulf Coast Association of Geological Societies, Volume 20, pp. 5-44.

5. Wilhelm, 0. and Ewing, M., 1972, Geology and History of the Gulf of Mexico: Geological Society of America Bulletin, Volume 83, pp. 575-600.

6. Murray, G. E., 1961, Geology of the Atlantic and Gulf Coastal Province of North America: Harper and Brothers, New York.

7. Woods, R. D., and Addington, J. W., 1973, Pre-Jurassic Geologic Framework, Northern Gulf Basin: Transactions-Gulf Coast Association of Geological Societies, Volume 23, pp. 92-108.

8. Scott, K. R., et al, 1961, Geology of the Eagle Mills Formation: Transactions-Gulf Coast Association of Geological Societies, Volume 11, p. 14.

9. Worzel, J. L., and Watkins, J. S., 1973, Evolution of the Northern Gulf Coast Deduced from Geophysical Data: Transactions-Gulf Coast Association of Geological Societies, Volume 23, pp. 84-91.

10. Hughes, D. J., 1968, Salt Tectonics as Related to Several Smackover Fields Along the Northeast Rim of the Gulf of Mexico: Transaction-Gulf Coast Association of Geological Societies, Volume 18, pp. 320-330.

11. Oxley, M. L., Minihan, E. D. and Ridgeway, J. M., 1967, A Study of the Jurassic Sediments in Portions of Mississippi and Alabama: Transactions-Gulf Coast Association of Geological Societies, Volume 17, pp. 24-48.

12. Wendlandt, E. A., and Shelby, T. H., Jr., 1948, Talco Oil Field-Franklin and Titus Counties, Texas: in Structure of Typical American Oil Fields -Volume II, American Association of Petroleum Geologists.

13. Lehner, P., 1966, Salt Tectonics and Pleistocene Stratigraphy on Continental Slope of Northern Gulf of Mexico: American Association of Petroleum Geologists Bulletin, Volume 53, pp. 2431-2479.

SECTION 2.5: REFERENCES (Cont'd)

14. Frye, J. C. and Willman, H. B., 1961, Continental Glaciation in Relation to McFarlan's Sea-level Curves for Louisiana: Geological Society of America Bulletin, Volume 72, Number 6, pp. 991-992.

15. Williamson, J. D. M., 1959, Gulf Coast Cenozoic History: Transactions-Gulf Coast Association of Geological Societies, Volume 9, pp. 15-29.

16. Wintz, W. A., Jr., Kasmann, R. G., and Smith, C. G., Jr., 1970, Subsidence and Ground Water Offtake in the Baton Rouge Area: Louisiana Water Resources Research Institute, Bulletin 6.

17. Zimmerman, T. J., 1958, Marine Pleistocene Deposits of the Mississippi Delta Platform: M. S. Thesis, Louisiana State University.

18. Akers, W. H., and Holch, A. J. J., 1957, Pleistocene Beds Near the Edge of the Continental Shelf, Southeastern Louisiana: Geological Society of America Bulletin, Volume 68, pp. 983-992.

19. Fisk, H. N., 1938, Pleistocene History of Central Louisiana (Abstract): Geological Society of American Proceedings 1937, pp81-82.

20. Fisk, H. N., 1939, Depositional Terrace Slopes in Louisiana: Journal of Geomorphology, Volume 2, Number 3, pp. 181-199.

21. Doering, J. A., 1958, Citronelle Age Problem: American Association of Petroleum Geologists Bulletin, Volume 42, Number 4, pp. 764-786.

22. Durham, C. O., Jr., et al, 1967, An Agnostic View of the Terraces: Natchez to New Orleans: Geological Society of American Field Trip Guidebook, New Orleans, pp. EI-E22.

23. Kolb, C. R., 1962, Distribution and Engineering Significance of Sediments Bordering the Mississippi from Donaldsonville to the Gulf: Dissertation, Louisiana State University.

24. Eardey, A. J., 1951, Structural Geology of North America: Harper and Brothers, New York.

25. River Bend Nuclear Generating Station Units I and II PSAR and SER-Section 2.5, Geology and Seismology.

26. Halbouty, M. T., 1967, Salt Domes: Gulf Publishing Company, Houston, Texas.

27. Hanna, M. A., 1958, Tectonics of Gulf Coast Salt Domes (Abstract): Transactions-Gulf Coast Association of Geologic Societies, Volume 8, P. 100.

SECTION 2.5: REFERENCES (Cont'd)

28. Bruce, C. H., 1972, Pressured Shale and Related Sediment Deformation: A Mechanism for Development of Regional Contemporaneous Faults: Transactions-Gulf Coast Association of Geological Societies, Volume 22, pp. 23-31.

29. Hardin, F. R., and Hardin, G. C., Jr., 1961, Contemporaneous Normal Faults of the Gulf Coast and Their Relation to Flexures: American Society of Petroleum Geologists Bulletin, Volume 45, pp. 238-248.

30. Ocamb, R. D., 1961, Growth Faults of Southern Louisiana: Transactions-Gulf Coast Association of Geological Societies, Volume 11, pp. 139-175.

31. Thorsen, C. E., 1963, Age of Growth Faulting in Southeast Louisiana: Transactions-Gulf Coast Association of Geological Societies, Volume 13, pp. 103-110.

32. Fisk, H. N., 1944, Geological Setting of the Mississippi Alluvial Valley: Mississippi River Commission, Vicksburg, Mississippi.

33. Oxley, P. 1971, Salt Ridge-Salt Dome Origins in Gulf Coast Area (Abstract): American Association of Petroleum Geologists Bulletin, Volume 55, Number 2, p. 357.

34. Durham, C. 0. Jr., and Peeples, E. M., III, 1956, Pleistocene Fault Zone in Southeastern Louisiana: Transactions-Gulf Coast Association Geological Societies, Volume 6, p. 65.

35. Carsey, B. J., 1950, Geology of the Gulf Coastal Area and Continental Shelf: American Association of Petroleum Geologists Bulletin, Volume 34, pp. 361-385.

36. Doering, J. A., 1956, Review of Quarternary Surface Formations of Gulf Coast Region: American Association of Petroleum Geologists Bulletin, 40, Number 8, pp. 764-786.

37. Murray, G. E., 1966, Salt Structures of the Gulf of Mexico Basin; American Association of Petroleum Geologists Bulletin, Number 50, pp. 439-478.

38. Case, J. E., and Moore, W. R., 1968, Gravity Anomalies, Basement Rocks, and Crustal Structure, Central and Southeast Texas Transactions-Gulf Coast Association of Geological Societies, Volume 28, pp. 331-333.

39. Deitz, R. A., Holden, J. C., and Sprool, W. P., 1970, Geotectonic Evolution and Subsidence of Bahama Platform: Geological Society of America Bulletin, Volume 31, pp. 1915-1928.

40. Powers, M. C., 1967, Fluid-release Mechanism in Compacting Marine Mudrocks and their Importance in Oil Exploration: American Association of Petroleum Geologist Bulletin, Volume 51, pp. 1240-1254.

SECTION 2.5: REFERENCES (Cont'd)

41. Burst, J. F., 1969, Diagenesis of Gulf Coast Clayey Sediments and Its Possible Relation to Petroleum Irrigation: American Association of Petroleum Geologists Bulletin; Volume 53, pp. 73-93.

42. Jones, P. H., 1970, Geothermal Resources of the Northern Gulf of Mexico Basin: U. N. Symposium on the Development and Utilization of Geothermal Resources, Pisa, Italy, 1970 Volume 2, Part I.

43. Yerkes, R. F. and Castle, R. O., 1970, Surface Deformation Associated with Oil and Gas Field Operations in the United States: International Association of Scientific Hydrology, Proceedings of the 1969 Symposium on Land Subsidence, Tokyo, Japan, Volume 1, pp. 55-66.

44. Zimmerman, T. J., 1957, Recent and Pleistocene Deposits of the Mississippi Delta Platform (Abstract): Transactions-Gulf Coast Association of Geological Societies, Volume 7, pp. 165-166.

45. Kazmann, R. G., and Heath, M. M., 1968, Land Subsidence Related to Ground Water offtake in the New Orleans Area: Transactions-Gulf Coast Association of Geological Societies, Volume XVIII, pp. 108-113.

46. Poland, J. F., 1969, Land Subsidence and Aquifer System Compaction, Santa Clara Valley, California, USA: Land Subsidence, Proceedings of the Tokyo Symposium, September 1969.

47. Geertsma, J., 1973, Land Subsidence Above Compacting Oil and Gas Reservoirs: Journal of Petroleum Technology, Volume 25, Number 6, pp. 734-744.

48. van der Knaap, W., and van der Vlis, A. C., 1967, On the Cause of Subsidence in Oil Producing Areas: Proceedings, 7th World Petroleum Congress, Mexico City.

49. Allen, D. R., 1968, Physical Changes of Reservoir Properties Caused by Subsidence and Repressuring Operations: Journal of Petroleum Technology, Volume 20, November 1, pp. 23-29.

50. Gilluly, J., and Grant, U. S., 1949, Subsidence in the Long Beach Harbor Area, California: Geological Society of America Bulletin, Volume 60, pp. 461-530.

51. D'Appolonia, D. J. and Lambe, T. W., 1970, Subsidence due to Oil Production: unpublished report.

52. Pratt, W.E., and Johnson, D.W., 1926, Local Subsidence of Goose Creek Oil Field: Journal of Geology, Volume XXXIV, Number 7, Part 1, pp. 577-590.

53. Hawkins, M. E., and Jirik, C.J., 1966, Salt Domes in Texas, Louisiana, Mississippi, Alabama, and Offshore Tidelands: A Survey: U. S. Department of the Interior, Bureau of Mines Information Circular 8313.

SECTION 2.5: REFERENCES (Cont'd)

54. Akers, W. H., 1965, Pliocene-Pleistocene Boundary, Northern Gulf Coast of Mexico: Science, Volume 149 pp. 741-742.

55. United States Department of Commerce, United States Earthquake: National Oceanic and Atmospheric Administration.

56. United States Department of Commerce, 1973, Earthquake History of the United States (through 1970): National Oceanic and Atmospheric Administration, Environmental Data Service Publication 41-1.

57. United States Geological Survey, 1974, Preliminary Determination of Epicenters (1973-1974).

58 Moneymaker, Berlin C., 1954, some Early Earthquakes in Tennessee and Adjacent States (1699-1850): Journal of the Tennessee Academy of Science, Vol. 29, No. 3, July, pp. 227-233.

59. Moneymaker, Berlin C., 1955, Earthquakes in Tennessee and Nearby Sections of Neighboring States (1851-1900):
Journal of Tennessee Academy of Science, Vol. 30, No. 3, July, pp. 223-233

60. Moneymaker, Berlin C.m 1957, Earthquakes in Tennessee and Nearby Sections of Neighboring States (1901 to 1925):
Journal of the Tennessee Academy of Science, Vol. 32, No. 2, April, pp. 91-105.

61. Moneymaker, Berlin C., 1958, Earthquakes in Tennessee and Nearby Sections of Neighboring States (1926 to 1950):
Journal of the Tennessee Academy of Science, Vol. 33, No. 3, July, pp. 224-239.

62. United States Coast and Coastal Survey, 1930, News Release of October 19, 1930, Donaldsonville Earthquake, Issued November 8, 1930.

63. Neumann, F. and Bodle, R. R., 1932, United States Earthquakes, 1930: U. S. Coast and Geodetic Survey.

64. Nuttli, 0. W., 1973, The Mississippi Valley Earthquakes of 1811 and 1812: Intensity Ground Motion and Magnitude: Bulletin of the Seismological Society of America, Volume 63, Number 1, pp. 227-248.

65. Fuller, M. L., 1912, The New Madrid Earthquake: U. S. Geological Survey Bulletin 494.

66. Schnabel, P. B., Lysmer, J., and Seed, H. B., 1972, SHAKE A Computer Program for Earthquake Response Analysis of Horizontally Layered Sites: Report No. EERC 72-12, University of California, Berkeley, California.

SECTION 2.5: REFERENCES (Cont'd)

67. Seed, H. B. and Idriss, I. M., 1970, Soil Moduli and Damping Factors for Dynamic Response Analysis: Report No. EERC 70-10, University of California, Berkeley, California.

68. Dehlinger, P., and Jones, B.R., 1965, Free Air Gravity Anomaly Map of the Gulf of Mexico and Its Tectonic Implications, 1963 Edition: Geophysics, Volume 30, pp. 102-110.

69. Hershberger, J., 1956, A Comparison of Earthquake Accelerations with Intensity Ratings: Seismological Society of America, Volume 46, Number 4, Number 4, pp. 317-320.

70. Shepard, F.P., 1960, Rise of Sea Level Along the Northwest Gulf of Mexico: in Recent Sediments, Northwest Gulf of Mexico, Shepard, F.P., et al, editions: American Association of Petroleum Geologists Symposium, pp. 338-344.

71. Swanson, R.L., Thurlow, C.I., 1973, Recent Subsidence Rates Along the Texas and Louisiana Coasts as Determined from Tile Measurements: Journal of Geophysical Research Volume 78, Number 15, pp. 2665-2671.

72. Unified Soil Classification System, Technical Memorandum 3-357, U.S. Waterways Experiment Station Vicksburg, 1953.

73. Whitman, Robert V. "Evaluation of Soil Properties For Site Evaluation and Dynamic Analysis of Nuclear Plants", From: Seismic Design for Nuclear Power Plants, 1970. The MIT Press, Cambridge, Massachussetts and London, England.

74. Hardin, Bobby D. and Drnevich, Vincent P. (1970) "Shear Modulus and Damping in Soils", Vol. 1, Measurement and Parameter Effects. Technical Report, University of Kentucky, UKY 26-70-CE2.

75. Seed, H. Bolton and Idriss, I.M. (1969), "The Influence of Soil Conditions on Ground Motions During Earthquake", Journal of the Soil Mechanics and Foundations Division. ASCE, 95, 99-137.

76. Pettitt, R.A. (1967), "Statistical Analyses of Density Tests", Journal of The Highway Division, ASCE , 37-51.

77. Cook, H.K, "Recommended Practice for Evaluation of Compression Test Results of Field Concrete", (AC1 214-65), American Concrete Institute, pp. 214-1-214-29.

78. Seed, H., Bolton and Iris, I.M. (1971), "Simplified Procedure For Evaluating Soil Liquefaction Potential", Journal of the Soil Mechanics and Foundation Division. ASCE, 1249-1273.

79. Lee, K.L. and Fritton. American Society For Testing Materials, STP 450 (1969).

SECTION 2.5: REFERENCES (Cont'd)

80. Bowles, J.E. "Foundation Analysis and Design", McGraw Hill, New York, 1968 Chapter 2, pp 47-53.

81. Geomap Company, Structure Contour Map on Horizon B, South Louisiana Quads 16, 17, 26, and 27, Dallas, Texas.

82. Hosman, R.L., "Grand Water Resources of the Norco Area, Louisiana", Louisiana Geological Survey, and Louisiana Department of Public Works, Water Resources Bulletin No. 18, 1972, Baton Rouge, Louisiana.

83. Durham, D.O., Jr., 1965, (abs.), Stream Activity in the Central Gulf Coast Area during Wisconsin Glacial: Geological Society of America Special Paper No. 82, p. 289.

84. Saucier, R.T., 1974, Quaternary Geology of the Lower Mississippi Valley: Publications on Archeology, Research Series No. 6, Arkansas Archeological Survey, Fayetteville, Arkansas.

85. Fisk, H.N., and McFarlan, E., Jr., 1955, Late Quaternary Deltaic Deposits of the Mississippi River: in Crust of the Earth Geological Society of America Special Paper 62, pp. 279-302.

86. Kolb, C.R., Smith, F.L., and Silva, R.C., 1975, Pleistocene Sediments of the New Orleans - Lake Pontchartrain Area: U.S. Army Engineer Waterways Experiment Station, Technical Paper S-75-6.

87. U.S. Army Engineer Waterway Experiment Station, 1958, Geology of the Mississippi River Deltaic Plain, Southeastern Louisiana: Technical Report 3-483.

88. Durham, C.O., Jr., 1964, (abs.), Late Pleistocene - Early Recent Stream Shrinkage and Crustal Fracturing in the Gulf Coast Area: Geological Society of America Special Paper No. 76, p. 52.

89. Smith, D.A., 1980, Sealing and Nonsealing Faults in Louisiana Gulf Coast Salt Basin: American Association of Petroleum Geologists Bulletin, V-64, No. 2, pp. 145-172.

90. J. Devine. "Clarification of the USGS Position on the Seismic Potential 13 of Certain Regions in the Eastern United States." U.S. Geologi-r-al Survey letter to R. Jackson (NRC), November 1982.

91. Electric Power Research Institute (EPRI) Report NP-6395-D, April 1989, Titled "Probabilistic Seismic Hazard Evaluations at Nuclear Plant Sites in the Central and Eastern United States, Resolution of the-Charleston Earthquake Issue."

92. Electric Power Research Institute Report RP 101-53, April 1989, Titled "Probabilistic Seismic Hazard Evaluation for Waterford Steam Electric Station."

SECTION 2.5: REFERENCES (Cont'd)

93. Louisiana Power and Light Problem Evaluation Information Request (PEIR) 20027, approved February 21, 1989.

SECTION 2.5: BIBLIOGRAPHY

1. Akers, W. H., 1965, Pliocene-Pleistocene Boundary, Northern Gulf Coast of Mexico: Science, Volume 149, pp. 741-742.

2. Akers, W. H., and Holch, A. J. J., 1957, Pleistocene Beds Near the Edge of the Continental Shelf, Southeastern Louisiana: Geological Society of America Bulletin, Volume 68, pp. 983-992.

3. Allen, D. R., 1968, Physical Changes of Reservoir Properties Caused by Subsidence and Repressuring Operations: Journal of Petroleum Technology, Volume 20, November 1, pp. 23-29.

4. Allens Creek Nuclear Generating Station Units 1 and 2 PSAR and SER Section 2.5, Geology and Seismology.

5. American Geophysical Union and the U. S. Geological Survey, 1964, Bouguer Gravity Amomaly Map of the United States.

6. Amery, G. B., 1969, Structure of Sigsbee Scarp, Gulf of Mexico: The American Association of Petroleum Geologists Bulletin, Volume 53, Number 12, pp. 2480-2482.

7. Andrews, D. I.. 1960, Louann Salt and Its Relationship to Gulf Coast Salt Domes: Transactions-Gulf Coast Association of Geological Societies, Volume 10, pp. 215-240.

8. Antoine, J. W.. 1968, A Study of the West Florida Escarpment: Transactions-Gulf Coast Association of Geological Societies, Volume 18, pp. 297-303.

9. Antoine, J. W. Bryant, W. R., and Jones, B. R., 1967, Structural Features of Continental Shelf, Slope, and Scarp, Northeastern Gulf of Mexico: American Association of Petroleum Geologists Bulletin, Volume 51, pp. 257-262.

10. Antoine, J. W., and Bryant, W. R., 1968, The Major Transition Zones of the Gulf of Mexico: Desoto and Campeche Canyons: Transactions-Gulf Coast Association of Geological Societies, Volume 18, p. 55.

11. Antoine, J. W., and Bryant, W. A., 1969, Distribution of Salt and Salt Structures in Gulf of Mexico: American Association of Petroleum Geologists Bulletin, Volume 53, pp. 2543-2550.

12. Antoine, J. W., and Harding, J. L., 1965, Structure Beneath Continental Shelf, Northeastern Gulf of Mexico: American Association of Petroleum Geologists Bulletin, Volume 49, pp. 268-286.

13. Antoine, J. W., and Jones, B. R., 1967, Geophysical Studies of the Continental Slope, Scarp and Basin, Eastern Gulf of Mexico: Transactions-Gulf Coast Association of Geological Societies, Volume 17, pp. 268-286.

SECTION 2.5: BIBLIOGRAPHY (Cont'd)

14. Atwater, G. I., 1968, Gulf Coast Salt Dome Field Area: in Saline Deposits, Geological Society of American Special Paper Number 88, pp. 29-40.

15. Atwater, G. I.. and Forman, M. J., 1959, Nature of Growth of Louisiana Salt Domes: Transactions-Gulf Coast Association of Geological Societies, Volume 88, pp. 20-21.

16. Ball, M. M., and Harrison, C. G. A., 1969, Origin of the Gulf and Caribbean and Implications Regarding Ocean Ridge Extension, Migration, and Shear: Transactions-Gulf Coast Association of Geological Societies, Volume 19, pp. 287-294.

17. Bergantino, R. N., 1971, Submarine Regional Geomorphology of the Gulf of Mexico: Geological Society of American Bulletin Volume 82, pp. 741-752.

18. Bornhauser, M., 1959, Gulf Coast Tectonics: American Association of Petroleum Geologists Bulletin, Volume 42 pp. 339-370.

19. Brannon, H. R., Jr., et al., 1957, Humble Oil and Refining Co. Radiocarbon Dates, Part II: Science, Volume 125, Number 3254, pp. 919-923.

20. Broacher, W., 1961, Radiocarbon Dating of Late Quaternary Deposits South Louisiana: A Discussion: Geological Society of America Bulletin, Volume 72, pp. 159-162.

21. Brooks, H. K., 1973, Geological Oceanography. in a Summary of Knowledge of the Eastern Gulf of Mexico: Coordinated by the State University System of Florida, Institute of Oceanography, St. Petersburg, Florida, pp. IIE-1 to IIE-41.

22. Broughton, M. N., 1944, Geology of the Lafitte Oil Field, Jefferson Parish, Louisiana: unpublished report presented to the Louisiana Department of Conservation.

23. Bruce, C. H., 1972, Pressured Shale and Related Sediment Deformation: A Mechanism for Development of Regional Contemporaneous Faults: Transactions-Gulf Coast Association of Geological Societies, Volume 22, pp. 23-31.

24. Bryant, W. R. Meyerhoff, A. A., Brown, N. K., Jr. Furrer, M. A., Pyle, T. E., and Antoine, J. W., 1969. Escarpments, Reef Trends and Diapiric Structures, Eastern Gulf of Mexico: American Association of Petroleum Geologists Bulletin, Volume 53, pp. 2506-2542.

25. Burst, J. F., 1969, Diagenesis of Gulf Coast Clayey Sediments and Its Possible Relation to Petroleum Irrigation: American Association of Petroleum Geologists Bulletin; Volume 53, pp-73-93.

26. Carsey, B. J., 1950, Geology of the Gulf Coastal Area and Continental Shelf: American Association of Petroleum Geologists Bulletin, Volume 34, pp. 361-385.

SECTION 2.5: BIBLIOGRAPHY (Cont'd)

27. Carver, R. E., 1968, Differential Compaction as a Cause of Regional Contemporaneous Faults: American Association of Petroleum Geologists Bulletin, Volume 52, Number 3, pp. 414-419.

28. Case, J. E., amd Moore, W. R., 1968, Gravity Anomalies, Basement Rocks, and Crustal Structure, Central and Southeast Texas Transactions-Gulf Coast Association of Geological Societies, Volume 28, pp. 331-333.

29. Castle, R. O., Yerkes, R. F., and Riley, F. S., 1970, A Linear Relationship between Liquid Production and Oil Field Subsidence: International Association of Scientific Hydrology, Proceedings of the 1969 Symposium on Land Subsidence, Tokyo, Japan, Volume 1, pp. 162-173.

30. Clark, T. H., and Stearn, C. W., 1968, Chapter 14: The Atlantic and Gulf Coastal Plains: The Geological Evolution of North America , 2nd Edition, Ronald Press Company, New York.

31. Coleman, J. M., and Gagliano, S. M., 1964, Cyclic Sedimentation in the Mississippi River Deltaic Plain: Transactions-Gulf Coast Association of Geological Societies, Volume 14, pp. 67-80.

32. Coleman, J. M., Gagliano, S. M., and Morgan. J. P., 1969, Mississippi River Subdeltas: Natural Models of Deltaic Sedimentation: Coastal Studies Bulletin Number 3, Coastal Studies Institute, Louisiana State University, pp. 23-27.

33. Crouch, R. W., 1955, Pragmatic Approach to Correlation of Miocene Strata in Southern Louisiana: American Association of Petroleum Geologists Bulletin, Volume 39, pp. 2321-2328.

34. Crouch, R. W., 1959, Inspissation of Post-Oligocene Sediments in Southern Louisiana: Geological Society of America Bulletin, Volume 70, pp. 1283-1293.

35. Curtis, D. M., 1970, Miocene Deltaic Sedimentation, Louisiana Gulf Coast (Abstract): Geological Society of America, Abstracts with Programs for 1970 Annual Meeting, pp. 277-278.

36. D'Appolonia, D. J. and Lambe, T. W., 1970. Subsidence due to Oil Production: unpublished report.

37. Davis, S. N. and DeWiest, R. J. M., 1966, Hydrogeology : John Wiley and Sons, New York.

38. DeBlieux, C., 1949, Photogeology in Gulf Coast Exploration: American Association of Petroleum Geologists Bulletin, Volume 33, Number 7, pp. 1251-1259.

39. DeBlieux, C., 1962, Photogeology in Louisiana Coastal Marsh and Swamp: Transactions-Gulf Coast Association of Geological Societies, Volume 12, pp. 231-241.

SECTION 2.5: BIBLIOGRAPHY (Cont'd)

40. Dehlinger, P., and Jones, B. R., 1965, Free Air Gravity Anomaly Map of the Gulf of Mexico and Its Tectonic Implications, 1963 Edition: Geophysics, Volume 30, pp. 102-110.

41. Deitz, R. A., Holden, J. C., and Sprool, W. P., 1970, Geotectonic Evolution and Subsidence of Bahama Platform: Geological Society of America Bulletin, Volume 31, pp. 1915-1928.

42. Doering, J. A., 1956, Review of Quarternary Surface Formations of Gulf Coast Region: American Association of Petroleum Geologists Bulletin, 40, Number 8, pp- 764-786.

43. Doering, J. A., 1958, Citronelle Age Problem: American Association of Petroleum Geologists Bulletin, Volume 42, Number 4, pp. 764-786.

44. Durham, C. L., 1967, A Study of Three Foraminiferal Assemblages from a Well in South Pass Area, Block 30, Louisiana: M. S. Thesis, Louisiana State University.

45. Durham, C. O., Jr. et al., 1964, Iron Ore of Central North Louisiana: Louisiana Geological Survey Bulletin Number 41.

46. Durham, C. O., Jr., et al, 1967, An Agnostic View of the Terraces: Natchez to New Orleans: Geological Society of America Field Trip Guidebook, New Orleans, pp. El-E22.

47. Durham, C. O., Jr., and Peeples, E. M., III. 1956, Pleistocene Fault Zone in Southeastern Louisiana: Transactions-Gulf Coast Association Geological Societies, Volume 6, p. 65.

48. Eardley, A. J., 1951, <u>Structural Geology of North America</u>: Harper and Brothers, New York.

49. Ewing, J. I., Worzel, J. L., and Ewing, M., 1962, Sediments and Oceanic Structural History of the Gulf of Mexico: Journal of Geophysical Research, Volume 67, pp. 2509-2527.

50. Fails, T., 1968, Pleistocene of the Louisiana Continental Shelf (Abstract): Lafayette Geological Society, Volume XII, Number 10.

51. Ferrando, A. and Richardson, H. T., 1941, Barataria Field, Jefferson Parish, Louisiana: American Association of Petroleum Geologists Bulletin, Volume 25, Number 2, pp. 322-323.

52. Fisk, H. N., 1938, Pleistocene History of Central Louisiana (Abstract): Geological Society of America Proceedings 1937, pp. 81-82.

53. Fisk, H. N., 1939, Depositional Terrace Slopes in Louisiana: Journal of Geomorphology, Volume 2, Number 3, pp. 181-199.

SECTION 2.5: BIBLIOGRAPHY (Cont'd)

54. Fisk, H. N., 1944, Geological Investigation of the Alluvial Valley of the Lower Mississippi River: Mississippi River Commission, Vicksburg, Mississippi.

55. Fisk, H. N., 1944, Geological Setting of the Mississippi Alluvial Valley: Mississippi River Commission, Vicksburg, Mississippi.

56. Fisk, H. N., 1955, Sand Facies of Recent Mississippi Delta Deposits: Proceedings, Fourth World Petroleum-Congress, Rome, Italy.

57. Fisk, H. N., 1956, Near Surface Sediments of the Continental Shelf Off Louisiana: Proceedings of the Eighth Texas Conference on Soil Mechanics and Foundation Engineering.

58. Fisk, H. N., 1958, Recent Mississippi River Sedimentation and Peat Accumulation: Compte Rendu Du Quatrieme Congres Pour 1"Advancement des Etudes de Stratigraphie et de Geologie du Carbonifere, Heerlen, Netherlands, pp. 187-199.

59. Fisk, H. N., and McClellan, B., 1959, Geology of Continental Shelf Off Louisiana: Its Influence on Offshore Foundation Design: Geological Survey of America Bulletin, Volume 70, pp. 1369-1394.

60. Fisk, H. N., and McFarlan, E., 1955, Late Quaternary Deltaic Deposits of the Mississippi River: Crust of the Earth, Geological Society of America Special Paper Number 62, pp. 279-302.

61. Fisk, H. N., McFarlan, E., Kolb, C. R., and Wilbert, L. J., 1954, Sedimentary Framework of the Modern Mississippi Delta: Sedimentary Petrology, Volume 24, Number 2, pp. 76-99.

62. Forman, M. J., and Dekker, J. H., 1969, Geological and Geophysical Study, Waterford Plant Site, St. Charles Parish, Louisiana: unpublished report for Louisiana Power and Light Company.

63. Foster, J. W., 1869, The Mississippi Valley; Its Physical Geography: Chicago, pp. 19-22.

64. Frazier, D. E., 1967, Recent Deltaic Deposits of the Mississippi River: Their Development and Chronology: Transactions-Gulf Coast Association of Geological Societies, Volume 17, pp. 287-311.

65. Frye, J. C., 1962, Comparison Between Pleistocene Deep-Sea Temperatures and Glacial and Interglacial Episodes: Geological Survey of American Bulletin, Volume 73, pp. 263-266.

66. Frye, J. C. and Willman, H. B., 1961, Continental Glaciation in Relation to McFarlan's Sea-level Curves for Louisiana: Geological Society of America Bulletin, Volume 72, Number 6, pp. 991-992.

SECTION 2.5: BIBLI0GRAPHY (Cont'd)

67. Frye, J. C., Willman, H. B., Meyer, R. and Black, R., 1968, Definition of Wisconsinan Stage: Geological Society of America Bulletin 1274-E.

68. Gabrysch, R. K., 1970, Land-Surface Subsidence in the HoustonGalveston Region, Texas: International Association of Scientific Hydrology, Proceeding of the 1969 Symposium on Land Subsidence, Tokyo, Japan, Volume I, pp. 43-54.

69. Gabrysch, R. K., McAdoo, G. D., 1973, Development of Groundwater Resources in the Orange County Area, Texas, and Louisiana, 1963-1971: Texas Water Development Board, Report 156.

70. Gagliano, S. M., Van Beek, J. L., 1973, New Era for Mudlumps: Water Spectrum, Volume 5, Number 1, pp. 25-31.

71. Garrison, L. E., and Martin, R. G., Jr., 1973, Geologic Structures in the Gulf of Mexico Basin: U. S. Geological Survey Professional Paper 773, p. 85.

72. Gealy, B. L., 1955, Topography of the Continental Slope in Northwest Gulf of Mexico: Geological Society of America Bulletin, Volume 66, pp. 203-228.

73. Geertsma, J., 1973, Land Subsidence Above Compacting Oil and Gas Reservoirs: Journal of Petroleum Technology, Volume 25, Number 6, pp. 734-744.

73A. Geomap Company, Structure Contour Map on Horizon B, South Louisiana Quads 16, 17, 26 and 27, Dallas, Texas.

74. Gilluly, J., and Grant, U. S., 1949, Subsidence in the Long Beach Harbor Area, California: Geological Society of America Bulletin, Volume 60, pp-461-530.

75. Gough, D. I., 1967, Magnetic Anomalies and Crustal Structure in Eastern Gulf of Mexico: American Association of Petroleum Geologists Bulletin, Volume 51, pp. 200-211.

76. Granata, W. H., Jr., Structural Development of the Sabine Uplift Area: Transactions-Gulf Coast Association of Geological Societies, Volwne 12, pp. 117-119.

77. Green, J. H., 1964, The Effect of Artesian-Pressure Decline on Confined Aquifer Systems and its Relation to Land Subsidence: U.S. Geological Survey Water-Supply Paper 1779-T, pp. TI-Tll.

78. Halbouty, M. T., 1967, Salt Domes Gulf Publishing Company, Houston, Texas.

79. Hanna, M. A., 1958, Tectonics of Gulf Coast Salt Domes (Abstract): Transactions-Gulf Coast Association of Geologic Societies, Volume 8, p. 100.

80. Harbison, R. N., 1968, Geology of DeSoto Canyon: Journal of Geophysical Research, Volume 73, pp- 5175-5185.

SECTION 2.5: BIBLIOGRAPHY (Cont'd)

81. Hardin, F. R., and Hardin, G. C., Jr., 1961, Contemporaneous Normal Faults of the Gulf Coast and Their Relation to Flexures: American Society of Petroleum Geologists Bulletin, Volume 45, pp. 238-248.

82. Haung, T. C. and Goodell, H. G., 1970, Sediments and Sedimentary Processes of Eastern Mississippi Cone, Gulf of Mexico: American Association of Petroleum Geologists Bulletin, Volume 54, pp. 20702100.

83. Hawkins, M. E., and Jirik, C. J., 1966, Salt Domes in Texas, Louisiana, Mississippi, Alabama, and Offshore Tidelands: A Survey: U. S. Department of the Interior, Bureau of Mines Information Circular 8313.

84. Holdahl, S. R., and Morrison, N. L., 1973, Regional Investigations of Vertical Crustal Movements in the U. S. Using Precise Relevelings and Mareograph Data: Symposium on Recent Crustal Movements and Associated Seismic and Volcanic Activity, Randung, Indonesia November, 1973.

84A. Hosman, R. L., "Groundwater Resources of the Norco Area, Louisiana", Louisiana Department of Conservation, Louisiana Geological Survey, and Louisiana Department of Public Works, Water Resources Bulletin No. 18, 1972, Baton Rouge, Louisiana.

85. Howe, H. W., 1936, Louisiana Petroleum Stratigraphy: Louisiana Department of Conservation Bulletin Number 27.

86. Howe, H. V. and McGuirt, J. H., 1936, Salt Domes of Plaquemines and St. Bernard Parishes: Louisiana Geological Survey, Bulletin 8, pp. 200-278.

87. Hughes, D. J., 1968, Salt Tectonics as Related to Several Smackover Fields Along the Northeast Rim of the Gulf of Mexico: Transaction-Gulf Coast Association of Geological Societies, Volume 18, pp. 320-330.

88. James, L. B., 1968, Failure of the Baldwin Hills Reservoir, Los Angeles, California: Geological Society of America, Engineering Geology Case Histories, Number 6, pp. 1-11.

89. Johnson, H. A., Bredeson, D. H., 1971, Structural Development of Some Shallow Salt Domes in Louisiana Miocene Productive Belt: American Association of Petroleum Geologists Bulletin, Volume 55, Number 2, pp. 204-226.

90. Jones, P. H., 1970, Geothermal Resources of the Northern Gulf of Mexico Basin: U. N. Symposium on the Development and Utilization of Geothermal Resources, Pisa, Italy, 1970 Volume 2, Part I.

91. Kazmann, R. G., and Heath, M. M., 1968, Land Subsidence Related to Ground Water offtake in the New Orleans Area: Transactions-Gulf Coast Association of Geological Societies,,Volume XVIII, pp. 108-113

SECTION 2.5: BIBLIOGRAPHY (Cont'd)

92. King, P. B., 1964, Tectonics of Quaternary Time in Middle North America: H. E. Wright, Jr. and D. G. Frey, Editors, The Quaternary of the United States, Princeton University Press, pp. 831-870.

93. Kolb, C. R., 1961, Geology of the Lower Mississippi River Valley and its Economic Aspects: Mississippi Industrial and Technological Research Commission, Publication Number 10, Jackson, Mississippi.

94. Kolb, C. R., 1962, Distribution and Engineering Significance of Sediments Bordering the Mississippi from Donaldsonville to the Gulf: Dissertation, Louisiana State University.

95. Kolb, C. R., and Shockley, W. G., 1957, Mississippi Valley Geology Its Engineering Significance: Proceedings, American Society of Civil Engineers, Journal of the Soil Mechanics and Foundation Division, Number SM3, Proceedings Paper 1289, pp. 1289-1 to 1289-14.

96. Kulp, J. L., 1961, Geologic Time Scale: Science, Volume 133, No 3459, pp. 1105-1114.

97. Kupfer, D. H., 1963, Structure of Salt in Gulf Coast Domes: Symposium on Salt, Northern Ohio Geological Society, Inc., Cleveland, Ohio, pp. 104-123.

98. Kupfer, D. H., et al, 1970, North Central Louisiana Salt Domes, Gulf Coast Association of Geologic Societies, 20th Annual Meeting Field Trip Guide.

99. Lehner, P., 1966, Salt Tectonics and Pleistocene Stratigraphy on Continental Slope of Northern Gulf of Mexico: American Association of Petroleum Geologists Bulletin, Volume 53, pp. 2431-2479.

100. Leutze, 1972, Generalized Biostratigraphic Zones South Louisiana: Transactions-Gulf Coast Association of Geological Societies, Volume 22, Figure 2, p. 151.

101. Leutze, W. P., 1972, Stratigraphy of Cibicides Carstensi Zone, Miocene of Louisiana: American Association of Petroleum Geologists Bulletin, Volume 56, Number 4, pp. 775-789.

102. Limes, L. L., and Stripe, J. C., 1959, Occurrence of Miocene Oil in South Louisiana: Transactions-Gulf Coast Association of Geological Societies, Volume 9, pp. 77-90.

103. Lowman, S. W., 1949, Sedimentary Facies in the Gulf Coast: American Society of Petroleum Geologists Bulletin, Volume 33, pp. 1937-1999.

104. Lyons, P. I., 1957, Geology and Geophysics of the Gulf of Mexico: Transactions-Gulf Coast Association of Geological Societies, Volume 7, pp. 1-10.

SECTION 2.5: BIBLIOGRAPHY (Cont'd)

105. Martin, R. G., and Case, J. E., (in press), Geophysical Studies in the Gulf of Mexico: in Ocean Basins and Margins, Volume II, The Gulf of Mexico and Caribbean Sea, Plenum Press, New York.

106. Martinez, J. D., 1969, The Impact of Salt on Man's Environment: Transactions-Gulf Coast Association of Geologic Societies, Volume 19, pp. 49-62.

107. McFarlan, E., Jr., 1957, Subsurface Quaternary Stratigraphy in Coastal Louisiana and Adjacent Continental Shelf (Abstract): Transactions-Gulf Coast Association of Geological Societies, Volume 7, p. 12.

108. McFarlan, E. Jr., 1961, Radiocarbon Dating of Late Quaternary Deposits, South Louisiana: Geological Society of America Bulletin, Volume 72, pp. 129-158 and 159-162.

109. McIntire, W. G., 1959, Methods of Correlating Cultural Remains with Stages of Coastal Development: 2nd Coastal Geography Conference, Coastal Studies Institute, Louisiana State University, pp. 341-359.

110. Morgan, A. L., 1952, A Structural Analysis of the Delta Farms Field LaFourche parish, Louisiana, with Notes of the Stratigraphy: Transactions-Gulf Coast Association of Geological Societies, Volume 2, pp. 129-163.

111. Morgan, J. P., 1967, Ephemeral Estuaries of the Deltaic Environment: Estuaries, American Association for the Advancement of Science, pp. 115-120.

112. Morgan, J. P., 1972, Impact of Subsidence and Erosion on Louisiana Coastal Marshes and Estuaries: Preprint, Coastal Marsh and Estuary Symposium, Louisiana State University.

113. Morgan, J. P., and Larimore, P. B., 1957, Changes in the Louisiana Shoreline: Transactions-Gulf Coast Association of Geological Societies, Volume 7, pp. 303-310.

114. Muchlberger, W. R., 1968, Internal Structures and Mode of Uplift of Texas and Louisiana Salt Domes: In Saline Deposits: Geological Society of America, Special Paper Nwnber 88, pp. 359-364.

115. Murray, G. E., 1961, <u>Geology of the Atlantic and Gulf Coastal Province of North America:</u> Harper and Brothers, New York.

116. Murray, G. E., 1966, Salt Structures of the Gulf of Mexico Basin: American Association of Petroleum Geologists Bulletin, Number 50, pp. 439-478.

117. Myers, R. L. and Van Siclen, D. C., 1964, Dynamic Phenomena of Sediment Compaction, Matagorda County, Texas: Transactions-gulf Coast Association of Geological Societies, Volume 14, pp. 241-252.

SECTION 2.5: BIBLIOGRAPHY (Cont'd)

118. Nettleton, L. L., 1952, Geophysical Aspects, Part VI of Sedimentary Volumes in Gulf Coastal Plain of the United States and Mexico: Geological Society of America Bulletin, Volume 63, pp. 1221-1228.

119. New Orleans Geological Society, 1954, Cross-Sections Through South Louisiana: New Orleans Geological Society Cross-Sections Study Group.

120. Ocamb, R. D., 1961, Growth Faults of Southern Louisiana: Transactions-Gulf Coast Association of Geological Societies, Volume 11, pp. 139-175.

121. Ohnoutka, R. C., 1963, Recent and Ancient Beach and Bar Deposits (Abstract): Transactions-Gulf Coast Association of Geological Societies, Volume 13, p. 126.

122. Oxley, M. L., Minihan, E. D. and Ridgeway, J. M., 1967, A Study of the Jurassic Sediments in Portions of Mississippi and Alabama: Transactions-Gulf Coast Association of Geologcal Societies, Volume 17, pp. 24-48.

123. Oxley, P. 1971, Salt Ridge-Salt Dome Origins in Gulf Coast Area (Abstract): American Association of Petroleum Geologists Bulletin, Volume 55, Number 2, p. 357.

124. Paine, W. R., and Meyerhoff, A. A., 1970, Gulf of Mexico Basin: Interactions Among Tectonics, Sedimentation, and Hydrocarbon Distribution: Transactions-Gulf Coast Association of Geological Societies, Volume 20, pp. 5-44.

125. Poland, J. F., 1969, Land Subsidence and Aquifer System Compaction, Santa Clara Valley, California, USA: Land Subsudence, Proceedings of the Tokyo Symposium, September, 1969.

126. Poland, J. F., and Davis, G. H., 1969, Land Subsidence Due to Withdrawal of Fluids: Geological Society of America, Reviews in Engineering Geology 11.

127. Powers, M. C., 1967, Fluid-release Mechanism in Compacting Marine Mudrocks and their Importance in Oil Exploration: American Association of Petroleum Geologists Bulletin, Volume 51, pp. 1240-1254.

128. Pratt, W. E., and Johnson, D. W., 1926, Local Subsidence of Goose Creek Oil Field: Journal of Geology, Volume XXXIV, Number 7, part 1, pp. 577-590.

129. Pusey, W. C., III, 1973, Paleotemperatures in the Gulf Coast Using the ESR-Kerogen Method: Transactions-Gulf Coast Association of Geological Societies, Volume 23, pp. 195-202.

130. Quarles, M., Jr., 1953, Salt-Ridge Hypothesis on Origin of Texas Gulf Coast Type of Faulting: Bulletin of the American Association of Petroleum Geologists, Volume 37, Number 3, pp. 489-508.

SECTION 2.5: BIBLIOGRAPHY (Cont'd)

131. Rainwater, E. H., 1964, Regional Stratigraphy of the Gulf Coast Miocene: Transactions-Gulf Coast Association of Geological Societies, Volume 14, pp. 81-124.

132. Reid, W. M., 1973, Active Faults in Houston, Texas: Ph.D. Dissertation, University of Texas at Austin.

133. River Bend Nuclear Generating Station Units I and II PSAR and SER Section 2.5, Geology and Seismology.

134. Russell, R. J., 1934, Slump Near Fort Adams, Mississippi (Abstract): Geological Society of America, Proceedings, p. 104.

135. Russell, R. J., 1939, Louisiana Stream Patterns: American Association of Petroleum Geologists Bulletin, Volume 23, Number 8, pp 1199-1227.

136. Russell, R. J., 1967, River and Delta Morphology: Coastal Studies Institute, Louisiana State University Baton Rouge, Louisiana, Technical Report Number 52.

137. Russell, R. J. (editor), 1968, Glossary of Terms Used in Alluvial, Deltaic, and Coastal Morphology and Processes: Coastal Studies Institute, Louisiana State University, Technical Report Number 63.

138. Saucier, R. T., 1963, Recent Geomorphic History of the Pontchartrain Basin: Louisiana State University, Coastal Studies Series Number 9.

139. Saucier, R. T., 1969, Geological Investigation of the Mississippi River Area, Artonish to Donaldsonville, Louisiana: U. S. Army Engineer Waterways Experiment Station, Vicksburg, Mississippi, Technical Report Number S-69-4.

140. Scott, K. R., et al, 1961, Geology of the Eagle Mills Formation: Transactions-Gulf Coast Association of Geological Societies, Volume 11. p. 14.

141. Seglund, J. A., 1974, Collapse Fault Systems of the Louisiana Gulf Coast: Transactions-Gulf Coast Association of Geological Societies, Volume 24, pp. 1-3.

142. Sellards, E. H., 1930, Subsidence at Goose Creek Oil Field University of Texas, Bulletin 3001, pp. 29-36.

143. Shelton J. W., 1968, Role of Contemporaneous Faulting During Basinal Subsidence: American Association of Petroleum Geologists Bulletin, Volume 52, pp- 399-413.

144. Shepard, F. P., 1960, Rise of Sea Level Along the Northwest Gulf of Mexico: in Recent Sediments, Northwest Gulf of Mexico, Shepard, F. P., et al, editors: American Association of Petroleum Geologists Symposium, pp. 338-344.

145. Smith, W. G., 1970, Spartina "Die-Back" in Louisiana Marshlands: Louisiana State University, Coastal Studies Bulletin Number 5, Special Sea Grant Issue, pp. 89-96.

SECTION 2.5: BIBLIOGRAPHY (Cont'd)

146. Stearns, R. G., 1956, Paleocene and Lower Eocene Geologic History of the Upper Mississippi ENbayment (Abstract): Transactions-Gulf Coast Association of Geological Societies, Volume 6, p. 152.

147. Swanson, R. L., Thurlow, C. I., 1973, Recent Subsidence Rates Along the Texas and Louisiana Coasts as Determined from Tide Measurements: Journal of Geophysical Research Volume 78, Number 15, pp. 2665-2671.

148. Thorsen, C. E., 1963, Age of Growth Faulting in Southeast Louisiana: Transactions-Gulf Coast Association of Geological Societies, Volume 13, pp. 103-110.

149. Trabant, P., Bryant, W. R., Bouma, A. H., 1972, High Resolution Subbottom Profiles and Sediment Characteristics of the Mississippi Delta (Abstract): Transactions-Gulf Coast Association of Geological Societies, Volume 22, p. 156.

150. Trowbridge, A. C., 1930, Building of Mississippi Delta: American Association of Petroleum Geologists Bulletin, Volume 14, pp. 867-901.

151. Trowbridge, A. C., 1954, Mississippi and Gulf Coast Terraces and Sediments as Related to Pleistocene History - A Problem: Geological Society of America Bulletin, Volume 65, pp. 793-812.

152. Uchupi, E., 1967, Bathymetry of the Gulf of Mexico: TransactionsGulf Coast Association of Geological Societies, Volume 17, pp. 161-172.

153. Uchupi, E., and Emery, K. O., 1968, Structure of Continental Margin off Gulf Coast of United States: American Association Petroleum Geologists Bulletin, Volume 52, pp. 1162-1193.

154. U.S. Geological Survey and American Association of Petroleum Geologists, 1962, Tectonic Map of the United States.

155. U.S. Geological Survey, 1932, Geologic Map of the United States.

155A. U.S. Geological Survey, Earthquakes in the United States (1976-1979), Circulars 766, 788, and 819.

156. van Andel, T. H. and Poole, D. M., 1960, Sources of Recent Sediments, Northern Gulf of Mexico: Journal of Sedimentary Petrology, Volume 30, pp. 91-122.

157. van der Knaap, W., and van der Vlis, A.C., 1967, On the Cause of Subsidence in Oil Producing Areas: Proceedings, 7th World Petroleum Congress, Mexico City.

158. van Lopik, J. R. and McIntire, W. G., 1957, Cheniers of Vermilion Parish, Louisiana - Their Relation to Mississippi River Delta Chronology (Abstract): Transactions-Gulf Coast Association of Geological Societies, Volume 7, p. 302.

SECTION 2.5: BIBLIOGRAPHY (Cont'd)

159. Vidrine, L. O., 1958, Regional Study of Portions of Jefferson, Plaquemines, and St. Charles Parishes, Louisiana: Transactions-Gulf Coast Association of Geological Societies, Volume 8, pp. 105-115.

160. Walker, J. R., and Massingill, J. V., 1970, Slump Features on the Mississippi Fan, Northeastern Gulf of Mexico: Geological Society of America Bulletin, Volume 81, pp. 3101-3108.

161. Wallace, W. E., 1944, Structure of South Louisiana Deep-Seated Domes: American Association of Petroleum Geologists Bulletin, Volume 28, Number 9, pp. 1249-1312.

162. Wallace, E. E. (editor), 1957, Fault Map of South Louisiana: Transactions-Gulf Coast Association of Geologic Societies, Volume 7, p. 240.

163. Warren, D. H., 1966, Crustal Seismic Measurements in Southern Mississippi: Journal of Geophysical Research, Volume 71.

164. Welder, F. A., 1959, Processes of Deltaic Sedimentation in the Lower Mississippi River: Louisiana State University, Coastal Studies Institute.

165. Wendlandt, E. A., and Shelby, T. H., Jr., 1948, Talco Oil Field Franklin and Titus Counties, Texas: in Structure of Typical American Oil Fields -Volume II, American Association of Petroleum Geologists.

166. Wilhelm, 0. and Ewing, M., 1972, Geology and History of the Gulf of Mexico: Geological Society of America Bulletin, Volume 83, pp. 575-600.

167. Williamson, J. D. M., 1959, Gulf Coast Cenozoic History: Transactions-gulf Coast Association of Geological Societies, Volume 9, pp. 15-29.

168. Wintz, W. A., Jr., Kasmann, R. G., and Smith, C. G., Jr., 1970, Subsidence and Ground Water Offtake in the Baton Rouge Area: Louisiana Water Resources Research Institute, Bulletin 6.

169. Woodbury, H. O., Murray, I. B., Pickford, P. J., Akers, W. H., 1973, Pliocene and Pleistocene Depocenters, Outer Continental Shelf, Louisiana and Texas: American Association of Petroleum Geologists Bulletin, Volume 57, Number 12, pp. 2428-2439.

170. Wood, M. L., and Walper, J. L., 1974, The Evolution of the Interior Mesozoic Basin and the Gulf of Mexico: Transactions-Gulf Coast Association of Geological Societies, Volume 24, pp. 31-40.

171. Woods, R. D., 1956, The Northern Structural Rim of the Gulf Basin: Transactions-Gulf Coast Association of Geological Societies, Volume 6, pp. 3-11.

172. Woods, R. D., and Addington, J. W., 1973, Pre-Jurassic Geologic Framework, Northern Gulf Basin: Transactions-Gulf Coast Association of Geological Societies, Volume 23, pp. 92-108.

SECTION 2.5: BIBLIOGRAPHY (Cont'd)

173. Worzel, J. L., and Watkins, J. S., 1973, Evolution of the Northern Gulf Coast Deduced from Geophysical Data: Transactions-Gulf Coast Association of Geological Societies, Volume 23, pp. 84-91.

174. Yarborough, J. Jr., 1967, Geologic Framework of Gulf of Mexico Basin (Abstract): American Association of Petroleum Geologists Bulletin, Volume 51, p. 2172.

175. Yerkes, R. F. and Castle, R. O., 1970, Surface Deformation Associated with Oil and Gas Field Operations in the United States: International Association of Scientific Hydrology, Proceedings of the 1969 Symposium on Land Subsidence, Tokyo, Japan, Volume 1, pp. 55-66.

176. Zimmerman, T. J., 1957, Recent and Pleistocene Deposits of the Mississippi Delta Platform (Abstract): Transactions-Gulf Coast Association of Geological Societies, Volume 7, pp. 165-166.

177. Zimmerman, T. J., 1958, Marine Pleistocene Deposits of the Mississippi Delta Platform: M. S. Thesis, Louisiana State University.

178. Berggren, W. A., 1969, Cenozoic Chronostratigraphy, Planktonic Foraminiferal Zonation and the Radiometric Time Scale: Nature, Volume 224, pp. 1072-1075.

179. Eargle, D. H., and Herbst, E. R., 1967, Regional Geology and the Samon Event: Proceedings of the Symposium on the Geology and Technology of Gulf Coastal Salt, Louisiana State University, Baton Rouge, Louisiana.

180. Fuller, M. L., 1912, The New Madrid Earthquake: U.S. Geological Survey Bulletin 494.

181. Gutenburg, B., and Richter, C. F., 1956, Earthquake Magnitude, Intensity, Energy and Acceleration: Seismological Society of America Bulletin, Volume 46, Number 2, pp. 105-145.

182. Henley, A. D., 1966, Seismic Activity Near the Texas Gulf Coast: Engineering Geology, Volume 3, Numbers 1-2, pp. 33-39.

183. Hershberger, J., 1956, A comparison of Earthquake Accelerations with Intensity Ratings: Seismological Society of America, Volume 46,
Number 4, pp- 317-320.

184. Hughes, D. J., 1960, Faulting Associated with Deep-seated Salt Domes in the Northeast Portion of the Mississippi Salt Basin: Transactions-Gulf Coast Association of Geological Societies, Volume 10, pp. 154-173.

185. Kovach, R. L., 1974, Source Mechanisms for Wilmington Oil Field California Subsidence Earthquakes: Bulletin of the Seismological Society of America, Volume 64, No. 3, pp. 699-711.

SECTION 2.5: BIBLIOGRAPHY (Cont'd)

186. Macelwane, J. B., 1930, The Mississippi Valley Earthquake Problem: Bulletin of the Seismological Society of America, Volume 20, Number 2. pp. 95-98.

187. Nuttli, 0. W., 1973, The Mississippi Valley Earthquakes of 1811 and 1812: Intensity Ground Motion and Magnitude: Bulletin of the Seismological Society of America, Volume 63, Number 1, pp. 227-248.

188. Nuttli, 0. W., 1973, Seismic Wave Attenuation and Magnitude Relationships, for Eastern North America: Journal of Geophysical Research, Volume 78, Number 5, pp. 876-885.

189. Nuttli, 0. W., 1973, State-of-the-Art for Assessing Earthquake Hazards in the United States: United States Army Engineers Waterway Experiment Station, Miscellaneous Paper S-73-1, Report 1.

190. Richter, C. F, 1958, Elementary Seismology, W. H. Freeman and Company, San Francisco.

191. Seed, H. Bolton, Idriss, 1. M., and Kiefer, F. W., 1968, Characteristics of Rock Motions During Earthquakes: University of California, Report Number EERC 68-5, September.

192. Sheets, M. M., 1947, Diastrophism During Historic Time in Gulf Coastal Plain: American Association of Petroleum Geologists Bulletin, Volume 31, pp. 201-226.

193. United States Army Corps of Engineers, 1950, Geological Investigation of the Faulting in the Lower Mississippi Valley: Waterways Experiment Station, Vicksburg Mississippi, Technical Memorandum Number 3-311.

194. United States Department of Commerce, United States Earthquakes: National Oceanic and Atmospheric Administration.

195. United States Department of Commerce, 1973, Earthquake History of the United States (through 1970): National Oceanic and Atmospheric Administration, Environmental Data Service Publication 41-1.

196. Neumann, F. and Bodle, R. R., 1932, United States Earthquakes, 1930: U.S. Coast and Geodetic Survey.

197. United States Coast and Coastal Survey, 1930, News Release of

October 19, 1930, Donaldsonville Earthquake. Issued November 8, 1930

198. United States Geological Survey, 1974. Preliminary Determination of Epicenters (1973-1974)

199. Wood, H. C. and Neumann, F., 1931. Modified Mercalli Intensity Scale of 1931: Bulletin of the Seismological Society of America. Volume 21, Number 4

SECTION 2.5: BIBLIOGRAPHY (Cont'd)

200. Moneymaker, Berlin C., 1974, Some Early Earthquakes in Tennessee and Adjacent States (1969-1850): Journal of the Tennessee Academy of Science, Vol. 29, No. 3, July, pp. 227-233.

201. Moneymaker, Berlin C., 1955, Earthquakes in Tennessee and Nearby Sections of Neighboring States (1851 to 1900): Journal of the Tennessee Academy of Science, Vol. 30, No. 3, July, pp. 222-233.

202. Moneymaker, Berlin C., 1957, Earthquakes in Tennessee and Nearby Sections of Neighboring States (1901 to 1925): Journal of the Tennessee Academy of Science, Vol. 32, No. 2, April, pp. 91-105.

203. Moneymaker, Berlin C., 1958, Earthquakes in Tennessee and Nearby Sections of Neighboring States (1926 to 1950): Journal of the Tennessee Academy of Science, Vol. 33, No. 3, July, pp. 224-239.

204. Schnabel, P. B., Lysmer, J., and Seed H. B., 1972, SHAKE - A Computer Program for Earthquake Response Analysis of Horizontally layered Sites: Report No. EERC 72-12, University of California, Berkeley, California.

205. Seed, H. B., Ugas, C., and Lysmer J., 1974, Site-Dependent Spectra for Earthquake-Resistant Design: Report No. EERC 74-12, University of California, Berkeley, California.

206. Seed, H. B. and Idriss, I. M., 1970, Soil Moduli and Damping Factors for Dynamic Response Analysis: Report No. EERC 70-10, University of California, Berkeley, California.

207. U.S. Atomic Energy Commission, 1973, Recommendations for Shape of Earthquake Response Spectra: WASH 1254 Prepared by John A. Blume and Associates, Engineers of Directorate of Licensing.

208. U.S. Atomic Energy Commission, 1973, A Study of Vertical and Horizontal Earthquake Spectra: WASH 1255, prepared by Nathan M. Newmark, Consulting Engineering Services for Directorate of Licensing.

209. Durham, D. O., Jr., 1965, (abs.), Stream Activity in the Central Gulf Coast Area during Wisconsin Glacial: Geological Society of America Special Paper No. 82, p. 289.

210. Saucier, R. T., 1974, Quaternary Geology of the Lower Mississippi Valley: Publications on Archeology, Research Series No. 6, Arkansas Archeological Survey, Fayetteville, Arkansas.

211. Fisk, H. N., and McFarland, E., Jr., 1955, Late Quaternary Deltaic Deposits of the Mississippi River: in Crust of the Earth, Geological Society of America Special Paper 62, pp. 279-302.

SECTION 2.5: BIBLIOGRAPHY (Cont'd)

212. Kolb, C. R., Smith, F. L., and Silva, R. C., 1975, Pleistocene Sediments of the New Orleans - Lake Pontchartrain Area: U. S. Army Engineer Waterways Experiment Station, Technical Paper S-75-6.

213. U.S. Army Engineer Waterway Experiment Station, 1958, Geology of the Mississippi River Deltaic Plain, Southeastern Louisiana: Technical Report 3-483.

214. Durham, C. O., Jr., 1964, (abs.), Late Pleistocene - Early Recent Stream Shrinkage and Crustal Fracturing in the Gulf Coast Area: Geological Society of America Special Paper No. 76, p. 52.

215. Smith, D. A., 1980, Sealing and Nonsealing Faults in Louisiana Gulf Coast Salt Basin: American Association of Petroleum Geologists Bulletin, V-64, No. 2, pp. 145-172.

TABLE 2.5-1

APPROXIMATE PERIODS OF MOVEMENTS ALONG GROWTH FAULTS IN LOUISIANA

(From References 6)

AGE	EPOCH OR STAGE	PALEONTOLOGICAL HORIZON
11,000 years-5.5 MYBP*		
	PLIO-PLEISTOCENE	
5.5 MYBP		
	MIOCENE	
		Bigenerina "A"
		Bigenerina "B"
		Textularia "L"
		Cibicides cartensi
		Bigenerina nodosaria directa
		Textularia "W"
		Bigenerina humbeli
		Cristellaria "I"
		Cibicides opima
		Amphistegina "B"
		Robulus "2"
		Operculinoides (Cristellaria "2")
		Robulus chambersi
	ANAHUACIAN	
		Discorbis Zone
		Heterostegina Zone
		Marginulina Zone
	CHICKASAWHAYAN	
		Camerina
		Cibicides hazzardi
		Marginulina texana
		Nonion struma
		Nodosaria blanpiedi
22.5 KYBP		
	OLIGOCENE VICKSBURGIAN	
36.0 MYBP		
	EOCENE JACKSONIAN CLAIBORNIAN	
53.5 MYBP		
	PALEOCENE SABINIAN - MIDWAYAN	
65.0 MYBP		
	CRETACEOUS GULFIAN	

GROWTH FAULT
GULFWARD--->

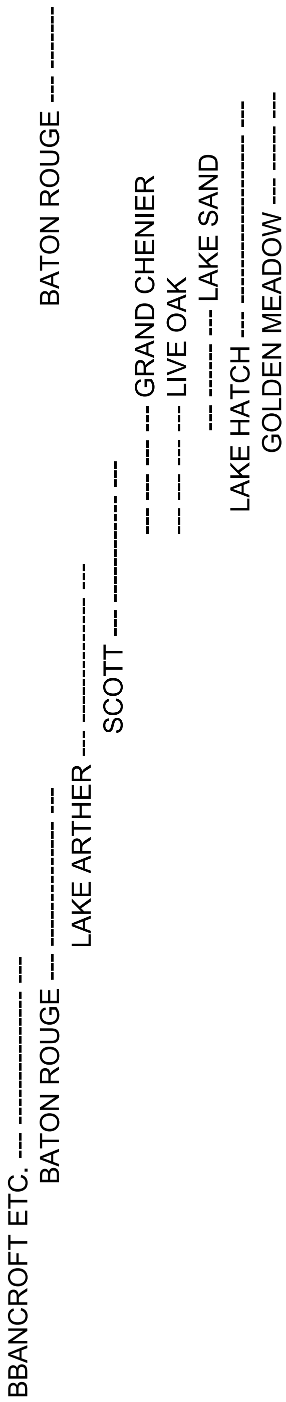

*MILLION YEARS BEFORE PRESENT (Ref. Bibliography 178).

TABLE 2.5-2 (Sheet 1 of 4)

OIL WELL LOGS USED IN STRUCTURAL CORRELATIONS

OIL WELL NUMBER	OIL WELL NAME	TOTAL DEPTH in ft.
0	Patrick Petr., Lanaux, No. 1	10500
1	Humble, Rogers Est., No. B1	11000
2·	Calco et al., L.A. Lauaux et al, No. 1	10400
3·	Humble, Cox et al, No. 1	10500
4·	Mag., S. Cox, No. 1	11056
5·	Drew, Lanaux et al, No. 1	10709
6·	Humble, Rathborne, No. (B) 1	11032
7·	HOR., Darensbourg, et al, No. 1	10340
8·	Calco, Haydel, No. 1	10386
9·	Calco, Montgomery, No. 1	11600
10	Stern, Landeche, No. 1	10528
11	Calco, Montgomery et al, No. 2	11050
12	Un. Cal., Montgomery, No. 1	10987
13	El Tres Pet., Casadaban, No. 1	10410
14	Tesoro, Landeche, No. 1	10800
15	Felmont, Landeche et al, No. 1	10871
16	Ratliff, Milliken & Farwell, No. 1	10823
19	Callery et al, Milliken & Farwell, No. 1	11300
20	Humble, Monterey, Landeche, No. 2	10525
21	Helis, Milliken & Farwell, No. 1	10026
22	Chevron, Milliken & Farwell, No. 1	12503
23	Un. Cal., Milliken & Farwell, No. 1	9981
24	Helis, Milliken & Farwell, No. 3	9027
25	Helis, Milliken & Farwell, No. 2	10023
26	Shell, Milliken & Farwell, No. 1	11003
27	Un. Cal., Milliken & Farwell, No. 2	9934
28	Cons. Gas, Boyle-Vial, No. 1	11500
29	Ashland-American Petrofina, Occidental Pet., No. 1	15715
30	Lone Star, Newman, No. 1	10935
31	Ashland, Union Carbide, No. 1	229
32	Union Texas Pet. & Clark, E.P. Creecy, No. 1	10515
33	Calco, Parquet et al, No. 1	10300
34	Samedan, Bougera, No. 1	10399
35	Lone Star, Barnes, No. 1	11500
36	Lone Star, Zimmer, No. 1	11250
37	McAlester, U.S.A., No. 2	12633
38	Calco, Smart-U.S.A., No.1	11600
39	Mac. Pet., U.S.A., No. 1	12633
40	Chevron, U.S.A., No. 2	10307

TABLE 2.5-2 (Sheet 2 of 4)

OIL WELL NUMBER	OIL WELL NAME	DATE LOGGED	TOTAL DEPTH in ft
41	Shenandoah, U.S.A., No. 1		10189
42	Chevron, U.S.A., No. 4		10300
43	Mesa, U.S.A., No. 1		7440
44	Coast St., U.S.A., No. 2		10825
45	Anson, U.S.A., No. 1		9270
46	Hellenic, Perrilloux, No. 1		11000
47	Coast St., U.S.A., No. 1		10817
48	Mullins-Pritchard, U.S.A., No. 1		9615
49	Calco, U.S.A., No. 3		11600
50	Wall & Assoc., U.S.A., No. 1		9800
51	Mac Pet., U.S.A., No. 1		11160
52	Calco, Spillway Fed. Un., No. 1		10435
53	Wall & Assoc., U.S.A., No. 1		10126
54	Stuarco, U.S.A., Clayton, No. 1		10209
55	Van Dyke, Dr. Clayton, No. 1		10410
56	Dirthright, Landeche, No. 1		10120
57	Dyanmic et al, Szubinski, No. 1		10100
58	Huskey Oil, M.M. Keller, No. 1		11020
59	Van Dyke, G. Mule, No.		10730
60	Midwest, L.L. & E. No. 1		11698
61	Davis, S/L 7162, No. 1	1/26/78	11315
62	Martin, S/L 2670, No. 1	12/11/77	10975
63	Martin, L.L.&E., No. 3	7/19/77	12100
64	Goodrich, L.L.&E., No. 1	10/20/76	11586
65	McCulloch, L.L.&E., No. 1	10/27/72	11512
66	Sunray, St. Charles Sch. Bd., No. 1	7/26/65	11995
67	Seaboard, S/L 1838, No. 1	1/2/53	11532
68	Kilroy, S/L 5777, No. 1	12/22/75	11300
69	Hilliard, S/L 7252, No.1	10/27/77	11450
70	Florida Gas, Duke, No. 1	10/25/75	11433
71	Forest - Texas Gas, McMillan, No. 1	3/30/77	11250
72	McCormick - Extex - First Miss., Rathborne, No. 1	1/1/79	11410
73	Forest, Rathborne, No. 1	6/10/78	12167
74	Texas, L.L.&E., No. 40	7/27/57	12003
75	Cayman, L.L.&E., No. 2	8/9/75	11700
76	Dykes - Clinton, DuFresne, No. 1	3/30/74	10525
77	Florida Gas, DuFresne, No. 1	3/17/77	11415
78	Callery, Home for Incurables, No. 1	8/15/52	11900
79	Union, DuFresne, No. 1	9/22/69	12500
83	Pel-Tex, Steinberg, No. 1	8/30/75	11525
84	Humble, L.L.&E., No. AA	2/27/65	11700
85	Humble, L.L.&E., No. U-5	2/6/57	12006

TABLE 2.5-2 (Sheet 3 of 4)

OIL WELL NUMBER	OIL WELL NAME	DATE LOGGED	TOTAL DEPTH in ft.
86	Union, L.L.&E., No. 2-C	11/22/55	11205
87	Atlantic, Steinberg, No. 1	4/18/56	12475
88	Owen, Gendron, No. 1	1/11/58	11280
89	Pelto-Mosbacher, Lanaux, No. 1	5/23/79	10650
90	Pel-Tex Oil, Goldmine, No. 2	3/14/76	10387
91	Occidental, Rayne, No. 1	12/10/65	10577
92	Hurley, Columbia, No. 1	5/11/54	10220
93	Braun, Columbia, No. 1	12/20/75	10414
94	Stone Oil, Landmark, No. 1	9/2/73	10100
96	Callery, La. & Ark, Rwy. No. 1	1/3/60	10870
97	Callery, Citizen, No. 1	9/18/58	10303
98	Brock Expl., Montegut, No. 2	11/19/78	12818
99	Brock Expl., Montegut, No. 1	5/13/77	12763
100	Chevron, Lanaux, No. 1	6/23/78	11010
101	Great Southern, Woods, No. 1	4/19/80	11412
102	California, Bougere, No. 1	3/23/64	11200
103	Tesch, Reine, No. 1	8/12/65	10315
104	Texaco, Milling, No. 2	7/9/65	11303
105	Texaco, Milling, No. B-1	6/14/67	11367
106	Houston, Oil, S/L 1838, No. 1	7/6/51	11271
107	Eason, Lasseigne, No. 1	11/9/60	10706
108	Crystal, Bougere, No. 1	4/9/66	10678
109	Callery, Cox, No. 27-1	7/4/59	9630
110	Callery, Milioto, No. 25-1	7/31/59	9623
111	Callery-Texaco, Ory, No. 1	7/15/62	11532
112	Texaco, Cambre, No. 1	2/17/62	9577
113	Ratliff, Godchaux, No. 1	2/23/54	10220
114	Damson, Sarpy, No. 1	12/30/70	10881
115	Pel-Tex, Gulf St. Ld. & Ind., No. 1	11/13/63	9716
116	Argo, Sarpy, No. 1	8/29/60	10030
117	Texaco, Callery Unit 23, No. 1	10/24/59	10318
118	Callery-Texaco, Montz Unit 10,No.1	11/22/58	9558
119	Callery, Montegut Unit 22, No.1	6/9/59	10669
120	Callery, Montegut Unit 28, No.1	11/28/59	10476
121	Callery, Montegut Unit 12, No.1	12/19/58	9565
122	Callery, Montegut Unit 5, No. 1	4/7/59	9605
123	Callery-Texaco, Montegut Unit 6, No. 1	8/29/58	10905
124	Callery, Bourgere Unit 8, No. 1	10/23/58	10123
125	El Toro, et. al., Morehead, No. 1	6/6/75	10825
126	Callery-Texaco, Marion, Unit 3, No. 1	4/25/58	9525
127	Callery-Texaco, Lasseigne Unit 7, No.1	9/22/58	9601
128	Callery-Texaco, CaVillino Unit 11, No. 1	11/22/58	9565
129	Callery-Texaco, Ory-No. 1	3/8/63	8120
130	Gulf States Land, Fee, No. 1	9/9/56	10505

TABLE 2.5-2 (Sheet 4 of 4)

OIL WELL NUMBER	OIL WELL NAME	DATE LOGGED	TOTAL DEPTH in ft.
131	Gulf States Land, Fee, No. 1A	9/30/57	9591
132	Callery-Texaco, Russel Unit 16, No. 1	2/9/59	9550
133	Callery-Texaco, Hymel Unit 20, No. 1	3/3/59	10325
134	Callery-Texaco, Call Unit 15, No. 1	1/13/59	9570
135	Callery-Texaco, Burg Unit 12, No. 1	12/22/58	10322
136	Callery-Texaco, Lasseigne Unit 19, No. 1	3/24/59	10923
137	Humble, Sarpy, No. 1	1/7/45	9690
138	Exchange, Brown, No. 1	1/22/64	10973
139	Pure, G.A.T.X., No. 7	8/20/51	10472
140	Frankel, Bride, No. 1	1/18/48	10347
141	Pure, G.A.T.X., No. 10	8/6/63	9727
142	Brock, Sarpy, No. 1	2/22/77	10121
143	Exxon, Sarpy, No. 25	5/27/79	7786
144	Exxon, PRA Sun-Sarpy , No. 24	6/13/77	7865
145	Exxon, Sarpy, No. 28	3/10/79	7800
146	Shell, R & RT, No. 29	9/24/67	9710
147	Shell, R & RT, No. 41	7/16/77	10863
148	Shell, Roy Realty, No. 1	8/3/48	8500
149	Pure, G.A.T.X., No. 11	10/13/63	9557
150	Texaco, Montegut, Unit 17, No. 1	2/1/59	11521
151	Energy Reserves, Dorvin, Devel., No. 1	4/26/78	11531

TABLE 2.5-3

TONAL ANOMALIES AND LINEAR TRENDS IN THE SITE AREA

INDENTITYING SYMBOL (SEE FIG. 2.5-31)	TYPE OF FEATURE	DESCRIPTION/EXPLANATION
F-1	Fisk Linear Trend	Follows general trend of the Mississippi River through site area
S-1 Through S-5	Linear Trend	Several features following straight sections of drainage features.
TA-1	Tonal Anomaly	Probably a topographic high caused by crevasse, deposition accented by vegetation.
TA-2	Tonal Anomaly	Probably an abandoned distribution or crevasse channel and natural levee.
TA-3	Tonal Anomaly	Linear topographic low, possibly associated with natural levess subsidence.
TA-4	Tonal Anomaly	Group of linear features possibly related to revegetation of a disturbed area (man-made) and overbank deposits along canals.
TA-5	Tonal Anomaly	Linear vegetation trend, possibly related to the TA-1 crevasse.

TABLE 2.5-4

UTILIZED SOUTHERN LOUISIANA SALT DOMES

Name	DISTANCE FROM SITE	DEPTH OF CAPROCK (FEET)	DEPTH TO TOP OF SALT (FEET)	SALT MINE	BRINE PRODUCTION	UNDERGROUND STORAGE	SULFUR MINING	QUARRY
Anse La Butte	90 mi WNW	-	137		X	X		
Avery	87 mi W	-	8	X				
Bay St. Elaine	62 mi S	710	1407				0	
Bayou Choctaw	55 mi NW	237	629		X	X		
Belle Isle	64 mi SW	110	135	X				
Chacahoula	29 mi SW	875	1100		X		0	
Cote Blanche	77 mi WSW	257	298	X				
Darrow	32 mi WNW	-	4595		X			
East Hackberry	170 mi W	2934	3330			X		
Garden Island Bay	98 mi SE	1350	1658				X	
Grand Isle Block 18*	65 mi SE	1773	2265				X	
Jefferson Island	90 mi W	530 (flank)	31	X			0	
Lake Hermitage	42 mi SE	904	1400				0	
Lake Pelto	62 mi S	1487	1982				X	
Lake Washington	57 mi SE	1094	1565				X	
Napoleonville	37 mi W	415	657		X			
Pine Prairie	128 mi NW	Surface	346			X		0
Port Barre	93 mi NW	3551	3642			X		
Sorrento	22 mi NW	1568	1717		X	X		
Starks	189 mi W	1157	1538		X		0	
Sulfur Mines	174 mi W	390	1460		X	X	X	
Weeks Island	81 mi WSW	Surface	43	X				
West Hackberry	176 mi W	1200	1790		X			

*offshore

X - active

O - abandoned

TABLE 2.5-5

SALT DOMES NEAR WATERFORD SITE

	Distance and Direction From Site (Miles)	Oil or Gas Production	Utilization	Top of Cap Rock (ft. below MSL)	Top of Salt (ft. below MSL)
Good Hope	5 E	yes			9580
Paradis	7 S	yes			13538
Bayou Des Allemandes	15 S	yes		7552	7560
Bayou Couba	15 SE	yes			6160
Hester	16 W	yes			6780
Raceland	17 S	yes			8170
Lake Salvador	22 SSE	yes			11270
Sorrento	22 NW	yes	LPG Storage, Brine	1568	1717
Valentine	24 S	yes			6575
Barataria	25 SE	yes			7730
Stella	28 SE	yes			13190
Chacahoula	29 SW	yes	Brine, Sulphur	875	1100
Cut off	30 SSE	yes			9708
Darrow	32 WNW	yes	Brine		4595
Bully Camp	33 S	yes	Frasch Sulphur (planned)	1256	1296
Lafitte	34 SE	yes			13947
Clovelly	35 SSE	yes		389	1168
Napoleonville	37 W	yes	Brine	415	657
St. Gabriel	39 NW	yes			11230
Golden Meadow	41 SSE	yes			15344
Lake Hermitage	42 SE	yes	Sulphur	904	1400
Bay de Chene	44 SE	yes			7950
White Castle	46 WNW	yes		1693	2313

TABLE 2.5-6 (Sheet 1 of 8)
LISTING OF HISTORIC EARTHQUAKES IN ORDER OF DISTANCE FROM WATERFORD SITE

YEAR	MONTH	DAY	HOUR (LOCAL TIME)	LATITUDE (N)	LONGITUDE (W)	MM INTEN-SITY	MAGNITUDE (MB)	HYPOCENTER DEPTH (MI.)	AREA (SQ. MI.)	DISTANCE TO SITE (MI.)	REMARKS
1930	10	19	0617	30.00	91.00	V-VI			15000	31.7	Donaldsonville, La.
1958	11	19	1215	30.30	91.10	V				43.3	Baton Rouge, La.,Felt Locally
1975	09	09	0553	30.66	89.25			3.0		86.2	Mississippi (Mag. 2.9 MBLG)
1955	02	01	0845	30.40	89.10	V				86.6	Gulfport, Miss
1978	12	10	2006	31.95	88.48	V	3.5	3.0		180.0	Mississippi, Alabama
1977	05	03	2000	31.98	88.42	V	3.6	3.0		183.3	Mississippi, Alabama
1978	06	09	1815	32.09	88.58	IV	3.3	6.0		183.0	Mississippi, Alabama
1976	10	22	1841	32.20	88.73	IV	3.0	3.0		184.0	Mississippi
1963	11	05	1645	27.80	92.40		4.8	20		191.0	Gulf of Mexico
1974	12	10	0002	31.35	87.47	V		6		202.0	S.W. Alabama (Mag 3.0 ML)
1964	04	28	1519	31.70	93.60	V	4.4			220.0	Western Louisiana
1964	08	16	0536	31.40	93.80	V				220.5	Hemphill, Texas
1964	04	23	1921	31.50	93.80	V	3.7			223.6	Western Louisiana
1964	04	27	1831	31.50	93.80	V	3.4			223.6	Western Louisiana
1964	04	24	0134	31.60	93.80	V	3.7			226.8	Western Louisiana
1886	02	04	2000	32.80	88.00	V			1600	242.7	Alabama
1886	02	13	0000	32.80	88.00					245.7	Alabama (* Time)
1967	06	04	1014	33.60	90.90	VI	3.8		25000	250.7	Greenville, Miss.
1967	06	29	0757	33.60	90.90	V	3.4			250.7	Greenville, Miss.
1917	06	29	2023	32.70	87.50	V				257.0	Alabama, Felt Only Locally
1971	03	14	1128	33.10	87.90		3.9	1.0		262.8	Carrollton, Alabama
1973	01	08	0312	33.80	90.60		3.5	4.0		234.4	Mississippi

TABLE 2.5-6 (Sheet 2 of 8)

YEAR	MONTH	DAY	HOUR (LOCAL TIME)	LATITUDE (N)	LONGITUDE (W)	MM INTEN-SITY	MAGNITUDE (MB)	HYPOCENTER DEPTH (MI.)	AREA (SQ. MI.)	DISTANCE TO SITE (MI.)	REMARKS
1911	03	31	1057	33.80	92.20	V			18000	282.1	Rison, Ark.
1911	03	31	1210	33.80	92.20	V			18000	282.1	Rison, Ark.
1975	03	01	0550	33.50	88.00			10.8		282.6	Mississippi (Mag 3.2 MBLG)
1957	03	19	1038	32.00	95.00	V			10000	302.1	Northeast Texas (*Coords)
1891	01	08	0000	31.70	95.20	VII				304.4	Rusk, Texas
1975	11	07	1740	33.55	87.36			3		307.0	Alabama (Mag 3.5 MBLG)
1974	02	15	1649	34.00	93.00	V	3.8	1.0		313.0	Whelen Springs, Ark.
1939	06	19	1543	34.10	93.10	V				323.0	Arkadelphia, Ark., Felt Locally
1974	02	15	1636	34.10	93.10		4.2	1.0		323.0	Arkansas, Several Weaker Shocks
1974	12	12	2304	34.67	91.88	V		3.0		333.7	N.E. Ark. (Mag. 3.4 MBLG)
1975	01	02	0319	34.87	90.94			15.0		338.3	Ark. (Mag. 2.9 MBLG)
1931	05	05	0718	33.70	86.60	V			6500	340.0	Cullman, Alabama
1918	10	04	0321	34.70	92.30	V			3000	342.5	Lonoke Co., Arkansas
1975	08	28	2223	33.82	86.60	VI	3.5	3		347.0	Alabama
1818	03	01	0000	35.00	90.00	IV-V				347.3	Miss. R. Valley
1916	10	18	1604	33.50	86.20	VII			100000	348.0	Irondale, Alabama
1969	01	01	1736	34.80	92.60	VI	4.2	7.0	23000	354.8	Central Arkansas
1923	11	26	1725	35.20	90.20	VI				360.3	Miss. R. Valley (*Coords, Date-Time)
1843	01	04	2045	35.20	90.00	VIII				361.0	Memphis, Tenn., Felt To East
1889	07	19	1932	35.20	90.00	VI			400000	361.0	Memphis, Tenn., Felt Only Locally
1922	03	30	1053	35.20	90.00	V				361.0	Miss. River Valley (*Coords)
1954	04	26	2009	35.20	90.00	V				361.0	Memphis, Tenn.

TABLE 2.5-6 (Sheet 3 of 8)

YEAR	MONTH	DAY	HOUR (LOCAL TIME)	LATITUDE (N)	LONGITUDE (W)	MM INTEN-SITY	MAGNITUDE (MB)	HYPOCENTER DEPTH (MI.)	AREA (SQ. MI.)	DISTANCE TO SITE (MI.)	REMARKS
1958	01	26	1056	35.20	90.00	V				361.0	Memphis, Tenn., Felt Locally
1918	10	15	2130	35.20	89.20	V			20000	367.5	West Tennessee
1923	12	31	2105	35.40	90.30	V			30000	373.9	Arkansas
1957	04	23	0424	34.50	86.80	VI			11500	379.0	Birmingham, Alabama
1923	10	28	1110	35.50	90.30	VII			40000	380.9	Marked Tree, Arkansas
1938	09	17	2134	35.50	90.30	IV-V			90000	380.9	Northeastern Ark.
1947	12	15	2127	35.50	90.00	V			10000	381.7	Near Osceola, Ark. (*Coords)
1941	11	16	2109	35.50	89.70	V-VI				383.3	Covington, Tenn., Locally
1976	03	24	1841	35.59	90.48	VI	4.9	9.0		386.9	Arkansas
1955	01	25	0124	35.60	90.30	VI			30000	387.8	Tenn.-Ark.-Mo
1976	09	25	0807	35.61	90.45	V		3.0		388.3	Ark., (Mag 3.6 MBLG)
1956	01	28	2214	35.60	89.60	VI				390.9	Tenn,-Ark. Border
1936	03	14	1120	34.00	95.20	V			900	391.8	Southeastern Oklahoma
1974	03	04	0824	35.70	90.40		3.0	3.0		394.6	Arkansas
1974	03	12	0630	35.70	89.80		3.2	3.0		396.5	Tennessee
1934	04	11	1140	33.90	95.50	V			3000	399.9	Texas Oklahoma
1959	08	12	1306	35.00	87.00	V			2800	400.0	Ala.-Tenn. Border
1971	10	01	1250	35.80	90.40	V		12.0	55000	401.5	Northeastern Arkansas
1974	02	24	0154	35.80	90.40		3.2	4.0		401.5	Arkansas
1933	12	09	0240	35.80	90.20	V			100	401.8	Manila, Ark.
1882	10	12	1615	35.00	94.00	VI-VII			135000	402.6	Arkansas

TABLE 2.5-6 (Sheet 4 of 8)

YEAR	MONTH	DAY	HOUR (LOCAL TIME)	LATITUDE (N)	LONGITUDE (W)	MM INTEN-SITY	MAGNITUDE (MB)	HYPOCENTER DEPTH (MI.)	AREA (SQ. MI.)	DISTANCE TO SITE (MI.)	REMARKS
1956	04	02	1003	34.20	95.40	V				409.6	Southeastern Oklahoma
1965	12	19	1619	35.90	89.90		5.3	3.0		409.7	Northeastern Arkansas
1970	11	16	2014	35.90	89.90	VI	3.6	17.0	78000	409.7	Arkansas
1905	08	21	2308	36.00	90.00	VI			40000	416.2	Miss. Valley (*Coords)
1918	10	13	0330	36.00	91.10	V				416.9	Blackrock, Ark.
1955	03	29	0303	36.00	89.50	VI				419.1	Finley, Tenn
1955	09	05	1945	36.00	89.50	V				419.1	Finley, Tenn
1955	12	13	0143	36.00	89.50	V				419.1	Dyer Co. Tenn., (Aftershock at 0156)
1959	12	21	1025	36.00	89.50	V			400	419.1	Finley, Tenn
1960	01	28	1538	36.00	89.50	V				419.1	Dyer Co., Tenn., Felt Locally
1976	05	22	0141	36.04	89.84	V		6.0		419.6	New Madrid, Mo. (Mag, 3.2 MBLG)
1975	08	25	0111	36.05	89.84			6.6		420.3	New Madrid, Mo. (Mag, 3.0 MBLG)
1937	05	16	1850	36.10	90.60	IV-V			25000	422.3	N.E. Ark.
1897	04	30	2200	36.00	89.00	IV-V				423.9	Tenn. and Ill. (*Corrds)
1962	07	23	0005	36.10	89.80	VI		11.0		424.0	Southern Mo.
1956	10	29	0324	36.10	89.40	V				426.7	Caruthersville, Mo.
1919	11	03	1440	36.20	90.90	IV-V				429.8	Arkansas Felt Only Locally
1952	07	16	1748	36.20	89.60	VI				432.0	Dyersburg, Tenn
1972	03	29	1439	36.20	89.60	V	3.7	6.0	65800	432.0	New Madrid, Mo.
1973	12	20	0445	36.20	89.60		3.4	6.0		432.0	New Madrid, Mo.
1975	07	06	0248	36.19	89.49			3.0		432.1	New Madrid, Mo. (Mag. 2.9 MBLG)
1959	02	13	0237	36.20	89.50	V			170	432.7	Bogota, Tenn.
1974	03	09	2234	36.20	89.50		2.5	3.0		432.7	New Madrid Region, Mo.

TABLE 2.5-6 (Sheet 5 of 8)

YEAR	MONTH	DAY	HOUR (LOCAL TIME)	LATITUDE (N)	LONGITUDE (W)	MM INTEN-SITY	MAGNITUDE (MB)	HYPOCENTER DEPTH (MI.)	AREA (SQ. MI.)	DISTANCE TO SITE (MI.)	REMARKS
1974	01	07	1913	36.20	89.39	V	4.1	.6		433.6	New Madrid, Mo.-Tenn. Region
1961	01	10	1940	35.00	95.00	V				435.2	S.E. Okla, (*Coords)
1961	04	27	0130	35.00	95.00	V				435.2	S.E. Okla, (*Coords-Time)
1958	04	08	1626	36.20	89.10	V			400	436.3	Obion Co. Tenn.
1958	04	26	0130	36.30	89.50	V				439.6	Lake Co. Tenn.
1960	04	21	0445	36.30	89.50	V				439.6	Lake Co. Tenn. Felt Locally
1965	08	13	2346	36.30	89.50		5.0			439.6	Southwestern Illinois
1883	12	05	0920	36.30	91.80	V				442.7	Izard Co. Ark. Felt Only Locally
1972	01	31	2342	36.40	90.80	V	3.9	8.0		443.3	Northeastern Arkansas
1965	02	10	2140	36.40	89.70		4.6	11.0		445.1	Southeastern Missouri
1915	04	28	1740	36.40	89.50	IV-V			200	446.4	New Madrid, Mo.
1927	08	13	1000	36.40	89.50	V				446.4	Hiss. Valley (Tiptonville Tn) (*Coords)
1949	01	13	2145	36.40	89.50	V			7000	446.4	Miss. River Valley
1952	02	20	1635	36.40	89.50	V				446.4	Tenn.-Mo. Border
1841	12	27	2350	36.40	89.20	V				448.9	Near Hickman, Ky (*Coords)
1964	05	23	0526	36.50	90.00		4.5	11.0		450.6	Southeastern Missouri
1964	05	23	0901	36.50	89.90		4.3	11.0		451.0	Southeastern Missouri
1968	02	09	1935	36.50	89.90		3.8			451.0	Southeastern Missouri
1970	03	26	2144	36.50	89.70		3.5	3.0		452.0	Southeastern Missouri
1962	02	02	0044	36.50	89.60	VI		15.0	35000	452.6	New Madrid, Mo.
1865	08	17	0900	36.50	89.50	VII			24000	453.3	Southeast Mo.

TABLE 2.5-6 (Sheet 6 of 8)

YEAR	MONTH	DAY	HOUR (LOCAL TIME)	LATITUDE (N)	LONGITUDE (W)	MM INTEN-SITY	MAGNITUDE (MB)	HYPOCENTER DEPTH (MI.)	AREA (SQ. MI.)	DISTANCE TO SITE (MI.)	REMARKS
1903	11	27	0320	36.50	89.50	V			70000	453.3	New Madrid, Mo.
1908	09	28	1334	36.50	89.50	IV-V			5000	453.3	New Madrid, Mo.
1975	02	13	1344	36.52	89.56			3.0		454.3	New Madrid, Mo. (Mag. 3.3 MBLG)
1975	06	13	1640	36.54	89.68	VI	4.3	1.2		454.9	New Madrid, Mo.
1975	12	02	2101	36.54	89.57	V		3.0		455.6	New Madrid, Mo. (Mag. 2.8 MBLG)
1975	08	20	0314	36.56	89.80			3.0		455.6	New Madrid, Mo. (Mag. 2.9 MBLG)
1927	05	07	0228	36.50	89.00	VII			130000	457.8	Mississippi Valley
1811	12	16	0200	36.60	89.60	XII			2000000	459.5	New Madrid Mo., Felt To The East
1812	01	23	0900	36.60	89.60	XII				459.5	New Madrid, Missouri
1812	02	07	0345	36.60	89.60	XII				459.5	New Madrid, Missouri
1916	12	18	2342	36.60	89.30	VI-VII				461.7	Hickman, Ky, Felt Only Locally
1878	11	18	2352	36.70	90.40	VI			150000	463.7	Southeastern Missouri
1954	02	02	1053	36.70	90.30	VI				463.7	Poplar Bluff Mo.
1963	03	03	1130	36.70	90.10	VI	4.5		100000	464.1	Southeast Missouri
1974	12	13	0413	36.70	91.63			3.0		468.4	S. Missouri (Mag. 2.8 MI)
1974	05	13	0052	36.71	89.39	VI	4.3	1.0		468.5	New Madrid, Missouri
1915	12	07	1240	36.70	89.10	V-VI			60000	470.3	Near Mouth of Ohio River
1964	01	16	2310	36.80	89.50		4.5	11.0		473.9	Southeastern Missouri
1915	10	26	0140	36.70	88.60	V				476.0	Mayfield, Ky., Felt Locally
1925	05	13	0600	36.70	88.60	V			3000	476.0	Kentucky
1878	03	12	0400	36.80	89.20	V				476.2	Columbus, Ky., Felt Locally
1974	08	11	0830	36.92	91.17	V	3.6	2.0		480.5	Fremont, Missouri

TABLE 2.5-6 (Sheet 7 of 8)

YEAR	MONTH	DAY	HOUR (LOCAL TIME)	LATITUDE (N)	LONGITUDE (W)	MM INTEN-SITY	MAGNITUDE (MB)	HYPOCENTER DEPTH (MI.)	AREA (SQ. MI.)	DISTANCE TO SITE (MI.)	REMARKS
1856	11	09	0000	37.00	89.00	IV-V				491.7	Ill.-KY.-Tenn. (*Coords-Time)
1930	08	29	0027	37.00	89.00	V				491.7	Ky.-Tenn.-Ill.-Mo. (*Coords)
1958	01	27	2357	37.00	89.00	V			300	491.7	Ill.-Ky.-Ho. Borders
1965	11	04	0144	37.10	91.00		4.5	20.0		492.2	Southeastern Missouri
1966	02	13	1720	37.10	91.00		4.7	4.2		492.2	Southeastern Missouri
1924	03	02	0518	36.90	89.10	V			15000	483.9	Kentucky
1922	11	26	2131	37.00	90.50					484.4	Miss. R. Valley (*Coords)
1963	07	08	1752	37.00	90.50		4.1	15.0		484.4	Southeastern Missouri
1909	10	23	0110	37-00	89.50	V			40000	487.6	Southeastern Missouri
1895	10	31	0508	37.00	89.40	VIII			1000000	488.3	Missouri, Felt To The East
1855	05	02	2133	37.00	89.20	IV-V				489.9	Cairo, Ill. (*Coords)
1883	01	11	0112	37.00	89.20	VI			80000	489.9	Cairo, Illinois
1883	04	12	0230	37.00	89.20					489.9	Cairo, Illinois, Felt Locally
1883	07	14	0130	37-00	89.20					489.9	Cairo, Ill., (*Coords)
1887	08	02	1236	37.00	89.20	V				489.9	Cairo, Ill., Widespread Effects
1891	09	26	2255	37.00	89.20	V				489.9	Cairo, Illinois (*Coords)
1908	10	27	1827	37.00	89.20	V			5000	489.9	Cairo, I11.
1934	08	19	1847	37.00	89.20	VI			28000	489.9	Rodney, Mo.
1956	11	25	2213	37.10	90.60	VI			21500	491.3	Wayne County Mo.
1963	08	02	1838	37.00	88.80	V	3.6	11.0		493.8	Ill.-Ky. Border
1965	08	14	0714	37.10	89.20	VII	5.0	3.0		496.7	Southwestern Illinois

TABLE 2.5-6 (Sheet 8 of 8)

YEAR	MONTH	DAY	HOUR (LOCAL TIME)	LATITUDE (N)	LONGITUDE (W)	MM INTEN-SITY	MAGNITUDE (MB)	HYPOCENTER DEPTH (MI.)	AREA (SQ. MI.)	DISTANCE TO SITE (MI.)	REMARKS
1957	03	26	0227	37.00	88.40	V				498.8	Paducah, Ky., Felt Only Locally
1966	02	26	0210	37.20	91.00		3.8	20.0		499.1	Southeastern Missouri
1975	08	24	2101	37.23	90.88			3.0		500.8	Eastern Missouri (Mag. 2.8 MBLG)
1975	08	24	1844	37.23	90.89			3.0		500.8	Eastern Missouri (Mag. 2.7 MBLG)
1956	10	30	0436	36.20	95.00	VII			3700	502.7	Northeastern Oklahoma
1922	03	23	1545	37.00	88.00	V				504.8	Western Kentucky (*Coords)
1940	05	31	1302	37.00	88.00	IV-V			1000	504.8	Ohio River (*Coords)
1820	11	09	1600	37.30	89.50	IV-V				508.2	Cape Girardeau, No.
1965	08	15	0007	37.40	89.50	V	5.1	3.0		515.0	Southwestern Illinois
1922	03	22	1630	37.30	88.60	V			25000	516.4	South Illinois (*Coords)
1967	07	21	0315	37.50	90.40	VI	3.9			518.9	Southeastern Mo.
1950	02	08	0437	37.40	92.40	V				523.9	Lebanon, Mo.
1973	01	07	1656	37.40	87.30		3.2	9.0		542.0	Kentucky
1976	04	15	0104	37.40	87.30	V		9.0		542.0	Kentucky

* ESTIMATE

TABLE 2.5-7 (Sheet 1 of 8)

LISTING OF HISTORIC EARTHQUAKES IN ORDER OF DECREASING INTENSITY

YEAR	MONTH	DAY	HOUR (LOCAL TIME)	LATI-TUDE (N)	LONGI-TUDE (W)	MM INTEN-SITY	MAGNI-TUDE (MB)	HYPOCENTER DEPTH (MI.)	AREA (SQ.MI.)	DISTANCE TO SITE (MI.)	REMARKS
1812	02	07	0345	36.60	89.60	XII				459.5	New Madrid, Mo
1812	01	23	0900	36.60	89.60	XII				459.5	New Madrid, Missouri
1811	12	16	0200	36.60	89.60	XII			2000000	459.5	New Madrid Mo., Felt To The East
1895	10	31	0508	37.00	89.40	VIII			1000000	488.3	Missouri, Felt To The East
1843	01	04	2045	35.20	90.00	VIII			400000	361.0	Memphis, Tenn., Felt To East
1965	08	14	0714	37.10	89.20	VII	5.0	3.0		496.7	Southwestern Illinois
1956	10	30	0436	36.20	95.00	VII			3700	502.7	Northeastern Oklahoma
1927	05	07	0228	36.50	89.00	VII			130000	457.8	Mississippi Valley
1923	10	28	1110	35.50	90.30	VII			40000	380.9	Marked Tree, Arkansas
1891	01	08	0000	31.70	95.20	VII				304.4	Rusk, Texas
1865	08	17	0900	36.50	89.50	VII			24000	453.3	Southeast Mo.
1916	10	18	1604	33.50	86.20	VII			100000	348.0	Irondale, Alabama
1916	12	18	2342	36.60	89.30	VI-VII				461.7	Hickman Ky, Felt Only Locally
1883	04	12	0230	37.00	89.20	VI-VII				489.9	Cairo, Illinois, Felt Locally
1882	10	22	1615	35.00	94.00	VI-VII			135000	402.6	Arkansas
1976	03	24	1841	35.59	90.48	VI	4.9	9.0		386.9	Arkansas
1963	03	03	1130	36.70	90.10	VI	4.5		100000	464.1	Southeast Missouri
1975	06	13	1640	36.54	89.68	VI	4.3	1.2		454.9	New Madrid, Missouri
1974	05	13	0052	36.71	89.39	VI	4.3	1.0		468.5	New Madrid, Missouri
1969	01	01	1736	34.80	92.60	VI	4.2	7.0	23000	354.8	Central Arkansas
1967	07	21	0315	37.50	90.40	VI	3.9			518.9	Southeastern Mo.

TABLE 2.5-7 (Sheet 2 of 8)

YEAR	MONTH	DAY	HOUR (LOCAL TIME)	LATI-TUDE (N)	LONGI-TUDE (W)	MM INTEN-SITY	MAGNI-TUDE (MB)	HYPOCENTER DEPTH (MI.)	AREA (SQ.MI.)	DISTANCE TO SITE (MI.)	REMARKS
1967	**06**	**04**	**1014**	**33.60**	**90.90**	**VI**	**3.8**		**25000**	**250.7**	**Greenville, Miss.**
1970	**11**	**16**	**2014**	**35.90**	**89.90**	**VI**	**3.6**	**17.0**	**78000**	**409.7**	**Arkansas**
1968	**10**	**14**	**0843**	**34.00**	**96.80**	**VI**				**462.8**	**Durant, Okla.**
1962	**07**	**23**	**0005**	**36.10**	**89.80**	**VI**		**11.0**		**424.0**	**Southern Mo.**
1962	**02**	**02**	**0044**	**36.50**	**89.60**	**VI**		**15.0**	**35000**	**452.6**	**New Madrid, Mo.**
1956	**11**	**25**	**2213**	**37.10**	**90.60**	**VI**			**21500**	**491.3**	**Wayne County Mo.**
1956	**01**	**28**	**2214**	**35.60**	**89.60**	**VI**				**390.9**	**Tennessee-Arkansas Border**
1955	**03**	**29**	**0303**	**36.00**	**89.50**	**VI**				**419.1**	**Finley, Tennessee**
1955	**01**	**25**	**0124**	**35.60**	**90.30**	**VI**			**30000**	**387.8**	**Tenn., Arkansas, Missouri**
1954	**02**	**02**	**1053**	**36.70**	**90.30**	**VI**				**463.7**	**Poplar Bluff, Mo.**
1952	**07**	**16**	**1748**	**36.20**	**89.60**	**VI**				**432.0**	**Dyersburg, Tenn.**
1934	**08**	**19**	**1847**	**37.00**	**89.20**	**VI**			**28000**	**489.9**	**Rodney, Mo.**
1931	**12**	**16**	**2136**	**34.10**	**89.80**	**VI**			**65000**	**286.7**	**Batesville, Miss.**
1923	**11**	**26**	**1725**	**35.20**	**90.20**	**VI**				**360.3**	**Miss. R. Valley (*Coords)**
1905	**08**	**21**	**2308**	**36.00**	**90.00**	**VI**			**40000**	**416.2**	**Miss. Valley (*Coords)**
1889	**07**	**19**	**1932**	**35.20**	**90.00**	**VI**				**361.0**	**Memphis Term., Felt Only Locally**
1883	**01**	**11**	**0112**	**37.00**	**89.20**	**VI**			**80000**	**489.9**	**Cairo, Illinois**
1878	**11**	**18**	**2352**	**36.70**	**90.40**	**VI**			**150000**	**463.7**	**Southeastern Missouri**
1957	**04**	**23**	**0424**	**34.50**	**86.80**	**VI**			**11500**	**379.0**	**Birmingham, Alabama**
1959	**08**	**12**	**1306**	**35.00**	**87.00**	**VI**			**2800**	**400.0**	**Ala-Tenn. Border**
1975	**08**	**28**	**2223**	**33.82**	**86.60**	**VI**	**3.5**	**3.0**		**347.0**	**Alabama**
1941	**11**	**16**	**2109**	**35.50**	**89.70**	**V-VI**				**383.3**	**Covington, Tenn., Local**

TABLE 2.5-7 (Sheet 3 of 8)

YEAR	MONTH	DAY	HOUR (LOCAL TIME)	LATI-TUDE (N)	LONGI-TUDE (W)	MM INTEN-SITY	MAGNI-TUDE (MB)	HYPOCENTER DEPTH (MI.)	AREA (SQ.MI.)	DISTANCE TO SITE (MI.)	REMARKS
1930	10	19	0617	30-00	91.00	V-VI			15000	31.7	Donaldsonville, La.
1915	12	07	1240	36.70	89.10	V-VI			60000	470.3	Near Mouth of Ohio River
1965	08	15	0007	37.40	89.50	V	5.1	3.0		515.00	Southwestern Illinois
1964	04	28	1519	31.70	93.60	V	4.4			220.1	Western Louisiana
1974	01	07	1913	36.20	89.39	V	4.1	.6		433.6	New Madrid, Mo-Tenn. Region
1972	01	31	2342	36.40	90.80	V	3.9	8.0		443.3	Northeastern Arkansas
1974	02	15	1649	34.00	93.00	V	3.8	1.0		314.2	Whelen Springs, Ark.
1972	03	29	1439	36.20	89.60	V	3.7	6.0	65800	432.0	New Madrid, Mo.
1964	04	24	0134	31.60	93.80	V	3.7			226.8	Western Louisiana
1964	04	23	1921	31.50	93.80	V	3.7			223.6	Western Louisiana
1974	08	11	0830	36.92	91.17	V	3.6	2.0		480.5	Fremont, Missouri
1963	08	02	1838	37.00	88.80	V	3.6	11.0		493.8	Ill.-KY. Border
1977	05	03	2000	31.98	88.42	V	3.6	3.0		183.0	Mississippi, Alabama
1978	12	10	2006	31.95	88.48	V	3.5	3.0		180.0	Mississippi, Alabama
1967	06	29	0757	33.60	90.90	V	3.4			250.7	Greenville, Miss.
1964	04	27	1831	31.50	93.80	V	3.4			223.6	Western Louisiana
1976	09	25	0807	35.61	90.45	V		3.0		388.3	Arkansas (Mag. 3.6 MBLG)
1976	05	22	0141	36.04	89.84	V		6.0		419.6	New Madrid, Mo. (Mag. 3.2 MBLG)
1975	12	02	2101	36.54	89.57	V		3.0		455.6	New Madrid, Mo. (Mag. 2.8 MBLG)
1974	12	12	2304	34.67	91.88	V		3.0		333.7	N.E. Arkansas (Mag. 3.4 MBLG)
1971	10	01	1250	35.80	90.40	V		12.0	55000	401.5	Northeastern Arkansas
1964	08	16	0536	31.40	93.80	V				220.5	Hemphill, Texas

TABLE 2.5-7 (Sheet 4 of 8)

YEAR	MONTH	DAY	HOUR (LOCAL TIME)	LATITUDE (N)	LONGITUDE (W)	MM INTENSITY	MAGNITUDE (MB)	HYPOCENTER DEPTH (MI.)	AREA (SQ.MI.)	DISTANCE TO SITE (MI.)	REMARKS
1961	04	27	0130	35.00	95.00	V				435.2	Southeasten Okla., (*Coords-Time)
1961	01	10	1940	35.00	95.00	V				435.2	Southeastern Okla. (*Coords)
1960	04	21	0445	36.30	89.50	V				439.6	Lake Co., Tenn., Felt Locally
1960	01	28	1538	36.00	89.50	V				419.1	Dyer Co., Tenn., Felt Locally
1959	12	21	1025	36.00	89.50	V			400	419.1	Finley, Tenn.
1959	02	13	0237	36.20	89.50	V			170	432.7	Bogota, Tenn.
1958	11	19	1215	30.30	91.10	V				43.3	Baton Rouge, La., Felt Locally
1958	04	26	0130	36.30	89.50	V				439.6	Lake Co., Tenn
1958	04	08	1626	36.20	89.10	V			400	436.3	Obion Co., Tenn.
1958	01	27	2357	37.00	89.00	V			300	491.7	Ill.-Ky.-Mo. Borders
1958	01	26	1056	35.20	90.00	V				361.0	Memphis, Tenn., Felt Locally
1957	03	26	0227	37.00	88.40	V				498.8	Paducah, Ky., Felt Only Locally
1957	03	19	1645	32.00	95.00	V			10000	302.1	Northeast Texas (*Coords)
1956	10	29	0324	36.10	89.40	V				426.7	Caruthersville, Mo.
1956	04	02	1003	34.20	95.40	V				409.6	Southeastern Oklahoma
1955	12	13	0143	36.00	89.50	V				419.1	Dyer Co., Tenn. (Aftershock at 0156)
1955	09	05	1945	36.00	89.50	V				419.1	Finley, Tenn.
1955	02	01	0845	30.40	89.10	V				86.6	Gulfport, Miss.
1954	04	26	2009	35.20	90.00	V				361.0	Memphis, Tenn.
1952	02	20	1635	36.40	89.50	V				446.4	Tennessee-Missouri Border
1950	02	08	0437	37.40	92.40	V				523.9	Lebanon, Mo.
1949	01	13	2145	36.40	89.50	V			7000	446.4	Miss. River Valley

TABLE 2.5-7 (Sheet 5 of 8)

YEAR	MONTH	DAY	HOUR (LOCAL TIME)	LATI-TUDE (N)	LONGI-TUDE (W)	MM INTEN-SITY	MAGNI-TUDE (MB)	HYPOCENTER DEPTH (MI.)	AREA (SQ.MI.)	DISTANCE TO SITE (MI.)	REMARKS
1947	12	15	2127	35.50	90.00	V			10000	381.7	Near Osceola, Ark. (*Coords)
1939	06	19	1543	34.10	93.10	V				323.0	Arkadelphia, Ark., Felt Locally
1936	03	14	1120	34.00	95.20	V			900	391.8	Southeastern Oklahoma
1934	04	11	1140	33.90	95.50	V			3000	399.9	Texas-Oklahoma Border
1933	12	09	0240	35.80	90.20	V			100	401.8	Manila, Ark.
1930	08	29	0027	37.00	89.00	V				491.7	Ky., Tenn., Ill., Mo. (*Coords)
1927	08	13	1000	36.40	89.50	V				446.4	Miss. Valley (Tiptonville Tn) (*Coords)
1925	05	13	0600	36.70	88.60	V			3000	476.0	Kentucky
1924	03	02	0518	36.90	89.10	V			15000	483.9	Kentucky
1923	12	31	2105	35.40	90.30	V			30000	373.9	Arkansas
1922	03	30	1053	35.20	90.00	V				361.0	Miss. River Valley (*Coords)
1922	03	23	1545	37.00	88.00	V				504.8	Western Kentucky (*Coords)
1922	03	22	1630	37.30	88.60	V			25000	516.4	South Illinois (*Coords)
1918	10	15	2130	35.20	89.20	V			20000	367.5	West Tennessee
1918	10	13	0330	36.00	91.10	V				416.9	Blackrock, Ark.
1918	10	04	0321	34.70	92.30	V			30000	342.5	Lonoke Co., Arkansas
1915	10	26	0140	36.70	88.60	V				476.0	Mayfield, Ky., Felt Locally
1911	03	31	1210	33.80	92.20	V			18000	282.1	Rison, Ark.
1911	03	31	1057	33.80	92.20	V			18000	282.1	Rison, Ark.
1909	10	23	0110	37-00	89.50	V			40000	487.6	Southeastern Missouri
1908	10	27	1827	37-00	89.20	V			5000	489.9	Cairo, 111.
1903	11	27	0320	36.50	89.50	V			70000	453.3	New Madrid, Mo.

TABLE 2.5-7 (Sheet 6 of 8)

YEAR	MONTH	DAY	HOUR (LOCAL TIME)	LATITUDE (N)	LONGITUDE (W)	MM INTENSITY	MAGNITUDE (MB)	HYPOCENTER DEPTH (MI.)	AREA (SQ.MI.)	DISTANCE TO SITE (MI.)	REMARKS
1891	09	26	2255	37.00	89.20	V				489.9	Cairo, Illinois (*Coords)
1887	08	02	1236	37.00	89.20	V				489.9	Cairo, Ill., Widespread Effects
1886	02	04	2000	32.80	89.00	V			1600	242.7	Alabama
1883	12	05	0920	36.30	91.80	V				442.7	Izard Co. Ark., Felt Only Locally
1878	03	12	0400	36.80	89.20	V				476.2	Columbus, Ky, Felt Locally
1841	12	27	2350	36.40	89.20	V				448.9	Near Hickman, Ky- (*Coords)
1931	05	05	0718	33.70	86.60	V			6500	340.0	Cullman, Alabama
1917	06	29	2023	32.70	87.50	V				257.0	Alabama, Felt Only Locally
1974	12	10	0002	31.35	87.47	V		6.0		202.0	S.W. Ala (Mag. 3.0 ML)
1976	04	15	0104	37.40	87.30	V		9.0		542.0	Kentucky
1940	05	31	1302	37.00	88.00	IV-V			1000	504.8	Ohio River (*Coords)
1938	09	17	2134	35.50	90.30	IV-V			90000	380.9	Northeastern Ark.
1937	05	16	1850	36.10	90.60	IV-V			25000	422.3	Northeastern Ark.
1919	11	03	1440	36.20	90.90	IV-V				429.8	Arkansas Felt Only Locally
1915	04	28	1740	36.40	89.50	IV-V			200	446.4	New Madrid, Mo.
1908	09	28	1334	36.50	89.50	IV-V			5000	453.3	New Madrid, Mo.
1897	04	30	2200	36.00	89.00	IV-V				423.9	Tenn. and Illinois (*Coords)
1883	07	14	0130	37.00	89.20	IV-V				489.9	Cairo, 111. (*Coords)
1856	11	09	0000	37.00	89.00	IV-V				491.7	Ill., Ky., Tenn. (*Coords-Time)
1855	05	02	2133	37.00	89.20	IV-V				489.9	Cairo, 111. (*Coords)
1820	11	09	1600	37.30	89.50	IV-V				508.2	Cape Girardeau, Mo.

TABLE 2.5-7 (Sheet 7 of 8)

YEAR	MONTH	DAY	HOUR (LOCAL TIME)	LATI-TUDE (N)	LONGI-TUDE (W)	MM INTEN-SITY	MAGNI-TUDE (MB)	HYPOCENTER DEPTH (MI.)	AREA (SQ.MI.)	DISTANCE TO SITE (MI.)	REMARKS
1818	03	01	0000	35.00	90.00	IV-V				347.3	Miss. R. Valley (*Coords, Date-Time)
1978	06	09	1815	32.09	88.58	<IV	3.3	6.0		183.0	Mississippi, Alabama
1976	10	22	1841	32.20	88.73	<IV	3.0	3.0		184.0	Mississippi
1965	12	19	1619	35.90	89.90		5.3	3.0		409.7	Northeastern Arkansas
1965	08	13	2346	36.30	89.50		5.0			439.6	Southwestern Illinois
1966	02	13	1720	37.10	91.00		4.7	4.0		492.2	Southeastern Missouri
1965	02	10	2140	36.40	89.70		4.6	11.0		445.1	Southeastern Missouri
1975	06	24	0512	33.72	87.84		4.5	6.0		300.4	Alabama
1965	11	04	0144	37.10	91.00		4.5	20.0		492.2	Southeastern Missouri
1964	05	23	0526	36.50	90.00		4.5	11.0		450.6	Southeastern Missouri
1964	01	16	2310	36.80	89.50		4.5	11.0		473.9	Southeastern Missouri
1964	05	23	0901	36.50	89.90		4.3	11.0		451.0	Southeastern Missouri
1974	02	15	1636	34.10	93.10		4.2	1.0		323.0	Ark., Several Weaker Shocks
1975	11	07	1740	33.55	87.36			3.0		307.0	Alabama (Mag 3.5 MBLG)
1963	07	08	1752	37.00	90.50		4.1	15.0		484.4	Southeastern Missouri
1971	03	14	1128	33.10	87.90		3.9	1.0		262.8	Carrollton, Alabama
1968	02	09	1935	36.50	89.90		3.8			451.0	Southeastern Missouri
1966	02	26	0210	37.20	91.00		3.8	20.0		499.1	Southeastern Missouri
1973	01	08	0312	33.80	90.60		3.5	4.0		263.4	Mississippi
1970	03	26	2144	36.50	89.70		3.5	3.0		452.0	Southeastern Missouri
1973	12	20	0445	36.20	89.60		3.4	6.0		432.0	New Madrid, Mo.

TABLE 2.5-7 (Sheet 8 of 8)

YEAR	MONTH	DAY	HOUR (LOCAL TIME)	LATITUDE (N)	LONGITUDE (W)	MM INTENSITY	MAGNITUDE (MB)	HYPOCENTER DEPTH (MI.)	AREA (SQ.MI.)	DISTANCE TO SITE (MI.)	REMARKS
1974	03	12	0630	35.70	89.80		3.2	3.0		396.5	Tennessee
1974	02	24	0154	35.80	90.40		3.2	4.0		401.5	Arkansas
1974	03	04	0824	35.70	90.40		3.0	3.0		394.6	Arkansas
1974	03	09	2234	36.20	89.50		2.5	3.0		432.7	New Madrid Region, Mo-
1975	09	09	0553	30.66	89.25			3.0		86.2	Miss. (Mag. 2.9 MBLG)
1975	08	25	0111	36.05	89.84			6.6		420.3	New Madrid, Mo. (Mag. 3.0 MBLG)
1975	08	24	2101	37.23	90.88			3.0		500.8	Eastern Mo. (Mag. 2.8 MBLG)
1975	08	24	1844	37.23	90.89			3.0		500.8	Eastern Missouri (Mag 2.7 MBLG)
1975	08	20	0314	36.56	89.80			3.0		455.6	New Madrid, Mo. (Mag 2.9 MBLG)
1975	07	06	0248	36.19	89.49			3.0		432.1	New Madrid, Mo. (Mag 2.9 MBLG)
1975	03	01	0550	33.50	88.00			10.8		282.6	Miss. (Mag 3.2 MBLG)
1975	02	13	1344	36.52	89.56			3.0		454.3	New Madrid, Missouri (Mag 3.3 MBLG)
1975	01	02	0319	34.87	90.94			15.0		338.3	Arkansas (Mag 2.9 MBLG)
1974	12	13	0413	36.70	91.63			3.0		468.4	S. Mo. (Mag 2.8 ML)
1922	11	26	2131	37.00	90.50					484.4	Miss. R. Valley (*Coords)
1886	02	13	0000	32.80	88.00					242.7	Alabama (*Time)
1963	11	05	1645	27.80	92.40		4.8	20.0		191.0	Gulf of Mexico
1973	01	07	1656	37.40	87.30		3.2	9.0		542.0	Kentucky

*** ESTIMATE**

TABLE 2.5-8 (Sheet 1 of 8)

LISTING OF HISTORIC EARTHQUAKE IN CHRONOLOGICAL ORDER

YEAR	MONTH	DAY	HOUR (LOCAL TIME)	LATITUDE (N)	LONGITUDE (W)	MM INTEN-SITY	MAGINITUDE (MB)	HYPOCENTER DEPTH (MI.)	AREA (SQ. MI.)	DISTANCE TO SITE (MI.)	REMARKS
1811	12	16	0200	36.60	89.60	XII			2000000	459.5	New Madrid Mo Felt To The East
1812	01	23	0900	36.60	89.60	XII				459.5	New Madrid, Missouri
1812	02	07	0345	36.60	89.60	XII				459.5	New Madrid, Kissouri
1818	03	01	0000	35.00	90.00	IV-V				347.3	Miss R. Valley (*Coords, Date-Time)
1820	11	09	1600	37.30	89.50	IV-V				508.2	Cape Girardeau, Mo.
1841	12	27	2350	36.40	89.20	V				448.9	Near Hickman, Ky, (*Coords)
1843	01	04	2045	35.20	90.00	VIII			400000	361.0	Memphis, Tenn., Felt To East
1855	05	02	2133	37.00	89.20	IV-V				489.9	Cairo, Ill. (*Coords)
1856	11	09	0000	37.00	89.00	IV-V				491.7	Ill., KY., Tenn. (*Coords-Time)
1865	08	17	0900	36.50	89.50	VII			24000	453.3	Southeast Mo.
1878	03	12	0400	36.80	89.20	V				476.2	Columbus, Ky., Felt Locally
1878	11	18	2352	36.70	90.40	VI			150000	463.7	Southeastern Missouri
1882	10	22	1615	35.00	94.00	VI-VII			135000	402.6	Arkansas
1883	01	11	0112	37.00	89.20	VI			80000	489.9	Cairo, Illinois
1883	04	12	0230	37.00	89.20	VI-VII				489.9	Cairo, Ill., Felt Locally
1883	07	14	0130	37.00	89.20	IV-V				489.9	Cairo, Ill. (*Coords)
1883	12	05	0920	36.30	91.80	V				442.7	Izard Co., Ark. Felt Only Locally
1886	02	04	2000	32.80	88.00	V			1600	242.7	Alabama
1886	02	13	0000	32.80	88.00					242.7	Alabama (*Time)
1887	08	02	1236	37.00	89.20	V				489.9	Cairo, Ill, Widespread Effects
1889	07	19	1932	35.20	90.00	VI				361.0	Memphis Tenn., Felt Only Locally
1891	01	08	0000	31.70	95.20	VII				304.4	Rusk, Texas
1891	09	26	2255	37.00	89.20	V				489.9	Cairo, Illinois (*Coords)

TABLE 2.5-8 (Sheet 2 of 8)

YEAR	MONTH	DAY	HOUR (LOCAL TIME)	LATITUDE (N)	LONGITUDE (W)	MM INTEN-SITY	MAGINITUDE (MB)	HYPOCENTER DEPTH (MI.)	AREA (SQ. MI.)	DISTANCE TO SITE MI.)	REMARKS
1895	10	31	0508	37.00	89.40	VIII			1000000	488.3	Missouri, Felt To The East
1897	04	30	2200	36.00	89.00	IV-V				423.9	Tennessee and Illinois (*Coords)
1903	11	27	0320	36.50	89.50	V			70000	453.3	New Madrid, Mo.
1905	08	21	2308	36.00	90.00	VI			40000	416.2	Mississippi Valley (*Coords)
1908	09	28	1334	36.50	89.50	IV-V			5000	453.3	New Madrid, Mo.
1908	10	27	1827	37.00	89.20	V			5000	489.9	Cairo, Ill.
1909	10	23	0110	37.00	89.50	V			40000	487.6	Southeastern Missouri
1911	03	31	1057	33.80	92.20	V			18000	282.1	Rison, Ark.
1911	03	31	1210	33.80	92.20	V			18000	282.1	Rison, Ark.
1915	04	28	1740	36.40	89.50	IV-V			200	446.4	New Madrid, Mo.
1915	10	26	0140	36.70	88.60	V				476.0	Mayfield, Ky. Felt Locally
1915	12	07	1240	36.70	89.10	V-VI			60000	470.3	Near Mouth Of Ohio River
1916	10	18	1604	33.50	86.20	VII			100000	348.0	Irondale, Alabama
1916	12	18	2342	36.60	89.30	VI-VII				461.7	Hickman Ky., Felt Only Locally
1917	06	29	2023	32.70	87.50	V				257.9	Alabama, Felt Only Locally
1918	10	04	0321	34.70	92.30	V			30000	342.5	Lonoke, Co., Arkansas
1918	10	13	0330	36.00	91.10	V				416.9	Blackrock, Ark.
1918	10	15	2130	35.20	89.20	V			20000	367.5	West Tennessee
1919	11	03	1440	36.20	90.90	IV-V				429.8	Arkansas, Felt Only Locally
1922	03	22	1630	37.30	88.60	V			25000	516.4	South Illinois (*Coords)
1922	03	23	1545	37.00	88.00	V				504.8	Western Kentucky (*Coords)
1922	03	30	1053	35.20	90.00	V				361.0	Mississippi River Valley (*Coords)
1922	11	26	2131	37.00	90.50					484.4	Miss R. Valley (*Coords)
1923	10	28	1110	35.50	90.30	VII			40000	380.9	Marked Tree, Arkansas

TABLE 2.5-8 (Sheet 3 of 8)

YEAR	MONTH	DAY	HOUR (LOCAL TIME)	LATITUDE (N)	LONGITUDE (W)	MM INTEN-SITY	MAGINITUDE (MB)	HYPOCENTER DEPTH (MI.)	AREA (SQ. MI.)	DISTANCE TO SITE (MI.)	REMARKS
1923	11	26	1725	35.20	90.20	VI				360.3	Miss R. Valley (*Coords)
1923	12	31	2105	35.40	90.30	V			30000	373.9	Arkansas
1924	03	02	0518	36.90	89.10	V			15000	483.9	Kentucky
1925	05	13	0600	36.70	88.60	V			3000	476.0	Kentucky
1927	05	07	0228	36.50	89.00	VII			130000	457.8	Mississippi Valley
1927	08	13	1000	36.40	89.50	V				446.4	Miss. Valley (Tiptonville Tn)(*Coords)
1930	08	29	0027	37.00	89.00	V				491.7	Ky., Tenn., Ill., Mo., (*Coords)
1930	10	19	0617	30.00	91.00	V-VI			15000	31.7	Donaldsonville, La.
1931	05	05	0718	33.70	86.60	V			6500	340.0	Cullman, Alabama
1931	12	16	2136	34.10	89.80	VI			65000	286.7	Batesville, Miss.
1933	12	09	0240	35.80	90.20	V			100	401.8	Manila, Ark.
1934	04	11	1140	33.90	95.50	V			3000	399.9	Texas-Oklahoma Border
1934	08	19	1847	37-00	89.20	VI			28000	489.9	Rodney, Mo.
1936	03	14	1120	34.00	95.20	V			900	391.8	Southeastern Oklahoma
1937	05	16	1850	36.10	90.60	IV-V			25000	422.3	Northeastern Ark.
1938	09	17	2134	35.50	90.30	IV-V			90000	380.9	Northeastern Ark.
1939	06	19	1543	34.10	93.10	V				323.0	Arkadelphia, Ark, Felt Locally
1940	05	31	1302	37-00	88.00	IV-V			1000	504.8	Ohio River (*Coords)
1941	11	16	2109	35.50	89.70	V-VI				383.3	Covington, Tenn., Local
1947	12	15	2127	35.50	90.00	V			10000	381.7	Near Osceola, Ark. (*Coords)
1949	01	13	2145	36.40	89.50	V			7000	446.4	Miss. River Valley
1950	02	08	0437	37.40	92.40	V				523.9	Lebanon, Mo.
1952	02	20	1635	36.40	89.50	V				446.4	Tenn. Mo. Border
1952	07	16	1748	36.20	89.60	VI				432.0	Dyersburg, Tenn.

TABLE 2.5-8 (Sheet 4 of 8)

YEAR	MONTH	DAY	HOUR (LOCAL TIME)	LATITUDE (N)	LONGITUDE (W)	MM INTEN-SITY	MAGINITUDE (MB)	HYPOCENTER DEPTH (MI.)	AREA (SQ. MI.)	DISTANCE TO SITE (MI.)	REMARKS
1954	n2	02	1053	36.70	90.30	VI				463.7	Poplar Bluff, Mo.
1954	04	26	2009	35.20	90.00	V				361.0	Memphis, Tenn.
1955	01	25	0124	35.60	90.30	VI			30000	387.8	Tennessee-Arkansas-Missouri
1955	02	01	0845	30.40	89.10	V				86.6	Gulfport, Miss.
1955	03	29	0303	36.00	89.50	VI				419.1	Finley, Tenn.
1955	09	05	1945	36.00	89.50	V				419.1	Finley, Tenn.
1955	12	13	0143	36.00	89.50	V				419.1	Dyer Co., Tenn.
1956	01	28	2214	35.60	89.60	VI				390.9	Tenn.-Ark. Border
1956	04	02	1003	34.20	95.40	V				409.6	Southeastern Oklahoma
1956	10	29	0324	36.10	89.40	V				426.7	Caruthersville, Mo.
1956	10	30	0436	36.20	95.00	VII			3700	502.7	Northeastern Oklahoma
1956	11	25	2213	37.10	90.60	VI			21500	491.3	Wayne County Mo.
1957	03	19	1038	32.00	95.00	V			10000	302.1	Northeast Texas (*Coords)
1957	03	26	0227	37.00	88.40	V				498.8	Paducah, Ky., Felt Only Locally
1957	04	23	0424	34.50	86.80	V			11500	379.0	Birmingham, Alabama
1958	01	26	1056	35.20	90.00	V				361.0	Memphis, Tenn., Felt Locally
1958	01	27	2357	37.00	89.00	V			300	491.7	Ill.-Ky.-Mo. Borders
1958	04	08	1626	36.20	89.10	V			400	436.3	Oblion Co., Tenn
1958	04	26	0130	36.30	89.50	V				439.6	Lake Co., Tenn
1958	11	19	1215	30.30	91.10	V				43.3	Baton Rouge, La., Felt Locally
1959	02	13	0237	36.20	89.50	V			170	432.7	Bogota, Tenn.
1959	08	12	1306	35.00	87.00	VI			2800	400.0	Ala-Tenn. Border
1959	12	21	1025	36.00	89.50	V			400	419.1	Finley, Tenn.
1960	01	28	1538	36.00	89.50	V				419.1	Dyer Co., Tenn., Felt Locally

TABLE 2.5-8 (Sheet 5 of 8)

YEAR	MONTH	DAY	HOUR (LOCAL TIME)	LATITUDE (N)	LONGITUDE (W)	MM INTEN-SITY	MAGINITUDE (MB)	HYPOCENTER DEPTH (MI.)	AREA (SQ. MI.)	DISTANCE TO SITE (MI.)	REMARKS
1960	04	21	0445	36.30	89.50	V				439.6	Lake Co. Tenn., Felt Locally
1961	01	10	1940	35.00	95.00	V				435.2	Southeastern Okla. (*Coords)
1961	04	27	0130	35.00	95.00	V				435.2	Southeastern Okla. (*Coords)
1962	02	02	0044	36.50	89.60	VI		15.0	35000	452.6	New Madrid, Mo.
1962	07	23	0005	36.10	89.80	VI		11.0		424.0	Southern Mo.
1963	03	03	1130	36.70	90.10	VI	4.5		100000	464.1	Southeast Missouri
1963	07	08	1752	37.00	90.50		4.1	15.0		484.4	Southeastern Missouri
1963	08	02	1838	37.00	88.80	V	3.6	11.0		493.8	Ill. Ky Border
1963	11	05	1645	37.80	92.40		4.8	20.0		191.0	Gulf of Mexico
1964	01	16	2310	36.80	89.50		4.5	11.0		473.9	Southeastern Missouri
1964	04	23	1921	31.50	93.80	V	3.7			223.6	Western Louisiana
1964	04	24	0134	31.60	93.80	V	3.7			226.8	Western Louisiana
1964	04	27	1831	31.50	93.80	V	3.4			223.6	Western Louisiana
1964	04	28	1519	31.70	93.60	V	4.4			220.1	Western Louisiana
1964	05	23	0526	36.50	90.00		4.5	11.0		450.6	Southeastern Missouri
1964	05	23	0901	36.50	89.90		4.3	11.0		451.0	Southeastern Missouri
1964	08	16	0536	31.40	93.80	V				220.5	Hemphill, Texas
1965	02	10	2140	36.40	89.70		4.6	11.0		445.1	Southeastern Missouri
1965	08	13	2346	36.30	89.50		5.0			439.6	Southwestern Illinois
1965	08	14	0714	37.10	89.20	VII	5.0	3.0		496.7	Southwestern Illinois
1965	08	15	0007	37.40	89.50	V	5.1	3.0		515.0	Southwestern Illinois
1965	11	04	0144	37.10	91.00		4.5	20.0		492.2	Southeastern Missouri
1965	12	19	1619	35.90	89.90		5.3	3.0		409.7	Northeastern Arkansas
1966	02	13	1720	37.10	91.00		4.7	4.0		492.2	Southeastern Missouri

TABLE 2.5-8 (Sheet 6 of 8)

YEAR	MONTH	DAY	HOUR (LOCAL TIME)	LATITUDE (N)	LONGITUDE (W)	MM INTEN-SITY	MAGINITUDE (MB)	HYPOCENTER DEPTH (MI.)	AREA (SQ. MI.)	DISTANCE TO SITE (MI.)	REMARKS
1966	02	26	0210	37.20	91.00		3.8	20.0		499.1	Southeastern Missouri
1967	06	04	1014	33.60	90.90	VI	3.8		25000	250.7	Greenville, Miss
1967	06	29	0757	33.60	90.90	V	3.4			250.7	Greenville, Miss
1967	07	21	0315	37.50	90.40	VI	3.9			518.9	Southeastern Missouri
1968	02	09	1935	36.50	89.90		3.8			451.0	Southeastern Missouri
1969	01	01	1736	34.80	92.60	VI	4.2	7.0	23000	354.8	Central Arkansas
1970	03	26	2144	36.50	89.70		3.5	3.0		452.0	Southeastern Missouri
1970	11	16	2014	35.90	89.90	VI	3.6	17.0	78000	409.7	Arkansas
1971	03	14	1128	33.10	87.90		3.9	1.0		262.8	Carrollton, Alabama
1971	10	01	1250	35.80	90.40	V		12.0	55000	401.5	Northeastern Arkansas
1972	01	31	2342	36.40	90.80	V	3.9	8.0		443.3	Northeastern, Arkansas
1972	03	29	1439	36.20	89.60	V	3.7	6.0	65800	432.0	New Madrid, Ho.
1973	01	07	1656	37.40	87.30		3.2	9.0		542.0	Kentucky
1973	01	08	0312	33.80	90.60		3.5	4.0		263.4	Mississippi
1973	12	20	0445	36.20	89.60		3.4	6.0		432.0	New Madrid, Mo.
1974	01	07	1913	36.20	89.39	V	4.1	0.6		433.6	New Madrid, Mo.-Tenn. Region
1974	02	15	1636	34.10	93.10		4.2	1.0		323.0	Arkansas, Several Weaker Shocks
1974	02	15	1649	34.00	93.00	V	3.8	1.0		314.2	Whelen Springs, Ark.
1974	02	24	0154	35.80	90.40		3.2	4.0		401.5	Arkansas
1974	03	04	0824	35.70	90.40		3.0	3.0		394.6	Arkansas
1974	03	09	2234	36.20	89.50		2.5	3.0		432.7	New Madrid Region, Mo.
1974	03	12	0630	35.70	89.80		3.2	3.0		396.5	Tennessee
1974	05	13	0052	36.71	89.39	VI	4.3	1.0		468.5	New Madrid, Missouri
1974	08	11	0830	36.92	91.17	V	3.6	2.0		480.5	Fremont, Missouri

TABLE 2.5-8 (Sheet 7 of 8)

YEAR	MONTH	DAY	HOUR (LOCAL TIME)	LATITUDE (N)	LONGITUDE (W)	MM INTEN-SITY	MAGINITUDE (MB)	HYPOCENTER DEPTH (MI.)	AREA (SQ. MI.)	DISTANCE TO SITE (MI.)	REMARKS
1974	12	10	0002	31.35	87.47	V		6.0		202.0	S. W. Alabama (Mag. 3.0 ML)
1974	12	12	2304	34.67	91.88	V		3.0		333.7	N. E. Ark. (Mag. 3.4 MBLG)
1974	12	13	0413	36.70	91.63			3.0		468.4	S. Missouri (Mag. 2.8 ML)
1975	01	02	0319	34.87	90.94			15.0		338.3	Arkansas (Mag. 2.9 NBLG)
1975	02	13	1344	36.52	89.56			3.0		454.3	New Madrid, Mo. (Mag. 3.3 MBLG)
1975	03	01	0550	33.50	88.00			10.8		282.6	Mississippi (Mag. 3.2 MBLG)
1975	06	13	1640	36.54	89.68	VI	4.3	1.2		454.9	New Madrid, Missouri
1975	06	24	0512	33.72	87.84		4.5	6.0		300.4	Alabama
1975	07	06	0248	36.19	89.49			3.0		432.1	New Madrid, Mo. (Mag. 2.9 MBLG)
1975	08	20	0314	36.56	89.80			3.0		455.6	New Madrid, Mo. (Mag. 2.9 MBLG)
1975	08	24	1844	37.23	90.89			3.0		500.8	Eastern Missouri (Mag. 2.7 MBLG)
1975	08	24	2101	37.23	90.88			3.0		500.8	Eastern Missouri (Mag. 2.8 MBLG)
1975	08	25	0111	36.05	89.84			6.6		420.3	New Madrid, Mo. (Mag. 3.0 MBLG)
1975	08	28	2223	33.82	86.60	VI	3.5	3.0		347.0	Alabama
1975	09	09	0553	30.66	89.25			3.0		86.2	Mississippi (Mag. 2.9 MBLG)
1975	11	07	1740	33.55	87.36			3.0		307.0	Alabama (Mag- 3.5 MBLG)
1975	12	02	2101	36.54	89.57	V		3.0		455.6	New Madrid, Mo. (Mag. 2.8 MBLG)
1976	03	24	1841	35.59	90.48	VI	4.9	9.0		386.9	Arkansas
1976	04	15	0104	37.40	87.30	V		9.0		542.0	Kentucky
1976	05	22	0141	36.04	89.84	V		6.0		419.6	New Madrid, Mo. (Mag. 3.2 MBLG)
1976	09	25	0807	35.61	90.45	V		3.0		388.3	Arkansas (Mag. 3.6 MBLG)

TABLE 2.5-8 (Sheet 8 of 8)

YEAR	MONTH	DAY	HOUR (LOCAL TIME)	LATITUDE (N)	LONGITUDE (W)	MM INTEN-SITY	MAGINITUDE (MB)	HYPOCENTER DEPTH MI.)	AREA (SQ. MI.)	DISTANCE TO SITE (MI.)	REMARKS
1976	10	22	1841	32.20	88.73	<IV	3.0	3.0		184.0	Mississippi
1977	05	03	2000	31.98	88.42	V	3.6	3.0		183.0	Mississippi, Alabama
1978	06	09	1815	32.09	88.58	<IV	3.3	6.0		183.0	Mississippi, Alabama
1978	12	10	2006	31.95	98.48	V	3.5	3.0		180.0	Mississippi, Alabama

* ESTIMATE

TABLE 2.5-9 (Sheet 1 of 7)

SUMMARY OF INTENSITY DATA CONCERNING THE NEW MADRID SERIES, DONALDSONVILLE EARTHQUAKE, GULFPORT EARTHQUAKE AND BATON ROUGE EARTHQUAKE

SUMMARY OF INTENSITY DATA FOR 1811-1812 NEW MADRID SERIES

EPICENTRAL INTENSITY (MODIFIED MERCALLI)	SUMMARY
XII	These were the strongest shocks of the great series of earthquakes of 1811-1812 centered in the Mississippi Valley and known collectively as the New Madrid earthquake. This series consisted of thousands of individual shocks, many of which were strong. The three strongest shocks had an intensity of XIT in their epicentral area at the following dates and coordinates: December 16, 1811, 36.6°N-89.6°W; January 23, 1812, 36.6°N-89.6°W; and February 7, 1812, 36.6°N-89.6°W. The three strong shocks were felt over an area of about 2,000,000 square miles. "The shock was felt from Canada to New Orleans, Louisiana, and from the heatwaters of the Missouri to the Atlantic, including Boston, Massachusetts, 1,100 miles away. Caving of river banks occurred as far away as Vicksburg, Mississippi. About 1 million square miles, or half the area, was so shaken that vibrations were distinctly felt. This far exceeds in land area any previous earthquake on this Continent". "The most seriously affected area was characterized by raised and sunken lands, fissures, sinks, sand blows, and large landslides. This area was 30,000 to 50,000 square miles in extent, from a point west of Cairo, Illinois, to the latitude of Memphis, Tennessee, and from Crowleys Ridge to Chicksaw Bluffs, Tennessee, a distance of 50 miles." "According to contemporary accounts, waves with visible depressions between the swells rolled across the earth and finally broke open leaving parallel fissures. These were reported to be from 600 to 700 feet long; one had a length of 5 miles. Another wave of smaller size resulted from the settling and caving of river banks". "There is some evidence of vertical faults, one of which is believed to have caused quite marked falls in the river, that lasted until the slope had been leveled off. Landslides occurred wherever the river banks were steep and where there were steep bluffs. In places, sections of forest were carried down or overthrown by the slides; many were split. In some cases, trees were thrown over to a sharp angle, beginning to grow in their new positions when the slide came to rest, with the lower parts of the trunks inclined and the upper parts vertical. In other areas, the vibration alone threw down trees." "Large areas dropped by amounts reaching 15 feet in some cases, though 5 to 8 feet was more common. In eastern Arkansas, Lake St. Francis, so formed, is 40 miles long by a half mile wide. Over the sunken country, trees were killed by water overflowing the lower parts of the trunks. Valuable evidence is given by cypress trees, killed when the knees were submerged. The cumulative effects of the earthquake destroyed forests over an area of 150,000 acres. The most typical sunken land of the area is Reelfoot Lake in Tennessee. The lake is 8 to 10 miles in length and 2 to 3 miles in width. The submergence ranged from 5 to perhaps 20 feet, although greater depths were reported." "Ejection of water, sand, mud, and gas were noticeable features of the quake.

EPICENTRAL INTENSITY
(MODIFIED MERCALLI) — SUMMARY

XII (Cont'd)

Sand, the most comon, was mixed with carbonaceous material in some cases, undoubtedly the source of the gas, was very noticeable in places". (Reference 56)

Recently, all available references to this series of earthquakes were compiled and studied. This comprehensive evaluation concludes that the three major shocks the New Madrid series were felt at New Orleans at the following intensities

DATE OF MAJOR SHOCK	MODIFIED MERCALLI INTFNSITY AT NEW ORLEANS:
December 16, 1811	III
January 23, 1812	IV-V
February 7, 1812	V

SUMMARY OF INTENSITY DATA CONCERNING DONALDSONVILLE, LOUISIANA EARTHQUAKE ON OCTOBER 19, 1930

EPICENTRAL INTENSITY
(MODIFIED MERCALLI) — SUMMARY

V-VI

The following was taken from "The Donaldsonville Chief" November, 1930 -"Earth Tremors Felt Over Wide Area of State".

"Two distinct tremors or vibrations from an earthquake or similar phenomenon, believed to have occurred deep within the floor of the Gulf of Mexico, 300 miles or more from shore, were felt over a wide area of southeast Louisiana early Sunday morning."

"The disturbance occurred shortly after 6 o'clock and affected an area within a radius of 100 miles of New Orleans. The tremors shook floors and beds and caused dishes to rattle and house foundations to creak, but not one was injured and no property damage was done."

"The shocks lasted from six to fifteen seconds, gradually subsiding. In some instances beds were rolled two or three feet, causing their occupants to awaken startled, and pictures were loosened from walls."

"Professor R. A. Steinmayer, head of the geological department of Tulane University, pointed out that the soil cushion under New Orleans and southeast Louisiana generally, which is 2300 feet deep, is sufficient to take up the shock from earthquake tremors and prevent serious damage."

"This is said to be the first earthquake that ever occurred in Louisiana. The shocks were felt as far north as Slidell, Covington and Bogalusa, to the south as far as Pilottown, and to the west and northwest at Morgan City, Franklin, New Iberia, Plaquemine, Donaldsonville, White Castle, Baton Rouge, New Roads and St. Francisville."

TABLE 2.5-9 (Sheet 3 of 7)

EPICENTRAL INTENSITY (MODIFIED MERCALLI)	SUMMARY
V-VI (Cont'd)	"Numerous incidents are reported from various cities and sections in the earthquake area. The shocks occurred at about the time of the beginning of the morning devotion in the churches where many people had already assembled. This was notably the case in New Orleans, where the worshippers, upon feeling the tremors, left the churches in fright. It is reported that in Morgan City, when the worshippers felt the benches rock and saw the walls tremble they fled from the church in panic." "There was a large number of people already assembled in the Ascension Catholic Church in this city for the first mass. Many left the building when it shook, but there was not panic, and they returned when the vibrations subsided." "It is said that at New Roads that three of the tremors was great enough to shake house doors open, and in Pilottown persons were thrown from their beds." "Assessor J. Paul Bourgeois, who resides in Gonzales, this parish, reports that the tremors were seriously felt in that section. He says that the brick chimneys of several residences were damaged, some being cracked almost from the top to bottom while parts of others, above the roof, were knocked down. No one was injured, Mr. Bourgeois said." "It is said that definite local data concerning the force and location of the earthquake was made impossible by a breakdown of the seismograph at Loyola University, New Orleans. "Professor Steinmnayer of Tulane University explained that the "areas where earthquakes are likely to be frequent" are as follows: 1. Where geological changes are a rapid progress. 2. In the vicinity of young mountains. 3. On submarine slopes. 4. In the vicinity of deltas of large rivers. He gave three general causes: "1. Faulting, slumping or fracture of the earth's strata." "2. Earth adjustment to stresses." "3. Volcanic disturbances." "Discussing the phenomena, he said: "Earthquakes are tremors of appreciable violence. They usually have small amplitude and their effectiveness, therefore, is not dependent upon their suddenness of movement." "Earthquakes cause an oscilation of the rock particles. Normally they are greater where the materials are densest. Therefore, here in the deltaic area, with our thousands of feet of thickness of loose, incoherent material, they are not likely to be disastrous."

TABLE 2.5-9 (Sheet 4 of 7)

EPICENTRAL INTENSITY (MODIFIED MERCALLI)	SUMMARY
V-VI (Cont'd)	The following was taken from the "Baton Rouge State Times", October 20, 1930 "Baton Rouge and Vicinity Shared in Earth Tremors of Early Sunday Mornings - First Quake Ever Recorded in Louisiana Mild in Form - First Quake in State's History Injuries Sustained When Morgan City Worshippers Leave Church". "Living through an earthquake was the novel experience of Baton Rougeans early Sunday morning and while some failed to recognize the gentle swaying as an actual shake-up of old mother earth, others give vivid accounts of the tremors, which were felt also throughout southeast Louisiana. Beds rocked back and forth and in some homes window panes rattled and ornaments tilted. The earthquake was a very real one and while no damage is reported anywhere in the state, the event has been chronicled by scientists as something new in Louisiana's history, so far as the records of hundreds of years reveal. The time of the tremor here was about 6:10 o'clock, possibly a few minutes earlier or later." "Father D. Blasco, Pastor of the Sacred Heart Church, who was in Naples during the fearful earthquake that shocked southern Italy last summer, felt the tremors yesterday morning, but so slight were they in comparison that at the time he attributed them to blasting by some of the oil companies in this vicinity." "Father Blasco was reading in his study at the time and felt a sensation which he describes more as a vibration. Very different was the shock in Naples he relates, when the effect was more like the continued swinging of a pendulum for a period of 45 seconds." "The first thought of many others in Baton Rouge was the swaying was possibly caused by blasting; although the sensation was different and there was no accompanying noise. Hundreds were awakened from their sleep by the moving back and forth of their beds, shortly after 6 o'clock. Some report a gentle swaying, while others felt a sharp rocking. Within a few seconds it was over and men and women were left wondering just what happened." "Until it was thoroughly established that a quake had occurred, many were left wondering over what had happened and numerous calls came into the State-Times office from those puzzled by the phenomenon. Weather beautifully clear and crisp prevailed and there was nothing saving the slight swaying over a period of a few seconds to indicate anything unusual in nature." "Father F. L. Gassier, Pastor of St. Joseph's Catholic Church was in the confessional box at the time and did not notice that anything out of the ordinary had occurred. Those in the rectory felt the tremors decidedly. Father Gassier who was sitting in the study at St. Anthony's rectory, says he saw the books in the library moving and the ornaments on top of the bookcase tilting. Mass was in progress at St. Anthony's Church but Father Edward Tombouis said no one there seemed to notice anything unusual."

TABLE 2.5-9 (Sheet 5 of 7)

EPICENTRAL INTENSITY (MODIFIED MERCALLI)	SUMMARY
V-VI (Cont’d)	"It was natural for many in Baton Rouge to first attribute the movement to oil blasting. Last winter some of the companies exploring for oil in this vicinity set off blasts, in order to take off records on the seismograph and most of this blasting was done at night. Frequent jars were felt throughout this entire territory but caused little concern after their sources was explained." "But the swaying motion of early Sunday morning, while scarcely more than a vibration in some sections, was real earth tremor, and Louisiana geologists and scientists are now seeking to locate the probable center, and to find out as nearly as possible its direct and remote causes." "New Orleans, October 20 (AP) Southeastern Louisiana, including New Orleans and Baton Rouge was strongly rocked yesterday by the first earthquake in the state’s known history but no loss of life or serious damage resulted." "A resilient cradle of alluvial silt and moist loam, 2300 feet deep underlying the region affected, was credited by scientific authorities with softening the tremors which nevertheless were sufficiently strong to throw scores into a panic." "The only injury reported was in Morgan City, when worshippers in a Catholic Church became frightened at apparently seeing the walls of the church sway and scratched and bruised each other in a hurried dash for the exits." "The quake occurred between 6:15 and 6:30 a.m. awakening sleepers and shocking many into wide awakening awakeness at Pilottown, at the mouth of the Mississippi River, a number of sleepers said they were literally shaken out of bed." The seismographic record at Georgetwon University of Washington, fixed the geostratic disturbance at 6:22 (C.S.T.). No record was made at the geostatic laboratories at Loyola University here or at Spring Hill College in Mobile as the instruments at both institutions were reported out of commission." "More than a score of cities and towns outside New Orleans as far west as New Iberia, as far north as St. Francisville, and eastward to Slidell report experiencing earth shocks." "Newspaper offices were beseiged with hundreds of telephone calls seeking information about the vibrations." "Those telling of the tremors differed as to whether there were more than one shock. Many were certain that they felt one lasting about 30 seconds and a second about five minutes later." "Among the cities outside New Orleans affected were Baton Rouge, New Iberia, Franklin, St. Francisville, Slidell, Bogalusa, New Roads, Plaquemine, White Castle, Lockport, and Donaldsonville, The earth trembled so violently that many inhabitants rushed into the streets in dismay."

EPICENTRAL INTENSITY (MODIFIED MERCALLI)	SUMMARY
V-VI (Cont'd)	"No shock was reported very far east of New Orleans and the Mississippi Gulf Coast was not affected." Professor R. A. Steinmayer head of the Tulane University geological department said that the crushing of alluvia soils underlying south Louisiana 2300 feet in depth was sufficient to take up strata shocks and prevent serious damage." "Professor J. Adair Lyon of the Physics Department Sophie Newcomb College expressed the view that as the vibrations gradually faded out in western, northerly and easterly directions the disturbances might have had its origin in the floor of the Gulf of Mexico several hundred miles from shore." "A group of nuns of the historic Uraubine Convent in New Orleans reported that the Dieu of more than one tremble and swayed during the morning prayers." "No record had been found of any previous earthquake in Louisiana history." The following was taken from the "Morgan City News", Morgan City, Louisiana, 1930 - "Earthquake Shocks Felt Here". "Two distinct earthquake shocks lasting from three to five seconds each were felt here at 6:15 o'clock Sunday morning. The same quakes were noted over a territory extending from New Orleans to Lafayette and as far north as Alexandria. No damage was reported but the trembles were of sufficient violence to cause momentary uneasiness. Members of the Sacred Heart Church, at early mass, left the building on account of the vibrations. Houses throughout the city were distinctly rocked, and many sleepers were awakened by the motion of their beds." "Scientists have decided that some shifting of the earth under the Gulf of Mexico somewhere off the central coast of Louisiana caused the earth to tremble. While the disturbance may have been very severe at the point of occurrence, it is believed that the formations of this part of the coast country are a splendid shock absorber and that no serious damage from an earthquake can be likely. The alluvial deposits of thousands of years have buried the bed rock formations so deeply that the cushion of loose upper soils will hardly ever be broken by a subterranean disturbance. Nevertheless, those who felt the shocks Sunday morning seem to be fully satisfied to limit the if experience with earthquakes to this one incident."

SUMMARY OF INTENSITY DATA FOR GULFPORT, MISSISSIPPI EARTHQUAKE ON FEBRUARY 1, 1955

EPICENTRAL INTENSITY (MODIFIED MERCALLI)	SUMMARY
V	Maximum Modified Mercalli intensity V. "Felt by and frightened many. Felt strongly by many along a 12 mile strip of the Mississippi Gulf Coast. In Gulfport, occupants of the building housing the highway patrol substation rushed outside. Houses shook; windows and dishes rattled.." (Reference 55)

TABLE 2.5-9 (Sheet 7 of 7)

EPICENTRAL INTENSITY (MODIFIED MERCALLI)	SUMMARY
V (Cont'd)	"Rumbling sounds. Also felt at Biloxi, Mississippi City and Bay St. Louis." (Reference 56)

EPICENTRAL INTENSITY (MODIFIED MERCALLI)	SUMMARY OF INTENSITY DATA FOR BATON ROUGE, LOUISIANA EARTHQUAKE ON NOVEMBER 19, 1958 SUMMARY
V	"Maximum Modified Mercalli intensity V. "Felt by and alarmed many. Scores of anxious residents telephoned the Weather Bureau, Civil Defense, police, newspaper, and radio stations. Houses shook; windows rattled. Also felt at Baker and Denham Springs." (References 55 and 56) The following was taken from the "State Times", Baton Rouge, Louisiana, November 19, 1958 - "Feel Tremor Over Large Area Here". "The State Times switchboard was flooded with calls from Baton Rougeans who reported that they felt a sharp tremor shortly before noon today." "Some said their houses shook. Others said their windows rattled. One resident thought someone was walking on the roof." "Speculation that the tremor was an earthquake was ruled out by the seismologist at Loyola University in New Orleans. But he said there was the possibility it was a surface distrubance, felt locally but recorded on the seismograph." "The Weather Bureau said an explosion was ruled out because nobody reported hearing a blast. Reports came from all over the city, as far east as the Air Force depot and as far west as Port Allen." "The Air Force and the tower at Ryan Airport said there were no jets in the area ruling out the possibility of a jet cracking the sound barrier." "The first reports of the tremor started coming in about 11:30 a.m." "State workers in the Capitol Annex reported feeling the shock." "Some of the calls came from the north Baton Rouge area. Others came from LSU and sections in the southern part of the city." "The industrial plants said they could not account for the tremor."

TABLE 2.5-10

RESULTS FROM PARAMETRIC STUDY OF SEISMIC WAVE TRANSMISSION CHARACTERISTICS

Depth Ft.	Maximum Acceleration (g)			Depth Ft.	Shear Moduli from Final Iteration (KSF)		
	G ± 0%	G - 25%	G + 25%		G ± 0%	G - 25%	G + 25%
0.	0.12727	0.12727	0.15526	5	2927.	2927.	2856.
10.	0.12643	0.12643	0.15162	34.	2088.	2089.	2019.
58.	0.09117	0.09118	0.08369	77.	380.	233.	604.
96.	0.20251	0.22731	0.22320	121.	501.	295.	783.
146.	0.16034	0.23176	0.17558	158.	613.	380.	1135.
170.	0.17654	0.22358	0.16674	195.	686.	441.	1309.
220.	0.19184	0.24200	0.18913	245.	959.	472.	1152.
270.	0.17318	0.33921	0.24363	304.	1082.	536.	1509.
338.	0.20588	0.39194	0.23153	354.	5294.	3040.	6586.
370.	0.91603	0.35223	0.20321	385.	5190.	2612.	6475.
400.	0.16506	0.26612	0.15810				

Length of Soil Column (Ft.)	Significant Site Frequency (cps)			Site Period (seconds)		
	G ± 0%	G - 25%	G + 25%	G + 0%	G - 25%	G + 25%
400.	0.32	0.24	0.39	3.09	4.14	2.54

TABLE 2.5-11

RESULTS FROM PARAMETRIC STUDY OF SEISMIC WAVE TRANSMISSION CHARACTERISTICS

Elevation	Maximum Acceleration - %(g)X $\frac{1}{100}$		
MSL	G	G-25%	G+25%
+17	0.12727	0.12727	0.15526
+7	0.12643	0.12643	0.15162
-40	0.09117	0.09118	0.08369
-80	0.20251	0.22731	0.22320
-130	0.16034	0.23176	0.17558
-150	0.17654	0.22358	0.16674
-200	0.19184	0.24200	0.18913
-250	0.17318	0.33921	0.24363
-320	0.20588	0.39194	0.23153
-350	0.19603	0.35223	0.20321
-380	0.16506	0.26613	0.15810

Elevation	Shear Moduli from Final Iteration (KSF)		
MSL	G	G-25%	G+25%
+12	2927	2927	2856
-17	2088	2089	2019
-60	380	233	604
-105	501	295	783
-140	613	380	1135
-180	686	441	1309
-230	959	472	1152
-285	1082	536	1509
-335	5294	3040	6586
-300	5190	2612	6475

Length of Soil Column (Ft.)	Significant Site Frequency (cps)			Site Period (seconds)		
	G	G-25%	G+25%	G	G-25%	G+25%
400	0.32	0.24	0.39	3.09	4.14	2.54

TABLE 2.5-12

PLEISTOCENE SOIL STRATA ZONES

Zone	Elevation (MSL)		Description of Pleistocene Strata
	From	To	
1	- 40 ft.	- 77 ft.	Stiff tan and gray fissured clay.
2	- 77 ft.	- 92 ft.	Very dense tan silty sand.
3 a	- 92 ft.	- 108 ft.	Medium stiff gray clay with silt lenses.
b	- 108 ft.	- 116 ft.	Stiff gray clay with organic matter.
c	- 116 ft.	- 127 ft.	Soft to medium stiff tan and gray clay with sand lenses.
4	- 127 ft-	- 317 ft.	Very stiff clay with silts and sands.

TABLE 2.5-13

UNIFIED SOIL CLASSIFICATIONS

Elevation (MSL)	Visual Description	Unified Soil Classification Description
Grade to -40'*	Soft to firm clay and silty clay with silt and sand lenses.	Predominate description is CH - clay of high plasticity.
-40' to -77'**	Stiff tan and gray fissured clay.	Predominate description is CH - clay of high plasticity.
-92' to -108'	Medium stiff gray clay with silt lenses.	CH - clay of high plasticity.
'108' to -116'	Stiff gray clay, organic.	CH and MH - clay and silt of high plasticity.
-116' to -127'	Soft to medium stiff tan and gray clay with sand lenses.	Predominately CL and ML - clay and silt of low plasticity.
-127' to -317'	Very stiff clays with silts and sands.	Predominately CL and CH - clays of low and high plasticity.

---

* Excavated and replaced with compacted backfill.

** Between -77 ft. and -92 ft. MSL is very dense tan silty sand.

TABLE 2.5-14

PROPERTIES OF SUBSURFACE MATERIALS DESIGN VALUES

Visual Stratum Description	Elev.(MSL)	Unified Soil Description	Specific Gravity (Gs)	Natural Density (PCF)	Coefficient of Permeability (k) - cm/sec	Unconfined Compressive Strength -qu(ksf)	Undrained Shear Strength	Drained Shear Strength	Overconsolidation Ratio (OCR)	Average Shear Modulus Gmax(ksf)	Young's Modulus E (ksf)	Poisson's Ratio - μ*
Clay and silty clay with silt and sand (Recent material**)	Grade to -40	CH	2.70	111	1.5x1O^{-6}	1.0	c = 0.5 KSF ∅ = 0°	c' = 0 KSF 0 = 25°	1.5 + 0 2.0	1200	3600	0.48
Stiff tan and gray fissured clay	-40 to -77	CH	2.72	119	1x10^{-8}	3.0	c = 1.5 KSF ∅ = 0°	c = 0.8 KSF 0 = 12.5°	3.4	3900	11,600	0.49
Very dense tan silty sand	-77 to -92	--	2.70	125	3x1O^{-5}	--	--	c' = 0 KSF	--	3900	11,500	0.48
Medium stiff gray clay with silt lenses	-92 to -108	CH	2.74	119	--	2.4	c = 1.2 KSF ∅ = 0°	c' = 0.8 KSF ∅ = 12.5°	1.4	3900	11,600	0.49
Stiff dark gray clay - organic	-108 to -116	MH & CH	2.68	104	--	3.6	c = 1.8 KSF ∅ = 0°	c' = 0.8 KSF ∅ = 12.5°	1.7	3900	11,600	0.49
Soft to medium stiff tan and gray clay with sand lenses	-116 -127	ML & CL	2.69	119	--	1.4	c = 0.7 KSF ∅ = 0°	c' = 0.8 KSF ∅ = 12.5°	2.0	3900	11,600	0.49
Very stiff clays with silts and sands	-127 to -317	CH & CL	2.71	119	--	4.0	c = 2.0 KSF ∅ = 0°	c' = 0.8 KSF ∅' = 12.5°	1.5 to 2.4	3900	11,500	0.48
Very dense sands and silty sands	-317 to -500	--	2.70	119 to 125	--	--	--	--	--	10,000	29,000	0.45

*Computed from field Vp and Vs measurements
**Excavated and replaced with compacted backfill

Note: The average shear moduli values are averaged from maximum shear moduli obtained from field geophysical test results. They are representative only for low shear strains of approximately 10^{-6} in./in.

TABLE 2.5-15

COMPACTED CLASS A BACKFILL INDEX PROPERTIES TEST RESULTS

Specimen Type	Grain Size Distribution % Passing #100 Sieve	Grain Size Distribution % Passing #200 Sieve	Specific Gravity	Maximum Dry Unit Weight Proctor	Maximum Dry Unit Weight Shake Table	Minimum Dry Unit Weight
Reconstituted	28.0	1.4	2.665 2.672	99.9pcf	98.4pcf 99.2pcf	86.Opcf
Triaxial Test Specimen	49.4	2.9	-	-	-	-
	49.5	2.5	-	-	-	-
	50.1	2.3	-	-	-	-
	47.6	2.2	-	-	-	-
	-	2.8	-	-	-	-

TABLE 2.5-16 (Sheet 1 of 3) Revision 12-A (01/03)

MONITORING POINT LOCATIONS
(for plant coordinate system see Figure 1.2-2)

	POINT	COORDINATES	
→(DRN 02-899, R12-A)			
←(DRN 02-899, R12-A)			
→(DRN 02-899, R12-A)			
*	SP-C1	N4304.50	W3770.50
*	SP-C2	N4195.50	W3770.50
*	SP-C3	N4195.50	W3879.50
*	SP-C4	N4304.50	W3879.50
*	SP-C5	N4240.00	W3747.00
*	SP-C6	N4270.00	W3900.00
←(DRN 02-899, R12-A)			
	SP-E1	N4394.50	W3771.75
	SP-E2	N4354.00	W3748.50
	SP-E3	N4323.00	W3748.50
	SP-E4	N4295.00	W3748.50
	SP-E5	N4271.50	W3750.12
	SP-E6	N4253.00	W3736.67
	SP-E7	N4232.00	W3730.67
	SP-E8	N4161.00	W3803.00
	SP-E9	N4162.00	W3734.00
	SP-E10	N4193.50	W3768.00
	SP-E11	N4193.50	W3737.00
	SP-E12	N3955.00	W3703.00
	SP-E13	N4326.75	W3703.00
	SP-E14	N4291.83	W3703.00

→(DRN 02-899, R12-A)

* = no longer in use

←(DRN 02-899. R12-A)

TABLE 2.5-16 (Sheet 2 of 3) Revision 12-A (01/03)

MONITORING POINT LOCATIONS
(for plant coordinate system see Figure 1.2-2)

	POINT	COORDINATES	
→(DRN 02-899, R12-A)			
*	SP-M1	N4029.00	W3699.00
*	SP-M2	N4391.00	W3699.00
*	SP-M3	N4377.00	W3959.00
*	SP-M4	N4029.00	W3959.00
*	SP-M5	N4179.00	W3699.00
*	SP-M6	N4313.50	W3699.00
*	SP-M7	N4288.00	W3959.00
*	SP-M8	N4179.00	W3959.00
←(DRN 02-899, R12-A)			
	SP-M9	N4395.50	W3703.00
	SP-M1O	N4396.00	W3955.00
	SP-M11A	N4270.00	W3903.00
	SP-M12	N4240.00	W3747.00
	SP-M13	N4271.00	W3955.00
	SP-A	N4132.25	W3953.17
	SP-B	N4151.50	W3870.50
	SP-C	N4088.17	W3902.00
	SP-D	N4033.00	W3891.00
	SP-E	N4027.50	W3799.75
	SP-F	N4079.50	W3707.33
	SP-W1	N4389.00	W3918.83
	SP-W2	N4354.00	W3915.50
	SP-W3	N4323.00	W3913.50
	SP-W4	N4295.00	W3913.50

→(DRN 02-899, R12-A)

* = no longer in use

←(DRN 02-899, R12-A)

TABLE 2.5-16 (Sheet 3 of 3) Revision 2 (12/88)

MONITORING POINT LOCATIONS
(for plant coordinate system see Figure 1.2-2)

POINT	COORDINATES	
SP-W5	N4277.00	W3921.50
SP-W6	N4242.33	W3907.40
SP-W7	N4227.50	W3929.00
SP-W8	N4193.50	W3913.00
SP-W9	N4193.50	W3880.00
➔		
SP-W10	N4357.00	W3955.00
SP-W11	N4320.00	W3955.00
SP-W12	N4198.25	W3955.00
←		